Boreskov Institute of Catalysis of the Siberian Branch
of the Russian Academy of Sciences

University of California

Scientific Council on Catalysis of the Russian Academy of Sciences

Russian-American Seminar

"Advances in the Understanding and Application of Catalysts"

ABSTRACTS

Novosibirsk-2003

SEMINAR ORGANIZERS

- Boreskov Institute of Catalysis, SB RAS, Novosibirsk, Russia
- University of California, Berkeley, USA
- Russian Foundation for Basic Research, Moscow, Russia
- Scientific Council on Catalysis, RAS, Moscow, Russia


Organizers express deep gratitude to BP International Ltd. for the financial support.

International Advisory Committee

B.C. Gates	- University of California, Davis, USA
V.B. Kazansky	- Zelinsky Institute of Organic Chemistry RAS, Moscow, Russia
K. Klier	- Lehigh University, USA
V.A. Likholobov	- Omsk Department of the Boreskov Institute of Catalysis SB RAS, Omsk, Russia
V.V. Lunin	- Lomonosov Moscow State University, Moscow, Russia
J. Lunsford	- Texas A&M University, USA
I.I. Moiseev	- Kurnakov Institute of General and Inorganic Chemistry RAS, Moscow, Russia
A.S. Noskov	- Boreskov Institute of Catalysis, SB RAS, Novosibirsk, Russia
G.A. Somorjai	- University of California, Berkeley, USA

Organizing Committee

Chairmen

A.T. Bell	- University of California, Berkeley, USA
V.N. Parmon	- Boreskov Institute of Catalysis SB RAS, Novosibirsk, Russia

Co-Chairmen

V. Guliants	- University of Cincinnati, USA
V.I. Bukhtiyarov	- Boreskov Institute of Catalysis SB RAS, Novosibirsk, Russia
M. Neurock	- University of Virginia, USA
U. Ozkan	- Ohio State University, USA
M.M. Slinko	- Semenov Institute of Chemical Physics RAS, Moscow, Russia
M.Yu. Sinev	- Semenov Institute of Chemical Physics RAS, Moscow, Russia

Secretary:

L.Ya. Startseva	- Boreskov Institute of Catalysis SB RAS, Novosibirsk, Russia

PLENARY LECTURES

EXAFS CHARACTERIZATION OF THE LOCAL STRUCTURE OF Fe IN Fe-ZSM-5

Choi S., Wood B. J., Ryder J., Bell A.T.

Department of Chemical Engineering, University of California, Berkeley, USA
E-mail: alexbell@uclink.berkeley.edu, bell@cchem.berkeley.edu

The local structure of Fe in Fe-ZSM-5 prepared by solid-state exchange was investigated with XAFS. Fe K-edge spectra were taken at liquid nitrogen temperature on samples with Fe/Al ratios of 0.33, 0.66, and 0.80. The radial structure function (RSF) of He- and CO-pretreated Fe-ZSM-5 shows two main peaks, one at 1.6 Å and the other at 2.5 Å. To interpret the origin of these peaks, RSFs were simulated for a number of mono- and di-iron structures obtained from quantum chemical calculations. By this means the peak in the RSF at 1.6 Å is clearly identified with back scattering from O atoms coordinated to a Fe atom. The peak at 2.5 Å has been previously ascribed to Fe-Fe scattering and has been used to argue for the presence of di-iron-oxo species; however, the origin of this peak and its interpretation remains an open question. The imaginary part of the Fourier-transformed data for the peak at 2.5 Å has the same characteristics as that generated theoretically for Fe-Al back scattering and is distinctly different from that generated theoretically for Fe-Fe back scattering. This evidence strongly suggests that the iron in Fe-ZSM-5 is present as isolated cations associated with framework aluminum. Further evidence for such a structure is the absence of any change in the magnitude of the peak near 2.5 Å with sample treatment. The RSFs and the information obtained from curve-fitting demonstrate that the structure of Fe in Fe-ZSM-5 does not change significantly with Fe/Al ratio. For both He- and CO-pretreated sample, the Fe-O coordination number is about 4 and correspondingly the Fe-Al coordination number is about 1, regardless of Fe/Al ratio. Therefore, the structure of Fe in Fe-ZSM-5 is best described as either $Z^-[Fe(O)_2]^+$ or $Z^-[Fe(OH)_2]^+$, where Z^- represents the charge-exchange site in the zeolite. Upon O_2 pretreatment, a new feature appears at about 1.1 Å in the RSF, which may be due to a migration of some of the Fe into the zeolite framework. This interpretation is qualitatively consistent with the observed RSF for Fe-silicalite.

SURFACE SCIENCE TECHNIQUES AND *IN-SITU* STUDY OF MECHANISMS OF HETEROGENEOUS CATALYTIC REACTIONS

Bukhtiyarov V.I.

Boreskov Institute of Catalysis SB RAS, Novosibirsk, Russia
Fax: (+7)-3832343056; E-mail: vib@catalysis.nsk.su

The application of modern surface science techniques to molecular-level investigations of different processes on surface of a solid has promoted our understanding of a broad range of phenomena such as chemisorption, adsorbate-adsorbate interactions and chemical reactions on the surface of single crystal. At the same time, the surface science results can not be directly transferred to technical catalysis due to the pressure gap problem. Indeed, weakly bound species present under reaction conditions ($P > 10^5$ Pa) may be absent under pressures at which almost all physical methods operate ($P < 10^{-4}$ Pa). If this species is catalytically active, so its non-observation by physical methods makes it impossible to characterize a surface of an operating catalyst. Tackling this problem requires the development of new physical methods working at high pressures.

Following this tendency, in nineties researchers have developed a number of novel physical methods and have modified existing ones for *in-situ* measurements at higher pressures. Among them are X-ray absorption near edge structure (XANES) spectroscopy, infra-red absorption spectroscopy (IRAS), polarization-modulated (PM) IRAS, sum frequency generation (SFG) spectroscopy, etc. Attempts to develop *in-situ* X-ray photoelectron spectroscopy (XPS), which in light of its universality and sensitivity to chemical state of an element occupies a special place among the physical methods of surface analysis, have been also made many times for last twenty years. General feature of all *in-situ* photoelectron spectrometers is a differential pumping of X-ray source and energy analyzer that allows one to shorten a path of photoelectrons in high-pressure region. Theoretical level of the highest pressure for *in-situ* measurement is ranging in 1-10 millibar depending on kinetic energy of photoelectrons, but experimental limit is affected by a number of factors. One of the main factors is a brightness of X-ray source, therefore modern *in-situ* spectrometers are usually attached to synchrotron radiation source. At the same time, routine XPS spectrometer can also be equipped for *in-situ* measurements.

In this presentation we would like to demonstrate the capabilities of our VG ESCALAB HP spectrometer to study the adsorption and mechanism of heterogeneous catalytic reactions.

Moreover, we will show that combination of XPS with other *in-situ* surface science techniques allows getting more convincing data about the system studied.

CO adsorption on Pd(111) was examined by high pressure SFG and XPS from 200 K to 400 K, and between 10^{-6} and 1 mbar CO. Even under high pressure both methods indicated that CO adsorbed in "regular" adsorption sites such as hollow, bridge and on-top. The high pressure CO structures were similar to those known from UHV studies. Our data clearly demonstrate that by combining SFG and XPS adsorbate structures and coverages can be obtained *in-situ* at high pressure and they even allow a quantitative analysis. We did not observe any indications of CO dissociation or carbonyl formation under our experimental conditions.

We also checked the influence of structural defects on CO adsorption. These experiments were carried out in light of previous studies on Pd(111) and Pd nanoparticles which suggested that CO dissociation requires the presence of low-coordination (defect) sites. However, our XPS data indicate that the structural defects induced by an ion sputtering does not facilitate CO dissociation. Only the same CO species are observed during CO adsorption both on the Pd(111) and on the sputtered Pd(111) surfaces.

Contrary to CO, adsorption of methanol on Pd(111) is affected by pressure. Both XPS and SFG data identifies two routes of methanol decomposition at room temperature: 1) dehydrogenation to CO and H_2 and 2) breaking C-O bond. The former route has identified on C1s feature from the adsorbed CO, the latter one – from elementary carbon. In full agreement with literature data, the route of dehydrogenation is preferable in UHV, whereas the rate of carbon formation is increased as the CH_3OH pressure rises. Total coverage of C_{ads} exceeds one a monolayer (up to 2) that indicates dissolution of carbon atoms into the subsurface metal layers.

Even more valuable data about mechanism of a catalytic reaction can be obtained if XPS is combined with mass-spectrometric analysis of the gas phase compositions. In this presentation we would like to demonstrate the capabilities of our spectrometer to study the mechanism of heterogeneous catalytic reactions on the example of partial oxidation of methanol to formaldehyde over copper. Analysis of the distribution of the reaction products and surface species depending on temperatures allowed us to show that:

1) Except for partial and total oxidation of methanol, the dehydrogenation routes of the reaction with the formation of CO and formaldehyde are observed.
2) Low activity of the copper at $T < 470$ K is explained by the saturation of the surface by methoxy-groups which are produced via the reaction of CH_3OH with O_{ads}.

3) Heating the sample above 500 K decomposes the methoxy-groups and develops the formation of the formaldehyde.
4) At intermediate temperatures (500 – 550 K) the formaldehyde formation proceeds presumably via the hydrogenation route, which displaces on the partial oxidation route at temperatures higher than 600 K.
5) Methoxy-groups are the only intermediates in the transformation of methanol to formaldehyde.
6) The catalyst surface exhibiting high catalytic activity is the metallic copper containing adsorbed oxygen and sub-oxide oxygen.

These data together with XANES results of Germany colleagues are used for discussion of the mechanisms of selective oxidation of methanol to formaldehyde.

The examples of the model studies described in this presentation unambiguously show that *in-situ* characterization of an operating catalyst is of great importance since allows elucidation of the real reaction mechanisms. As consequence, we can conclude that development and application of such techniques will be spread in the nearest future, and their results will be used more and more often to improve the catalyst performance.

IN SITU MAS NMR SPECTROSCOPY IN HETEROGENEOUS CATALYSIS: ADVANCES AND PERSPECTIVES

Ivanova I.I.

Lomonosov Moscow State University, Moscow, Russia
Fax: 7 (095) 9328846; E-mail: IIIvanova@phys.chem.msu.ru

More than 20 years ago G.K. Boreskov have formulated an idea that heterogeneous catalysts are self-tuning systems, in which the active surface of the catalyst is formed during catalytic reaction and the state of the "working" surface is different from those before or after reaction [1]. This fundamental idea, on the one hand, have stimulated many experimental and theoretical studies in the field of heterogeneous catalysis and, on the other hand, required development of novel experimental approaches for the investigation of heterogeneous catalysts directly under "working" conditions, in particular, development of *in situ* techniques.

The progress achieved in the field of spectroscopic methods of catalysts characterization allows now for investigation of the state of catalysts and reactants directly in the course of catalytic reactions - *in situ*. Among *in situ* spectroscopic techniques, NMR spectroscopy is considered to be one of the most informative.

The aim of this contribution is to review the advances in the *in situ* MAS NMR techniques for the unravel of the mechanisms of heterogeneous catalytic reactions. In the first part of the lecture, the different techniques for realization of *in situ* MAS NMR experiments in static and flow conditions are briefly considered. The experimental approaches including temperature-switch and pulse-quench methods, aimed at the investigation of fast reactions, and stopped-flow and separated-step techniques, directed at the study of stable reaction intermediates in continuous flow and batch conditions are discussed.

In the second part, the main application areas and the capabilities of the *in situ* MAS NMR techniques are analysed. It is demonstrated that *in situ* MAS NMR techniques can be used for the determination of surface active sites and their interaction with adsorbed reactants; the analysis of the state and mobility of adsorbed reactants and products; the identification of surface species formed and the investigation of their reactivity; the direct observation and the indirect identification of reaction intermediates; the studies of reaction kinetics; the observation of real primary products; the probing of reaction mechanisms using ^{13}C tracing techniques and various probe molecules (H_2, O_2, H_2O, CO, C_6H_6 etc.); finally, the direct observation of the shape selectivity, confinement effects in molecular-sieve catalysts and catalysts deactivation.

The advantages of the *in situ* MAS NMR techniques are illustrated with examples taken from the literature on the interaction of olefins, alcohols, ethers, alkanes, aromatics and halogen-containing compounds over mono- and bifunctional zeolite and oxide catalysts. The cross-reference index between the reactions studied, the catalysts used, the mechanistic information obtained and the corresponding literature sources are established.

Finally, in the last part, the perspectives of the *in situ* MAS NMR techniques are considered.

Acknowledgements

Financial support by the Volkswagen Foundation and RFBR is gratefully acknowledged. I.I. Ivanova thanks the Russian Science Support Foundation for a grant within the frame of the program supporting talented young researches.

References

[1] Boreskov G.K. “Catalysis: The questions of theory and practice”, Edts: K.I. Zamaraev and G.I. Panov, Novosibirsk, “Nauka”, 1987.

REACTIVITY OF ACIDIC ZEOLITES VIA QUANTUM CHEMICAL AND CAR-PARRINELLO MOLECULAR DYNAMIC METHODS

Lo C., Trout B.L.

Department of Chemical Engineering, MIT, Cambridge, USA
Fax: 1-617-258-5042; E-mail: trout@mit.edu

Zeolites are of major industrial importance as solid acid catalysts, being used throughout the petroleum and specialty chemical industry. They are microcrystalline silicon-oxide materials with various other species incorporated. For example, Brønsted acid sites are incorporated into the zeolite when certain atoms, such as Al, are substituted for Si in the zeolite framework.

Despite a tremendous amount of progress in characterizing zeolite acidity, there are still many unresolved issues which stem from the overall question of what is the nature of the active site or sites. The lack of understanding of acidity hinders the ability to synthesize zeolites with optimal properties for desired applications. While there are many experimental techniques, including microcalorimetry and solid-state NMR, to probe acid sites, there are often inconsistencies among the results of various methods. Also, there is no suitable scale for solid acidity, such as pH for acidity in aqueous solution. These remarks are quite understandable in light of the difficulties of evaluating heterogeneous catalytic processes in general, and in particular of isolating individual reaction steps that occur during processes on solid surfaces. Computational methods based on first-principles present a way to address these experimental difficulties.

We have performed a detailed investigation, via density functional theory (DFT) and constrained optimization, of the reactivity of acid sites in the zeolite chabazite, by calculating energies of adsorption of bases, proton affinities, and vibrational frequencies on a periodic chabazite model with one or two acid sites per unit cell and with and without a silanol defect. We chose to study chabazite as our model solid acid catalyst because it is industrially relevant, as shown to be active for the methanol to gasoline (MTG) process [1], but also because its unit cell size is much smaller than that of the more widely used ZSM-5 (36 atoms versus 288 atoms for the siliceous material).

We have found that there are two possible proton positions, one stable and the other metastable, per acidic oxygen at the acid site, not one as previously reported in the literature. We have also found that the individual acid site strengths do not vary significantly, within the accuracy of DFT calculations, with acid site concentration in the zeolite or framework defects,

and that the adsorption energy of various bases at the acid site does not correlate to the O-H stretch vibrational frequency at the Bronsted acid site. Our results suggest that all acid sites in chabazite have the same acid properties within the accuracy of the calculations. Given the range of local chemical structure that we investigated in chabazite, our results imply that for alumina-silica zeolites, in general, differences in catalytic activity are governed primarily by extrinsic factors such as diffusion and surface adsorption, rather than intrinsic differences in acid strength among zeolites.

We next turned our attention to studying coupling reactions of methanol in zeolites and zeotypes. From the industrial standpoint, such interest has been spurred from the possibilities of synthesizing olefins using methanol to olefins (MTO) processes and of developing more environmentally friendly processes for synthesizing gasoline using methanol to gasoline (MTG) processes. From the academic standpoint, it is of interest to understand the mechanism for the formation of the first C-C bond, since it is thought that this is the rate limiting first step, along with the initial physisorption to the zeolite acid site, of the MTG and MTO reactions. It is also thought that the formation of surface methoxonium groups and dimethyl ether is a necessary first step towards the formation of ethanol and higher hydrocarbons [2, 3, 4].

As a first step in studying the methanol-methanol coupling process, we performed full periodic constrained molecular dynamics simulations of two methanol molecules in the chabazite unit cell at 400 ^{o}C, using the Car-Parrinello formulation. We wanted to simulate the C-C bond formation process, and we chose the C-C intermolecular distance as our reaction coordinate. We performed geometry optimizations at 0 K of the two methanol molecules in chabazite, and from the optimized structure, we decreased the C-C distance and constrained its value. Initially, this decrease in distance occurred at 0.4 Angstrom intervals, and closer to the transition state, it occurred at 0.2 Angstrom intervals. At each point along the reaction coordinate, we evaluated the ensemble averaged force due to the constraint along the constrained direction. From the results of the constrained molecular dynamics simulations, we concluded that the process, which produces ethanol and water, involves stable intermediates of methane, protonated formaldehyde, and water, and calculated the free energy barrier of the reaction to be 223.5 kJ/mol using the method of Sprik et al. [5].

There is a major concern, however, in using the method of constrained dynamics with a very simple geometric reaction coordinate. We therefore used the method of transition path sampling developed by Chandler et al. [6] to find the true transition state ensemble and calculate the reaction rate and free energy barrier(s). This method involves “shooting” short,

unconstrained, molecular dynamics trajectories, and using a Monte Carlo approach, from an initial dynamical path connecting the reactant and product states; knowledge of an initial transition state is not required. By sampling a large portion of phase space, we hope to converge towards the true reaction mechanism.

We implemented this method in conjunction with Car-Parrinello molecular dynamics. We used the constrained dynamics trajectories from the ensemble of the 2.2 Angstrom C-C distance to investigate the initial C-O bond breaking that must occur to form methane, and the ensemble of the trajectory with 1.8 Angstrom C-C distance to investigate the C-C bond formation to form ethanol. For the first step, the reaction mechanism was similar to that predicted by constrained dynamics, which is expected since the C-C distance constraint does not dramatically affect C-O bond breaking. First, a proton is transferred from the zeolite acid site to one of the methanol molecules, forming a methoxonium cation, which subsequently splits into methyl cation and water, breaking the C-O bond. Then the remaining methanol transfers one of its protons to the methyl cation, forming methane and "protonated formaldehyde". We calculated the free energy barrier to be 197.26 kJ/mol.

However, the mechanism we found for the formation of the C-C bond was very different from that predicted by constrained molecular dynamics. See a snapshot presented in Figure 1. Ethanol forms by a simple combination of the methyl anion and protonated formaldehyde. Therefore, the rate-limiting step is not the formation of the C-C bond, but rather the proton transfer from methane to water. We also note that ethanol is formed directly from the intermediates, without the need for prior formation of dimethyl ether and surface methoxonium groups, as hypothesized by other researchers. The hydroxonium cation does transfer the proton back to the chabazite acid site, but one in an adjacent unit cell. This underscores the importance of doing full periodic calculations and taking into account the interactions of the reactants and products with the chabazite framework. We calculated the free energy barrier to be 195.59 kJ/mol.

In summary, we have elucidated a new mechanism for direct ethanol formation from methanol at 400 °C that does not require the formation of surface methoxy groups or a dimethyl ether intermediate. The mechanism involves stable intermediates of methane and protonated formaldehyde. Our calculated free energy barriers are roughly equal to or lower than those of other researchers who have reported other mechanisms. Part of this work has been submitted for publication and part is in preparation [7-8].

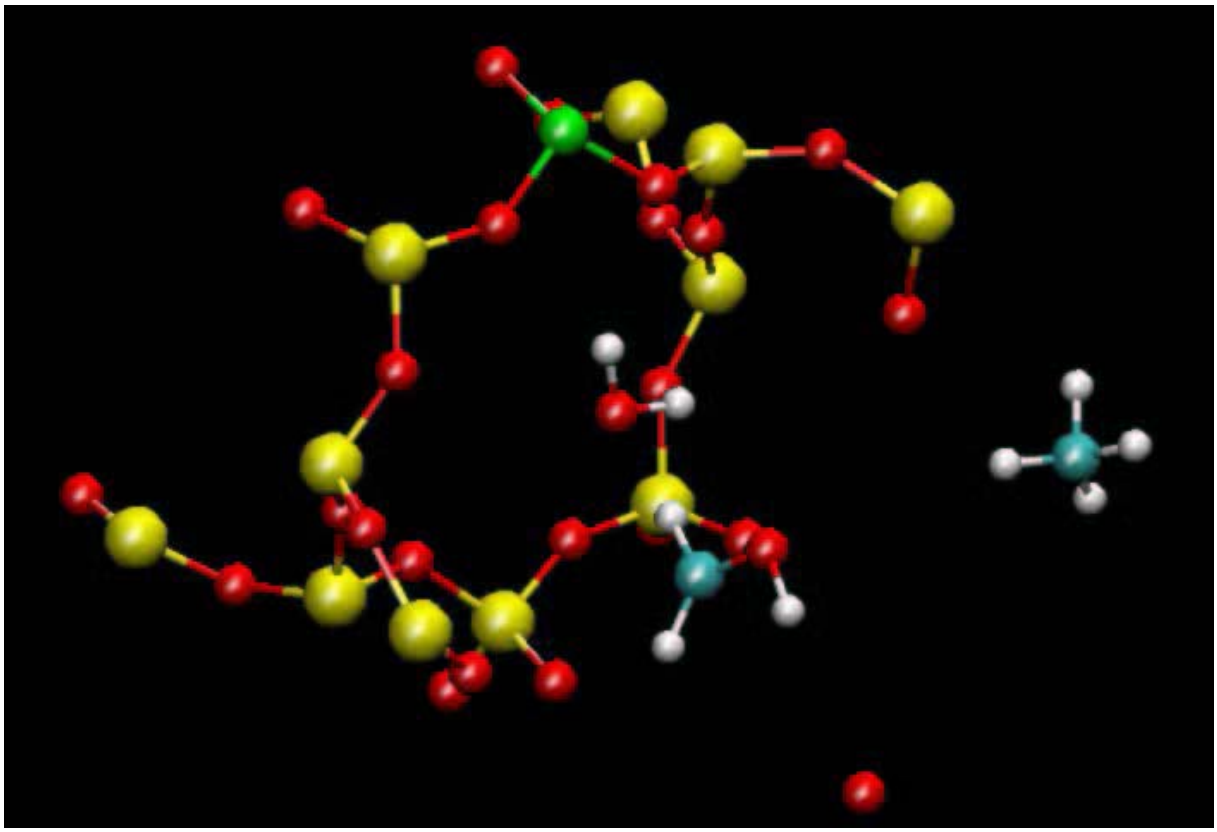

Fig. 1: Snapshot of transition state ensemble for C-C bond formation.

References:

[1] Yuen L.-T., Zones S. I., Harris, T. V., Gallegos, E. J. and Auroux A., *Microporous Mat.,* 2 (1994) 105.
[2] Blaszkowski S. R. and van Santen, R. A., *J. A. C. S.,* 119 (1997) 5020.
[3] Tajima N., Tsuneda T., Toyama F. and Hirao K., *J. A. C. S.,* 120 (1998) 8222.
[4] Govind N., Andzelm J., Reindel K. and Fitzgerald G., *Int. J. Molec. Sci.,* 3 (2002) 423.
[5] Sprik M. and Ciccotti G., *J. Chem. Phys.,* 109 (1998) 7737.
[6] Bolhuis P. G., Chandler D., Dellago C. and Geissler P. L., *Ann. Rev. Phys. Chem.,* 53 (2002) 291.
[7] Lo C. and Trout B. L., *J. Phys. Chem. B*, submitted.
[8] Lo C. and Trout B. L., in preparation.

SPECTRAL STUDY OF UNUSUAL LOCALIZATION AND SUPERACID PROPERTIES OF BIVALENT CATIONS IN THE ZEOLITES WITH HIGH Si/Al RATIO IN THE FRAMEWORK

Kazansky V.B.

Zelinsky Institute of Organic Chemistry RAS, Moscow, Russia
Fax: 135-53-28; E-mail: vbk@ioc.ac.ru

The unusual catalytic properties of high silica zeolites modified with bivalent cations have recently attracted the growing attention of different scientific groups. High silica zeolites modified with Zn^{+2} ions catalyze dehydrogenation and aromatization of paraffins[1,2]. Copper and cobalt modified ZSM-5 samples are active in selective reduction of NOx with hydrocarbons. CoZSM-5 catalyzes ammoxidation of ethane to acetonitryl[3,4], etc. Catalytic activity and selectivity of high silica zeolites in these reactions are much higher than of the low silica faujusites modified with the same cations. This is obviously connected with the unusual localization and properties of bivalent cations in the silica rich frameworks.

Indeed, according to ^{29}Si MAS NMR, distribution of aluminum in the framework of high silica zeolites is mostly random [5], while aluminum atoms are strongly separated from each other [6]. In this case neutralization of several distantly placed negative lattice charges by a single multi-charged cation is difficult. Therefore, in most part of published papers only stabilization of bivalent cations at the two adjacent aluminum atoms in the next-nearest positions to each other is usually discussed. However, the number of such dual sites at the very high Si/Al ratios is rather low and localization of the multivalent cations at the sites with the distantly placed aluminum should be also somehow considered.

Our very recent experimental results clarify this situation [7,8]. In contrast to the generally accepted models, we found that in HZSM-5 with Si/Al ratios of 25 or 40 all of the bridging acidic protons can be quantitatively substituted by Zn^{+2} ions via reaction with zinc vapor at 720 K (Fig. 1). Since the number of the pairing aluminum sites in the next - nearest positions in both of these zeolites is certainly much less than the total aluminum content, the complete substitution of protons by zinc ions presents a direct experimental evidence of localization of the bivalent cations at the isolated aluminum occupied oxygen tetrahedra with the single negative electric charges.

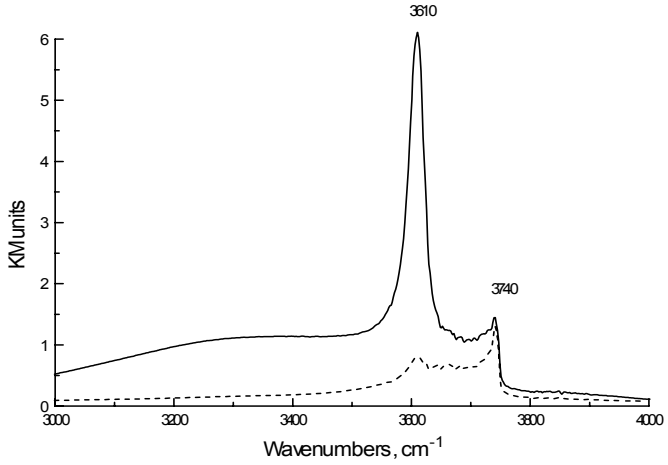

Fig. 1. Substitution of the bridging acidic protons by reaction with zinc vapor at 720 K. Solid line – DRIFT spectrum of OH groups in the initial sample. Dashed line – after reaction with zinc vapor.

The only reasonable way to explain this result for a zeolite modified with the bivalent cations is the following model with alternation of the positive and negative electric charges:

$$2\,Z^{-}\text{-}H^{+} \quad + \quad Zn^{0} \quad \rightarrow \quad Z^{-}\text{-}Zn^{+2} \quad + \quad Z^{-}\square \quad + \quad H_2 \qquad (1)$$

In this case one half of bivalent cations is localized at the singly negatively - charged aluminum occupied oxygen tetrahedra creating the sites with the excessive positive electric charges. The negative charges of the equivalent amount of aluminum centered oxygen tetrahedra with cationic vacancies at such sites are compensated in the indirect way by an electrostatic interaction with the surrounding positively charged Zn^{+2} ions. In other words, localization of bivalent cations at the isolated single lattice negative charges results in formation of the acid base pairs with the distantly separated excessively positively charged Lewis acid sites and the basic lattice oxygen atoms. For zeolites such possibility has been never discussed before, despite the structures with alternation of excessive positive and negative electric charges in the framework are well known for such oxides as γ-Al_2O_3, spinels or layered aluminum silicates.

DRIFT spectra of molecular hydrogen adsorbed at 77 K by Zn^{+2} ions at these sites indicated an unusually strong perturbation of H-H stretching frequency resulting in the H-H stretching band with the maximum at 3938 cm^{-1}. (Fig. 2). The strong low–frequency shift more than 200 cm^{-1} should be explained by interaction of hydrogen with the non-compensated positive charge of bivalent zinc cations. Moreover adsorption of hydrogen at room or slightly elevated temperatures resulted in its heterolytic dissociation with formation of hydride ions

and acidic protons. Recently we also found that zinc ions at such sites unusually strongly perturb adsorbed methane and dissociatively adsorb it at 473 K.

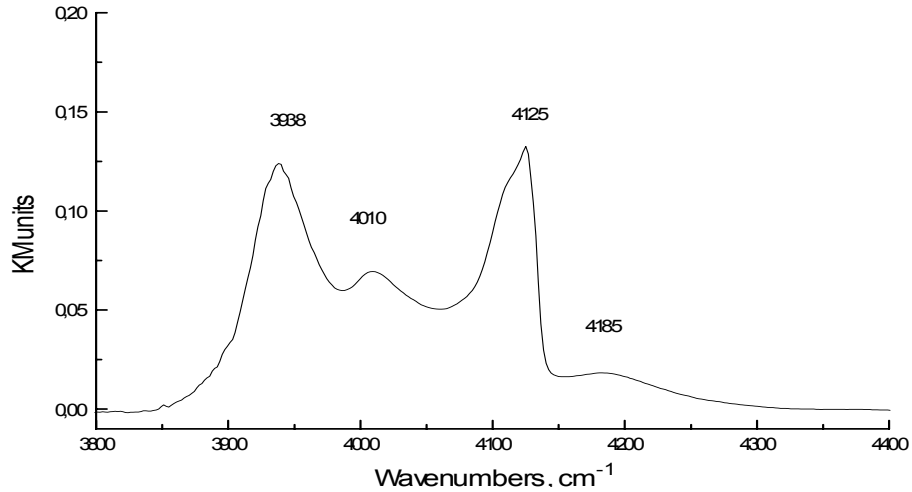

Fig. 2. DRIFT spectrum of H_2 adsorbed on zinc modified HZSM-5 zeolite at 77 K. The bands at 3938 and 4010 cm^{-1} belong to the stretching vibrations of H_2 perturbed by two different kinds of Zn^{+2} cations, respectively. The band at 4125 cm^{-1} is connected with H_2 adsorption on silanol groups remaining after substitution of acidic groups by Zn^{+2} ions.

Position of the second band in Fig. 2 at 4010 cm^{-1} is close to that one earlier reported by us for hydrogen adsorption on zinc modified HY prepared by ion exchange [9]. Therefore, similar to HY we also ascribe the corresponding sites to the Zn^{+2} ions localized at the conventional ion - exchangeable positions in the six- or five- membered rings of the ZSM-5 framework containing two aluminum – occupied oxygen tetrahedra per the ring.

The similar sites of the stronger and weaker perturbation of adsorbed hydrogen or methane were also observed in our work for zinc and cobalt modified ZSM-5 zeolites prepared by conventional incipient wetness impregnation of the corresponding hydrogen forms [8-13]. In addition, the study of zinc and cobalt modified zeolites with different aluminum content in the framework indicates that the sites of weaker hydrogen perturbation predominate at higher aluminum content when the density of aluminum atoms in the zeolite framework is high. In contrast, as one should expect, the sites of the strongest perturbation of adsorbed hydrogen and methane predominate in the zeoltes with the lower aluminum density in the framework. Therefore, formation in high silica zeolites of the above-discussed ions pairs with the distantly placed bivalent cations and basic oxygen in the framework is of a general importance. The only difference from the samples prepared via reaction with zinc vapor is the less selective substitution of protons by zinc ions.

Usually the catalytic properties of high silica zeolites are accounted for the shape selectivity effects connected with the porous structure of these materials. The above results

for the first time indicate importance in addition to the shape selectivity of the specific structure of the distantly separated acid–base active sites.

References

1. A.Hagen, F.Roessner, Catal. Rev., 2000, **42**, 403.
2. E. Iglesia, E. Baungarter, Catal. Today, 1996, **31**, 207.
3. M. Shelef, Chem. Rev., 1995, **95**, 209.
4. J. N. Armor., Catal. Today , 1995, **26,** 147.
5. G. Engelhardt, in *"Introduction to Zeolite Science and Technology"*, Chapter 8, p. 285-315, van Bekkum H., Flaningen E.M., Jansen J.C., eds., (Elsevier Amsterdam 1991).
6. X. Feng, W.K.Hall, Catal. Lett., 46(1997)11.
7. V. B. Kazansky, accepted for publication in J. Catal.
8. V. B. Kazansky, A. I.Serykh, submitted to Chem. Comm.
9. V. B. Kazansky, V.Yu. Borovkov, A.I. Serykh, R.A.van Santen, P. Stobbelar PCCP 1999, **1**, 2881.
10. V.B.Kazansky, V.Yu. Borovkov, A.I. Serykh, R.A. van Santen, B.G. Anderson., Catal. Lett., 2000, **66**, 39.
11. V.B. Kazansky, A.I. Serykh, R.A. van Santen, B.G. Anderson Catal. Lett., 2001, **74**, 55.
12. V.B. Kazansky, A.I. Serykh, A.T.Bell, accepted for publication in Catal. Lett.,
13. V.B.Kazansky , A.I. Serykh, submitted to Catal. Lett.

MIXED Mo-V-Te OXIDE CATALYSTS FOR ENVIRONMENTALLY BENIGN PROPANE OXIDATION TO ACRYLIC ACID

Guliants V.V., Al-Saeedi J., Vasudevan V.

Department of Chemical and Materials Engineering, University of Cincinnati, Cincinnati, USA
E-mail:Vadim.Guliants@uc.edu

Economic and environmental considerations have generated much recent interest in the oxidative catalytic conversion of alkanes to olefins, oxygenates and nitriles in the petroleum and petrochemical industries. The Mo-V-Te-Nb-O oxides have been disclosed in recent years as highly active and selective for the ammoxidation of propane to acrylonitrile [1, 2] and the propane oxidation to acrylic acid [3]. They contain so-called "M1" and "M2" mixed metal oxide phases proposed as active and selective for propane oxidation to acrylic acid. However, these mixed metal oxide catalysts traditionally synthesized by solution evaporation techniques are complex mixtures of mixed oxide phases with poorly defined crystal morphologies [4]. Therefore, these catalysts are unsuitable as model systems for fundamental studies of the bulk and surface molecular structure-activity/selectivity relationships in propane oxidation reaction.

Recently, the Mo-V-Te-O catalysts have been synthesized by hydrothermal methods that resulted in the M1 and M2 phases with well-defined rod-like crystal morphology [5, 6] highly promising as model catalysts for propane oxidation to acrylic acid. However, these recent reports provided an incomplete synthesis procedure only for a very narrow region of the Mo-V-Te-O synthesis diagram corresponding to the $Mo_{0.6}V_{0.3}Te_{0.1}O_x$ composition.

In this study, we investigated the role of the synthesis composition, solution pH, and thermal activation conditions on the solid-state chemistry of the model Mo-V-Te-O system. The hydrothermal synthesis of the $Mo_{0.6}V_{0.3}Te_{0.1}O_x$ composition previously reported [5, 6] revealed the critical role of the solution pH for the formation of the M1 and M2 phases. The $Mo_{0.6}V_{0.3}Te_{0.1}O_x$ composition crystallizes as rod-like crystals of 1-3 μm in diameter and 10-20 μm long. Hydrothermal synthesis results in a catalyst precursor that was thermally activated in an inert environment (N_2) at 500 ^oC in order to avoid the phase separation and obtain an active and selective catalyst. Two routes of thermal activation were utilized. The two-steps, air at 280 ^oC then N_2 at 500 ^oC, thermal activation route lead to morphological differences in comparison with the one step, N_2 at 500 ^oC, thermal activation route.

The Mo-V-Te-O phase diagram was systematically explored in order to elucidate the role of various hydrothermal synthesis parameters (synthesis route/pH/composition) in the nucleation and growth of different Mo-V-Te-O phases. This study revealed that the M1 and M2 phases crystallized under a much wider range of synthesis compositions than reported previously [5, 6]. We discuss the crystal morphology, microstructure, crystal structures, bulk and surface compositions, as well as the catalytic performance of this model mixed Mo-V-Te-O catalysts in selective propane oxidation to acrylic acid.

References:

1. Ushikubo, T., K. Oshima, A. Kayou, M. Vaarkamp, and M. Hatano, J. Catal., 169 (1997) 394.
2. Watanabe, H., and Y. Koyasu, Appl. Catal., 194 (2000) 479.
3. Mitsubishi Chemicals, JP 10-36311(1998)
4. Lin, M., Appl. Catal., 207 (2001) 1.
5. Ueda, W., N.F.Chen, and K. Oshihara, Chem.Comm., (1999) 517.
6. Oshihara, K., T. Hisano and W. Ueda, Top. in Catal., 15 (2001) 153.

NITROUS OXIDE: NEW OXIDATION REACTIONS IN ORGANIC CHEMISTRY

Panov G.I.

Boreskov Institute of Catalysis SB RAS, Novosibirsk, Russia
Fax: (007) 3832 344687; E-mail: panov@catalysis.nsk.su

Introduction

Selective oxidation of organic substrates is one of the most difficult fields of catalytic chemistry. Creation of selective catalyst is usually the main problem. Such a catalyst should perform a multifunctional role: to activate in a due way both dioxygen and the substrate, and to promote their further interaction so as to form desirable products. Optimization of these functions is a difficult challenge since at varying the catalyst composition one cannot tune them independently.

To solve the problem, the use of alternative oxidants in the form of various oxygen-containing molecules seems to be a promising approach in heterogeneous catalysis. The variation of the oxidant chemistry should primarily change the state of surface oxygen, while activation of organic molecules may remain unchanged, thus suggesting new opportunity for controlling the oxidation selectivity.

This report is devoted to nitrous oxide as an alternative oxidant and presents a review on its application in both the gas-phase and liquid-phase oxidation reactions.

Gas-phase oxidation

Until recently, N_2O was used only in the gas-phase catalytic oxidation. The most known example is the selective oxidation of benzene to phenol over FeZSM-5 zeolite, which underlies a pilot-scale development of a new phenol process. Recently, a significant progress has been achieved with another important reaction, i. e., the oxidation of phenol to dihydroxybenzenes.

According to a generally accepted view, the high oxidation efficiency of nitrous oxide relates to a particular form of surface oxygen ("α-oxygen"), which is generated from N_2O. α-Oxygen remarkably combines two seemingly incompatible features: high activity and high selectivity. α-Oxygen, even at room temperature, can oxidize a variety of hydrocarbons (alkanes, cycloalkanes, alkenes, aromatics) and provide selective formation of the corresponding hydroxylated products. These results demonstrate great potentialities of N_2O in selective oxidation catalysis, where many research groups are active currently in searching for new catalysts and new N_2O reactions.

The report will consider a number of fundamental issues in the field. In particular, the nature of the surface sites responsible for the α-oxygen stabilization. There are two alternatives, which are under long discussion in the literature: either Lewis acid centers or Fe-containing surface complexes. Last years, spectroscopic studies in combination with adsorption and catalytic measurements identified clearly a key role of the iron in the oxygen transfer from N_2O to an organic molecule.

The composition, structure and nano-scale description of the active Fe complexes remain to be open questions and are subjects of many studies.

Liquid-phase oxidation

This is a very new field, although the first attempt here has been made more than 50 years ago. Recently a very efficient way for the N_2O liquid-phase oxidation of cyclohexene and cyclopentene to the corresponding cyclic ketones was described [1–3]. The oxidation proceeds noncatalytically at 150–250 ^oC with 95–99% selectivity. This phenomenon was shown to relate to a remarkable ability of N_2O to interact directly with the alkene double bond and transfer its oxygen atom to the unsaturated carbon of the cycle. The simplicity and high selectivity of the above reactions stimulate attempts to extend this approach to the oxidation of other alkenes.

The report will discuss new results of a broad substrate screening (over 40 compounds), which show that the liquid-phase non-catalytic oxidation by nitrous oxide is applicable to aliphatic, cyclic, heterocyclic alkenes and their derivatives for the preparation of various carbonyl compounds widely used as intermediates and solvents.

Several research groups are taking efforts for developing an alternative liquid-phase approach, i.e., catalytic activation of N_2O in order to direct the reaction to other selective oxidation products, in particular, to epoxides. The first successful examples of this promising approach as well as economic aspects of using N_2O oxidant will be discussed.

Conclusion

The application of nitrous oxide offers remarkable opportunities for selective oxidation both in the gas and the liquid phases. This is a rapidly growing field, which enjoys currently the activity of more than 30 research groups. Many N_2O reactions provide high selectivity and open ways for developing new routes in organic chemistry.

[1] Panov G.I., Dubkov K.A., Starokon E.V. and Parmon V.N., *React. Kinet. Catal. Lett.*, 76 (2002) 401.
[2] Dubkov K.A., Panov G.I., Starokon E.V. and Parmon V.N., *ibid.*, 77 (2002) 197.
[3] Avdeev V.I., Ruzankin S.Ph. and Zhidomirov G.M., *Chem. Commun.*, (2003) 42.

ORAL PRESENTATIONS

STUDY OF THE LOW TEMPERATURE CO + O_2 REACTION OVER Pd(111), Pd(110) AND Pd TIP SURFACES USING ^{18}O TRACES, TPR, FEM AND MOLECULAR BEAMS

Gorodetskii V.V.[1], Matveev A.V.[1], Zaera F[2].

[1]Boreskov Institute of Catalysis SB RAS, Novosibirsk, Russia
[2]Department of Chemistry, University of California, California,USA

Introduction

The catalytic CO oxidation over noble metal surfaces has been a subject of scientific interest and plays an important role in air pollution control. There is a great interest in self-oscillatory phenomena in the reaction catalysed by platinum metal surfaces. The CO oxidation on Pd surface is a non-linear system, in which temporal and spatial organisation become possible. In the oscillating regime of the reaction, the reaction mixture periodically affects the properties of metal surfaces. On Pd(110) these processes can be accompanied by reversible formation of subsurface oxygen layers: $O_{ads} \Leftrightarrow O_{sub}$. Two different mesoscopic and microscopic analytical tools have been introduced and successfully applied to learn details about the reaction dynamics of CO oxidation at platinum metal surfaces [1,2]. During catalytic reactions the propagation of reaction-diffusion fronts were observed [2]. The purpose of the present work is to investigate the adsorption of O_2 and the reaction of atomic O_{ads} state as well as a subsurface atomic O_{sub} state with CO on the Pd(111), Pd(110) and Pd tip surfaces using TPD, TPRS, FEM and molecular beams (MB). The effect of atomic oxygen preadsorption $^{18}O_{ads}$ on the subsequent low temperature CO+O_2 reaction over Pd(111) surface has been studied. The results obtained with CO oxidation of $^{18}O_{sub}$ over Pd (110) surface have been compared.

Results and Discussion

The Pd surfaces are catalytically active at low temperature CO+O_2 reaction (~ 200 K) due to the ability to dissociate O_2 molecules. The oxygen O_{ads} diffusion process on Pd(110) surface may be proposed for the formation of *subsurface* oxygen layer O_{ss} which is an important intermediate species in CO+O_2 catalytic reaction on palladium surfaces. O_{ads} is highly active in comparison with O_{ss} species due to the rapid attachment of the carbon monoxide molecules, CO_{ads}, producing CO_2. A study of CO oxidation on Pd(111), Pd(110) single crystal surfaces by MB has shown that the oxygen penetration into the subsurface can lead to critical phenomena such as hysteresis, self-oscillations, and chemical waves. The modifying effect of both adsorbed (O_{ads}) and subsurface oxygen (O_{sub}) on the active centres

on the Pd(110) single crystal surface in the $CO+O_2$ reaction has been studied by TDS and TPR. The molecular beam results on the Pd(111) surface demonstrate, that the maximum rate of CO_2 molecules formation is attained on clean metal surface in accordance with our FEM results which were obtained in a narrow zone between O_{ads} and CO_{ads} layers with the highest concentration of empty sites.

Present experimental work shows that the field electron microscope (FEM) can also serve as an in situ catalytic flow reactor. Palladium field emitter expose different *nano* single-crystal planes (111), (100), (110) and (210) with well-defined crystallographic orientations are simultaneously exposed to the reacting gas. These tips were used for the first time as an excellent model for metal supported catalyst to study oscillations in $CO + O_2$ reaction *in situ*. Isothermal, non-linear dynamic processes of the $CO+O_2$ reaction on Pd tip have been studied as well as the formation of face-specific adsorption islands and the mobility of reaction/diffusion fronts. The initiating role of a nanoplanes Pd {110} was established for the generation of local waves on the Pd tip surface. Analysis of Pd surface with a local resolution of ~ 20 Å shows the availability of a sharp boundary between the mobile CO_{ads} and O_{ads} fronts. It has been found that subsurface oxygen formation plays an initiating function in the generation of chemical waves over Pd tip surface. The specificity of the kinetics of $CO + O_2$ reaction has been observed over Pd tip: (i) the maximum initial rate has been observed on the Pd(110); (ii) two spatially separated adlayers are formed on the tip surface. The oxygen layer forms only on the {111}, {110}, {320} and {210} planes, whereas CO_{ads} layer or empty sites forms on the {100} and $\{100\}_{step}$ planes. Chemical waves are O_{ads} and CO_{ads} layers, interacting by a sequence of reaction steps with the reversible-oxygen sites transition of $O_{ads} \leftrightarrow O_{sub}$, which involves the feedback step $O_{sub} \rightarrow O_{ads}$ during oscillations.

The principal result of these studies was that non-linear reaction kinetics is not restricted to macroscopic planes since: (i) the planes ~ 200 Å in diameter show the same non-linear kinetics; (ii) regular waves appear under the reaction rate oscillations; (iii) the propagation of reaction-diffusion waves includes the participation of the different crystal nanoplanes and indicates an effective coupling of adjacent planes.

The experimental movies will complement the presentation.

This work was supported partially by the Grant # 02-03-32568 and by NSF.

References

1. C.S. Gopinath, F. Zaera, J. Catalysis, 200 (2001) 270
2. V.V. Gorodetskii, W. Drachsel, Appl. Catal. A: General, 188 (1999) 267

INTERACTION OF H_2 AND $H_2 + O_2$ MIXTURES WITH $Pt/MoO_3/Mo$ MODEL CATALYSTS

Kalinkin A.V.[1], Pashis A.V.[1], Rodionov S.V.[1], Goodman D.W.[2], Bukhtiyarov V.I.[1]

[1]Boreskov Institute of Catalysis SB RAS, Novosibirsk, Russia
Fax: (+7)-3832343056; E-mail: vib@catalysis.nsk.su
[2]Texas A&M University, College Station, TX, USA

For the last decade, selective oxidation of hydrocarbons by mixture of oxygen and a reducing agent (f.e. hydrogen and carbon monoxide) has attracted an increasing attention of researchers [1-4]. The main advantage of these reactions from those where pure oxygen is used as an oxidant is their proceeding at low temperatures (not higher than 400 K) that decreases considerably the selectivity problems. It has been suggested that a reaction of O_2 with a reducing agent leads to *in situ* generation of a transient species active in the key reaction – selective oxidation of a hydrocarbon. In spite of evident perspectives of such processes, their commercial application is limited by the low yields of valuable products compared to the products of the coupled reaction (water or CO_2). It is evident that further progress in achieving adequate catalyst performance for these reactions requires a more detailed, molecular-level understanding of the nature of active species and the structure of the relevant surface sites.

In light of the notes, we have studied an interaction of $Pt/MoO_3/Mo$ model samples with pure H_2 and with mixtures of H_2 + O_2 using X-ray photoelectron spectroscopy. The designation of *$Pt/MoO_3/Mo$* means that our samples were prepared by oxidation of polycrystalline molybdenum surface (99.99% purity) followed by UHV deposition of platinum on the surface of MoO_3 films (the film depth was about 2-3 nm). The choice of Pt/MoO_3 surfaces as object for our study was based on the results of the catalytic studies mentioned above [1-4]. Platinum is one of precious metals exhibiting good activity for the reactions of interest and MoO_3 is a reducible oxide – reduced cations on surface of a supporting oxide are proposed to be responsible for the formation of the active species. Namely, the formation of the reduced Mo ions depending on Pt particle sizes and on reaction mixture composition was investigated in this work.

It has been shown that interaction of Pt/MoO_3 surface with 5 mbar of H_2 results in reduction of the MoO_3 surface even at room temperature – additional features characteristic of Mo(IV) ions are observed in Mo3d spectra. Kinetic analysis of its accumulation shows that there are two regimes of the reduction. Fast reduction is observed for the small doses (up to 10 minutes), whereas further raising the H_2 dose increases slowly, but constantly the

concentration of the Mo(IV) ions. Most probably, the former regime concerns with the reduction of MoO_3 on the perimeter of the Pt particles, and then the process is spreading on the rest MoO_3 surface. Then, the rate of the latter process is limited by diffusion of hydrogen atoms from the Pt particles on the MoO_3 surface. The fact that molecular H_2 does not affect on the MoO_3 surface is in line with the proposed mechanisms.

It should be however noted that in both regimes the amount of Mo(V) ions remains negligible. As opposed to this, interaction of the $Pt/MoO_3/Mo$ surfaces with $H_2 + O_2$ mixtures produces both Mo(IV) and Mo(V) ions, with their relative population being dependent on the ratio of reagent partial pressures. Only in high access of the hydrogen (H_2/O_2 = 10:1) their concentrations are similar, whereas raising the fraction of oxygen in the mixture decrease relative amount of the Mo(IV) ions. In oxygen-rich mixtures mainly Mo(V) ions are observed in XPS spectra.

Analysis of the Mo3d spectra variation during reduction indicates also that the accumulation of the reduced Mo ions depends on the platinum coverage, or Pt particle sizes. The lower is the coverage, the slower is the reduction. Moreover, decrease in the platinum coverage below critical value, which corresponds to Pt4f/Mo3d intensity ratio of 0.1, makes impossible to observe the reduction using XPS data even in the case of high doses to pure H_2. It has been also shown that no variation in the shape of Pt4f spectra takes place if the Pt coverage is higher than critical. Contrary to this, an additional component with higher binding energy is appeared in the Pt4f spectra, when H_2 interacts with the Pt/MoO_3 samples with platinum coverage below critical. On our opinion, these facts can be explained if we suggest the formation of platinum hydride in the case of small Pt particles. Indeed, the hydride formation should cause a positive shift of the core-level spectra of metallic platinum and may prevent the H_2 molecule from dissociation. As consequence, diffusion of hydrogen atoms and subsequent their participation in the MoO_3 reduction will be impossible. It is obvious that this hypothesis should be checked in future experiments.

This study was supported by CRDF program, grant No. 2331.

References

1. M.G. Clerici and P. Ingallina, Catal. Today, 41 (1998) 351.
2. N.I. Kuznetsova, L.G. Detusheva, L.I. Kuznetsova, M.A. Fedotov and V.A. Likholobov, J. Mol. Catal. A, 114 (1996) 131.
3. M. Lin, A. Sen and J. Am. Chem. Soc. 114 (1992) 7307.
4. T. Miyake, M.Hamada, Y. Sasaki and M. Oguri, Appl. Catal. A: General, 131 (1995) 33.

APPLICATION OF UV-VISIBLE SPECTROSCOPY STUDIES TO MEASURE THE REDOX PROPERTIES OF SUPPORTED VANADIA CATALYSTS FOR THE OXIDATIVE DEHYDROGENATION OF PROPANE

Argyle M.D.[1], Chen K.D.[2], Resini C.[3], Krebs C.[4], Bell A.T.[1], Iglesia E.[1]

[1]Lawrence Berkeley National Laboratory and Department of Chemical Engineering, University of California at Berkeley, Berkeley, USA
E-mail: alexbell@uclink.berkeley.edu, bell@cchem.berkeley.edu
[2]Chevron-Texaco Research and Technology Company, Richmond, USA
[3]University of Genoa, Genoa, Italy
[4]Technical University of Hamburg-Harburg, Hamburg, Germany

UV-visible spectroscopy was used to measure the density of reduced centers in supported metal oxides during propane ODH. Upon reduction, the absorbance of the pre-edge feature increased due to the formation of color centers in the oxide. The number of anionic vacancies associated with an individual cation was determined via temperature programmed oxidation, with results shown in the Fig. 1 inset. The concentration of reduced centers present during propane ODH was then determined by measuring the pre-edge absorbance under reaction conditions. As shown in Fig. 1, the fractional reduction of vanadia dispersed on Al_2O_3 was found to be small (<15%) and increased with increasing C_3H_8/O_2 ratio. The measured reduced center density is consistent with the redox mechanism

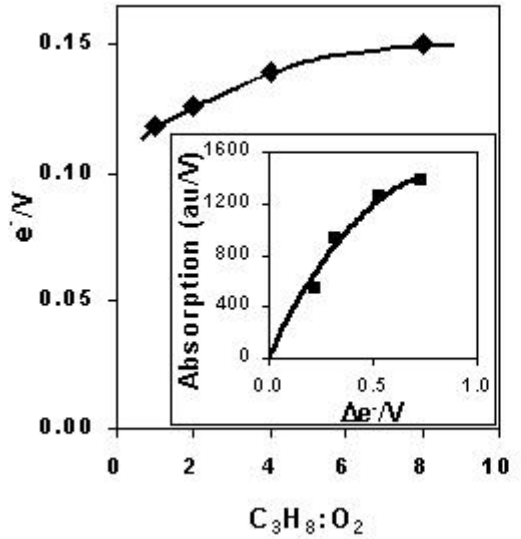

Fig. 1. Extent of reduction of 10 wt% V_2O_5/Al_2O_3 during propane ODH as a function of reactant concentration ratio [603 K, 4.0 kPa C_3H_8, 0.5-4.0 kPa O_2]. Inset: Calibration curve for UV-vis response during H_2 reduction [20 kPa H_2, 603 K] and corresponding electron transfer quantified by subsequent temperature programmed oxidation [5 kPa O_2, 298-773 K].

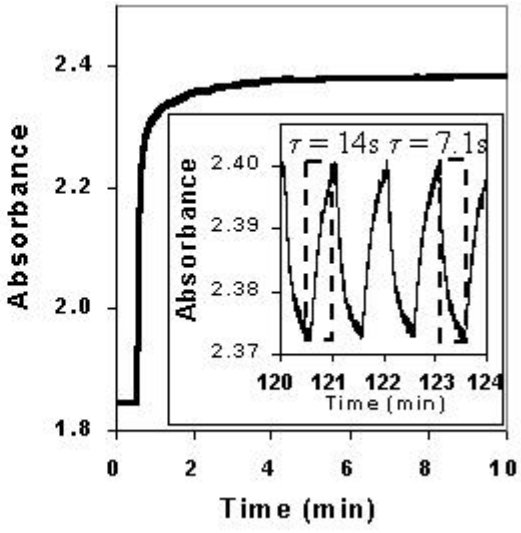

Fig. 2. Change in absorbance of 10 wt% V_2O_5/Al_2O_3 at 1.86 eV during switch from fully oxidized conditions (before 0.5 min) [603 K, 5 kPa O_2] to propane ODH [603 K, 4.0 kPa C_3H_8, 0.5 kPa O_2]. Inset: Transient response during ODH to changes in O_2 concentration [603 K; increasing curves, 4.0 kPa C_3H_8, 0.5 kPa O_2, balance He; decreasing curves, 4.0 kPa C_3H_8, 4.0 kPa O_2, balance He].

(shown in the first column of Table 1) proposed on the basis of isotopic tracer and kinetics studies. The small change in the concentration of reduced centers under dynamic conditions of varying C_3H_8 or O_2 pressure (Fig. 2 inset) compared to the overall number of reduced centers (n_r, proportional to absorbance in Fig 2) permitted linearization of the governing differential equations. The individual rate constants were then evaluated based on the relaxation time, τ (Eq. 1 and 2, with typical values shown in Fig. 2) and are shown in Table 1. Since the UV-visible results provide a direct measure of the active centers involved in C_3H_8 ODH, the fraction of all vanadium atoms in the catalyst active for ODH can be determined by comparison with results obtained from steady-state rate measurements. For the catalyst shown in Table 1, ~70% of the vanadia appears to be participating in the reaction.

$$(n_{r0} - n_r(t))/(n_{r0} - n_{r\infty}) = \exp(-t/\tau) \quad (1)$$

$$\tau = f(K_1k_2, k_3, K_4, k_5, [C_3H_8], [O_2], [H_2O]) \quad (2)$$

Table 1. Mechanism, rate parameters, and fraction of active sites for propane ODH reaction on 10 wt% V_2O_5/Al_2O_3 [603 K, 4 kPa C_3H_8, 0.5 kPa O_2, balance He].

ODH Mechanism	Rate Parameter	Transient Response	Steady State	Fraction active V
$C_3H_8 + O^* \rightleftarrows C_3H_8O^*$ $C_3H_8O^* + O^* \rightarrow C_3H_7O^* + OH^*$	K_1 k_2	$2.5\ 10^{-4}$ [a]	$1.9\ 10^{-4}$ [e]	0.74
$C_3H_7O^* \rightarrow C_3H_6 + OH^*$	k_3	$1.8\ 10^{-2}$ [b]	NA[f]	
$OH^* + OH^* \rightleftarrows H_2O + O^* + *$	K_4	560 [c]	NA[f]	
$O_2 + * + * \rightarrow O^* + O^*$	k_5	104 [d]	NA[f]	

[a]$(s \cdot kPa\ C_3H_8)^{-1}$, [b]$s^{-1}$, [c]$(kPa\ H_2O)^{-1}$, [d]$(s \cdot kPa\ O_2)^{-1}$, [e]$(s \cdot g\text{-atom V} \cdot kPa\ C_3H_8)^{-1}$, [f]Not accessible

UV-Visible spectroscopy was also used to characterize Al_2O_3-, ZrO_2-, and MgO-supported VO_x, MoO_x, WO_x, and NbO_x catalysts used for propane ODH. Each catalyst was also characterized by temperature-programmed reduction. For a given oxide, the propane turnover frequency increases with increasing rate of catalyst reduction by H_2, consistent with the propane ODH redox processes described above. However, for catalysts with different active phases (e.g., VO_x vs. MoO_x), the propane turnover frequency is quite different although these catalysts have a similar H_2 reduction rate. Independent of the active phase involved, the propane turnover frequency increases monotonically with a decrease in the UV-visible absorption edge energy of the active phase. This result suggests that the C-H bond dissociation step involved in the first step of propane activation proceeds via the transfer of single electrons from oxygen atoms to metal centers and that propane turnover frequencies can be inferred from measurements of UV-visible absorption energies.

APPLICATION OF THE NMR MICROIMAGING TO THE IN SITU INVESTIGATION OF CATALYTIC REACTIONS INSIDE CATALYST PELLETS AND GRANULAR BEDS

Koptyug I.V.[1], Lysova A.A.[1,2,3], Kulikov A.V.[2], Kirillov V.A.[2], Sagdeev R.Z.[1], Parmon V.N.[2]

[1]International Tomography Center, Novosibirsk, Russia
[2]Boreskov Institute of Catalysis SB RAS, Novosibirsk, Russia
[3]Novosibirsk State University, Novosibirsk, Russia
Fax: 7 3832 331399, 7 3832 343269;
E-mails: lysova@tomo.ncs.ru, koptyug@tomo.nsc.ru, parmon@catalysis.nsk.su

It has been shown in the last few years that nuclear magnetic resonance (NMR) imaging can be used as a powerful non-destructive method to study *in situ* some physical-chemical processes in porous media, for example, liquid sorption and desorption [1, 2]. It is challenge for scientists to attempt to apply the NMR imaging for the *in situ* investigation of the chemical reactions, especially the heterogeneous catalytic reactions. The most of studies of the catalytic reactions by the NMR imaging refer to the homogeneous Belousov-Zhabotinsky reaction [3, 4].

This reaction is the oxidation of some organic compounds (malonic acid, citric acid) by bromate-anions catalyzed by transition metal ions (Ce(III), Mn(II)). The inherent coupling of molecular diffusion and nonlinear stages of the chemical reaction under certain reagent concentrations gives the possibility for the appearance of the oscillations of the reagent and intermediate concentrations and for the formation of the various spatio-temporal structures. From the point of view of the peculiarity of the NMR imaging the periodic change of the oxidation state of the catalyst ions is essential to detect this process because the oxidized and reduced states of the metal ion have different influence on the relaxation times of the protons of solvent (water).

The NMR imaging was used earlier for the investigation of the Belousov-Zhabotinsky reaction in the homogeneous media, but influence of the medium inhomogeneities on the behavior of the system was not studied by this method before now. Our work shows the possibility to use the NMR imaging to detect and study the peculiarities of the propagation of the chemical waves in the model granular bed imitated the bed of the catalyst grains (fig.1). It is found that the transfer from the homogeneous to heterogeneous reaction medium diminishes the influence of the convective flows of the liquid on the propagation of the wave front and allows to detect the spherical and planar waves propagating in the bed directly *in situ*. Moreover, in the granular bed the chemical wave propagation is shown to be slower in comparison with the homogeneous phase. It is shown experimentally that the wave activity in

the bed is observed only under conditions when the size of the pores between the bed particles is more than certain critical sizes determined by the velocity of planar chemical wave propagation.

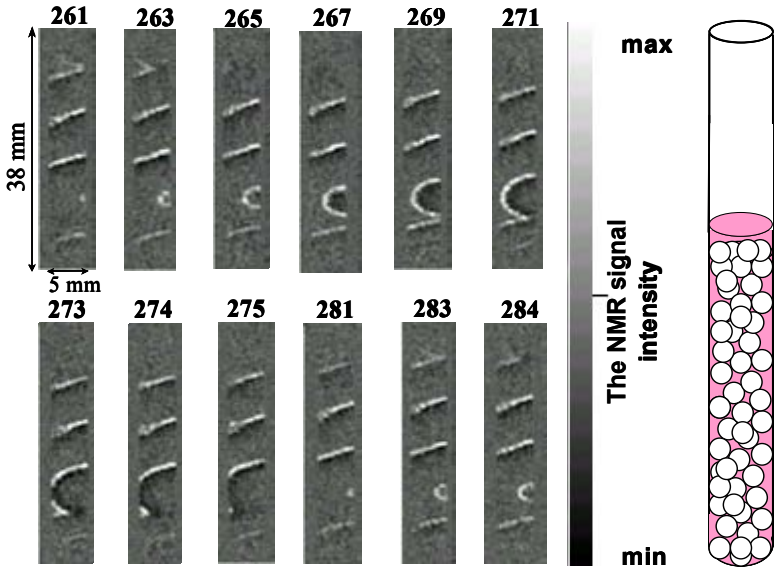

Fig.1. 2D images of the tube filled with the glass particles of 0.5 mm in diameter and the Belousov-Zhabotinsky reaction solution. The starting composition of reaction solution: $[NaBrO_3] = 0.05$ M, $[KBr] = 0.06$ M, $[CH_2(COOH)_2] = 0.15$ M, $[MnSO_4] = 0.0006$ M, $[H_2SO_4] = 0.2$ M, $[H_3PO_4] = 3.0$ M. The spatial resolution was (310×230) μm^2. The detection time of each 2D image was 14.3 s, the whole experiment time was 2 h 1 min 52 s. The number of each image is shown in the figure.

The *in situ* investigations of the real heterogeneous catalytic processes are much more difficult because these processes usually occur in the inner volume of the catalyst grain and are accompanied by the diffusion inside as well as outside the catalyst pellet. Such investigations are possible to perform only by the imaging methods. In our present work we try to use the NMR microimaging for the *in situ* studies of the heterogeneous catalytic reactions with strong exothermic effect (hydrogen peroxide decomposition and α-methylstyrene (AMS) hydrogenation). The NMR imaging allows to obtain for these reactions the images of the liquid phase inside the catalyst grain directly in the course of the catalytic process and thus allows to determine the state of the grain during the reaction.

We have found that the reaction of hydrogen peroxide decomposition at the moderate activity of the used catalysts and the low hydrogen peroxide concentrations occurs only in a thin surface layer. By the use of the NMR flow imaging technique [5, 6] we obtained a spatial map of flow velocities that shows the existence of a convective flow of the liquid along the catalyst grain because of the intensive dioxygen bubble formation on the grain surface and established that the dioxygen molecules are carried by convection rather than diffusion.

Another trend of our work concerning the heterogeneous catalytic reaction of AMS hydrogenation has theoretical as well as practical importance. Many heterogeneous catalytic reactions in industry occur in the reactors with the co-current gas-liquid flow. Such reactors usually work in stationary regimes but under some conditions the appearance of dangerous

critical phenomena such as catalyst overheating, hot spot formation as a result of the occurrence of the exothermic by-pass reactions is possible [7]. The detailed investigation of the peculiarities of the catalyst grain operation in such a type of reactor is necessary to perform to establish the safety conditions of the reactor operation.

We have carried out the experiment to establish the distribution of the liquid phase consisted of the reagent and product inside the catalyst grain under various regimes of the reagent supply in the reactor for the AMS hydrogenation [8, 9].

In particular, fig. 2 shows the subsequent two-dimensional images of the liquid phase redistribution inside the catalyst pellet under conditions of the simultaneous supply of liquid AMS and the hydrogen saturated with AMS vapor to the grain. The area void of signal in the left side of the images is connected with the suppressing of the NMR signal near the thermocouple put inside the pellet to measure the temperature of the pellet in the course of the reaction. The first image shows the existence of the liquid phase inside the grain despite no liquid AMS is supplied to the pellet at this stage, possibly due to adsorption/condensation of AMS and cumene – the product of the reaction – inside the pores. Then before the detection of the second image was started the liquid AMS supply was turned on to the top of the practically dry catalyst pellet. This led to the increase of the liquid content in the grain (image 2). In the upper part of the grain to which liquid AMS is permanently supplied the NMR signal intensity is much higher than in the lower part of the grain. That corresponds to the higher liquid content in the upper part of the grain. The NMR signal intensity is lower in the periphery of the grain. That is bound with the intensive evaporation process that occurs in this part of the grain. The front of evaporation is located inside the catalyst grain and the vapor produced reacts on the non-wetted part of the porous structure. That led to the increase of the grain temperature (3-4). The increase of the liquid AMS supply

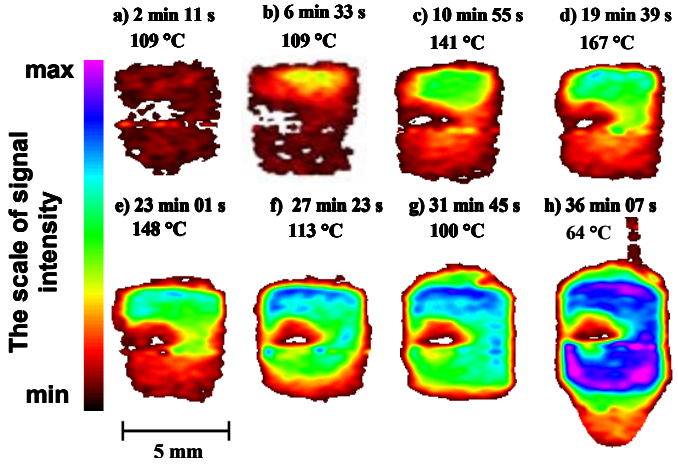

Fig.2. 2D images of the liquid phase distribution inside the catalyst grain of 15% Pt/Al_2O_3 in the process of AMS hydrogenation in the presence of hydrogen saturated with AMS vapor. The flow rate of hydrogen supply was 18.5 $см^3/с$; the temperature of hydrogen stream was 67°C; the liquid AMS supply: a – 0; b,c – $0.43 \cdot 10^{-3}$ g/s; d, e, f – $0.57 \cdot 10^{-3}$ g/s; g, h – $0.71 \cdot 10^{-3}$ g/s. The spatial resolution was (230×140) $мкм^2$; the acquisition time of each image was 4 min 22 s

was made during the detection of the fourth image. As the result the evaporation front moves deeper into the grain and the grain temperature decreases (image 5). In this regime the grain is almost completely filled with liquid phase and narrow front of the evaporation and vapor-phase reaction is located near the lower end of the grain. The front of the liquid phase propagation inside the grain has rough structure because of the intensive evaporation process and hydrogenation process. The liquid-filled area observed in the absence of reaction when no hydrogen gas is supplied has the smooth edges. When the liquid AMS supply was increased to $0.71 \cdot 10^{-3}$ g/s the grain became completely filled with liquid phase.

Therefore, the NMR imaging shows that impregnation of the porous catalyst with liquid reagent under conditions of the simultaneous endothermic reagent evaporation and its exothermic vapor-phase hydrogenation can lead to the formation inside the pellet of two domains with strongly different liquid phase content: the upper part of the grain completely filled with liquid phase and the lower part of the grain which is almost dry and filled with the vapor where the vapor-phase hydrogenation occurs.

The work was supported by grants of the Russian Foundation for Basic Research (02-03-32770, 00-15-97446, 00-15-97450) and of the Siberian Branch of the Russian Academy of Sciences (Integration project #46). A.A. Lysova gratefully acknowledges a scholarship awarded by the Zamaraev International Charitable Scientific Foundation.

References:

[1] I.V. Koptyug, V.B. Fenelonov, L.Yu. Khitrina, R.Z. Sagdeev, V.N. Parmon, J. Phys. Chem. B, 102 (1998) 3090.
[2] I.V. Koptyug, S.I. Kabanikhin, K.T. Iskakov, V.B. Fenelonov, L.Yu. Khitrina, R.Z. Sagdeev, V.N. Parmon, Chem. Eng. Sci., 55 (2000) 1559.
[3] A. Tzalmona, R.L. Armstrong, M. Menzinger, A. Cross, C. Lemaire, Chem. Phys. Lett., 174, (1990) 199.
[4] Y. Gao, A.R. Cross, R.L. Amstrong, J. Phys. Chem., 100, (1996) 10159.
[5] I.V. Koptyug, L.Yu. Ilyina, A.V. Matveev, R.Z. Sagdeev, V.N. Parmon, S.A. Altobelli, Catal. Today, 69 (2001) 385.
[6] E. Fukushima, Ann. Rev., 31 (1999) 95.
[7] A.V. Kulikov, N.A. Kuzin, A.V. Shigarov, V.A. Kirillov, A.E. Kronberg, K.R. Westerterp, Catal. Today, 66 (2001) 255.
[8] I.V. Koptyug, A.V. Kulikov, A.A. Lysova, V.A. Kirillov, V.N. Parmon, R.Z. Sagdeev, J. Amer. Chem. Soc., 124 (2002) 9684.
[9] I.V. Koptyug, A.V. Kulikov, A.A. Lysova, V.A. Kirillov, R.Z. Sagdeev, V.N. Parmon, Dokl. Akad. Nauk, 385 (2002) 205.

PROBING ELECTRONIC STATE OF Pt AND ALLOYING METALLIC COMPONENTS IN ALUMINA-SUPPORTED Pt-Cu CATALYSTS WITH FTIR SPECTROSCOPY OF ADSORBED $^{13}C^{18}O+^{12}C^{16}O$ ISOTOPIC MIXTURES

Borovkov V.Yu.[1], Kolesnikov S.P.[1], Kovalchuk V.I.[2], d'Itri J.L.[2]

[1]Zelinsky Institute of Organic Chemistry RAS; Moscow, Russia
Fax: (8-095) 135-53-28; E-mail: borovkov@ioc.ac.ru.
[2]Department of Chemical Engineering, University of Pittsburgh, Pittsburgh, USA

It is commonly recognized that electronic interactions between different metals can influence the catalysis of bimetallic surfaces [1]. One of the most convenient ways to probe the electronic state of Group VIII noble metals, particularly Pt, is to measure the singleton frequency of adsorbed CO and its shift due to dipole-dipole interaction between neighboring CO molecules. The singleton frequency is indicative of electronic state of the adsorption site [2], whereas the dipole-dipole shift provides information about the size of the ensemble of adjacent identical atoms [3].

With the isotopic dilution method, isotopic $^{13}C^{16}O+^{12}C^{16}O$ mixtures are commonly used for spectroscopic investigations of bulk [2,3] and supported [4] metals at saturation CO coverage. There is ~50 cm^{-1} difference in the frequencies of the $^{13}C^{16}O$ and $^{12}C^{16}O$ vibrations; thus, no dipole-dipole shift arises from vibrational interaction between neighboring $^{13}C^{16}O$ and $^{12}C^{16}O$ molecules adsorbed on the metallic surface [1]. Therefore, the position of the IR band for adsorbed $^{13}C^{16}O$ at very low concentrations, when each $^{13}C^{16}O$ molecule on the metal surface is surrounded by only the $^{12}C^{16}O$ molecules, corresponds to the singleton frequency. The difference between the band position at monolayer coverage of the $^{13}C^{16}O$ and its singleton frequency is the dipole-dipole shift arising from the dipole-dipole coupling between adsorbed $^{13}C^{16}O$ molecules. However, the strong intensity redistribution between the IR bands of adsorbed $^{13}C^{16}O$ and $^{12}C^{16}O$ molecules [4-6] does not allow precise determination of the band positions when the surface concentration of $^{13}C^{16}O$ is low.

To probe the electronic state of Pt in alumina-supported Pt-Cu catalysts, isotopic mixtures of $^{13}C^{18}O$ and $^{12}C^{16}O$ were used instead of $^{13}C^{16}O$ and $^{12}C^{16}O$. It was shown that the singleton frequency and dipole-dipole shift can be determined in one experiment with very low concentration of $^{13}C^{18}O$ in the $^{13}C^{18}O+^{12}C^{16}O$ mixture, because of absence of intensity redistribution between IR bands of adsorbed $^{13}C^{18}O$ and $^{12}C^{16}O$. In addition, the alloying of Pt and Cu in the Pt-Cu catalysts was probed based on analyses of CO adsorption with and without the gas phase.

Experimental

The catalysts were prepared by pore volume impregnation of γ-Al_2O_3 (Vista-B, 300 m^2/g, average pore diameter, 55 A) with aqueous solutions containing $H_2PtCl_6 \cdot 6H_2O$ or a mixture of $H_2PtCl_6 \cdot 6H_2O$ and $CuCl_2 \cdot 2H_2O$. The concentrations of the metals in the impregnating solutions were adjusted to obtain metal loadings of 3.0% for Pt/Al_2O_3, 3.0% Pt + 3.0% Cu and 3.0% Pt + 6% Cu for the two $Pt\text{-}Cu/Al_2O_3$. The bimetallic catalysts had Pt/Cu atomic ratios of 1:3 and 1:6, respectively. The self-supporting catalyst wafers (~20 mg/cm^2 thick) were pretreated *in situ* by evacuating at 623 K for 1 h, then heating in flowing H_2 to 623 K at the rate of 5 K min^{-1} and holding at this temperature for 1 h. Then, the gas phase was evacuated at 623 K for 1 h to a pressure of 1×10^{-5} Torr.

The infrared spectra were recorded with a Research Series II FTIR spectrometer (Mattson, Inc) equipped with a liquid N_2 cooled MCT detector. The IR cell with a volume of 200 cm^3 was similar to that described elsewhere [7]. The dipole-dipole coupling frequency shifts and singleton frequencies of CO adsorbed on the catalyst were measured by the isotopic dilution method [1] with mixtures of $^{13}C^{18}O$ (Isotec, 99+% ^{13}C, 95+% ^{18}O) and $^{12}C^{16}O$ (Praxair, 99.99+%) of different compositions. Initially, a mixture of known composition was adsorbed on the pretreated sample at ambient temperature and an equilibrium pressure of 12 Torr. After 20 min the spectrum of adsorbed CO in the presence of gas phase was recorded. The gaseous CO was evacuated at the same temperature for 20 min and the spectrum of adsorbed CO was recorded in the absence of gas phase. Then the catalyst wafer was exposed to a $^{13}C^{18}O$+$^{12}C^{16}O$ mixture of different composition. By repeating the procedure while systematically changing the composition of the isotopic mixture, the spectra of adsorbed CO as a function of $^{13}C^{18}O$+$^{12}C^{16}O$ mixture composition were determined.

It was shown that addition of a $^{13}C^{18}O$+$^{12}C^{16}O$ mixture into the IR cell results in a fast isotopic equilibration between adsorbed and gaseous CO molecules. This is important, because the dependence between band position for the adsorbed isotopic CO molecules and the composition of the gas phase $^{13}C^{18}O$+$^{12}C^{16}O$ mixture is determined using a catalyst surface already covered with adsorbed CO when the next $^{13}C^{18}O$+$^{12}C^{16}O$ mixture is introduced into the IR cell. Hence, the composition of the adsorption layer is initially different than that of the gas phase. However, because the number of gaseous CO molecules in the IR cell significantly exceeded the number of Pt atoms in the wafer, it is reasonable to assume that the composition of adsorbed layer would be the same as to that of gaseous $^{13}C^{18}O$+$^{12}C^{16}O$ mixture added after an equilibrium between gas phase and surface is reached. Thus, the ratio of isotopes in the gas phase was used to approximate that on the catalyst

surface. It was also shown that for CO linearly adsorbed on Pt the effect of the intensity redistribution between the bands of adsorbed $^{13}C^{18}O$ and $^{12}C^{16}O$ is weak. Without the intensity redistribution, it was possible to analyze spectra of adsorbed $^{13}C^{18}O$ at the concentrations in the $^{12}C^{16}O$+$^{13}C^{18}O$ mixture of few percents.

Results and Discussion

Analyses of the $^{13}C^{18}O$ band position vs. concentration of the $^{13}C^{18}O$ molecules in the $^{13}C^{18}O$+$^{12}C^{16}O$ mixture indicated that the dipole-dipole interaction between $^{13}C^{18}O$ molecules linearly adsorbed on Pt could be detected only at the concentrations higher than 10%. Therefore, at lower concentrations the band position of linearly adsorbed $^{13}C^{18}O$ corresponds to the singleton frequency. The singleton frequencies of adsorbed $^{13}C^{18}O$ and $^{12}C^{16}O$ measured at very low and very high concentrations of $^{13}C^{18}O$, respectively, differed by 100 cm^{-1}, similar to that for gaseous $^{13}C^{18}O$ and $^{12}C^{16}O$ molecules. The same difference in the IR band positions was observed for the $^{13}C^{18}O$ and $^{12}C^{16}O$ adsorbed on the metal at saturation surface coverage. Thus, the dipole-dipole shifts and singleton frequency for linearly adsorbed CO molecules can be calculated with high accuracy in an experiment with a $^{13}C^{18}O$+$^{12}C^{16}O$ mixture that contains less than 10% of the $^{13}C^{18}O$. The band position for the $^{13}C^{18}O$ in this case will be the singleton frequency. At the same time, the band position for $^{12}C^{16}O$ reduced by 100 cm^{-1} will give the $^{13}C^{18}O$ band position at saturation coverage, the value needed for the dipole-dipole shift calculation.

The IR spectra of adsorbed $^{13}C^{18}O$ at very low concentrations in the $^{13}C^{18}O$+$^{12}C^{16}O$ mixture indicated that for the Pt/Al_2O_3 catalyst there are two types of sites that adsorb CO in linear mode with singleton frequencies of 1945 cm^{-1} and 1965 cm^{-1}. An increase in the $^{13}C^{18}O$ concentration leads to the enhancement of the dipole-dipole coupling between $^{13}C^{18}O$ molecules and an intensity redistribution between low- and high-frequency absorption bands. This indicates that these sites are located in close vicinity to each other. The band at 1965 cm^{-1} is completely removed after evacuation of the catalyst wafer at room temperature for 20 min. Probably, the existence of such weakly adsorbed CO on Pt is a result of repulsive interaction between CO molecules at very high metal surface coverage [2,3]. This interaction can lead to an increase in C=O bond vibration frequency as well as to a decrease in the heat of CO adsorption [2,3]. In the absence of the gas phase and low concentration of the $^{13}C^{18}O$ in the $^{13}C^{18}O$+$^{12}C^{16}O$ mixture, the spectrum of $^{13}C^{18}O$ linearly adsorbed on metallic Pt consists of a single absorption band at 1945 cm^{-1}, which is shifted by 35 cm^{-1} to higher wavenumbers

as the $^{13}C^{18}O$ concentration in the $^{13}C^{18}O$+$^{12}C^{16}O$ mixture approaches 100% (dipole-dipole shift).

The $^{13}C^{18}O$ adsorbed on Pt in the Pt-Cu/Al_2O_3 catalyst with Cu/Pt atomic ratio of 3 is characterized by singleton frequency of 1945 cm^{-1} in the absence of gas phase $^{13}C^{18}O$+$^{12}C^{16}O$ mixture. This frequency is the same as for the Pt/Al_2O_3 catalyst. However, the dipole-dipole shift for the adsorbed $^{13}C^{18}O$ was 20 cm^{-1}, 15 cm^{-1} lower than for the Pt/Al_2O_3. This decrease suggests smaller Pt ensembles in the Pt-Cu/Al_2O_3 catalyst compared to that for the Pt/Al_2O_3. In the presence of the gaseous $^{13}C^{18}O$+$^{12}C^{16}O$ mixture the singleton frequency of adsorbed $^{13}C^{18}O$ shifted to lower wavenumbers by 5 cm^{-1}, indicating the influence of CO weakly adsorbed on Cu on the electronic state of Pt.

At higher relative Cu content in the Pt-Cu/Al_2O_3 catalyst (Cu/Pt = 1:6), the singleton frequencies for the $^{13}C^{18}O$ adsorbed on Pt in linear mode were found to be 1926 and 1940 cm^{-1} in the absence and in the presence of the gaseous $^{13}C^{18}O$+$^{12}C^{16}O$ mixture, respectively. As evacuation of the Pt-Cu catalyst with pre-adsorbed CO results in removing adsorbed CO only from Cu, the difference in the $^{13}C^{18}O$ singleton frequency for Pt of ~15 cm^{-1} with and without gas phase provide evidence that Pt and Cu are located next to each other. Only with adjacent Pt and Cu atoms would the electron withdrawing ability of CO adsorbed on Cu affect the frequency of CO adsorbed on Pt, suggesting alloying Pt and Cu. The dipole-dipole shifts of the $^{13}C^{18}O$ band measured in the absence or presence of gaseous $^{13}C^{18}O$+$^{12}C^{16}O$ were essentially the same (15 cm^{-1}) viz. 20 cm^{-1} lower than that of CO adsorbed on monometallic Pt/Al_2O_3 catalyst.

The further insight into probing electronic state of Pt and alloying the metallic components of the alumina-supported Pt-Cu catalysts with FTIR spectroscopy of the adsorbed $^{13}C^{18}O$+$^{12}C^{16}O$ isotopic mixtures will be given in the presentation.

References

1. Rodrigues, J.A. and Goodman, D.W., *J. Phys. Chem*., 95 (1991) 4196.
2. Hammaker, R.M., Francis, S. and Eischens, R.P., *Spectrochim. Acta.*, 21 (1965) 1295.
3. Crossley, A. and King, D.A., *Surf. Sci*., 68 (1977) 528.
4. Toolenaar, F.J.C.M., Stoop, F. and Ponec, V. *J. Catal.*, 82 (1983) 1.
5. Shpiro, E.S., Tkachenko, O.P., Jaeger N.I., Schulz-Ekloff G. and Grunert W., *J. Phys. Chem*., B 102 (1998) 3798.
6. Persson, B.N.J. and Ryberg, R., *Phys. Rev*., B 24 (1981) 6954.
7. Deshmukh, S.S., Borovkov, V.Yu., Kovalchuk V.I. and d'Itri J.L., *J. Phys. Chem.*, B 104 (2000) 1277.

APPLICATION OF RADIOISOTOPIC TECHNIQUE FOR THROUGHPUT SCREENING OF Co(Ni)Mo/Al_2O_3 SULFIDE CATALYSTS FOR HDS

Kogan V.M.

Zelinsky Institute of Organic Chemistry RAS, Moscow, Russia
E-mail: vmk@ioc.ac.ru

Why do we develop the method of radioisotopic screening?

The demand for new and more effective catalysts for the oil processing industry is growing. Reasons for this are: first, it has become necessary to use heavier fractions for processing and, second, processed products must meet strict ecological requirements. Among a vast range of possible combinations of catalytic systems it is sometimes difficult to select the right one for the given process. In industry only pilot plant tests remain as a way to select the best catalyst for given process so far. Every test takes long time and is very consuming.

The radioisotopic method for screening of hydrodesulfurization (HDS) catalysts developed during the last decade [1-7] is very informative, relatively inexpensive and it takes about 5-6 hours to test one catalyst sample. The method can be applied as a pre-selection step to reduce the number of commercial catalysts for further pilot plant testing and as a way to investigate dynamics of the active sites of newly designed catalysts and to forecast their catalytic properties depending on reaction conditions and the nature of crude.

What is the radioisotopic screening of sulfide catalysts like?

Catalysts of various composition labelled by ^{35}S during sulfidation are tested in the thiophene HDS reaction. In the course of the reaction over a CoMo sulfide catalyst labelled by ^{35}S, some part of the sulfur of the catalyst (mobile sulfur, equal to surface SH groups) is replaced by thiophene sulfur and leaves the catalyst surface in the form of H_2S. For catalyst tests, pulse microcatalytic technique with radiochromatographic analysis of the products is used. Mathematical treatment of the experimental curves (Fig. 1) allows us to approximate the dependencies obtained by exponential equations of the following type: $\alpha = \sum A_i exp(-\lambda_i x)$. From the equation it is possible to estimate catalyst sulfur amount (in mg) that can participate in H_2S formation (mobile part of sulfur) on the sites of the type *i*:

$$S_i = \frac{32}{22.4 \times 100} \int_0^\infty B_i \exp(-\lambda_i x) dx \ .$$

If conversion is known, it is possible to estimate the site productivity $P_i = 2.84 \times 10^{-3} \gamma \lambda_i$, where γ is thiophene conversion and λ_i is the order of magnitude in the equation of H_2S MR.

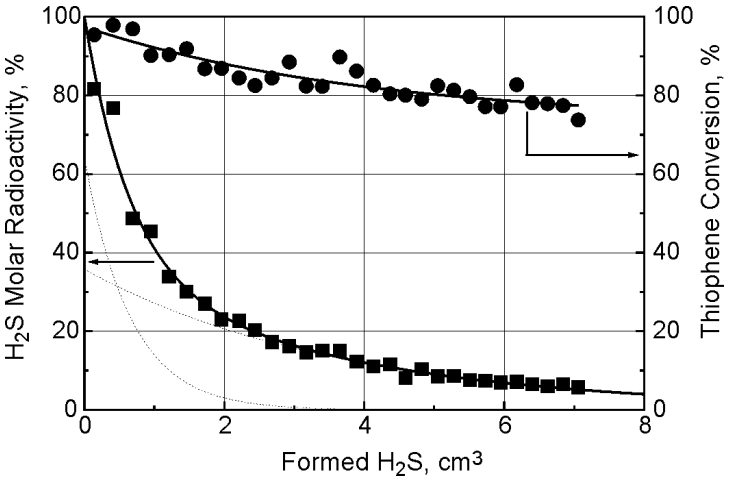

Fig. 1. Dependencies of MR of H_2S and thiophene conversion on the amount of H_2S formed in the course of the thiophene HDS over sulfidized-^{35}S $CoMo/Al_2O_3$ catalyst.

The amount of mobile sulfur in sulfide catalysts depends on the composition of the catalyst. Two types of HDS active sites containing mobile sulfur have been found - "rapid" and "slow". The amount of sulfide catalyst mobile sulfur, in its turn, depends on catalyst composition and sulfidizing technique. An original “forcing out” mechanism of thiophene HDS has been suggested [1, 5-7].

In the course of systematic radioisotopic tests of sulfided CoMo catalysts in the HDS of thiophene the effects of catalyst composition and the nature of the feed on the number, distribution and functioning of the active sites of these catalysts have been studied. A method to estimate the ratio between surface SH groups and coordinatively unsaturated sites (CUS) has been put forward [6]. The CUS, that directly participate in the reaction, *i.e.* on which thiophene molecules are adsorbed and react, are named “functioning vacancies”, or, simply, vacancies (V) and those that do not - “empty sites” (ES). Thus, $\sum CUS = \sum V + \sum ES$ (Fig. 2).

Since in promoted catalysts surface SH groups are not uniform and are differentiated into “rapid” and “slow” according to their mobility, anion vacancies should also be divided into those linked to “rapid” and “slow” SH groups (V_r and V_s respectively). When thiophene is adsorbed on V_r, H_2S is formed with the participation of a “rapid” SH group; when on V_s - with the participation of a “slow” SH group. After H_2S is formed, the vacancy of the same type is formed and the balance between “rapid” and “slow” active sites is not broken. The total of vacancies is the sum of “rapid” and “slow” vacancies: $\sum V = \sum V_r + \sum V_s$. It has been shown that the CoMo catalyst activity is determined not only by the number of SH groups and their mobility, but also by the number of the vacancies for thiophene adsorption.

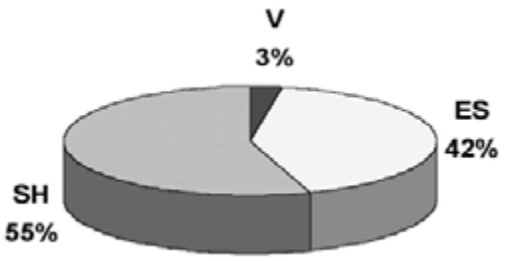

Fig. 2. Distribution of active sites and SH groups on an active phase surface of 8 % Mo/Al_2O_3 sulfide catalysts. **SH** – surface SH groups; **V** – functioning vacancies, **ES** – "empty sites" (explanations are given in the text).

On the basis of the obtained data, general conditions for the formation and functioning of active sites due to the nature of crude have been formulated and criteria to evaluate the efficiency of catalyst functioning have been formulated:

- If it is necessary to hydrodesulfurize light molecules, catalysts with the highest activity of the "rapid" sites should be preferred. In this case the catalyst composition would be determined by the area of Co and Mo concentrations limited by the highest density of V_r vacancies.If heavy oils are subjected to HDS, the catalysts with the most favorable conditions for the sites of the "slow" type would be most efficient, and the number of these sites and the density of V_s vacancies should be as high as possible.The comparison of the radioisotopic data and the results of pilot plant tests confirms a crucial role of the vacancies in catalysis by sulfides in the course of HDS and proves the correctness of our supposition about the criteria for selecting catalysts for HDS of different types of crude.

How have radioisotopic screening data been applied?

Regularities described above were used for pre-selection of commercial catalysts for HDS of light and heavy oil fractions, catalyst design for hydrotreatment of residuals and the investigation into the mechanism of poisoning of CoMo sulfide catalysts by basic N-containing compounds.

It has been found that catalyst poisoning by basic N-containing compounds results in a larger share of the active phase surface covered by SH groups and in a smaller number of functioning vacancies. As a result, some effective approaches to increase poison resistance of catalysts have been developed.

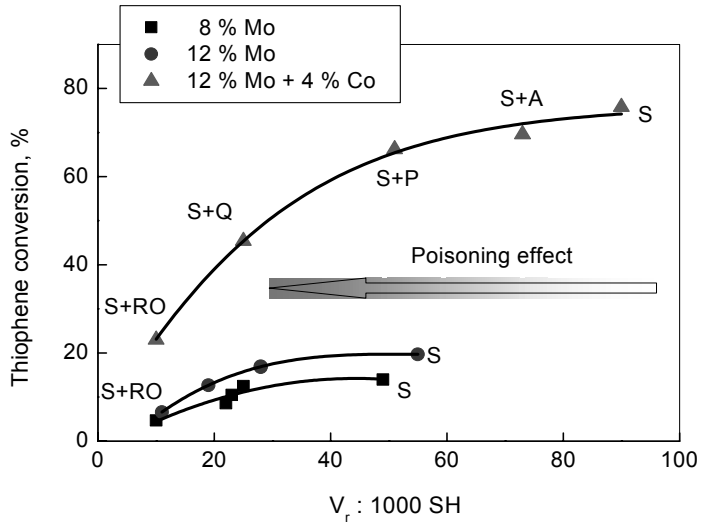

Fig. 3. Thiophene HDS conversion over (Co)Mo/Al_2O_3 catalysts treated by N-containing compounds during sulfidation vs. V_r density (V_r : 1000 SH groups ratio). S - sulfidation without poisoning; S + A -sulfidation in the presence of aniline; S + P - sulfidation in the presence of pyridine; S + Q - sulfidation in the presence of quinoline; S + RO - sulfidation in the presence of residual oil.

In the course of the wide range radioisotopic screening of alumina- and silica supported NiMo, CoMo Co, Ni and CoNi catalysts some crucial dependencies between catalyst composition, carrier support, the number, type and productivity of active sites, and catalyst functioning under of West-Siberian petroleum hydrotreating conditions have been found [4]. The results obtained have permitted us to determine an optimal catalyst composition for a definite refining process and to design some cheap Mo free CoNi catalysts-adsorbents for preliminary treating of heavy crudes.

References

1. G. V. Isagulyants, A. A. Greish, and V. M. Kogan, in M. J. Philips and M. Ternan (eds), *Proc. 9th Int.Congress on Catalysis*, Calgary, 1988, Ottawa, Ontario, Canada, (1988) vol. **1**, P.35.
2. G. V. Isagulyants, A. A. Greish, and V. M. Kogan, *Catal. Lett.,* **6** (1990) 157.
3. V. M. Kogan, Nguen Thi Dung, and V.I. Yakerson, *Bull. Soc. Chim. Belg.,* **104** (1995) 303.
4. V. M. Kogan, and N. M. Parfenova, in: "*Hydrotreating and hydrocracking of oil fractions*" (G. F. Froment, B. Delmon and P. Grange eds.), Elsevier Science B.V. (1997), P. 449.
5. V. M. Kogan, in: "*Transition Metal Sulfides. Chemistry and Catalysis*", (T. Weber, R. Prins, R. van Santen eds.), NATO ASI Series, Kluwer Academic Publishers, 1998, vol. **60**, P.235.
6. V. M. Kogan, N. N. Rozhdestvenskaya, I. K. Korshevets*, Appl. Catal. A: Gen*., **234** (2002) 207.
7. V. M. Kogan, *Appl. Catal. A: Gen*., **237** (2002) 161.

FTIR STUDY OF STERIC EXCITATIONS AT SURFACES

Storozhev P.Yu.[1], Otero A.C.[2], Turnes Palomino G.[2], Tsyganenko A.A.[1]

[1]Fock Institute of Physics, St. Petersburg State University, St. Petersburg, Russia
Fax: 4287240; E-mail stor@photonics.phys.spbu.ru
[2]Departamento de Química, Universidad de las Islas Baleares, Palma de Mallorca, Spain

The paper reports recent results of application of FTIR spectroscopy for studies of "sterically excited" surface species, i.e. adsorbed complexes that have non-optimal geometry and, hence, have certain extra energy stored as the energy of isomerization. Such species co-exist in a thermodynamic equilibrium with those normally present at the surface, at least in some temperature interval. Possible role of sterical excitation in catalysis is discussed.

The existence of sterically excited states was first reported and extensively studied for CO adsorbed on cationic sites in zeolites [1, 2]. IR spectroscopic measurements at variable temperatures provided evidence that this molecule forms with extra-framework cations not only carbon-bonded, but also oxygen-bonded adducts. The two species account for two IR bands of C–O stretching vibrations. The high-frequency (HF) band belongs to the more stable C-bonded species, while the weak LF band is due to O-bonded adducts that are energetically less preferable but co-exist with common adsorption due to the thermal excitation.

Later on, FTIR studies at low temperatures provided evidence that CO manifests the same amphipathic ability in hydrogen bonding with bridged acidic Si(OH)Al groups of zeolites [3], and with silica silanol groups [4] forming both OH···CO and OH···OC species.

The energy of isomerization between the two forms of CO adsorption could be estimated from the intensity ratio of LF and HF bands. More precise values can be derived from the temperature dependence of the ratio presented in the form of van't Hoff plots. The obtained values are summarized below in the table 1. Simultaneous pressure measurements enable the isosteric heat of adsorption to be obtained.

Table 1
The positions of HF and LF bands of adsorbed CO as well as experimental and theoretically estimated values of CO-OC isomerization energy for various adsorbents

Adsorbent	Reference	ν_{HF} (cm^{-1})	ν_{LF} (cm^{-1})	$\Delta\nu$(cm^{-1})	ΔH^{o}_{exp} (kJ/mol)	ΔE_{theor} (kJ/mol)
Li-ZSM-5	[7]	2195 2188	2100 2110	95 80	6,5 5,6	4,9 4,1
Na-ZSM-5	[1, 2]	2178	2112	66	3,8	3,4
K-ZSM-5	[8]	2166	2117	49	3,2	2,5
Rb-ZSM-5	[9]	2162	2119	43	1,8	2,2
Cs-ZSM-5	[9]	2157	2122	35	-	1,8
H-ZSM-5	[10]	2175	2112	63	4,2	3,2
H-Y	[3]	2173	2124	49	4,3	2,5
Na-Y	[2]	2171	2122	49	2,4	2,5
Ca-Y	[5]	2197 2191	2094 2099	103 92	11 8	5,3 4,7
Sr-Y	[6]	2191 2187	2095 2098	96 89	9,8 7,6	4,9 4,6
SiO_2	[4]	2154	2131	23	2	1,2
Silicalite	[4]	2160	2122	38	3	2,0

For Ca-Y, Sr-Y and Li-ZSM-5 zeolites [5-7], interaction of two CO molecules with the same cation was established. In this case, formation of M(CO,OC) species with one O-bonded molecule also occurs, where mutual interaction between the two ligands strongly affects the energetic parameters and IR spectra of the system. The same, but slightly weaker effect on the CO-OC equilibrium can be brought about by coadsorbed N_2.

Interaction of CO with a cation or OH group can be described by a simple electrostatic model, where the frequency shift is considered as a manifestation of the vibrational Stark effect for a molecule in the electric field of a point charge or of a dipole. The model explains the existence of two stable states and well reproduces the experimentally measured enthalpy of CO - OC isomerization, as could be seen from comparison of two right columns of table 1.

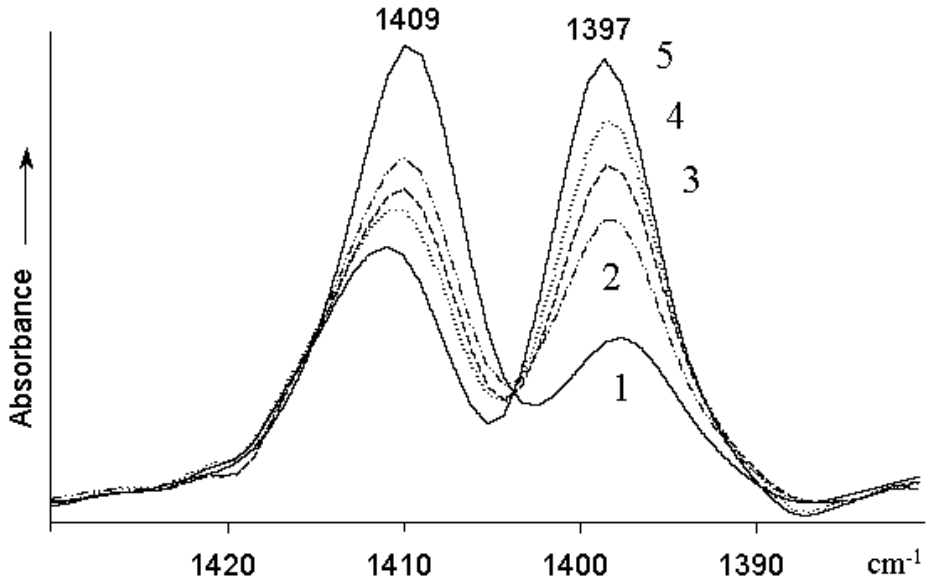

Figure 1. IR spectra of the thiophene adsorbed on silica before (1) and after addition of SO_2 (2-5), at 55 K (1, 2), 98 K (3), 112 K (4) и 138 K (5)

Our recent data show that thiophene adsorbed on silanol groups or on acidic hydroxyls of zeolites can also form two kinds of complexes with the same surface site, bonded via sulphur atom or π–electrons. The two species have two distinct IR bands at 1409 and 1397 cm^{-1}, respectively (see figure). Besides, thiophene can interact with oxygen atom of silanol group as an acid that also contributes into the intensity of the 1409 cm^{-1} band. In the presence of coadsorbed SO_2 this form of adsorption is suppressed, and one can see the intensity redistribution between the two bands with the temperature, demonstrating higher stability of the H-bond via π-electrons (band at 1397 cm^{-1}).

These examples demonstrate the capability of FTIR spectroscopy to detect thermally activated 'sterically' excited states with unusual orientation of the molecule with respect to the adsorption site. However, formation of different energetically inequivalent species has been established not only for molecular adsorption. Dissociative adsorption of HD on ZnO leads as well to two structures, OH-ZnD and OD-ZnH, inequivalent due to different zero-point energies. The two structures co-exist at 300 K or higher, but at low temperatures the equilibrium is frozen because of the high activation energy of isomerization.

On the other hand, it is well possible that, on molecular adsorption, isomerization inside the molecule could be favored by the surface, and less stable isomers could be formed due to thermal activation with their further desorption or reaction with other molecules. Thus, sterically activated species should be considered as intermediates of catalytic reactions and the energy of isomerization could be the activation energy of an elementary step. In the case

of CO, unusual geometry of O-bonded species with positively charged carbon atom should affect their chemical properties and enhance reactivity towards other molecules. The energy of isomerization between the two CO species that, according to our data, could be as high as 12-15 kJ/mol. This value is comparable with the activation energy of some catalytic reactions, such as CO oxidation on oxide catalysts, and we believe that notion on steric activation is important enough for understanding the detailed mechanism of different catalytic processes. Experiments on the reactivity of sterically excited surface species are in the course.

References

[1] Otero Areán C., Tsyganenko A.A., Escalona Platero E., Garrone E. and Zecchina A., *Angew. Chem. Int. Ed.,* 37 (1998) 3161

[2] Tsyganenko A.A., Escalona Platero E., Otero Areán C., Garrone E. and Zecchina A., *Catal. Lett.,* 61 (1999) 187

[3] Otero Areán C., Tsyganenko A.A., Manoilova O.V., Turnes Palomino G., Peñarroya Mentruit M., Garrone E., *J. Royal Soc. Chem., Chem. Commun.,* 2001, 455

[4] Storozhev P.Yu., Otero Areán C., Garrone E., Ugliengo P., Ermoshin V.A., Tsyganenko A.A., *Chem. Phys. Lett.,* Submitted

[5] Tsyganenko A.A. *In: Aspects of the Surface Chemistry of Oxidic Systems. A one-day symposium honouring the memory of Estrella Escalona Platero. Turin. Edizioni Libreria Cortina,* Torino, 1999, 51

[6] Garrone E., Bonelli B., Tsyganenko A. A., Rodriguez Delgado M., Turnes Palomino G., Manoilova O.V., Otero Areán C., *J. Phys. Chem. B.*, 106 (2002) .

[7] Otero Areán C., Manoilova O.V., Rodriguez Delgado M., Tsyganenko A.A. Garrone E., *Phys. Chem. Chem. Phys.,* 3 (2001) 4187

[8] Manoilova O.V., Peñarroya Mentruit M., Turnes Palomino G., Tsyganenko A.A., Otero Areán C., *Vibrational Spectroscopy*, 26 (2001) 107

[9] Otero Areán C., Turnes Palomino G., Tsyganenko A.A., Garrone E., *Int. J. Mol. Sci.*, 3 (2002) 764

[10] Turnes Palomino G., Peñarroya Mentruit M., Tsyganenko A. A., Escalona Platero E., Otero Areán C., *Studies in Surface Sci. and Catalysis*, *Elsevier,* v.135 (2001), 219

ESR STUDY OF NANOCRYSTALLINE AEROGEL-PREPARED MAGNESIUM OXIDE

Heroux D.S.[2], Richards R.M.[2], Volodin A.M.[1], Bedilo A.F.[1,2], Chesnokov V.V.[1], Zaikovskii V.I.[1], Klabunde K.J.[2]

[1]Boreskov Institute of Catalysis SB RAS, Novosibirsk, Russia
[2]Department of Chemistry, Kansas State University, Manhattan, Kansas, USA

Nanotechnology in its various manifestations is one of the fastest developing fields of science nowadays. Nanocrystalline metal oxides prepared via a sol-gel route from the corresponding alkoxides have small average crystallite sizes (4-8 nm), unusual crystallite shape, superior adsorption and catalytic properties.[1-3] Aerogel-prepared (AP) alkaline earth metal oxides have been shown to be efficient destructive sorbents in reactions with halogenated hydrocarbons, hazardous compounds and air pollutants containing phosphorous, sulfur, etc. Nanocrystalline MgO can be transformed in the reaction with 1-chlorobutane into $MgCl_2$ that acts as an effective catalyst for 1-chlorobutane dehydrohalogenation.[3,4] Recently high surface area AP-MgO has been demonstrated to be an effective support for synthesis of vanadia-magnesia catalysts for oxidative dehydrogenation of light alkanes.[5,6]

However, due to their enhanced hydrophilicity in all such reactions as well as during the period of storage before use, nanocrystalline alkaline earth metal oxides are rapidly deactivated in the presence of water vapor and CO_2. One of the possible ways to improve the hydrophobic properties of these materials is the formation of an “intelligent” carbon coating. Such coating will act as a hydrophobic barrier partially protecting the core metal oxide from water adsorption and conversion to magnesium hydroxide. However, destructive adsorption reactions can still proceed on the metal oxide surface, as evidenced by dehydrochlorination of 2-chloroethylethylsulfide (2-CEES) and 1-chlorobutane.[7] Meanwhile, the overall stability of the material in the presence of water vapor is significantly improved in comparison with non-coated nanocrystalline MgO.

High surface area metal oxides are known to exhibit acid and/or basic properties, depending on the nature of the metal cation. These are usually associated with surface low-coordinated ions as Lewis sites and surface OH groups as Bronsted acid sites. For nanoparticles in the size range of 2-10 nm the percentage of such coordinatively unsaturated sites is especially high. So, their properties and contribution to the reactivity of the nanoparticles as destructive adsorbents or catalysts have to be carefully evaluated.

Ion pairs with low coordination numbers can be found at corners, edges, or high Miller index surfaces. Ion pairs with different coordination numbers appear to correspond to basic

sites of different strength, so that M^{2+}_{3C}-O^{2-}_{3C} ion pair is most basic and most reactive.[6] At the same time such sites adsorb water and carbon dioxide most strongly making high pretreatment temperatures necessary for their removal. As a result, the nature of basic and acid sites varies with the severity of the pretreatment conditions for most heterogeneous oxide catalysts.

The present communication reports the results of a comprehensive ESR study of nanocrystalline aerogel-prepared MgO and carbon-coated MgO involving a variety of ESR approaches successfully used earlier for characterization of catalytic materials prepared by conventional methods.[8-10]

In addition to a typical Mn^{2+} signal present as an impurity in most MgO samples, two more species were detected in the spectrum of AP-MgO (Fig. 1). The first signal (**A**) is an easily saturated singlet (g = 2.0025, $\Delta H \cong 0.5$ G) with a Gaussian line shape. This signal dominates the spectra registered at low microwave power. An increase of the microwave power to 3 mW results in a significant decrease in its intensity, and it can hardly be seen in the spectrum registered at 48 mW. The concentration of sites observed in the form of signal **A** in the initial AP-MgO is about 2 x 10^{16} g^{-1}. The other signal (**B**) is a three-component spectrum (g = 2.0033, A^H = 18 G) with 1:2:1 ratio in the intensities of the components. This signal is not saturated as easily as signal **A** and is observed best at the microwave power 1-3 mW. The concentration of sites **B** is about 1 x 10^{16} g^{-1}.

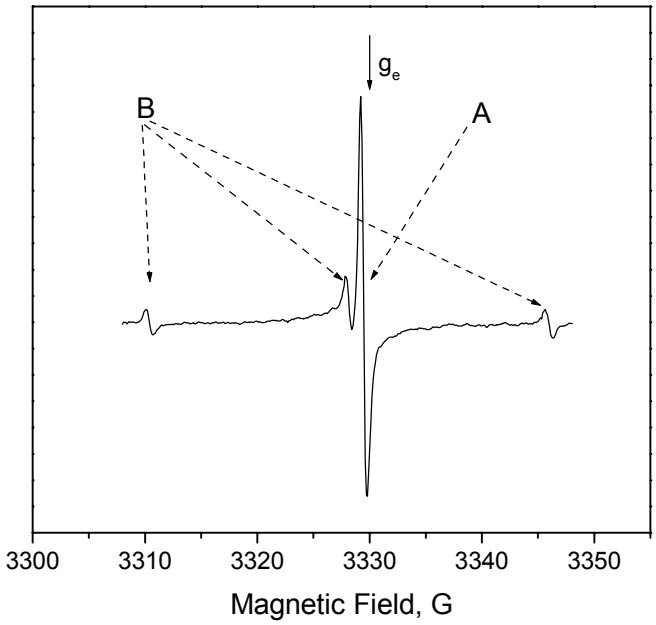

Signal **B** can be attributed to radical fragments -O-$^{\bullet}CH_2$ stabilized at the places of contact between the nanocrystals. The formation of such radicals can be expected for samples prepared from methanol solutions that are known to contain significant amounts of residual methoxyl groups on the surface of the nanocrystals. The parameters of

their spectra are similar to those of $^{\bullet}CH_2OH$ radicals in solution.[11] It is notable that all radicals observed in AP-MgO have isotropic ESR spectra both at room temperature and at 77 K. This fact can be attributed to fast rotation of the -O-$^{\bullet}CH_2$ fragment around the O-C bond. While the radicals have very high thermal stability under vacuum, heating in the presence of air at 400°C or higher temperatures appears to result in the oxygen diffusion into the places of contact between the nanocrystals and disappearance of the spectra.

Strong Lewis acid and basic sites on the surface of AP-MgO were characterized using the adsorption of 2,2,6,6-tetramethyl-4-oxo-1-oxyl-pyperidine (TEMPONE) and dinitrobenzene (DNB), respectively. These techniques are known to detect only strong sites of each type that are most reactive. Such sites have been identified on AP-MgO after heat treatment at 400°C or higher temperature that was required to remove any accumulated water or other adsorbed surface species. The concentrations of the Lewis acid and basic sties were determined to be $3.0 \pm 0.5 \times 10^{18}$ and $2.5 \pm 0.3 \times 10^{18}$ sites/g, respectively.

To study the effect of the carbon coating on the concentration of basic sites determined by the dinitrobenzene adsorption, samples with the carbon loadings of 1.2, 3.2, 5.0, 10.0 and 15.9 wt.% were prepared by coking AP-MgO with butadiene used as a source of carbon. The results are summarized in Table below.

% C	Coke peak width	DNB peak height	# sites (g^{-1})	% MgO sites
0	-	9.5	2.26E+18	100
1.2	5.0 G	6.1	1.88E+18	83
3.2	3.5 G	4.1	1.73E+18	65
5	3.6 G	2.7	9.60E+17	42
10	2.8 G	0.7	2.35E+17	10
15.9	1.9 G	0	0	0

The ESR spectra of carbon-coated samples showed singlets with g close to 2.0023 typical for coke on catalytic materials. The intensity of the peak grew with the increase of the carbon loading, while its width was getting smaller. Since the intensity of the coke signal for samples with significant amounts of carbon was much higher than that of the DNB signal, the concentrations of basic sites on the surface of carbon-coated samples were evaluated from the area of the leftmost hyperfine component in the spectrum of the nitroxyl radicals formed from dinitrobenzene. The results of our experiments indicate that about 40% of strong basic sites were still open in the sample with 5 wt.% carbon. Therefore, this sample can be expected to exhibit considerable reactivity in reactions typical for nanocrystalline MgO. Meanwhile, 15.9% carbon was enough to suppress the formation of radicals from DNB completely.

Hence, this sample is very unlikely to have any reactivity in the destructive adsorption and catalytic reactions. Thus, ESR with DNB used as a spin probe offers an alternative very effective technique for evaluation of the effect of carbon coating on the reactivity of nanocrystalline alkaline earth metal oxides.

Acknowledgement

This study has been supported by the U.S. Army Research Office, CRDF (Project RC1-2340-NO-02) and the Russian Foundation for Basic Research (Grant 03-03-33178).

References

1. S. Utamapanya, and J. R. Schlup, *Chem. Mater.*, 1991, **3**, 175.
2. K. J. Klabunde, J. V. Stark, O. B. Koper, C. Mohs, D. G. Park, S. Decker, Y. Jiang, I. Lagadic and D. Zhang, *J. Phys. Chem.,* 1996, **100**, 12142.
3. V. B. Fenelonov, M. S. Mel'gunov, I. V. Mishakov, R. M. Richards, V. V. Chesnokov,
4. A. M. Volodin and K. J. Klabunde, *J. Phys. Chem. B,* 2001, **105**, 3937.
5. I. V. Mishakov, A. F. Bedilo, R. M. Richards, V. V. Chesnokov, A. M. Volodin, V. I. Zaikovskii, R. A. Buyanov and K. J. Klabunde, *J. Catal.,* 2002, **206**, 40.
6. C. Pa, A. T. Bell and T. D. Tilley, *J. Catal*. 2002, **206**, 49.
7. V. V. Chesnokov, A. F. Bedilo, D.S. Heroux, I. V. Mishakov and K. J. Klabunde, *J. Catal*., 2003, in press.
8. A.F. Bedilo, M.J. Sigel, O.B. Koper, M.S. Melgunov and K.J. Klabunde, *J. Mater. Chem.,* 2002, **12**, 3599.
9. T. A. Konovalova, A. M. Volodin, V. V. Chesnokov, E. Paukshtis and G. V. Echevskii, *React. Kinet. Catal. Lett.,* 1991, **43**, 225.
10. A. M. Volodin, V. A. Bolshov and T. A. Konovalova, *Molec. Eng.,* 1994, **4**, 201.
11. A. M. Volodin, *Catal. Today*, 2000, **58**, 103.
12. R. Livingston and H. Zeldes, *J. Chem. Phys.,* 1966, **44**, 1245.

MESOSTRUCTURED MIXED METAL OXIDES FOR PARTIAL OXIDATION OF LOWER ALKANES

Carreon M.A.[1], Guliants V.V.[1], Pierelli F.[2], and Cavani F.[2]

[1]Department of Chemical and Materials Engineering, University of Cincinnati, Cincinnati, USA
E-mail: Vadim.Guliants@uc.edu, vguliant@alpha.che.uc.edu
[2] Dipartimento di Chimica Industriale e dei Materiali, Bologna, Italy

Introduction

Since the discovery of M41S family of silicate mesoporous molecular sieves [(1,2)], there has been great interest in the preparation of M41S-type non-silicate phases. Transition metal oxides are particulary attractive because of their interesting catalytic properties. Mesostructured transition metal oxides of antimony [(3)], molybdenum [(4)] and vanadium [(5)] have been prepared. However, the template removal from these phases resulted in the collapse of mesostructure. Recently, we reported [(6,7)] the novel synthesis of mesostructured vanadium-phosphorus-oxide (VPO) phases displaying improved thermal stability, desirable chemical compositions and pore structures for the partial oxidation of n-butane. We report here the catalytic properties of mesostructured VPO phases in n-butane oxidation to maleic anhydride, as well as disclose novel synthesis of mesostructured multicomponent Mo-V-M-O (M=Nb and Te) oxides promising for selective oxidation of propane to propylene and oxygenates.

Mesostructured lamellar, hexagonal and cubic vanadium-phosphorus-oxides were prepared by employing cationic (alkyl ammonium bromides), anionic (sulfonates and phosphonates) and alkylamine surfactants. In a typical synthesis, an aqueous solution containing the phosphorus and vanadium sources was added to an aqueous surfactant solution. The pH of the resultant solution was adjusted with HCl. The obtained sol was precipitated with NH_4OH and stirred for additional 24 hours. The resultant slurry was filtered, washed with deionized water and dried. Detailed synthesis conditions are described elsewhere [(6,7)].

The complete surfactant removal and preparation of thermally stable mesoporous mixed metal oxides systems are challenging. We have found that it was possible to remove most of the surfactant occluded in the mesopores by a two-step post-synthesis method, which led to the formation of microporous mesostructured phases. In the proposed method, fresh VPO phases were Soxhlet-extracted in toluene to remove the surfactant (3-7 days) and then thermally activated in nitrogen atmosphere at 673-723 K for 8 hours. The post-treated samples largely retained the original mesostructure as confirmed by the presence of a well-defined XRD peak at *d*-spacing ~3.85 nm. The bulk composition by ICP was P/V ~ 1.08

which is optimal for selective catalytic oxidation of n-butane. Nitrogen adsorption measurements of these post-treated samples showed the type I isotherms with a hysteresis loop characteristic of microporous phases with slit-shaped pores and specific surfaces areas in the 55-250 m^2/g range. It is important to mention that the surface areas reported for conventional VPO phases are in the 15-25 m^2/g range. The creation of microporosity in mesostructured VPO phases can be attributed in great extent to the Soxhlet extraction process. It has been previously demonstrated that post-synthesis treatments such as steaming and hydrothermal treatment can lead to the creation of microporosity in the walls of various mesostructured systems [8,9]. To the best of our knowledge, these mesostructured bulk mixed metal oxides displaying improved thermal stability have been prepared for the first time. These microporous mesostructured VPO phases are promising for the partial oxidation of n-butane. These novel phases displayed ~40 mol. % selectivity to maleic anhydride at 400 ^oC and ~70 mol. % selectivity at 460 ^oC and 20% n-butane conversion.

This self-assembly method was employed to synthesize other mesostructured mixed metal oxides, such as Mo-V-M oxides (where M= Nb and Te) promising for the partial oxidation of propane. In a typical preparation, an aqueous solution of niobium oxalate, ammonium metavanadate, ammounium heptamolybate and telluric acid was mixed with an aqueous surfactant solution and allowed to react for 24-48 h. The mesostructured lamellar and hexagonal phases obtained were filtered, washed with deionized water, and dried. These mixed metal oxide phases displayed promising catalytic properties in selective propane oxidation to propylene and acrylic acid.

References

1. C.T. Kresge, M.E. Leonowicz, W.J. Roth, J.C. Vartulli, J.S. Beck, *Nature,* 359 (1992) 710.
2. J.S. Beck, J.C. Vartulli, W.J. Roth, M.E. Leonowicz, C.T. Kresge, K.D. Schmitt, T.W. Chu, D.H. Olson, E.W. Sheppard, S.B McCullen, J.B. Higgins, J.L. Schlenker, *Journal of The American Chemical Society,* 114 (1992) 10834.
3. D.M. Antonelli, *Microporous and Mesoporous Materials,* 30 (1999) 315.
4. G.G. Janauer, A. Dobley, J. Guo, P. Zavalij, M.S. Whittingham, *Chemistry of Materials,* 8 (1996) 2096.
5. V. Luca, J.M. Hook, *Chemistry of Materials,* 9 (1997) 2731.
6. M.A Carreon, V.V.Guliants, *Studies in Surface Science and Catalysis,* 141 (2002) 301.
7. M.A. Carreon, V.V. Guliants, *Microporous and Mesoporous Material,s* 55 (2002) 297.
8. M.S. Wong, J.Y. Ying, *Chemistry of Materials,* 10 (1998) 2067.
9. M. Imperor-Clerc, P. Davidson, A. Davidson, *Journal of The American Chemical Society,* 122 (2000) 11925.

ANOMALOUS DESORPTION OF OXYGEN FROM TUNGSTEN AND ITS EXPLANATION BY LATERAL INTERACTIONS AND MIGRATION OF OXYGEN ADATOMS

Savkin V., Bychkov V., Kislyuk M.

Semenov Institute of Chemical Physics RAS, Moscow, Russia
Fax: (095)938-2156; E-mail: Savkin@polymer.chph.ras.ru

Several unusual phenomena were observed in TPD experiments performed for oxygen adsorbed layers on polycrystalline tungsten [1]. Similar effects were observed by Madix with co-workers for O/Pt (100) [2] and N/W (100) [3].

Fig.1a demonstrates the TPD spectra of oxygen atoms observed after O_2 adsorption at 300 K and various expositions leading to various initial surface concentrations of oxygen adatoms from Θ=0,21 (1) to Θ=1 (7). The calculations of the desorption rate constant gave the values of the activation energy $E_{des.}$=310±50 kJ/mol and the preexponential factor $k^o = 10^7$-10^9 s^{-1}.

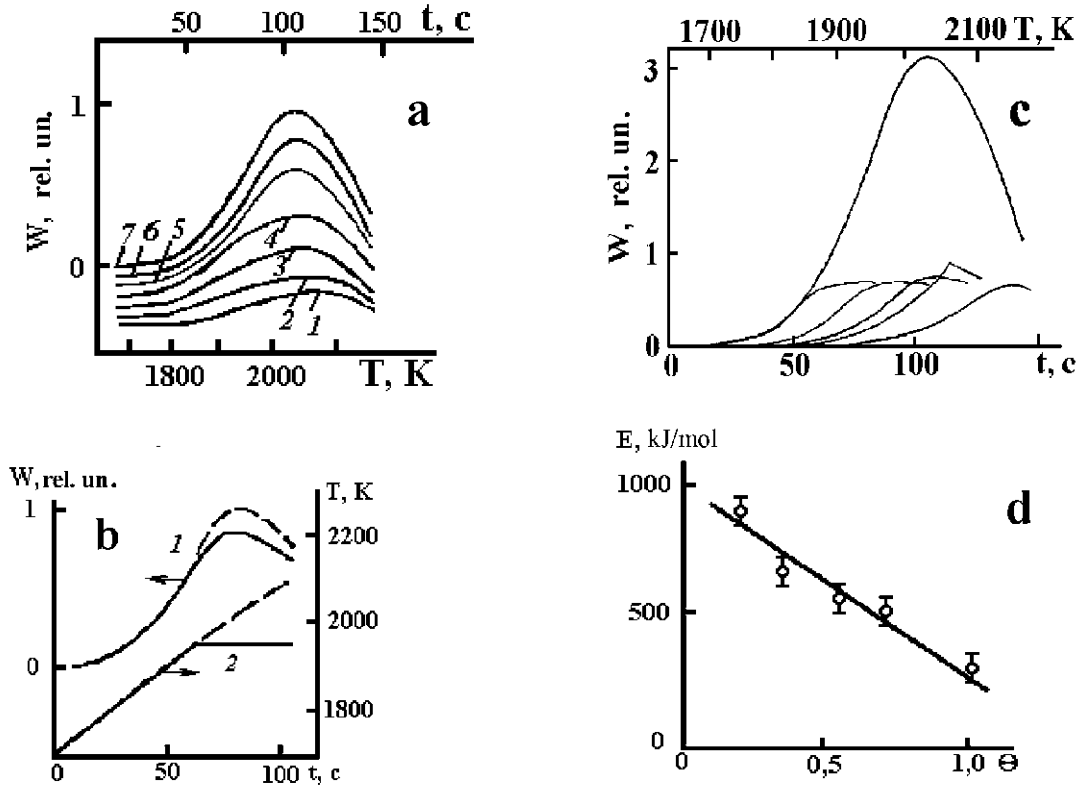

Fig. 1. Experimental results [1].

Fig. 1b shows the desorption kinetic curve obtained under the transition from linear heating of the sample to isothermic conditions. One can see that desorption rate still increases when temperature is constant. Only later it passes throw maximal value and then decreases.

This fact is in the contradiction with the classic kinetic theory, which describes the desorption rate by the equation

$$W_{des.} = -d\theta/dt = k^{o}\theta^{n}\exp(-E_{des.}/RT), \quad (1)$$

where: θ is a surface coverage by the adsorbate and **n** is a kinetic order of the desorption. At any values of **n > 1** and constant temperature (**T**) the equation (1) gives the desorption rate as a decreasing function of time (**t**).

Fig. 1c demonstrates the results of another type of TPD experiments where we used several cycles "heating-isothermal-cooling" (HIC) for initially saturated adlayer of oxygen atoms (lover curves). The upper shows the TPD spectrum from the saturated adlayer. One can see that these results drastically differ from those shown at Fig. 1a. The maxima of the TPD curves (Fig. 1a) are situated at about the same positions 2030-2090 K and correspond to the effective activation energy about 310 kJ/mole. The HIC experiments show the consecutive shift of the TPD curves to higher temperatures. As a result, the effective activation energy, calculated from the initial parts of the curves (Fig. 1c), increases from 280 to 880 kJ/mol (see Fig. 1d).

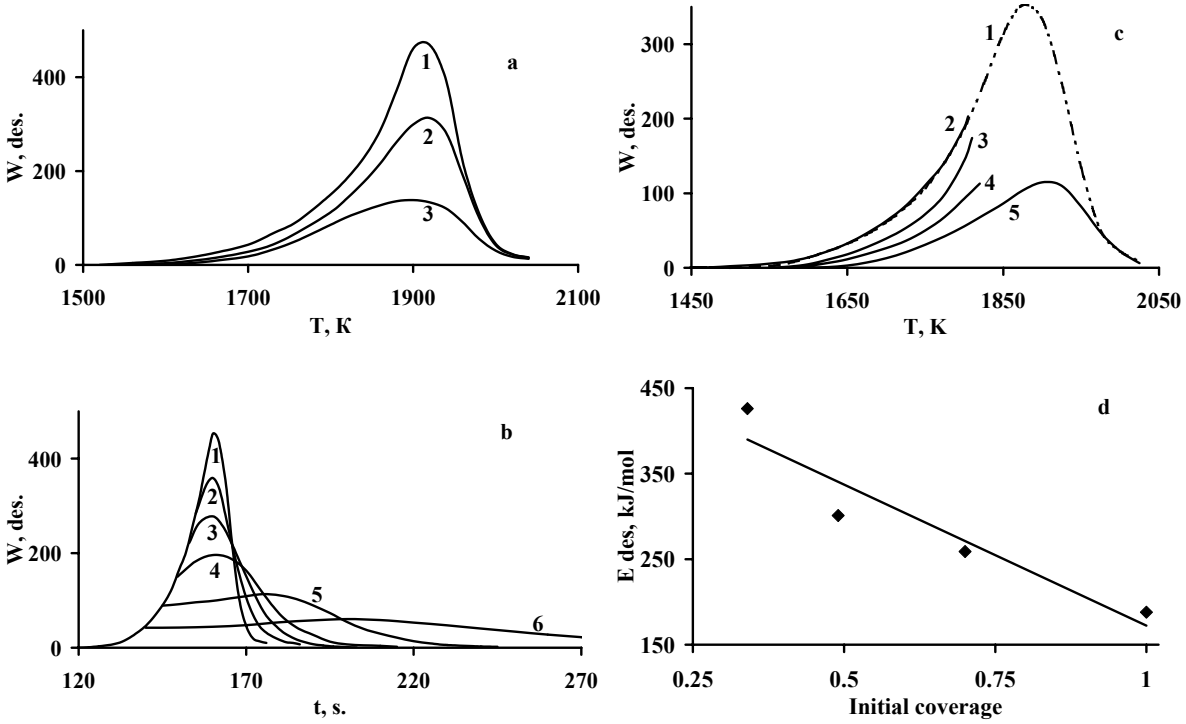

Fig. 2. Model calculations

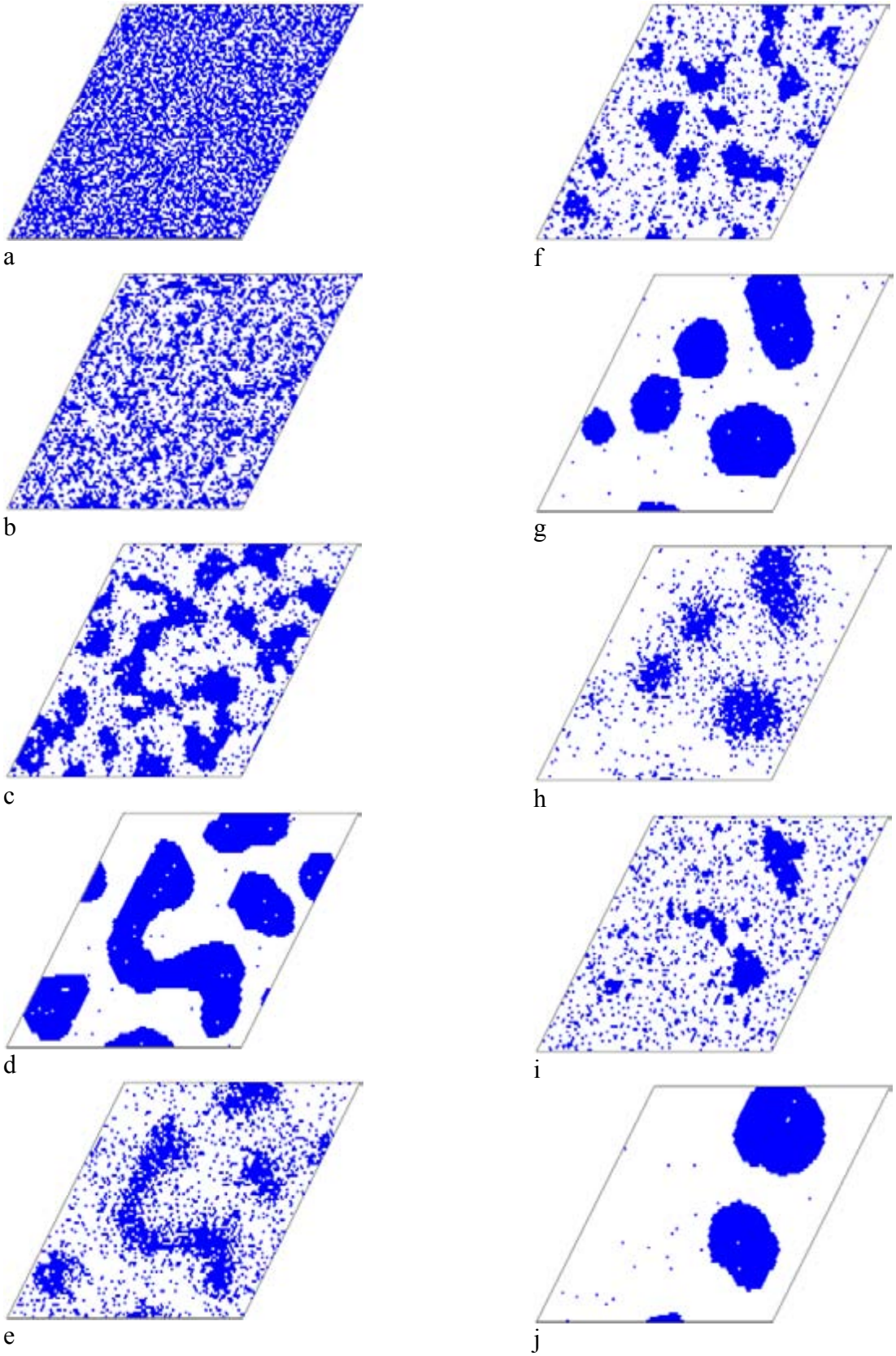

Fig. 3. Visual maps of the adsorbed layer

Each of the observed unusual effects (isothermal maxima (Fig. 1b), the shift of kinetic curves to higher temperatures (Fig. 1c) and the corresponding growth of the effective activation energy (Fig. 1d) at HIC experiments) may be explained individually [1-3].

We attempted to explain all the results by a model taking into account the surface migration of oxygen adatoms and their lateral interactions with each other. For this aim we used Monte Carlo simulation at the area W(110) 100×100 or 200×200 active cites. We assumed an attractive interaction of each O-adatom with any oxygen adatom, situated at the six nearest neighboring positions. According to [4] we considered the ratio $E_{des.}/E_{mig.}= 3$ between the desorption and migration activation energies of oxygen adatoms.

For fitting the calculated kinetic curves to the experimental ones we varied the values of k^o, $E_{des.}$, E_{mig}, and the attractive potential of the lateral interactions. The results are shown in Figs. 2a-2d. A comparison of these figures with Figs.1a-1d shows almost a quantitative agreement between the model and experiment. Figs. 3a-3j demonstrate the rearrangement of the adsorbed layer during HIC experiments, corresponding to Fig. 2c.

The model can be improved by taking into the consideration the lateral interactions with next nearest neighboring adatoms.

The present work was supported by the Russian Foundation for Basic Research, project No 02-03-33097

References.

[1] Savkin V. V., Kislyuk M. U., and Sklyarov A. V., *Kinetika i kataliz*, 29 (1988) 168.
[2] Barteau M. A., Ko E. I., Madix R. J., *Suface Sci*, 102 (1981) 99.
[3] Lee J., Madix R. J., Schlaegel J. E., Auerbach D. J., *Suface Sci*, 143 (1984) 626.
[4] Kislyuk M. U., *Kinetika i kataliz*, 40 (1999) 803.

MOLECULAR DESIGN AND CHARACTERIZATION OF CATALYSTS FOR NOx SELECTIVE REDUCTION BY HYDROCARBONS IN THE OXYGEN EXCESS BASED UPON ULTRAMICROPOROUS ZIRCONIA PILLARED CLAYS

Sadykov V.[1], Kuznetsova T.[1], Doronin V.[1], Moroz E.[1], Ziuzin D.[1], Kochubei D.[1], Novgorodov B.[1], Kolomiichuk V.[1], Alikina G.[1], Bunina R.[1], Paukshtis E.[1], Fenelonov V.[1], Derevyankin A.[1], Matyshak V.[2], Lunin V.[3], Rozovskii A.[4], Tretyakov V.[4], Burdeynaya T.[4], Ross J.[5]

[1]Boreskov Institute of Catalysis SB RAS, Novosibirsk Russia
E-mail: sadykov@catalysis.nsk.su
[2]Semenov Institute of Chemical Physics, Moscow, Russia
[3]Chemical Department of Lomonosov Moscow State University, Moscow, Russia
[4]Topchiev Institute of Petrochemical Synthesis RAS, Moscow, Russia
[5]Limerick University, Limerick, Ireland

Introduction

Clays pillared by nanosize zirconia particles (Zr PILC) are promising supports and catalysts for different petrochemical processes [1-2] and selective catalytic reduction of NO_x by hydrocarbons in excess oxygen [3]. Their performance strongly depends upon the size, shape and structure of nanosized zirconia pillars propping the alumosilicate layers, which are in turn determined by the properties of zirconium hydroxy polycations in pillaring solutions. However, such data are scares, which limits possibilities for molecular design of those systems.

In this work, to cover such a gap, approaches for controlling the size and structure of pillaring polynuclear zirconium hydroxospecies in solution was developed. It is based on tuning composition of solutions (concentrations of Zr and modifying Ca, Sr, Ba cations), time and temperature of aging. SAXS and EXAFS were applied to monitor evolution of pillaring species in solution. To elucidate their further rearrangement after pillaring into montmorillonite clay followed by calcinations, X-ray structural analysis, EXAFS, UV-Vis and FTIRS of adsorbed CO were used. By comparing those results with data obtained for bulk ultradispersed zirconias, specificity of nanosized zirconia oxides structure was thus revealed.

The effect of the pillars size and shape on Zr PILC structure (the inner arrangement of pillars and pores within crystallites) and texture (a type of crystallites packing into aggregates) was studied by using a new method based upon analysis of combined XRD and high resolution nitrogen absorption data in the frames of a geometrical model [4].

Approaches for supporting of transition metal cations (Cu) and precious metals (Pt) on nanosized pillars were elaborated, and their properties were elucidated using TEM, EXAFS, SAXS, ESR, UV-VIS, TPD/TPR and FTIRS of adsorbed CO/NO molecules. Specificity of

copper cations coordination in those systems is explained by their strong interaction with nanosized zirconia pillars.

Catalytic properties of these systems were characterized in the reactions of NO_x selective reduction in the excess of oxygen by propane, propylene and decane.

Results and discussion

Structure of pillaring species in solution and their control. The analysis of the particle size distribution by SAXS data revealed that in fresh diluted solutions of pure zirconium salts polynuclear zirconium hydroxocomplexes are mainly represented by species with typical sizes in the range of 15-30 Å. They are comprised of several Zr_4 tetramers stacked into nanorods. The EXAFS data confirm preservation of the parent Zr_4 structure in those species characterized by the next typical distances and coordination numbers (CN): Zr-O - 2.21 Å (CN 7), Zr-Zr - 3.34 Å (CN 0.8), Zr-Zr - 3.67 Å (CN 1) and Zr-Zr - 4.91 Å (CN 0.8). It implies a weak interaction (mainly through the hydrogen bonds) between stacked tetramers.

In aged solutions especially in those aged at 80 ^oC, the tetrameric units appear to be bound stronger, which is reflected in pronounced distortion of their structure. In this case, only two distances: Zr-O - 2.19 Å (CN 7) and Zr-Zr - 3.52 Å (CN 0.8) are revealed in the EXAFS spectra. These features can be tentatively explained by a structure of nanorods in which consecutively stacked Zr_4 units are rotated by 45 degrees relative to each other to ensure their connection by bridging OH groups formed by condensation of terminal OH groups situated at the vertexes of tetramers. The existence of sheet-like structures could not be excluded as well.

In pure solutions of zirconium salts, a part of zirconium hydroxocomplexes is aggregated into large (typical diameters in the range of 60-200 Å) colloidal particles. The addition of alkaline-earth cations into solutions helps to partly suppress formation of those particles not affecting appreciably the structure of nanorods, only slightly decreasing Zr-O and Zr-Zr coordination numbers. Some increase of nanorods mean sizes (up to 45 Å) was observed as well. As alkaline-earth cations are found to be completely removed from the pillared clays at the washing stage, it suggests that in solutions, they are located at the external surface of nanorods being coordinated by terminal hydroxyls or water molecules chemically bound with Zr cations of tetramers. Such an interaction explains a higher distortion of the tetramer structure leading to decrease of EXAFS coordination numbers (in aged solutions, in the presence of alkaline-earth cations, Zr-O CN are in the range of 6.6-6.3, while Zr-Zr CN are in the range of 0.7-0.3). The lowest coordination numbers were found for Sr-containing

solutions, and the highest - for solutions with added calcium chloride. Some variation in the structure of polynuclear species in the presence of different alkaline earth cations as suggested by these results can be tentatively explained by the difference in the hydration sphere of the latter cations in water solutions. Thus, for Ca the nearest sphere is comprised of regular octahedron, for Ba it is elongated octahedron, while for Sr it is a square antiprism. It can be speculated that Sr cations are included within the polynuclear species affecting the mode of their polymerization and condensation at aging.

Structure of nanosized zirconia pillars in clays. In the initial clay washed by the diluted HCl solution with the pH value 2.2 equal to that in pillaring solutions and then calcined at 400 ^{o}C, the basal (001) spacing was found to be ~ 11 Å (9.6 Å being the reference value for completely dehydrated parent montmorillonite). The mean particle size in the (001) direction was around 40 Å. After pillaring, washing and calcination at 400 ^{o}C, for all samples containing ~ 20 wt.% of zirconia prepared using optimized solutions and pillaring procedures, the basal spacing was increased up to ~ 18 Å, while the particle size remains rather constant (~ 30 Å), suggesting that pillaring has not caused the clay exfoliation. These results imply that for all samples studied here, the mean gallery height is around 7 Å. This value corresponds to the normal orientation of tetrameric units with respect to the host layers.

In all zirconia- pillared clays studied here, any reflections which could be assigned to separate zirconia-containing phases were not observed. It means that for predominant part of pillars, their typical sizes within the basal plane are less than 25-30 Å, and that in the basal direction is less than 10 Å. The differential radial distribution curve obtained by subtracting the initial clay data from those of pillared clays was found to contain maxima at 2–2.4; 3.6; 4–4.2; 4.5–4.8; 5.6–5.9 Å, thus proving incorporation of tetramers containing species into clay structure.

The negative peaks of the electron density in the differential curve show variation in the structure of a clay due to pillars incorporation. The interlayer distance between the tetrahedral SiO_4 layers in the alumosilicate sheets is increased up to 2.8 Å. Similarly, the distance between octahedrally coordinated cations (Me=Al, Mg) to the oxygen in the nearest tetrahedron is increased from 3.1 to 3.3 Å. These variations can be caused by strains generated by zirconia pillars situated between the alumosilicate layers. The incorporation of a big cation (first of all, Zr) into the vacant octahedral positions could not be excluded as well.

As follows from the results of UV-Vis, for Zr PILC the characteristic absorption corresponding to the anion-cation charge transfer is shifted to higher wavenumbers as

compared with that for the bulk analog -highly dispersed cubic zirconia stabilized by 2 mol. % of CaO. This feature can be explained by a lower O-Zr coordination number in nanosized pillars (maximum 2 for bridging oxygen anions or hydroxyls) as compared with the bulk zirconia lattice (each oxygen is surrounded by 4 Zr cations). As a result, the Zr-O bond in nanoparticles possesses a higher ionicity which is reflected in a higher energy of the charge transfer band. Decreased intensity of those bands in Zr PILCs can be related to a high disordering of the nanoparticle structure as revealed by EXAFS.

FTIRS data of adsorbed CO and hydroxyl groups indicate that on the surface of zirconia pillared clays evacuated at 400 ^{o}C, the number of coordinatively unsaturated Zr cations is much lower as compared with that for bulk highly dispersed zirconia samples. Moreover, in the hydroxyls stretching regions, only bands at ~ 3650-3700 cm $^{-1}$ corresponding to bridging hydroxyls are present. It implies that the surface of zirconium nanoparticles is covered by bridging hydroxyls binding either Zr cations or Zr cations and cations in the alumosilicate layers.

Structure and texture of zirconia pillared clays. According to analysis of the nitrogen adsorption isotherms by using the geometric model of pillared interlayer materials, the specific surface area of a free space within the pillared clay galleries is in the range of 350-400 m^2/g. A mean diameter of pillars approximated by discs was estimated to be in the range of 15-20 Å, which agrees rather good both with the predominant sizes of pillaring species in solution and the upper limit of the size of zirconia nanoparticles as determined by XRD (vide supra).

Pore structure withstands overheating up to 750 ^{o}C without collapse, which is comparable with the best results reported by Ohtsuka et al [5]. Such a stability implies reasonably uniform spatial distribution of pillars within galleries.

State of supported copper cations and Pt atoms. Results of UV-VIS and FTIRS of adsorbed CO test molecules imply that for ZrPILC samples loaded with up to 2-3 wt. % of Cu, three-dimensional reactive copper oxidic clusters dominating for copper supported bulk mesoporous zirconia catalysts are absent. This feature can be assigned to difference between the surface arrangement of the most developed (111) and (110) faces of the fluorite-like zirconia and that of nanosized zirconia pillars (vide supra). As the result, copper cations supported on nanosized pillars appear to sink into their bulk, thus being coordinated by bridging hydroxyls and/or oxygen atoms, reactive terminal oxygen forms being absent. Estimation of the number of Cu^{+} and Cu^{2+} cations by using known values of the integral absorption coefficients A_o revealed that around a half of copper cations is in the 1+ state. This

share is much higher than that revealed for copper-loaded bulk zirconia, thus implying Cu^{+} cations stabilization by pillars.

At room temperature, in oxidized Pt-loaded ZrPILC, Pt atoms are detected by a weak Pt-CO band at~ 2125 cm^{-1}, which indicates their predominant ionic state due to a strong interaction with nanosized pillars. For Pt+Cu-loaded samples, carbonyl band at ~ 2100 $cm^{-1.}$ is clearly observed indicating that metallic Pt is present here. Since for Pt-ZrPILC Pt is mainly in the ionic state due to strong interaction with pillars, pre-supporting of copper cations appears to make such an interaction much weaker. Moreover, Pt supporting on sample precovered by copper cations causes two-three fold decrease of the intensity of bands corresponding to all types of other CO adsorption centers including Cu cations, Zr^{4+} cations and hydroxyls. Hence, a part of copper cations is masked by superimposed Pt atoms.

Catalytic activity. Catalytic properties of these systems were characterized in the reactions of NO_x selective reduction in the excess of oxygen by propane, propylene and decane. Catalytic performance of best samples in the NO_x selective reduction by hydrocarbons in the low-temperature (200-300 ^{o}C) region is comparable with or higher than that of systems based upon ZSM-5 while being stable in the presence of water and sulfur dioxide.

In the case of Pt-promoted samples, a general level of activity is enhanced (NO_x conversion exceeding 60% at GHSV up to 50,000/h), which can be explained by enhanced oxidation ability of mixed active components. At high contents of water and oxygen (up to 10%) no trances of N_2O by-product were revealed.

Acknowledgments Financial support by INTAS under 97-11-720 project is gratefully acknowledged.

References

[1] Gil. A. and Gandia L.M,. Catal. Rev-Sci. Eng., 42 (2000) 146.
[2] Yang R. T., Trappiwattanannon N. and Long R.Q.,. Appl. Catalysis B: Environment., 19 (1998) 289.
[3] Sadykov V. A., Kuznetsova T.G. et al. In: Abstracts, EUROPACAT-5, Limerick, Ireland, Book 3, 7-O-03 (2001).
[4] Fenelonov V. B., Derevyankin A. Yu. and Sadykov V. A. Micropor. Mesopor. Mater. 47 (2001) 359.
[5] Ohtsuka K. Hayashi Y and Suda M., Chem. Mater., 5 (1993) 1823

LABORATORY-SCALE FLOW-RECYCLING CATALYTIC REACTORS: THEIR POTENTIALITIES AND PERSPECTIVES

Bobrov N.N., Bobrova I.I., Parmon V.N.

Boreskov Institute of Catalysis SB RAS, Novosibirsk, Russia
Fax: (3832) 34-30-56; E-mail: bobrov@catalysis.nsk.su

The flow-recycling reactor (FRR) is an important version of laboratory-scale catalytic reactors of ideal mixing in which a mixing devices placed outside of the reaction volume.

The main advantage of the FRR compared to other types of the "gradientless" catalytic reactors is a reliable provision of the catalyst bed thermal and concentration gradientlessness as well a possibility to remove the reaction products just after the catalyst bed. This permits to study the kinetics of both heterogeneous and hetero-homogeneous catalytic reactions with most accuracy. The most important kinetic parameter of catalysts, their "catalytic activity", can be easy and correctly determined by the FRR as specific stationary rate of the catalytic reaction at the given temperature, pressure and composition of the reaction mixture which is in contact with the catalyst. However, up today the FRR reactors did not found a wide application owing to a number of still unsolved complicated methodological and technical problems. In recent years, in the Boreskov Institute of Catalysis, both the FRR design and techniques of their use were sufficiently improved [1].

In the present work, we show possibilities of highly accurate kinetic studies carried out using the FRR on the particular example of catalytic processes of methane oxidative conversion (deep and partial methane oxidation by molecular oxygen, as well as methane steam reforming). The use of the FRR together with the new generation of digital pulse gas flow controllers permits to solve accurately and efficiently all typical kinetic tasks including an unequivocal comparison of the activity of different catalysts and the study of the catalyst activity in respect to the reaction temperature, the composition of the contact reaction mixture and diffusion effects. This provides an opportunity to create compact, simple in design and reasonably priced educational set-ups for the laboratory tasks performance on the tutorial course "Kinetics of heterogeneous catalytic reactions".

The FRR combined with a quenching unit for the formaldehyde absorption in water at room temperature easily provides a 100% selectivity of the methane oxidation to formaldehyde. This permits to compare unequivocally the activity of different chemical compounds and to choose more correctly the most perspective catalysts for the mentioned process. The application of the FRR to kinetic studies of methane steam reforming over Ni-

and Ru-based catalysts have shown that this process can proceed via either a heterogeneous or hetero-homogeneous mechanism. The specific activities of the Ni and Ru catalysts proved to be the same in the mode of heterogeneous occurence of the methane steam reforming, while at the hetero-homogeneous occurence the activity of Ru is much higher than that of Ni.

The most promising is the FRR application for the development of standardized methods for the catalyst properties studies since it provides comparable conditions of the catalyst testing for any catalysts and processes.

References.

1. Bobrov N.N., Parmon V.N. in *Principles and Methods for Accelerated Catalyst Design and Testing, (Eds. E.G.Derouane, V.Parmon, F.Lemos and F.R.Ribeiro), NATO Science Series, II. Mathematics, Physics and Chemistry,* 69 (2002) 197

HYDROXYLATION OF ORGANIC SUBSTRATES BY AN O_2 /H_2 MIXTURE

Likholobov V.A.

Boreskov Institute of Catalysis SB RAS, Omsk Department, Omsk, Russia
E-mail: Likhvl@catalysis.nsk.su, ofik@omsk.net.ru

An O_2/H_2 oxidant is considered as very promising alternative for dioxygen in reactions of hydrocarbons oxidation. It gains advantages over dioxygen, those are lower temperature of performances and resulting selective conversion of hydrocarbons into oxygenated compounds with minimal complete oxidation.

A group of catalytic systems consisted of Pt or Pd and different heteropoly compounds (HPC's), including transition metal containing HPC's, was studied in oxygenation of alkanes, cyclohexane, benzenes and alkenes. The liquid-phase versions of the systems were composed of (1) water soluble complexes of Pd(II) ions with heteropoly anions, (2) solid Pt catalysts and HPC solution and (3) supported or bulky solids of the same composition.

In addition the silica supported Pt-HPC and Pd-HPC samples were used in vapor-phase oxidation of hydrocarbons providing selective conversion of alkanes and benzenes into oxygenated compounds.

Data on both structure of the catalyst active components and relative reactivity of the hydrocarbons and composition of the oxygenated products were analyzed for elucidation nature of the active intermediate species responsible for oxygenation in the system under study .

PENETRABLE COMPOSITE MONOLITHS FOR THE FISCHER-TROPSCH SYNTHESIS. CONTROL OF THE PROCESS SELECTIVITY BY POROUS STRUCTURE PARAMETERS

Khassin A.A., Sipatrov A.G., Chermashentseva G.K., Yurieva T.M., Parmon V.N.

Boreskov Institute of Catalysis SB RAS, Novosibirsk, Russia

A new concept of the catalyst bed which uses penetrable composite monoliths (PCM) has been already shown to be efficient one for the Fischer-Tropsch synthesis (FTS). The PCM represents itself a single porous composite particle with a well developed structure of transport pores with the size ranging from 2 μm to 20 μm. A small effective diffusion length and a high intensity of the liquid-gas mass transfer provide a high effectiveness of the FTS process. The magnitude of the diffusion limitations was shown to correlate with the dispersion of the transport pore size distribution.

In this paper we present recent experimental results on the possibility to control the porous structure parameters at the PCM preparation stage. The variation of the pore size distribution was proved to be a tool to control the selectivity of the FTS process. E.g. weakening the transport limitations leads to a higher selectivity towards olefins; at the extreme, the propylene-to-propane ratio of *ca.* 6 is achieved. On the contrary, in the case of severe diffusion limitations, a high selectivity towards saturated branched hydrocarbons is observed.

Another aspect of the study is the effect of the PCM particle geometry. Three types of the PCM particle geometry were tested - a flat plate, a hollow cylinder with radial flow directed from the cylinder axis to the outer element, and a hollow cylinder with radial flow directed towards the cylinder axis. Unexpectedly, the data on the process productivity *versus* the gas velocity, as well as those on the process selectivity *versus* the CO conversion extent appear to depend dramatically on the PCM particle shape.

The nature of the observed phenomena is discussed.

References:

1. A.A. Khassin, T.M. Yurieva, A.G. Sipatrov, V.A. Kirillov, G.K. Chermashentseva and V.N. Parmon. Catal. Today, 2003 (in press)
2. I.Sh. Itenberg, V.A. Kirillov, N.A. Kuzin, V.N. Parmon, A.G. Sipatrov, A.A. Khassin, G.K.Chermashentseva, T.M. Yurieva. WO Patent Application PCT/RU 02/00507, priority date 21.12.2001.

RAPID TESTING OF SUPPORTED COBALT FISCHER-TROPSCH SYNTHESIS CATALYSTS: MAGNETIC TPO AND TPR

Lermontov A.S., Chernavskii P.A., Pankina G.V., Lunin V.V.

Chemical Department, Lomonosov Moscow State University, Moscow, Russia
E-mail: chern@kge.msu.ru

Fischer-Tropsch synthesis is one of the hardest catalytic reactions from the direct catalytic tests viewpoint. Nowadays, there is no effective way for quick in situ characterization of the reduced catalyst. However, the unique technique of in situ magnetization measurements allows continuous determination of cobalt metal content in catalyst during reduction, oxidation and hydrogenation of carbon deposits. Also magnetic measurements give a possibility to reconstruct cobalt particle size distribution during chemical reactions. In this work the possibility of catalyst properties prediction using magnetic temperature-programmed reduction (TPR) and temperature-programmed oxidation (TPO) techniques was investigated.

It was found that the magnetic TPO spectra of supported cobalt Fischer-Tropsch catalysts contain information about cobalt particle size distribution. The experiments show that the temperature of «oxygen consumption / metallic cobalt loss» maximum on TPO spectra is independent on support nature. It depends only on the mean size of cobalt crystallites. The cobalt crystallites are smaller the lower is the maximum of temperature of oxygen consumption. The theoretical modeling of TPO spectra was done using the Cabrera-Mott theory of oxidation and the conception of oxygen layer thickness independence from the particle sizes. It indicates that bimodality of particle size distribution can lead to the double peak appearances on magnetic TPO spectra.

From the magnetic TPR spectra it is possible to determine the structure of the catalyst. First of all using the continuous magnetization measurements technique it is possible to divide the reactions of different cobalt oxides reduction and identify true stages of metallic cobalt appearance. The diffusion limitations of cobalt oxide reduction caused by water generation during reaction in the narrow pores leads to the increasing of temperature maximum of metallic cobalt appearance. So the position of maximums on TPR spectra depends on the support pore structure. The size of particles plays not so important role as in the case of oxidation, because during the Co_3O_4 reduction to CoO the highly defect CoO nanoparticles are produced. From the magnetic TPR spectra it is possible to differ cobalt nanoparticles in narrow pores and cobalt in the wide pores or on the external surface of support grains. The

size of the first ones is limited by the size of the pores; the size of the second type of particles is «unlimited». The special series of experiments was used to show that the relatively big particles are reduced at lower temperatures than the smaller ones.

Comparison of TPR spectra with Fischer-Tropsch catalytic tests shows that the best results were obtained on the catalysts, which have only one peak in magnetic TPR spectra. The mean particles size for these catalysts was 8-10 nm and the mean pore diameter was 14-16 nm. All catalysts that have two peaks of metallic cobalt in the TPR spectra show higher methanation activity, higher carbon deposits and lower activity in the FT synthesis. Thus, the magnetic TPR and TPO are the powerful tools for the rapid prediction of the catalytic properties in Fischer-Tropsch synthesis.

This work was supported by Russian Foundation of Basic Research, Grant № 02-03-32556.

METHANOL STEAM REFORMING OVER Cu-CONTAINING CATALYSTS

Zavalishin I.N., Lin G.I., Kipnis M.A., Yashina O.V., Grafova G.M., Rozovskii A.Ya.

Topchiev Institute of Petrochemical Synthesis RAS, Moscow, Russia
Fax: (7 095) 230 22 42; E-mail: zaval@ips.ac.ru

Methanol steam reforming ($CH_3OH + H_2O = CO_2 + 3H_2$) is the process of significant interest in view of hydrogen generation, particularly promising for use in fuel cells. Kinetic study of proceeding reactions gives important information allowing to establish the mechanism and to optimize the process.

Kinetics of methanol steam reforming was studied over Cu-containing catalysts in flow reactor. The range of experimental conditions (temperature 240-310 ^oC, pressure 6-21 atm, methanol/water ratio from 1:1.3 to 1:3) was chosen so as to provide markedly differing results for interpretation of the kinetics.

Consideration of possible mechanism of the process was made on the basis of the following propositions:

1) Methanol steam reforming over Cu-containing catalysts is the reaction reverse to methanol synthesis. It proceeds in conjugation with reverse water gas shift reaction (WGSR):

$CO_2 + H_2 = CO + H_2O$;

2) All active sites are covered by strongly adsorbed species;

3) Reactions of adsorption substitution on the active sites play the key role in the overall mechanism;

4) Methanol decomposition into CO and H_2, the reaction which proceeds with very high rate already at 200 ^oC (through methyl formate formation as the intermediate product), is suppressed when water is present in high concentrations due to the peculiarities of reaction mechanism. In particular, methyl formate decomposition requires the existence of free centers on the catalyst surface.

As the question of the “right” mechanism of methanol steam reforming obviously revolves around the question of the “right” mechanism of methanol synthesis itself, a large body of previously obtained data [1, 2] was involved for accumulation of information on the character of individual steps and their possible participants. New kinetic experiments were made in order to make clear whether methanol steam reforming proceeds as the reverse methanol synthesis under its conditions, quite different from the conditions of methanol synthesis.

Proposed mechanistic scheme of methanol steam reforming includes seven surface species which participate in a number of adsorption substitution reactions. While it was not possible in the scope of this work to describe some of these intermediate species in more thorough way than simply by their stoichiometry, it was nevertheless possible to quantify their input into the overall kinetics in each case. Splitting of hydrogen molecule from the surface species which includes CO_2 and H_2 was found to be the rate-limiting step of methanol steam reforming.

As to the formation of CO, its concentration was found to be on the level of equilibrium CO concentration for reverse WGSR under all studied conditions. Some input of methanol decomposition (through methyl formate) was noticed only under 21 atm at 300 ^{o}C.

On the basis of this mechanism, kinetic model of methanol steam reforming is proposed. Computer modeling has shown that this model is in satisfactory agreement with experimental results in the range noted above. To check the validity of the model further, the data by Kuznetsov, Shub and Temkin [3] on methanol synthesis and methanol steam reforming under atmospheric pressure were used. For these data, the description of both methanol synthesis and methanol steam reforming was made using the same kinetic parameters. The success of this comparison pointed out that the approach undertaken in this work was a well-chosen one.

We would like to acknowledge the support of Russian Foundation for Basic Research (Grant 02-03-32202) and support of Program for Support of Scientific Schools (Grant 00-15-97389).

[1] Lin G.I., Kotyaev K.P. and Rozovskii A.Ya., *Kinetics and Catalysis*, 39 (1998) 798
[2] Rozovskii A.Ya. and Lin G.I., *Kinetics and Catalysis*, 40 (1999) 854
[3] Kuznetsov V.D., Shub F.S. and Temkin M.I., *Kinetika i Kataliz (Rus.)*, 25 (1984) 606

THE PROCESS FOR SYNTHESIS OF NITROUS OXIDE VIA SELECTIVE OXIDATION OF AMMONIA: FROM CATALYST SURFACE TO PILOT INSTALLATION

Noskov A.S., Zolotarskii I.A., Slavinskaya E.M., Mokrinskii V.V., Ivanova A.S., Korotkikh V.N., Kashkin V.N., Pokrovskaya S.A.

Boreskov Institute of Catalysis SB RAS, Novosibirsk, Russia
E-mail: noskov@catalysis.nsk.su

Nitrous oxide is traditionally used in a number of fields including medicine, semiconductor techniques, cosmetics and food industry. These industries consume relatively small amounts of nitrous oxide. Installations of unit capacities no more than several thousand tons of nitrous oxide per year (usually, no more than 5,000 t/y) are based on thermal decomposition of nitrite-nitrate salts. It is hardly possible to boost further their capacity because of the high process explosiveness.

Progress in the field of catalytic selective oxidation of hydrocarbons by nitrous oxide, for example, oxidation of benzene into phenol, have given impetus to development of processes for production of nitrous oxide at the unit capacity higher by orders of magnitude (50,000 – 100,000 t/y). One of the processes may be selective oxidation of ammonia with oxygen into N_2O.

The present work dealt with the results of development of a large-tonnage process for synthesis of nitrous oxide via selective oxidation of ammonia. The studies included the following stages: a) choice of catalyst, synthesis and characterization of manganese-bismuth oxide catalysts including establishment of surface active species responsible for the process selectivity; b) determination of kinetic parameters of the process and mathematical modeling of the reactor units; c) testing of catalysts and design of a pilot installation producing up to 8 t of N_2O per year.

At the first stage of studies, Mn-M-O/support samples [1], where M = Ni, Bi, Y, Ce, Sm etc., containing the active component in amount of 10 – 25 wt % were prepared using γ- and α-alumina as the support. Catalysts were prepared by impregnation of the support with a mixed solution of nitrates of the corresponding elements taken in certain ratio followed by drying and calcination. Comparative testing demonstrated high activity of all the samples. The highest selectivity to nitrous oxide (up to 90 %) at almost complete conversion of ammonia was observed with Mn-Bi-O composition supported on α-alumina, while the same composition supported on γ-alumina did not allow a selective catalyst to be obtained at the

comparable content of the active component, the selectivity to nitrous oxide was not higher than 54 %.

At the next stage the phase composition, surface state and catalytic properties of Mn-Bi-O catalysts different in the support nature and conditions of thermal treatment were thoroughly studied. For this purpose the pulse method and the method of temperature programmed surface reaction (TPSR) of ammonia were used to study interaction of individual components of the reaction mixture.

Experimental studies were carried out using an installation with a unit for mass spectrometric analysis by feeding pulses of ammonia or reaction mixture containing NH_3 and $^{16}O_2(^{18}O_2)$. Reduction of the catalyst with ammonia results in formation of the reaction products: N_2O, N_2 and NO. Approximately a half amount of all oxygen is removed from the catalyst along with the reaction products during reduction that indicated a high enough mobility of bulk oxygen. It is shown that the reduction rate decreases with an increase in the surface reduction degree, the rate of ammonia oxidation into N_2O being decreased more sharply than that into N_2 that leads to increasing selectivity to N_2.

TPSR studies of the catalysts reveal the presence of oxygen species with different bond energies. The weakly bonded oxygen is shown to be responsible for formation of nitrous oxide. Elimination of the weakly bonded oxygen results in a decrease in the overall reduction rate and in a more sharp decrease in the rate of oxidation to N_2O in comparison to the rate of oxidation to N_2. As a consequence, the selectivity to N_2 increases. The state of catalyst surface changes as the calcination temperature rises at the stage of catalyst preparation. Since the manganese-oxygen bond energy is lower in oxidized manganese species, an increase in the proportion of lower bond energy sites means am increase in the ratio of the oxidized to reduced manganese states. This conclusion is supported by XPS data indicating an increase in the $Mn^{3+}/Mn^{(2\div3)+}$ ratio with elevation of the catalyst calcination temperature. The selectivity to N_2O is cymbate to changes in the ratio. Another reason for decreasing reduction rate is blocking of the active surface by strongly bonded ammonia species, which can only be eliminated at the temperatures higher than the reaction temperature.

The same products, *viz.* N_2O, N_2 and NO, are shown to release during the catalyst reduction and the catalytic reaction, the rates being equal at equal surface reduction degrees. Comparison of the total oxygen consumption for formation of the reaction products and the oxygen consumption of formation of the products from gas phase gives an evidence of the participation of intrinsic oxygen of the catalyst in the catalytic cycle. This conclusion is supported by experimental data obtained by substitution of $^{18}O_2$ for $^{16}O_2$ in the reaction

mixture. In the course of the experiment, more than 2 monolayers of $^{16}O_2$, i.e. one third of the total amount of intrinsic oxygen, is eliminated with the reaction products. Such a degree of intrinsic oxygen contribution argues for the high mobility of bulk oxygen.

The whole set of results obtained leads to conclude that the stagewise mechanism is characteristic of the reaction of ammonia oxidation.

Kinetic regularities of ammonia oxidation were studied using the Mn-Bi-O/α-Al_2O_3 catalyst containing 13 wt % of MnO_2 and 11 wt % of Bi_2O_3. The influence of contact time, temperature, pressure and composition of the reaction mixture on ammonia conversion and selectivity to reaction products were studied. It was experimentally shown that ammonia oxidation produced N_2O, N_2 and NO. The study of the influence of contact time revealed a surprising fact: Selectivity to nitrous oxide increased with increasing ammonia conversion.

Temperature dependences of the reaction rates were studied at temperature varied between 315 and 370 °C at constant concentrations of ammonia, oxygen and water in the reactor. The data obtained were used for estimation of apparent activation energies of the ammonia oxidation and formation of the products. Nitrous oxide is formed at higher activation energy than nitrogen that accounts for the fact that a higher selectivity to nitrous oxide is observed at a higher temperature within the range under study. An increase in the oxygen concentration leads to an increase in the rate of ammonia oxidation, the rate of formation of nitrous oxide being more accelerated than the rate of formation of nitrogen that results in an increase in the selectivity to nitrous oxide.

The results obtained show that an increase in the ammonia concentration causes acceleration of the ammonia oxidation. The rate of nitrogen formation increases more rapidly than the rate of formation of nitrous oxide and nitrogen oxide. Correspondingly, the selectivity to nitrogen increases while the selectivities to nitrous and nitrogen oxides decrease. It also follows from the data obtained that the rate of ammonia oxidation decreases at an increase in the water concentration. The presence of water makes the formation of nitrogen more considerably decelerated than formation of nitrous oxide, while the rate of formation of nitrogen oxide increases slightly. This phenomenon accounts for the increase in the selectivity to nitrous oxide and nitrogen oxide and the decrease in the selectivity to nitrogen at an increase in the water concentration.

The data obtained were used for construction of kinetic models to describe experimental data and for mathematical modeling of basic reactor units for oxidation of ammonia into nitrous oxide, *viz.* a fluidized bed reactor and tube reactor [2, 3].

The studies allowed a pilot installation for synthesis of nitrous oxide via oxidation of ammonia to be designed for production of up to 8 t N_2O /y. Technological regimes were adapted using the reaction mixture containing ammonia in the amount of 18 to 50 vol %. Stable operation regimes were achieved at the temperature range of 330 to 370 °C that provided high conversions of ammonia (96 – 99 %) at the selectivity to nitrous oxide equal to 76 – 86 %. Concentration of NO_x was not higher than 10 ppm in the produced nitrous oxide.

Therefore, the accomplished studies allowed creation of a new large-tonnage process for synthesis of nitrous oxide via selective catalytic oxidation of ammonia.

The authors express their gratitude to P. Notte, S.A. Veniaminov, I.A. Polukhina.

References

1. V.V. Mokrinsii, E.M. Slavinskaya, A.S. Noskov, I.A. Zolotarsky, PCT Int. Appl. WO 9825698 (1998), priority: RU 96-96123343; A.S. Ivanova, E.M. Slavinskaya, I.A. Polukhina, A.S. Noskov, V.V. Mokrinskii, I.A. Zolotarskii, Rus. Pat. 2185237 (2002), Catalyst and the method for production of nitrous oxide.
2. V.N. Kashkin, V.S. Lakhmostov, I.A. Zolotarskii, A.S. Noskov, J.J. Zhou, Studies on the onset velocity of turbulent fluidization for alpha-alumina, Chem. Eng. Journal, in press.
3. A.S. Noskov, I.A. Zolotarskii, S.A. Pokrovskaya ., V.N. Korotkikh, E.M. Slavinskaya, V.V. Mokrinskii, V.N. Kashkin, Ammonia oxidation into nitrous oxide over Mn/Bi/Al catalyst. I. Single cooling tube experiments, Chemical Engineering Journal, 4073 (2002) 1–8.

SULFUR OXIDE CHEMICAL PROCESSES ON Pt SURFACES

Lin Xi[1], Tang H.[2], Trout B.L.[2]

[1]Department of Chemistry, MIT, Cambridge, USA
[2]Department of Chemical Engineering, MIT, Cambridge, USA
Fax: 1-617-258-5042; E-mail: trout@mit.edu

The thermodynamics of S, O, SO, SO_2, SO_3, and SO_4 chemisorption on the Pt(111) surface are studied using first-principles density functional theory (DFT) computations. The adiabatic potential energy surfaces of the sulfur oxides on Pt(111) are probed systematically to yield comprehensive sets of local minima[1-2]. The most energetically stable configurations of all the sulfur oxides are identified. These adsorbates demonstrate strong surface coverage effects due to dipole-dipole interactions. Based on the fact that the nature of these interactions is the same for all adsorbates, a general procedure is developed for computing adsorption thermodynamics as a function of coverage. Predicted isotherms of non-dissociative SO_2 and dissociative O_2 with these coverage-dependent adsorption thermodynamics are generated. The sulfur atoms of the most energetically stable SO_x (x= 1, 2, 3, and 4) surface species exhibit a general tetrahedron binding preference. Novel surface reconstructions are observed at high surface coverages. Dozens of surface reactions at the low, high, and oxygen-saturated surface coverage limits are examined at low temperatures, and the most energetically stable surface species at these limits are identified as atomic S, SO_4, and SO_4, respectively. Possible oxidation reaction channels are suggested, which are shown to be highly sensitive to the surface coverage.

The chemical kinetics of SO_2 oxidation reactions on the oxygen pre-adsorbed Pt(111), and the self-diffusion reactions of O, SO_2, and SO_3 on Pt(111) are studied using first-principles density functional theory (DFT) computations. The minimum energy paths are searched by the nudged elastic band method that requests only the first-derivatives of the Kohn-Sham energy functional. The transition states are identified as the maximum points along the minimum energy paths, the activation free energies being computed via the harmonic oscillation approximation at low and intermediate temperatures. Both Langmuir-Hinshelwood and Eley-Rideal mechanisms of the oxidation reactions are examined and the results indicate that the Langmuir-Hinshelwood mechanism is slightly favored. The selfdiffusivities of SO_2, SO_3, and O are also reported. Using all of this data, we are working towards developing a comprehensive reaction/diffusion model as described in the next paragraph.

Kinetic Monte Carlo (KMC) based on a lattice model is used to study the oxygen island formation on Pt (111). Only hopping from an fcc to an empty nearest fcc site is considered in our model, and all of the necessary parameters, such as energy barriers and lateral interactions, are obtained by DFT computation. KMC simulations indicate that most of the oxygen atoms aggregate in islands, wherein individual atoms are not closer than two lattice constants apart, p(2x2) symmetry (see figure 1). This is in agreement with experimental results (see figure 2)[3-5]. B. C. Stipe *et al.* owed this oxygen island formation on Pt(111) to nearest neighbor repulsion and second nearest neighbor attraction[3]. This is a little different from our preliminary DFT computational results which show that there is repulsion between nearest neighbors (strong) and second nearest (weak) neighbors, and attraction exists only between third nearest neighbors (see Table 1). More accurate interaction fitting is still in process.

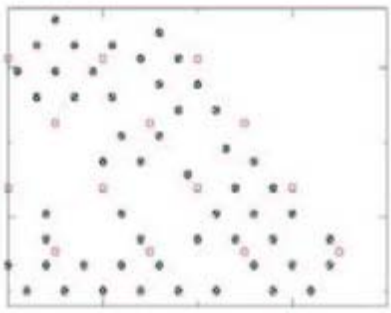

Figure 1: At 200 K, initial (cycle) and final (solid) configuration of oxygen islands on Pt (111) after KMC simulation.

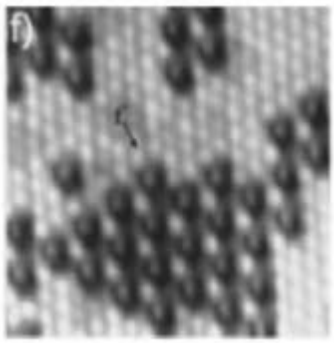

Figure 2: STM image (45Å×45Å) of small oxygen islands on Pt (111)[3].

Table 1: DFT calculated interaction parameters (in kJ/mol) for O on Pt(111).

Interactions	V_1	V_2	V_3	V_{lt}	V_{bt}	V_{tt}
Value/kJ/mol	22.431	3.210	-0.049	7.123	0.935	-10.584

References:

[1] Lin X., Hass K. C., Schneider W. F. and Trout, B. L., *J. Phys. Chem. B*, 106 (2002) 12575.

[2] Lin X. and Trout B. L., "Chemistry of Sulfur Oxides on Transition Metal Surfaces," in Interfacial Applications in Environmental Engineering, ed. Keane, M., ACS Symposium Proceedings (2002) 55-68.

[3] Zambelli T., Barth J. V., Wintterlin J. and Ertl G., *Nature*, 350 (1997) 495.

[4] Wintterlin J., Schuster R. and Ertl, G., *Phys. Rev. Lett*., 77 (1996) 123.

[5] Stipe B. C., Rezaei M. A. and Ho W., *J. Chem. Phys.*, 107 (1997) 6443.

MODEL DFT STUDY OF THE INTERMEDIATES OF BENZENE TO PHENOL OXIDATION BY N_2O ON HIGH-SILICA ZEOLITES

Zhidomirov G.M[1], Kachurovskaya N.A.[2], van Santen R.A.[2]

[1]Boreskov Institute of Catalysis, Novosibirsk, Russia
E-mail: Zhi@catalysis.nsk.su
[2]Schuit Institute of Catalysis, Laboratory of Inorganic Chemistry and Catalysis,
Eindhoven University of Technology, Eindhoven, The Netherlands

Recently considerable attention has been drawn to the selective oxidation of hydrocarbons with nitrous oxide in ZSM-5 zeolites, especially to the direct process of benzene to phenol oxidation [1].

Fe(II) ion in α-cationic position of ZSM-5, (Fe/Z), was suggested as active site of N_2O thermal decomposition and of selective oxidation center OFe/Z formation. Cluster model calculations of the intermediate of benzene hydroxylation by N_2O have been performed [2]. The calculated bond energy of oxygen in the structure OFe/Z is in reasonable agreement with experiment for α-oxygen. The study showed that the interaction of the center with benzene molecule resulted easily in arene oxide formation probably with rather low activation energy. Stepwise mechanism of the further transfer of arene oxide to phenol was suggested, like it was found early for the aromatization of arene oxides [3]. All the probable intermediates: benzene oxide, oxepin, zwitterion, keto-tautomer of phenol and phenol molecule have been calculated in adsorption state on Fe^{2+} containing AS. Arene oxide to zwitterion transfer was supposed to be the limiting stage of the reaction in full analogy with the arene oxide to phenol reaction in solutions [3], what allowed explaining the absence of H/D KIE in the reaction. It was concluded that appearance of unusual frequency band 2874 cm^{-1} during adsorption of benzene on α-sites of zeolite can be explain by formation of keto-tautomer of phenol as one of intermediates of the reaction. Adsorbed phenol occurs to be the most stable final product of the reaction and desorption of phenol molecules or their dislodging by N_2O substitution would be the key step in the reaction "in situ". This is in quite agreement with recent experimental investigations [4].

Periodic DFT calculations were carried out on a model for the α-oxygen active site present in Fe ions incorporated in zeolite. The model was constructed from an Fe(II) ions located at the α-cationic position of the Ferrierite structure. Then model was tested on appropriateness by calculating bond energy for α-oxygen. Performed periodic calculations supported conclusions on the rate limiting step of the reaction made in the cluster studies [2].

All possible intermediates were studied in the adsorbed state on the active site and the comparison with the results of the cluster calculations were performed.

[1] G.I.Panov, CATTECH, **2000**, 4, 18.
[2] N.A.Kachurovskaya, G.M.Zhidomirov,E.J.M.Hensen, R.A.van Santen, submitted to Catal.Lett.
[3] G.J. Kasperek, T.C. Bruce, H. Yagi, D.M. Jerina, *J. Am. Chem. Soc.*, **1973**, 95, 6041.
[4] A.A.Ivanov, V.S.Chernavsky, A.S.Kharitonov, G.I.Panov, submitted to Appl.Catal.

THE MECHANISM OF C–C BONDS HYDROGENOLYSIS IN ALKANES ON THE SILICA-SUPPORTED ZIRCONIUM HYDRIDES. A THEORETICAL DFT STUDY

Besedin D.V., Ustynyuk L.Yu., Ustynyuk Yu.A., Lunin V.V.

Department of Chemistry, Lomonosov Moscow State University, Moscow, Russia
Fax: +7-095-939-4575; E-mail: dmitri_b@kge.msu.ru

In the recent years, the reactions of alkane hydrogenolysis on a silica-supported zirconium hydride catalyst were investigated in a series of experimental works by Basset *et.al.* [1-4]. This catalyst is obtained by the reaction of the organozirconium compounds ZrR_4 (where R = allyl [8] or neopentyl [1-4]) with the partially dehydroxylated silica surface, followed by the heating in the hydrogen atmosphere at 423 K. According to the IR spectroscopic data [1, 8], the mixture of grafted zirconium monohydrides $(\equiv Si–O)_3ZrH$ [2] and dihydrides $(\equiv Si–O)_2ZrH_2$ [8] is obtained under these conditions. Some amounts of Zr(III) compounds are always formed as well, according to the ESR studies (up to 5% of the total amount of grafted zirconium). Among these compounds, the presence of Zr(III) hydrides has been supposed [5]. It is still unclear, up to the present time, which of the aforementioned centers are responsible for the catalysis of the alkane hydrogenolysis reactions.

In our earlier studies, we have investigated the reactions of the isotopic exchange in methane [9] and the polymerization of ethylene on a silica-supported Zr(III, IV) hydrides using the DFT approach [10-11]. As a continuation of these studies, we have investigated the mechanisms of the catalytic hydrogenolysis of the C–C bonds of linear alkanes (using propane, *n*-butane and *n*-pentane as examples) on model compounds **1**–**3** under the same approach as in [9-11].

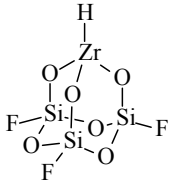

1

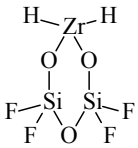

2

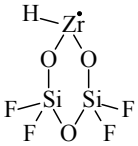

3

The mechanism of the interaction of the model compound **1** with linear alkanes (RH) considered by us is analogous to that proposed earlier by Basset *et.al.* [2-4] for the C–C bonds hydrogenolysis on Zr(IV) monohydrides $(\equiv Si–O)_3Zr^{IV}H$. It is essentially the same with the reverse sequence of transformations established for the ethylene polymerization on these centers [10-11].

Scheme 1

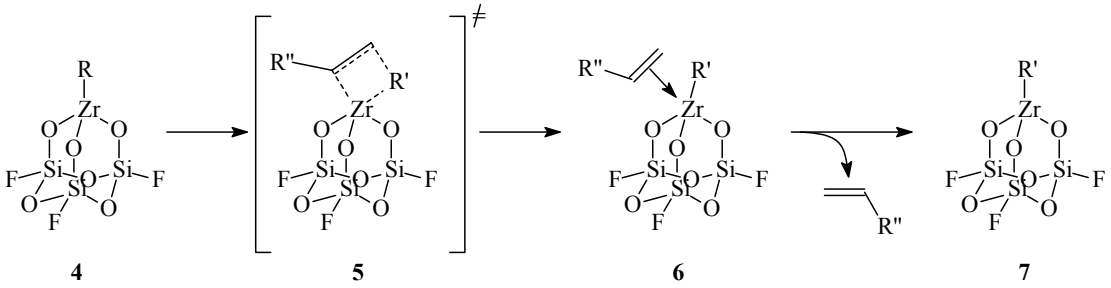

4 **5** **6** **7**

The rate-determinig step of the linear alkane hydrogenolysis on monohydride centers **1** is the cleavage of the aliphatic β-C–C bond in the zirconium alkyl species **4** (see Scheme 1). It proceeds by the migration of the R′ alkyl fragment in the sequence of transformations **4** → **5** → **6** and requires an overcome of considerable energy barriers ($\Delta G_{298}^{\neq}$ = 28.4 ÷ 30.9 kcal mol^{-1}). The formation of complexes **6** from **4** is extremely unfavorable from the thermodynamic point of view (ΔG_{298} = 8.3 ÷ 16.9 kcal mol^{-1}). The presence of branching at the α-position of the alkyl chain in **4** leads to the considerable lowering of the endothermicity of the process. The migration of β-methyl fragment proceeds easier than that of β-ethyl. The dissociation of the olefin molecule (C_2H_4, R″ = H, or C_3H_6, R″ = CH_3) from complexes **6** is allowed thermodynamically due to considerable increase of the system entropy, which results in lowering of the free energy of the system (ΔG_{298} = -6.9 ÷ -3.9 kcal mol^{-1}). As a result, the free energy changes in the sequence of transformations **4** → **7** + CH_2=CHR″ are ΔG_{298} = 4.3 ÷ 10.7 kcal mol^{-1}. For the process as a whole (**1** + RH → **7** + CH_2=CHR″), the ΔG_{298} values were found to be 8.3 ÷ 13.6 kcal mol^{-1}. The cleavage of the C–C bond of the linear alkanes by the mechanism depicted at Scheme 1 turns out to be thermodynamically unfavorable and therefore the mild hydrogenolysis of alkanes on Zr(IV) monohydrides is extremely unprobable.

Scheme 2

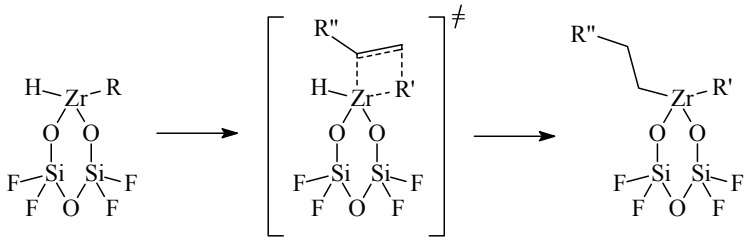

8 **9** **10**

The key (rate-determining) step of the mechanism of the catalytic hydrogenolysis of alkanes on Zr(IV) dihydride centers **2** is presented in Scheme 2. The cleavage of the aliphatic β-C–C bond in alkylhydrides **8** via transition states **9** requires an overcome of the energy

barriers ($\Delta G_{298}^{\neq}$ = 32.0 ÷ 34.1 kcal mol^{-1}) close to that found for the analogous process on the monohydride centers **1**. However, there's an important difference between dihydrides **2** and monohydrides **1** as catalytic centers. Namely, the relaxation of the transition state **9** leads directly to the zirconium dialkyl species **10**, bypassing the stage of the formation of olefin complexes. In the other words, the coordinated olefin molecule CH(R″)=CH$_2$ shifts from the alkyl fragment R′ toward the hydride ligand in the process of relaxation of **9** with the subsequent formation of the H–CH(R″)CH$_2$ bond at the one side and CH(R″)CH$_2$–Zr at the other side. Due to this fact, the transformation **8** → **10** considerably lowers the free energy of the system (ΔG_{298} = -11.3 ÷ -7.3 kcal mol^{-1}), the lowering being more pronounced in case of the *β*-methyl migration compared to the migration of the *β*-ethyl fragment. The influence of the R″ fragment structure on the energetics of this process is negligible. The estimation of the rate constants of the rate-determining step of the reaction and the equilibrium constants between the reagents and the products reveals that the process of the hydrogenolysis of linear alkanes on dihydride centers **2** is thermodynamically favorable and may proceed with noticeable rates under the experimental conditions normally used (T = 423K).

Taking into the account the fact that some amounts of Zr(III) compounds are always present in the real Yermakov-Basset catalytic system, we have considered the possibility for the silica-supported Zr(III) hydrides (≡Si-O)$_2$Zr^{III}H to catalyze the process under study, using the model compound **3**. The sequence of transformations leading to the cleavage of the C–C bond of alkane is presented in Scheme 3.

Scheme 3

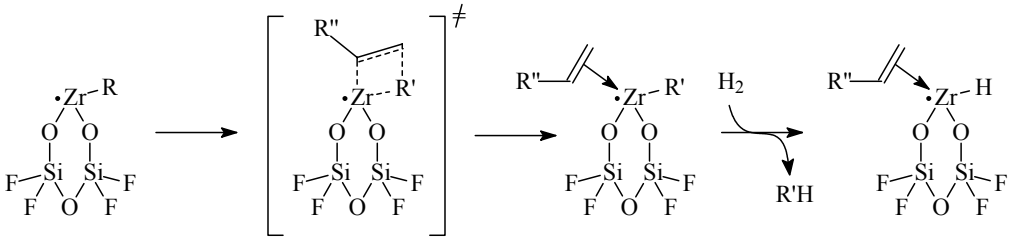

11 **12** **13** **14**

The cleavage of the aliphatic C–C bond in the intermediates **11** via transition states **12** leads to the complexes **13**. These transformations require an overcome of considerably lower energy barriers ($\Delta G_{298}^{\neq}$ = 23.8 ÷ 25.6 kcal mol^{-1}) compared to the C–C bonds cleavage on Zr(IV) hydrides. The great degree of coordinative unsaturation of Zr in compounds **11** makes the *β*-alkyl migration, which leads to the fulfilling of the coordinative vacancy of Zr exceptionally favorable from the thermodynamic point of view. The PES study of the **13** + H$_2$ system revealed that the compounds **13**, unlike the corresponding complexes of Zr(IV), are

able to come into the exchange reaction with the hydrogen molecule, leading to the substitution of the R′ ligand to the hydride while retaining the olefin molecule CH_2=CHR″ coordinated. These transformations (**13** → **14**) require an overcome of the energy barriers ($\Delta G_{298}^{\neq}$ = 22.1 ÷ 24.8 kcal mol^{-1}) comparable to the barriers for the *β*-alkyl migration and are accompanied by the energy gain (ΔG_{298} = -5.6 ÷ -3.2 kcal mol^{-1}). The insertion of the coordinated olefin molecule to the Zr–H bond followed by the exchange of the alkyl ligand to the hydride allows the catalytic cycle to restart.

The comparison of the mechanisms and the energy profiles of the reactions of the model compounds **1**–**3** with RH lets us conclude that the hydrogenolysis of linear alkanes on Zr(IV) monohydrides $(\equiv Si–O)_3ZrH$ is unlikely to proceed efficiently as the process turns out to be thermodynamically unfavorable. Contrary, Zr(IV) dihydrides $(\equiv Si–O)_2ZrH_2$ and Zr(III) hydrides $(\equiv Si–O)_2Zr^{III}H$ are able to act as the catalysts of the hydrogenolysis of linear alkanes under the conditions experimentally used by Basset *et.al.* [2-4].

References:

[1] Quignard F., Lecuyer C., Choplin A. and Basset J.-M., *J. Chem. Soc. Dalton Trans.,* (1994) 1153.
[2] Corker J., Lefebvre F., Lecuyer C., Dufaud V., Quignard F., Choplin A., Evans J. and Basset J.-M., *Science*, 271 (1996) 966.
[3] Lefevbre F., Thivolle-Cazat J., Dufaud V., Niccolai G. P. and Basset J.-M., *Appl. Catal.*, 182 (1999) 1.
[4] Lefebvre F. and Basset J.-M., *J. Mol. Catal.*, 146 (1999) 3.
[5] Zakharov V.A., DudchenkoV.K., Kolchin A.M. and Yermakov Yu.I., *Kinet. Catal.*, 16 (1976) 808.
[6] Zakharov V.A., DudchenkoV.K., Minkov A.I., Efimov O.N., Khomyakova L.G., Babenko V.P. and Yermakov Yu.I., *Kinet. Catal.*, 17 (1976) 643.
[7] DudchenkoV.K., Echevskaya L.G., Bukatov G.D. and Yermakov Yu.I., *Kinet. Catal.*, 19 (1978) 278.
[8] Zakharov V.A., Dudchenko V.K., Paukshtis E.A., Karakchiev L.G. and Yermakov Yu.I., *J. Mol. Catal.*, 2 (1977) 421.
[9] Ustynyuk L.Yu., Ustynyuk Yu.A., Laikov D.N. and Lunin V.V., *Russ. Chem. Bull., Int. Ed.*, 50 (11) (2001) 2050.
[10] Ustynyuk L.Yu., Besedin D.V., Lunin V.V. and Ustynyuk Yu.A., *Fiz. Khim.*, 2003, in press.
[11] Besedin D.V., Ustynyuk L.Yu., Ustynyuk Yu.A. and Lunin V.V. *Organometallics*, 2003, in press.

A DFT STUDY OF THE WATER EFFECT ON CATALYTIC BEHAVIOUR OF Cp_2TiCl_2/AlR_2Cl SYSTEM

Fushman E.A.[1], Ustynyuk L.Yu.[2], Margolin A.D.[1], Lalayan S.S.[1]

[1]Semenov Institute of Chemical Physics RAS, Moscow, Russia
Fax: (095)135-1521; E-mail: elga@polymer.chph.ras.ru
[2]Department of Chemistry, Lomonosov Moscow State University, Moscow, Russia

The homogeneous systems $CoX_2/AlEt_2Cl$ have been the first metal-complex catalysts for which exhaustive removal of H_2O resulted in complete lost of the catalytic activity (in diene polymerization) [1, a-c]. Meanwhile, the addition to the desiccated system of minute amounts of water (in the ppm range) restored the activity [1 c] (these studies were performed in the middle of 60's). According to ref. [1a], water has the function of a Lewis base in the system $CoCl_2$/ethylaluminium sesquichloride and must present to enable the formation of the active species.

Later (in 70's), it has been found that the same situation occurs in the ethylene polymerization with the systems Cp_2TiCl_2/AlR_2Cl and $Cp_2TiEtCl/AlEtCl_2$. They become inactive after removal of the traces of water, while their activity regains when water is added [2 a-d]. In particular, Reichert and Meyer reported [2 a] that the rate of the ethylene polymerization with the $Cp_2TiEtCl/AlEtCl_2$ catalyst system increased with an increase in the concentration of water. Analysis of the data of ref. [2 a], let us to conclude [3] that it is the concentration of water that determines the number of C^* in the experiments of Reichert and Meyer, that is, $[C^*] = [H_2O]$.

The positive effect of water was explained by both the formation of chloralumoxanes *via* hydrolysis [2b, 4] and formation of $AlCl_3$ via dismutation process ($AlEtCl_2 \cdot H_2O + AlEtCl_2 \rightarrow AlCl_3 \cdot H_2O + AlEt_2Cl$) [2d]. In this contribution authors considered theoretically adducts of $Cp_2TiMeCl$ both with $AlMeCl_2$ and with the products formed from this component in the presence of H_2O, namely, with $AlCl_3$, $Cl_2AlOAlCl_2$, and complexes $AlCl_3 \cdot Cl_2AlOAlCl_2$ and $AlMeCl_2 \cdot Cl_2AlOAlCl_2$ (scheme 1)

Criteria for activity of ion pairs given in recent papers of Marks et al [5a,b] were taken into consideration. First, dramatic increase in polymerization activity of ion pairs $LL'Mt(R)^+$--F-PBA^- (Mt=Ti, Zr; PBA-perfluobiphenylaluminate) was observed [5a] if the ligands L afford weakening of ion pairing. Second, through analysis of experimental and calculation data, it was found [5b] that increasing energy of formation (ΔH_{form}) of the Ti-CH_3-B bridged adduct of $R_2Si(R'\text{-}Cp)(R''NTi(CH_3)R'''$ with $B(C_6F_5)_3$ and increasing (even moderate) the length of the Ti-CH_3 bridge bond in this adduct result in the important increase

in polymerization activity. Third, this increase was found [5b] to correlate with the decrease of energy of heterolytic dissociation (ΔH_{ips}).

Scheme 1

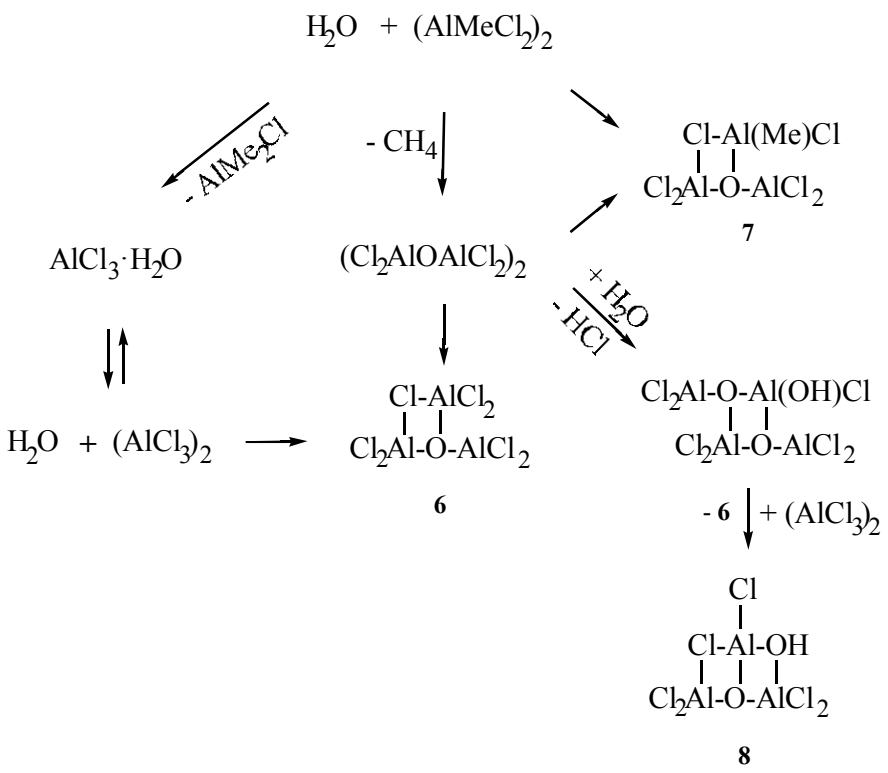

On analyzing Ti-Al adducts we considered aforementioned criteria and also some others: energy gain due to adding anion Cl^- to Al-containing Lewis acid, the difference in length of Ti-Cl and Cl-Al bonds in the bridge, and the Cl-Al length in an anion.

All criteria testify that the adducts of $Cp_2TiMeCl$ with $AlCl_3$, $AlCl_3 \cdot Cl_2AlOAlCl_2$, and $AlMeCl_2 \cdot Cl_2AlOAlCl_2$ are more active than that with the starting compound $AlMeCl_2$. The most promising precursor for active site is the adduct $Cp_2Ti(Me)..Cl..AlCl_2\text{-}OAl_2Cl_5$ (Fig. a and b). It has greatest ΔH_{form}, lowest ΔH_{ips}, the longest Ti-Cl bridge bond, the most difference in Ti-Cl and Cl-Al bonds, greatest stabilization of anion with minimal Cl-Al distance and besides the unfavourable oxygen atom in this adduct is shielded (contrary to the adduct with individual alumoxane Al_2OCl_4). Shielding is achieved due to complexed $AlCl_3$ (as does $AlMe_3$ in the MAO-based moieties proposed by us earlier [3]).

One way of looking at the structure of this "optimal" adduct is in terms of the ion pair $[Cp_2TiMe]^+[Al_3Cl_8O]^-$. In such a representation, anionic part is the anion characterized by X-ray diffraction structural analysis [6]. Calculated geometric parameters of the anion

$[Al_3Cl_8O]^-$ are agree (with an accuracy of 2-4%) with experimental values. This agreement lends support to the validity of the calculation procedure used in our analysis.

Fig. Isomers of the adduct $Cp_2TiMeCl$ with $AlCl_3 \cdot Cl_2AlOAlCl_2$

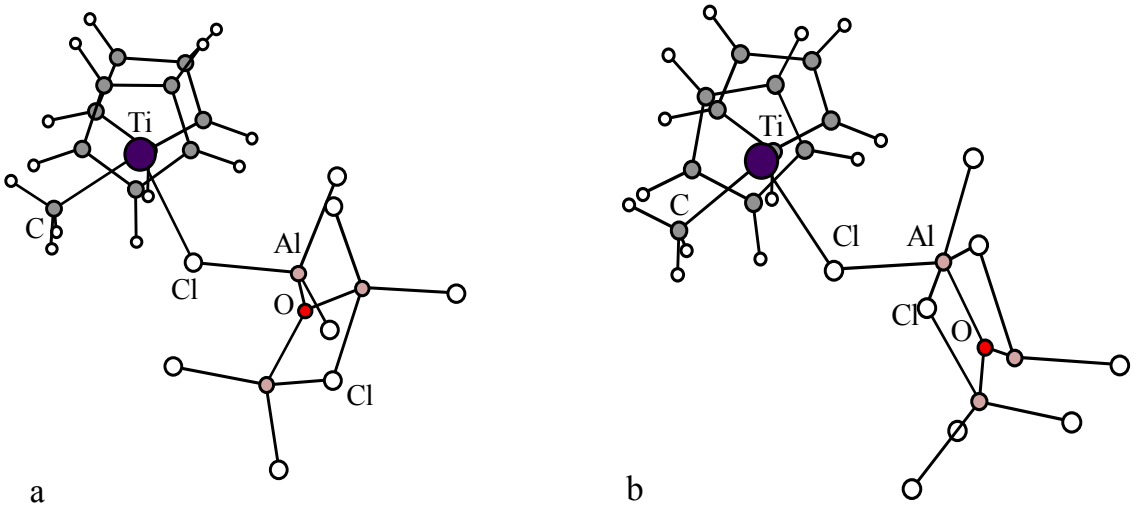

The data obtained explain the majority of peculiarities in polymerization characteristics: a) why super-dried systems Cp_2TiCl_2/AlR_2Cl and $Cp_2TiRCl/AlRCl_2$ are inactive, b) the regimes in which polymerization rate is virtually independent of both dozing components (Ti and Al), c) why the polymer precipitation is accompanied by a dramatic growth in polymerization rate, c) why bi-modal MMD is observed in certain cases, etc.

It is known that chlorine-containing Al-compounds are not able to activate zirconocenes, contrary to titanocene complexes considered above. On substituting Ti with Zr atom in adducts whose criteria were the best, it was found that ΔH_{form} of $[Cp_2ZrMe]^+[Al_3Cl_8O]^-$ is essentially lower (by 5-10 kcal/mole) and ΔH_{ips} higher as compared with these parameters for Ti. For this reason the Zr-complexes should be less active in conjunction with chloroaluminum compounds than their Ti-analogues.

On the basis of aforementioned criteria, chlorine-Al-components containing Me-group (not only $AlMeCl_2$ but also its complex with alumoxane $AlMeCl_2.Cl_2AlOAlCl_2$) should be the less efficient activators than those containing stronger Lewis acid $AlCl_3$. This is in line with finding of Meizlik et al [4] that increasing the number of ethyl groups in the product of hydrolysis of $EtAlCl_2$ leads to considerable loss of activity in ethylene polymerization.

At the same time, the productivity of the titanocenes-MAO catalyst was almost two order of magnitudes higher than the productivity of Cp_2Ti-based compounds activated by

Cl-Al-derivatives [7]. However, in [7], MAO emerged its unique potential at [Al]:[Ti] ratio about 3000. It is believed that a minor quantity of MAO units are extremely acidic or MAO ensures some other type of activation process.

Computational Details

DFT calculations within this contribution were carried out using an original program PRIRODA developed by D.N. Laikov [8]. The generalized gradient approximation for the exchange-correlation functional by Perdew, Burke, and Ernzerhof [9] is employed. The orbital basis sets of contracted Gaussian-type functions of size (4s)/[2s] for H, (8s4p1d)/[4s2p1d] for C and O, (15s11p2d)/[10s6p2d] for Al and Cl, (17s13p8d)/[12s9p4d] for Ti is used for the remaining electrons in conjunction with the density-fitting basis sets of uncontracted Gaussian-type functions of size (4s1p) for H, (7s2p2d) for C and O, (14s3p3d1f1g) for Al and Cl and (18s6p6d5f5g) for Ti. Full geometry optimization of all structures is performed using analytical gradients and is followed by analytical calculations of the second derivatives of energy with respect to coordinates in order to characterize the nature of the resulting stationary points (minima or saddle points) on the potential energy surface.

Acknowledgements This work was financially supported by the Russian Foundation for Basic Research (projects nos. 01-03-33307 and 02-03-32781) and the Complex Program for Scientific Research in 2001-2002 of the Russian Academy of Sciences (subprogram Basic Studies of Chemical Bonding and Chemical Structure).

References:

[1] a) Van de Kamp F.P. *Makromolek. Chem*., 93 (1966) 202; b) Sinn H., Von Tirpitz W. *Makromolek. Chem.,* 85 (1965) 280; c) Volkov L.A., Medvedev S.S. *Dokl. Akad. Nauk SSSR,* 184 (1969) 125.

[2] a) Reichert K.H., Meyer K.R. *Makromol. Chem*., 169 (1973) 163; b) Long W.P., Breslow D.S. *Liebigs Ann.Chem*., 3 (1975) 463; c) Cihlar J., Mejzlik J., Hamrik O. *Makromol.Chem*., 179 (1978) 2553; d) Borisova L.F., Fushman E.A., Shupik A.N., Vizen E.I., Sosnovskaya L.N., Lalayan S.S. *Vysokomol. Soed. (Russian),* A 23 (1981) 1984.

[3] Margolin A.D., Fushman E.A., Lalayan S.S., L'vovskii V.E. *Polymer Science (Russian),* A 38 (1996) 1812.

[4] Cihlar J., Mejzlik J., Hamrik O., Hudec P., Majer J. *Makromol.Chem*., 182 (1981) 1127.

[5] a) Chen E.Y.-X., Stern C.L., Marks T.J. *J.Am.Chem.Soc.,* 119 (1997) 2582; b) Lanza G., Fragala I.L., Marks T.J. *J.Amer.Chem.Soc*., 122 (2000) 12764.

[6] Thewalt U., Stollmaier F. *Angew.Chem.Suppl*., (1982) 211.

[7] Conti G., Arribas G., Altomare A., Ciardelli F. *J.Mol.Cat.,* 89 (1994) 41.

[8] Laikov D.N. *Chem. Phys. Lett*., 281 (1997) 151.

[9] Perdew J.P., Burke K., Ernzerhof M. *Phys. Rev. Lett.*, 77 (1996) 3865.

NEW BIS(CYCLOALKYL-ARYLIMINO)PYRIDYL COMPLEXES AS COMPONENTS FOR ETHYLENE POLYMERIZATION CATALYSTS

Ivanchev S.S.[1], Tolstikov G.A.[2], Badaev V.K.[1], Oleinik I.I.[2], Ivancheva N.I.[1], Rogozin D.G.[1], Oleinik I.V.[2], Myakin S.V.[1]

[1]St-Petersburg Department of the Boreskov Institute of Catalysis SB RAS, St-Petersburg, Russia
Fax: +7 812 2330002; E-mail: ivanchev@SM2270.spb.edu
[2]Vorozhtzov Institute of Organic Chemistry SB RAS, Novosibirsk, Russia

13 novel cycloalkyl-substituted 2,6-bis(arylimino)pyridyl complexes of the general formula

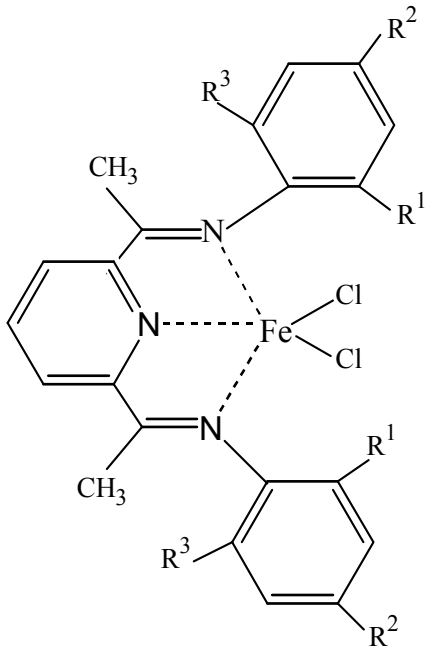

(R^1=cyclopentyl, cyclohexyl, cyclooctyl, cyclododecyl; R^2 = Me, H; R^3 = the same cycloalkyl as R^1, Me, H) are prepared by reacting the corresponding 2- or 2,6-cycloaliphatic amines with iron chloride. The composition and structure of the synthesized compounds are confirmed by elemental analysis, NMR- and IR-spectroscopy and 3D structure is simulated by molecular mechanics using HyperChem computer program.

The obtained catalyst systems are studied in homogeneous ethylene polymerization using methylalumoxane (MAO) as a cocatalyst in toluene at 30-80 °C, 0.3 MPa, MAO:Fe=1500:1. Their activity is found to grow with the increase of methylene units number in the cycloalkyl substituents, with this growth being more prominent at elevated

temperatures. The polymerization is featured with non-stationary kinetics depending on the number of cycloalkyl substituents in the ortho-positions of the aryl ring.

Generally the comparison of the achieved polymer yields with the reference data indicates that these novel cycloalkyl-substituted bis(arylimino)pyridyl ligands provide catalyst systems retaining quite high polymerization activity at commercially applied increased temperatures.

The developed catalysts afford high density polymers with MW slightly depending on the cycloalkyl substituent size and decreasing with the polymerization temperature growth.

Supporting of the prepared complexes onto SiO_2 subjected a special pretreatment allows performing the polymerization with the cocatalyst replaced by $Al(C_4H_9)_3$ and decrease of the total cocatalyst amount up to Al:Fe ~ (50-100):1.

In contrast to homogeneous processes, the efficiency of the supported catalysts in slurry and gas phase polymerizations drops with the increase of the cycloalkyl substituent size. The supported catalyst initiated polymerization proceed with almost stationary kinetics yielding polymers with MW approaching super-high levels and being easily controlled via H_2 addition. The resulting polymers are featured with quite broad MWR and strength performances similar to those for commercial brands of gas phase polyethylene for pipe applications.

HYDROGENATION OF ACETYLENE ALCOHOL WITH Pd AND Pd-Au COLLOIDAL CATALYSTS PREPARED IN BLOCK-COPOLYMERS MICELLE

Sulman E., Matveeva V., Sulman M., Bykov A., Demidenko G., Doluda V., Bronstein L., Chernyshov D., Valetsky P.

Department of Biotechnology and Chemistry, Tver Technical University, Tver, Russia
Fax: (0822)449317; E-mail:sulman@online.tver.ru

Polymeric catalysts, both organometallic polymers and polymer-protected, colloidal noble metals are of great interest since they are very promising for many catalytic applications [1-3]. Pd-, Rh-, and Pt-containing polymer systems were studied as catalysts for olefin hydrogenation [4, 5], however no paper was related to polymer catalysts dealing with hydrogenation of long chain acetylene alcohols which are intermediate products in preparation of some important vitamins and fragrant substances.

Linalool (LN, 3,7-dimethyl-octadiene-1,6-ol-3), the product of selective hydrogenation of dehydrolinalool (DHL, 3,7-dimethyl-octaene-6-yne-1-ol-3) is a fragrant substance of terpenic series. This is also a part of many cosmetic preparations and a number of scent compositions. The selective hydrogenation of triple bond to double one is one of the steps of LN syntheses (see Scheme 1). When hydrogenation goes on non-selectively, LN transforms into dihydrolinalool (DiHL, 2,6-dimethyl-octen-2-ol-6), which are possible side products of these reactions.

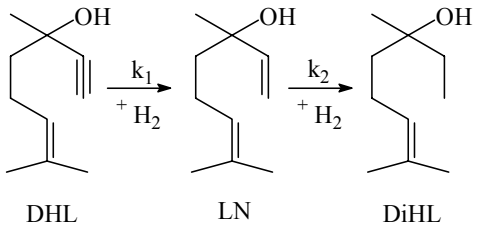

Scheme 1. Acetylene alcohols hydrogenation processes

Selective hydrogenation of acetylene compounds to olefins (including, alcohols) was mainly carried out with supported Pd catalysts, such as Pd/C, Pd/SiO_2, $Pd/CaCO_3$, Pd/Al_2O_3 and others, modified with organic (for example, pyridine, quinoline) and inorganic (Zn, Cd, Pb and other salts) substances [6-12]. Such a modification allowed to increase the selectivity of hydrogenation, but resulted in polluting the end products with the modifiers.

Another imperfection of this way of modification was poor stability of such catalysts: modifiers adsorbed on the catalyst surface often left the surface during usage, thus decreasing the catalyst selectivity. Previously we have developed for the first time the synthesis of

Pd-containing polymers derived from polystyrene-polybutadiene triblock copolymers (SBS) and bis(acetonitrile) palladium chloride (SBS-Pd) [13, 14]. These polymers deposited on Al_2O_3 seemed to be catalytically active in hydrogenation of dehydrolinalool [14] and allowed to reach 98.7 % selectivity without any modification. Recently a novel type of Pd-polymer catalysts was elaborated [15, 16] via synthesis of Pd colloids in cores of block copolymer micelles derived from polystyrene-poly-4-vinylpyridine (PS-b-P4VP) in selective solvents (toluene, THF). The present report is focused on the study of Pd and Pd-Au colloidal catalyst synthesized in PS-b-P4VP micelles in preparations of linalool.

The preparation of Pd colloids stabilized in block copolymer micelles in toluene was described elsewhere [15]. The reactor for hydrogenation was described in [14]. DHL concentration (C_o), catalyst amount (C_c) and hydrogenation temperature (T_h) have been varied: C_o from 33.4 to 250.8 g/L for DHL, C_c from 1.67 to 5.00 g/L for DHL and T_h from 50 to 95°C. The experiments were carried out at atmospheric pressure. The optimal conditions for hydrogenation were chosen experimentally. The best selectivity in DHL hydrogenation (99.8%) was achieved at C_o = 66.6 g/L, C_c = 3.33 g/L in toluene at 90 °C.

Based on kinetics, relative rates, r, of DHL hydrogenation which are the relation of reaction rate at 20 % of hydrogen uptake to catalyst and DHL amounts were calculated. The Table includes these values for the processes carried out both over the catalyst studied and conventional Pd catalysts under the same optimal conditions. Comparing these results one can see that the reaction rates are much smaller for traditional catalysts at the same selectivity.

Table 1

The relative rates of DHL hydrogenation over different Pd catalysts
(20% hydrogen uptake, solvent - toluene)

Catalyst	DHL hydrogenation rate, $m^3 H_2/(g\ Pd \cdot mol\ DHL \cdot s)$
Pd colloidal catalyst	0.55
Pd-Au colloidal catalyst	1,31
Pd/Al_2O_3	$3.2 \cdot 10^{-2}$
$Pd/CaCO_3$	$5.9 \cdot 10^{-3}$

The mathematical treatment of kinetic data carried out in the way depicted in [17] shows that formally all experimental results for DHL can be well-described by the equation 1 (Pd colloidal catalyst) and 2 (Pd-Au colloidal catalyst):

$$W = k\,, \tag{1}$$

$$W = \frac{kx_1}{(x_1 + Qx_2)^2} \tag{2}$$

where k is the kinetic parameter; x_1 is the acetylene alcohol concentration; x_2 is the olefin alcohol concentration; Q is the adsorption parameter. $Q = K_2/K_1$ where K_2 and K_1 are the adsorption equilibrium constants of olefin alcohol (linalool) and acetylene alcohol (dehydrolinalool), respectively. Thus, the denominator of equation (2) characterizes the substrate adsorption. For graphic construction of the curves the parameter θ was used which is a relative time: $\theta = \tau'/q$, τ' - current reaction time, $q = C_o / C_c$ (see Fig. 1). These figures demonstrate a good agreement of calculated curves and experimental data. For each q value the total time τ required for the reaction completion is also shown.

The influence of solvent nature on catalytic properties of Pd and Pd-Au colloidal catalyst was studied. Maximum relative rate was found to be in methanol, but the highest selectivity was achieved in toluene. Indeed, toluene is a selective solvent for PS-b-P4VP providing a complete dissolution of PS corona and maximum accessibility of active centers located in micelle cores.

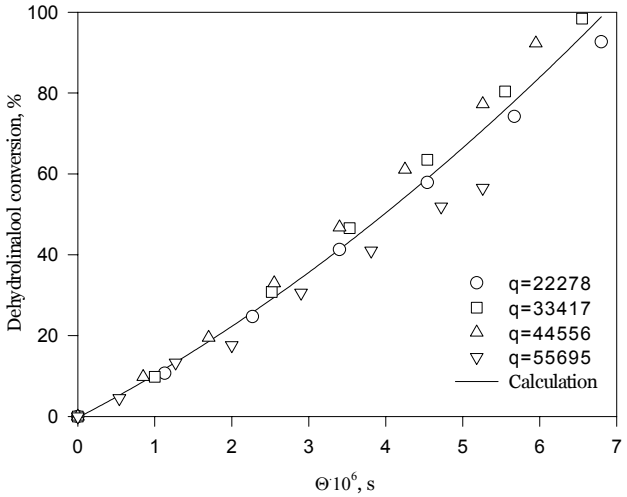

Fig. 1. Dependence of DHL conversion on relative time (for Pd-Au colloidal catalyst)

Conclusion

Mono-(Pd) and bimetallic (PdAu) colloids formed in the PS-*b*-P4VP block copolymer micelles were studied in DHL hydrogenation. FTIR spectra of CO adsorbed on PdAu sample show only one band for terminal adsorption. This testifies the presence of only Pd atoms on the PdAu nanoparticle surface and existence of only one type of active centers. Based on

FTIR and XPS data, it can be concluded that the modifying metal (Au) influences both electronic properties and surface geometry of the particles. Due to this influence, the catalytic activities of bimetallic catalyst are different and higher then for Pd catalyst, the optimal conditions were found allowing the high selectivity of hydrogenation up to 99.8%, which is mainly determined by the modifying influence of pyridine groups in the P4VP cores. The study of the kinetics of DHL hydrogenation with catalysts developed allowed us to suggest the hypothesis for hydrogenation mechanism, which fits well to computational kinetic models.

Acknowledgments

We sincerely thank NATO Science for Peace Programme (grant SfP - 974173) and Russian Foundation for Basic Research (grant 01-03-32937) for financial support.

References

[1] Holy N.L., Shelton S.R., *Tetrahedron*, 37 (1981) 25
[2] Sobczak J.W., Wernish J., *J. Phys. Chem.*, 137 (1983) 119
[3] Warshavsky A., Kramer R., Levy M., *Ind. Eng. Chem. Res*., 34 (1995) 2821
[4] Komiyama M., Ohtaki M. *J. Coord. Chem*., 18 (1988) 185
[5] Mayer A.B.R., Mark J. E., *Colloid. Polym. Scie*., 275 (1997) 333
[6] Tedeschi R.J., Clark V., *J. Org. Chem.,* 27 (1962) 12
[7] Wells P.B., *Platinum Met. Rev.,* 7 (1963) 1
[8] Rajaram J., Narula A.P.S., Chawla H.R.S., Sukh D. *Tetrahedron*, 39 (1983) 13
[9] Patent Application N 56-150022 (Japan). C.A. 1982. V.96. N 48. 143512m.
[10] Patent Application N 2311767 (France). C.A. 1977. V.86. N 17. 72026m.
[11] Patent Application N 57-185229 (Japan). C.A. 1983. V.98. N 17. 142934e.
[12] Patent Application N2431929 (Germany). C.A. 1976. V.84. N 21. 150183k.
[13] Mirzoeva E.Sh., Bronstein L.M., Valetsky P.M., Sulman E.M., *Reactive Polymers*, 24 (1995) 243
[14] Sulman E.M., Matveeva V.G., Bronstein L..M., Ankudinova T.V., Mirzoeva E.Sh., Sidorov A.I., Valetsky P.M. *Russ. Chem. Farm. J*, 5 (1995) 149
[15] Antonietti M., Wenz E., Bronstein L., Seregina M. *Adv. Mater.,* 7 **(**1995**)** 1000
[16] Seregina M. V., Bronstein L.M., Platonova O. A., Chernyshov D.M., Valetsky P.M., Hartmann J., Wenz E., Antonietti M. *Chem. Mater*., 9 (1997). 923
[17] Yermakova A., Anikeev V.I., Bobrin A.S. *Appl. Catal*., 101 (1993) 25

OXIDATIVE DEHYDROGENATION OF BUTANE ON NANOCRYSTALLINE MgO, Al_2O_3 AND VO_x/MgO CATALYSTS IN THE PRESENCE OF SMALL AMOUNTS OF IODINE

Chesnokov V.V.[1], Bedilo A.F.[2], Heroux D.S.[2], Mishakov I.V.[1], Klabunde K.J.[2]

[1]Boreskov Institute of Catalysis SB RAS, Novosibirsk, Russia
Phone: (3832) 34-49-01; Fax: (3832)-34-30-56; E-mail: chesn@catalysis.nsk.su
[2]Department of Chemistry, Kansas State University, Manhattan, Kansas, USA

A large number of studies are devoted to development of new dehydrogenation catalysts and improvement of the existing ones. Of special interest are catalysts for dehydrogenation of n-butane to butadiene. There are several specific features of dehydrogenation reactions that limit choices of the reaction conditions, process engineering and type of catalysts. Dehydrogenation reactions of paraffins and olefins are very endothermic. The yields of desired products are usually limited by equilibrium conditions. Acceptable yields are typically achieved only above 520 °C for dehydrogenation of paraffins and above 570 °C for dehydrogenation of olefins. Therefore, dehydrogenation processes are usually carried out at very high temperatures (550-620 °C) where cracking of the hydrocarbons and carbon deposition on the catalysts become significant. In order to decrease the partial pressure of the starting hydrocarbons and increase the yield of the desired products, one-stage dehydrogenation of n-butane to butadiene is performed under vacuum over alumina-chromium catalysts.

Our analysis of available approaches to butane dehydrogenation indicates that prospects for improvement of the conventional dehydrogenation method seem to be exhausted since butene and butadiene yields achieved are very close to the corresponding equilibrium values. In most processes employed, the butadiene content in the dehydrogenated C_4 stream from the reactor after separation of other byproducts is limited to about 20 percent.

In the last few years numerous papers have appeared devoted to oxidative dehydrogenation of propane and butane (1-6). Oxidative dehydrogenation of these hydrocarbons has a number of advantages in comparison with conventional dehydrogenation, such as high exothermicity that eliminates the need for heat supply to the reactor, removal of the thermodynamic limitations on the yield of the desired products, decrease of the reactor temperature and lower yields of side reactions (cracking and carbon deposition). Oxidative dehydrogenation of butane is usually performed over catalysts containing VO_x or MoO_y on various supports. The best results so far have been obtained on a VO_x/MgO system. However,

the main problem of oxidative dehydrogenation – improvement of the selectivity to butadiene – remains unsolved.

In the present communication we demonstrate an increase in butadiene selectivity of this process by performing oxidative dehydrogenation in the presence of small amounts of iodine. The idea of "iodine dehydrogenation" was popular in the 60s and 70s. The key reagent in this case is molecular iodine that reacts with butane and butenes at about 500 °C to form butadiene and HI (7, 8). This idea was first researched by Shell Development at Emeryville, California, leading to a process concept known as Temescal.

Further development of this approach involved introduction of an HI acceptor that could be easily regenerated by oxygen or air (9). Many different oxides and hydroxides can be used as HI acceptors. The following reactions take place in the case of a group II metal oxide:

$$C_4H_{10} + I_2 + MO \rightarrow C_4H_8 + MI_2 + H_2O \quad [1]$$

$$C_4H_8 + I_2 + MO \rightarrow C_4H_6 + MI_2 + H_2O \quad [2]$$

$$2\ MI_2 + O_2 \rightarrow 2\ MO + 2\ I_2 \quad [3]$$

The use of an acceptor that reacts with HI easily and completely shifts the equilibrium of the dehydrogenation reactions to the right and makes it possible to achieve high butane conversion with high selectivity to butadiene.

Shell scientists have suggested a process based on the acceptor circulation in the reactor (10). In this case, the acceptor was introduced into the bottom part of the reactor where it was regenerated with oxygen or air to yield molecular iodine. Then, it was transferred to the middle section of the reactor where it was mixed with butane. Butane dehydrogenation took place in the top part of the reactor with the formation of C_4H_6, HI and some by-products. HI formed in the reaction was absorbed by the acceptor. Then the gas-solid mixture was subjected to separation in cyclones, and the acceptor recovered was returned into the reactor. Despite the above advantages of oxidative iodine dehydrogenation, this method proved to be economically adverse due to significant losses of iodine and its high cost. Due to iodine high concentrations used, the yield of iodinated hydrocarbons could reach 0.10-0.15 kg per 1 kg of butadiene (11).

In this communication we suggest a different approach. In order to increase the efficiency of iodine-mediated oxidative dehydrogenation, we suggest combining the HI destructive adsorption by acceptor and I_2 regeneration in one place. This requires the catalyst-acceptor to have oxidative properties and significant amounts of oxygen to be present in the feed.

Nanocrystalline metal oxides prepared by a modified aerogel procedure developed in our laboratory at KSU are known to have high surface areas, small crystallite sizes, unusual morphology, and enhanced adsorption properties in comparison with conventionally prepared materials. These properties make them very good candidates for various applications as catalysts and catalyst supports. In the present communication we report our first results on the use of nanocrystalline MgO, Al_2O_3 and MgO*Al_2O_3 as butane dehydrogenation co-catalysts and use of nanocrystalline AP-MgO as a support for vanadium in the same reaction.

The performance of different catalysts in iodine-mediated oxidative dehydrogenation was studied in a 10 cm^3 quartz flow reactor. The reactor was placed inside an electrical furnace. The reaction was carried out at 500-580 °C. The catalyst loadings were varied between 0.05 and 0.8 g. The feed flow rate was 10 l/h. The catalysts were diluted with quartz powder to prevent removal of the oxide particles by the gas flow. The composition of feed (vol. %) was 92.5 % He: 2.5 % C_4H_{10}: 5 % O_2. The iodine concentration in the feed was varied between 0 and 0.25 vol. %.

High surface area nanocrystalline MgO, Al_2O_3 and MgO-Al_2O_3, commercial MgO, and a series of 10 % VO_x/MgO samples have been used as catalysts in one-step selective oxidative dehydrogenation of butane to butadiene in the presence of oxygen and iodine. Molecular iodine shifts the equilibrium of the dehydrogenation reactions to the right and makes it possible to achieve high butane conversion with high selectivity to butadiene. When excess oxygen is present in the feed, iodine is completely regenerated and can be recycled. Butadiene selectivity as high as 67 % has been achieved in the presence of small amounts of iodine (0.25 vol. %) over a vanadia-magnesia catalyst at 56 % butane conversion. The best performance has been observed over a catalyst containing magnesium orthovanadate phase.

The results obtained in this study for iodine-mediated oxidative dehydrogenation of butane over vanadia-magnesia catalysts are very promising for future practical application of this approach. Very high selectivity to butadiene can be achieved in the presence of iodine. When excess oxygen is present in the feed, molecular iodine is successfully regenerated and can be recycled. Besides butadiene, this method can be applied for synthesis of many other olefins, e.g. propene, isobutene or isoprene.

Acknowledgment

The financial support of the US Army Research office, CRDF (Project RC1-2340-NO-02) and RFBR (Project 00-15-97440) is acknowledged with gratitude.

References

1. Tellez, C., Abon, M., Dalmon, J.A., Mirodatos, C., and Santamaria, J., *J. Catal*., **195**, 113 (2000).
2. Pa, K. C., Bell, A.T., and Tilley, T.D., *J. Catal*., **206**, 49 (2002).
3. Chaar, M.A., Patel, D., and Kung, H.H., *J. Catal*., **109**, 483 (1987).
4. Kung, H.H., *Adv. Catal*., **40**, 1 (1994).
5. Kung, H.H, and Kung, M.C., *Appl. Catal. A,* **157**, 105 (1997).
6. Blasco, T., Lopez-Nieto, J.M., Dejoz, A., and Vazquez, M.I., *J. Catal*., **157**, 271 (1995).
7. Canadian Patent 576.172. (18/2/55) Shell Development Co.
8. U.S. Patent 2,890,253 (16/5/56) Shell Development Co.
9. British Patent 895.500 (29/12/59) Shell International Research Maatschappij N.V.
10. King, R.W., *Hydrocarbon Processing* **45** (11). (1966) 189.
11. King, R., *Process Engineering,* March, (1977) 85.

CONTROL OF HETEROGENEOUS BASE CATALYST ACTIVITY USING MATERIALS SYNTHESIS BY DESIGN

Bass J.D., Anderson S.L., Parra-Vasquez N., Katz A.

Department of Chemical Engineering, University of California at Berkeley, Berkeley, California, USA
E-mail: katz@cchem.berkeley.edu

Introduction

A general characteristic of biological catalysts (enzymes) has been their ability to induce large rate enhancements via organization of chemical functionality on the nanoscale. One of the most common organizational motifs used by enzymes has been the placement of an acid-base pair in close proximity to one another within a catalytically active site. These two moieties can function in concert during catalysis to polarize a substrate for nucleophilic attack using the acid while simultaneously conducting nucleophlic attack with the base. This acid-base charge-relay results in a significantly higher effective pKa of the base during catalysis than would be possible in the case without the acid in close proximity. We wish to reproduce the acid-base relay found in enzymes in a synthetic material. Our approach is to use the templating of bulk silica as a tool to synthesize base catalysts with and without accessible silanol groups that can act as acids, which is possible because catalyst immobilization using a templating strategy does not use silanols for anchoring.

Model base-catalyzed reactions for exploring the role of acid-base pairing in the catalytic materials were chosen. The Knoevenagel C-C bond-forming condensation represents a most interesting class of reactions in which a silanol-amine concerted mechanism has been proposed previously [1, 2]. These mechanistic studies have demonstrated that the catalyst support contributes significantly to the activity of the reaction by possibly affecting transition-state stabilization with the silanols acting as an acid and amines as a base in a concerted mechanism. Relying on our recent discovery of hydrophilic bulk silica imprinting [3], here we present a fundamental study of the effects of changing the hydrophobicity of the inorganic matrix and examine the resulting impact on the activity of the base catalyst while keeping all other catalyst and material attributes the same. These results have a significant impact on the rational design of the local environment surrounding a catalytically active site.

Results and Discussion

A templating strategy is used to synthesize primary amine base sites within mesoporous bulk silica. Materials synthesis is accomplished using two different templating strategies. To create a hydropohobic support in which there are no accessible silanols, a capping and deprotection strategy involving trimethylsilyliodide is performed to synthesize material **1** [4]. A novel bulk silica templating strategy developed in our research group results in the hydrophilic material **2**, which retains accessible silanols [3].

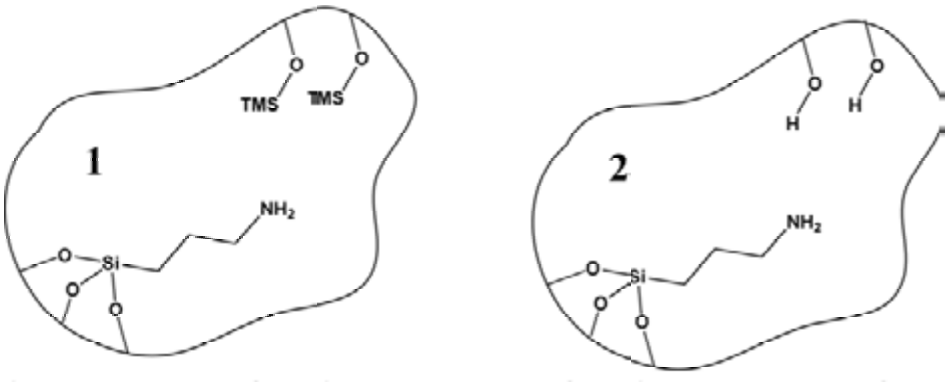

The activity of catalysts **1** and **2** was examined in the Knoevenagel condensation of isophthalaldehyde and malononitrile under various conditions and solvents (reaction scheme shown below). Figure 1 shows the typical enhanced activity of the hydrophilic material in relation to the hydrophobic material. The observed turnover frequencies are approximately 30-fold higher for **2** compared with **1** under the same conditions during initial conversion. We are currently extending these observations to other base catalyzed systems, and will describe how framework hydrophobicity can serve as a means to control catalyst activity.

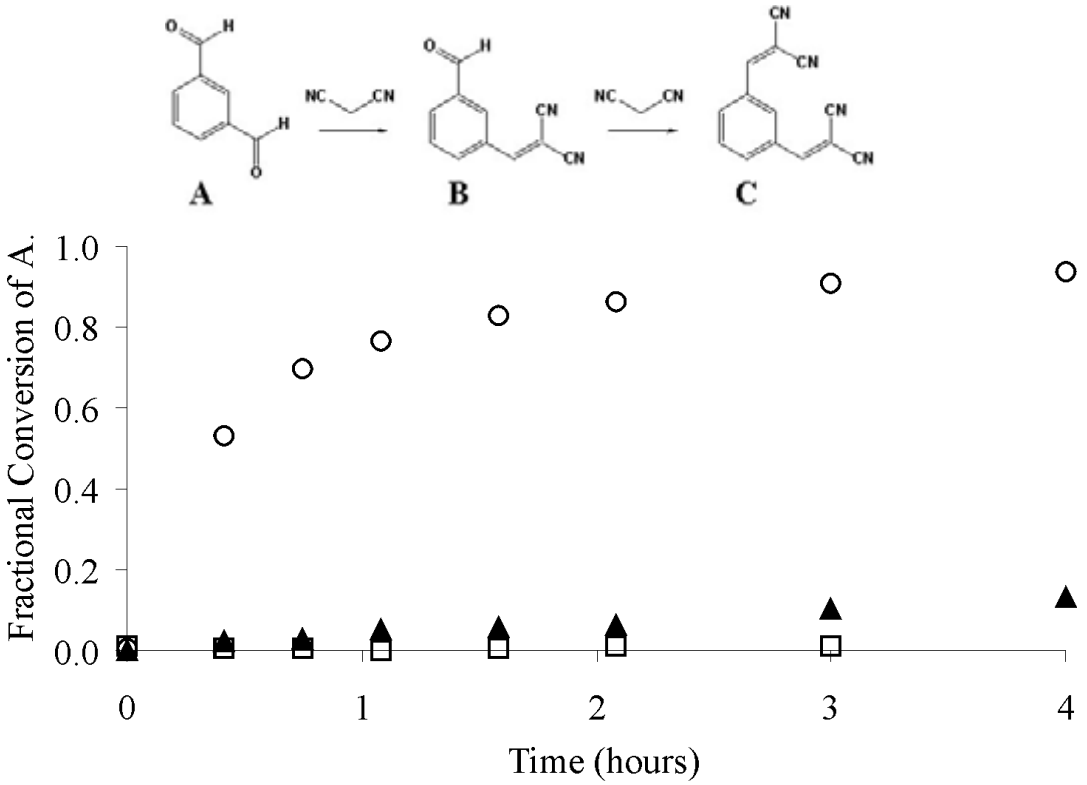

Figure 1. Knoevenagel condensation of isophthaldehyde with malononitrile with 0.5 mol% catalyst in benzene at RT: material **1** (▲), material **2** (○), and without catalyst (□).

References

1. E. Angeletti, C. Canepa, G. Martinetti, P. Venturello, Tetrahedron Lett., 29 (1988) 2261.
2. A. Corma, S. Iborra, I. Rodriguez, F. Sanchez, J. Catal., 211 (2002) 208.
3. J. D. Bass, A. Katz, in preparation.
4. A. Katz, M. E. Davis, Nature, 403 (2000) 286.

ESR STUDY OF HIGH-TEMPERATURE METHANE INTERACTION WITH AMMONIUM HEPTAMOLYBDATE SUPPORTED ON HZSM-5 ZEOLITE: DETECTION OF MOLYBDENUM-ALKYL COMPLEXES FORMATION

Vasenin N.T., Matus E.V., Tsykoza L.T., Ismagilov I.Z., Kerzhentsev M.A., Anufrienko V.F., Ismagilov Z.R.

Boreskov Institute of Catalysis SB RAS, Novosibirsk, Russia
Fax: + 7 (3832) 39-73-52; E-mail: zri@catalysis.nsk.su

In 1993 was discovered the catalytic reaction of methane dehydro–aromatization into benzene and other aromatic hydrocarbons without oxygen over the zeolite catalyst Mo/HZSM–5 [1]. The catalysts of this type are prepared via the ammonium heptamolybdate (AHM) $(NH_4)_6Mo_7O_{24}\cdot H_2O$ deposition on the zeolite HZSM–5, with subsequent thermal activation of the catalyst in methane medium at the temperatures up to 700 °C. Recently, the analysis of ESR spectra of AHM/HZSM–5 system after activation by methane with an inert gas additive (9.5 $\%N_2/CH_4$) was conducted [2].

On the other hand, earlier in the works [3, 4] ESR method was used to study the thermolysis of bulk AHM and 2 types of Mo^{5+} ions were detected. It was shown, that Mo^{5+} ions of the first type, with rhombic anisotropy of g–factor, are present in the tetrahedral oxygen coordination, and are stabilized as characteristic structural defects in the forming rhombic phase of MoO_3 oxide (denoted as T–type ESR spectra: g_x = 1.958, g_y = 1.048, g_z = 1.877). The Mo^{5+} ions of the second type, with axial symmetry of the oxygen surroundings, are existing due to the molybdenum stabilization as polymolybdate structures (denoted as PM–type ESR spectra: $g_\perp$ = 1.936, $g_\parallel$ = 1.895). They are characterized by the appearance of molybdenyl bond $[Mo=O]^{3+}$, leading to the axial spectrum. It is also possible to assign these spectra to the phase of hexagonal MoO_3, similar to the polymolybdate structures [5]. Besides the Mo^{5+} ions, after the AHM decomposition appears an anisotropic spectrum of hole center, stabilized on the MoO_4^{2-} fragment according to the scheme: $MoO_4^{2-} + \oplus \rightarrow MoO_4^{-}$ [3, 4]. For this center, regardless of the thermolysis conditions, appear the hyperfine structure (HFS) from molybdenum nuclei and super–hyperfine structure (SHFS) from nitrogen nuclei (denoted as R–type ESR spectra: g_x = 1.976, g_y = 2.002, g_z = 2.070, A_x^N = 12 Gs, A_y^{Mo} = 19 Gs, A_z^{Mo} = 8 Gs). It is important, that for such center the spin density is localized on the oxygen ions [6].

In the present work, the ESR method was used to study the electronic states of Mo after thermolysis of the AHM/HZSM–5 system in the atmospheres of air and methane at the temperatures up to 500 °C.

ESR spectra of the AHM/HZSM–5 system after thermolysis in the air

The dependencies of ESR spectra of the AHM/HZSM–5 samples, with molybdenum content 5 and 10 wt.%, on the temperature and time of thermolysis in the air have been studied: 200, 300, 400 and 500 °C, from 15 min to 7 h. Based on the analysis of spectra, the following results can be emphasized:

1. Thermolysis of samples with Mo content 10 wt.% leads to the appearance of spectra of Mo^{5+} ions and radicals, similar to the paramagnetic centers observed after thermolysis of the bulk AHM, while for the samples with Mo content 5 wt.% only the traces of such spectra are observed.

2. At these conditions of supported AHM thermolysis, none of the spectra of Mo^{5+} ions were found, whose peculiarities would allow to suppose that Mo^{5+} are stabilized in the channels of HZSM–5 zeolite. Some indication of such channel positions of Mo^{5+} ions could be the SHFS from aluminum nuclei, which was suggested in work [2], but no such SHFS was found here.

ESR spectra of the AHM/HZSM–5 system after thermolysis in the flow of methane–argon mixture

Using the same AHM/HZSM–5 samples and thermolysis conditions as in the air, the ESR method was used to study the samples after treatment in the flow of methane–argon mixture. In the work [2] for the first time are studied ESR spectra obtained in the similar conditions, however the authors did not provide sufficiently exact analysis of these data.

The spectra of samples after 1 and 2 h of treatment with the mixture 10%CH_4/Ar at 300 and 400 °C in the vicinity of g_z are non–uniform and wide, containing the superposition of several spectra – types T, PM and a new spectrum, which will be described below. This spectrum appears in the pure form both at 77 and 293 K scanning temperatures already after thermolysis at 500 °C. It can be assigned to the 2 types of Mo^{5+} ions in axially–distorted coordination with the following parameters: $g_{\perp}^{(1,2)} = 1.935$, $g_{\parallel}^{(1)} = 1.910$, $g_{\parallel}^{(2)} = 1.895$. These new states are not the above–mentioned Mo^{5+} ions of T and PM types, though the values of their parameters are close. Since the new spectrum vanishes upon the contact of sample with atmospheric oxygen at the room temperature, this means that before were observed the Mo^{5+} ions with coordination surroundings consisting not only of the oxygen ions. The additional

proof of this effect is that if the coordination surroundings of Mo^{5+} ions would consist only of oxygen ions, it would not undergo changes upon the contact with atmospheric oxygen and, consequently, the spectra would not change [6].

The nature of observed ESR spectra becomes more understandable, if one will suppose, that in the process of samples thermolysis takes place alkylation of Mo^{5+} ions in the methane medium (with Mo–C bond formation). At the temperatures 300–400 °C and short times of thermolysis (1–2 h) can preferentially proceed the reduction of Mo^{6+} ($4d^0$–ions) to Mo^{5+} ($4d^1$–ions) by methane molecules, and thus there is practically no alkylation. However further thermolysis at higher temperatures 400–500 °C can lead to the alkylation of Mo^{5+} ions, which becomes apparent in the spectra as widened axially–anizotropic signals. As it follows from [2], such spectra are vanishing after sample thermolysis at 700 ^oC, which is probably associated with the transformation of molybdenum alkyl complexes into molybdenum carbide – Mo_2C. It is also important to note the absence of coke depositions, which would give the spectra with g_e, even after thermolysis at 500 °C for 10 h.

It is necessary to consider more thoroughly the peculiarities of obtained ESR spectra, corresponding to the alkylated Mo^{5+} ions. The spectra of similar alkylated d^1–ions have been studied in detail using the titanium–based catalysts for ethylene polymerization, obtained via the interaction of bulk $TiCl_4$ or supported titanium complexes with aluminum–organic compounds (AOC) [7–^{9}]. Upon such interaction, in addition to the reduction of initial Ti^{4+} ions ($3d^0$–ions), takes place the alkylation of produced Ti^{3+} ions ($3d^1$–ions), that is formation of Ti–C bond, the presence of which is an essential condition for the accomplishment of ethylene polymerization. The spectra of such Ti^{3+} ions have 2 features. First, due to the formation of Ti–C bond, is observed the tetragonal compression, so strong that the value of $g_\perp$, determined by the formation of covalent bond of Ti^{3+} ion with p_π–orbitals of alkyl ligand, becomes larger than $g_\parallel$. Second, the spectra are very sensitive to ethylene coordination, its insertion into the Ti–C bond and to the polymer chain growth, which for the first time was shown by ESR method [9]. It is obvious, that the absolute values of $g_\perp$ for $4d^1$–ions Mo^{5+} with alkyl bonds are noticeably smaller than the values of $g_\perp$ for similar $3d^1$–ions Ti^{3+}. Analysis of the spectra of Mo^{5+} ions with alkyl bonds indicates, that corresponding values of $g_\perp$ are in the range 1.92–1.94.

For the more complete confirmation of assumption about the formation of molybdenum–alkyl bonds and their possible role in the oligomerization of hydrocarbon forms (C_1, C_2) during thermolysis of AHM/HZSM–5 in the CH_4 medium, it is worth to study how

the ESR spectra are influenced by the processes of reacted samples reduction using various AOC without oxygen, as well as by the ethylene adsorption and its oligo– and polymerization.

Conclusions

Using the ESR method it was shown, that: first, after thermolysis of supported AHM/HZSM–5 in the air, no principally new states of Mo^{5+} ions stabilized in the channels of zeolite HZSM–5 were observed, compared with the thermolysis of bulk AHM [3, 4]; second, in contrast with the work [2], after thermolysis in the flow of methane–argon mixture, were not observed spectra of any Mo^{5+} ions forming the bond with zeolite framework, giving SHFS from aluminum nuclei; third, it is very probable that after thermolysis in the flow of methane–argon mixture are observed the spectra of Mo^{5+} ions with alkyl bonds, which requires to carry out further experiments.

Acknowledgements

Catalyst preparation part of this work was financially supported by INTAS Grant 99–01044.

References

[1] Wang L., Tao L., Xie M., Xu G., Huang J., Xu Y., *Catal. Lett.*, 21 (1993) 35.
[2] Ma D., Shu Y., Bao X., Xu Y., *J. Catal.*, 189 (2000) 314.
[3] Maksimov N.G., Andrushkevich T.V., Tiurin Yu.N., Anufrienko V.F., *Kinet. Katal.* (in Russian), 15 (1974) 472.
[4] Ravilov R.G., Maksimov N.G., Mikhailenko E.L., Kalechits I.V., Anufrienko V.F., *Izvestiya SO AN SSSR. Ser. khim.* (in Russian), 3 (1981) 65.
[5] Olenkova I.L., Plyasova L.M., Kiric S.D., *React. Kinet. Catal. Lett.*, 16 (1980) 81.
[6] Ravilov R.G., Chemistry Ph.D. Thesis (in Russian), Novosibirsk, Institute of Geology and Geophysics SB AS USSR, 1980.
[7] Maksimov N.G., Nesterov G.A., Zakharov V.A., Stchastnev P.V., Anufrienko V.F., Yermakov Yu.I., *React. Kinet. Catal. Lett.*, 8 (1978) 81.
[8] Maksimov N.G., Nesterov G.A., Zakharov V.A., Stchastnev P.V., Anufrienko V.F., Yermakov Yu.I., *J. Mol. Catal.*, 4 (1978) 167.
[9] Poluboyarov V.A., Chemistry Ph.D. Thesis (in Russian), Novosibirsk, Institute of Catalysis SB AS USSR, 1986.

OBSERVATION OF LINEAR COPPER-OXYGEN STRUCTURES IN CHANNELS OF ZSM-5 ZEOLITES

Ismagilov Z.R., Yashnik S.A., Anufrienko V.F., Larina T.V., Vasenin N.T., Bulgakov N.N., Vosel S.V., Tsykoza L.T.

Boreskov Institute of Catalysis SB RAS, Novosibirsk, Russia
Phone: +7 3832 341219; Fax: +7 3832 397352; E-mail: zri@catalysis.nsk.su

The interest in Cu-ZSM-5 catalysts, which are highly active to direct decomposition of NO and selective catalytic reduction of NO with hydrocarbons including propane, gives an impetus to studies of the electron states of copper in the catalyst (oxidation level and coordination) and their influence on the catalytic properties. It is shown in a number of papers that the catalytic activity of Cu-ZSM-5 expressed as conversion of NO increases with the level of Cu-exchange to reach maximum at the ratio Cu/Al≈100% [1-3]. At the further increase in Cu/Al (to as high ratio as 450% [1, 3, 4]) the NO conversion keeps constant.

The present work deals with EPR and ESDR studies of electron states of copper depending on the method used for preparation of Cu-ZSM-5 (ion exchange, wet impregnation, deposition), basic conditions of synthesis (pH of copper solution, copper precursor, temperature etc.) and copper loading.

For calcined Cu-ZSM-5 samples treated in vacuum at 400°C, axial EPR spectra of O^- ion radicals with $g_\perp$=2.05 and $g_\parallel$=2.02, which are presumably assigned to linear $–O^––Cu^+–O^––Cu^+–O^–$ chains in zeolite channels [5], are observed against the background of EPR signal of isolated octahedral Cu^{2+} ions with different extents of tetragonal distortion.

The studies of the copper electron states in Cu-ZSM-5 have allowed a copper state with absorption bands at the unexpected region of 18000 to 23000 cm^{-1} to be discovered for the first time in the samples treated in vacuum at 150 – 400°C (Fig.). Along with this state, isolated Cu^{2+} ions (a.b. 12500 – 14000 cm^{-1}) and clustered copper oxide species (CTB 27000 – 32000 cm^{-1}) are observed (Fig.). The discovered absorption bands (18000 – 23000 cm^{-1}) relate to the ligand-metal CTB in $–O^{2–}–Cu^{2+}–O^{2–}–Cu^{2+}–O^{2–}–$like chains in the zeolite channels. Probably, the chain structures are easy to reduce (they are even capable of self-reduction) and may play an important role, along with $Cu^{2+}\cdots Cu^{1+}$ sites (a.b. 15000 – 17000 cm^{-1}), in selective reduction of nitrogen oxides.

ADF quantum chemical calculations argue for the probable occurrence of charge transfer bands at 18000 – 23000 cm^{-1} for copper with coordination number equal to 2, such as linear $Cu^{2+}–O^{2–}–Cu^{2+}–O^{2–}–$ chains, and, in principle, for the possibility for intrachain reduction $Cu^{2+}O^{2–} \rightarrow Cu^+O^–$.

Formation of the chains is caused by copper hydrolysis during synthesis of Cu-ZSM-5 followed by stabilization of polynuclear [$Cu^{2+}O^{2-}$] species in the zeolite channels. The ratio of copper states in Cu-ZSM-catalysts depends both on the preparation procedure and conditions (pH, concentration of copper salt solute, temperature) and on conditions of the thermal post-treatment in vacuum (temperature and time).

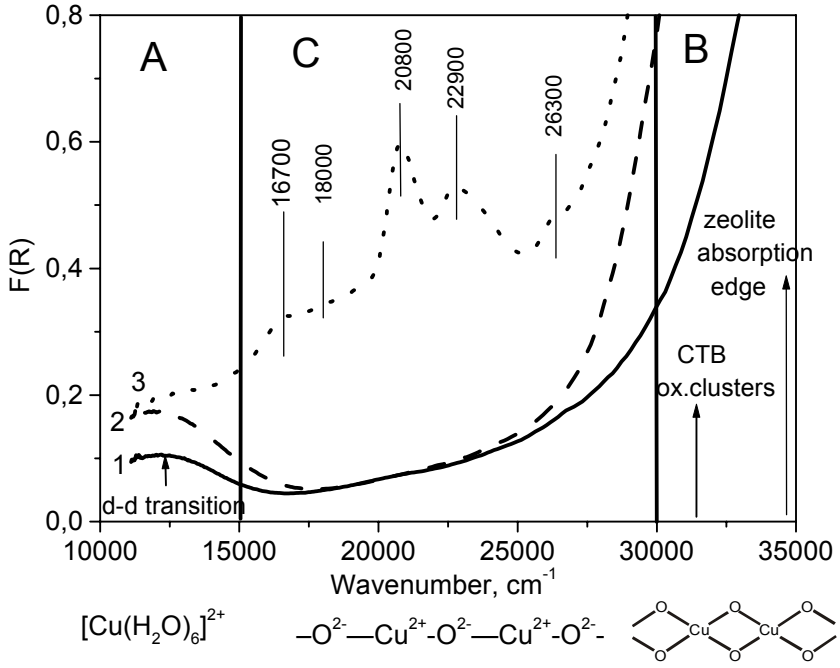

Fig. ESDR spectra of Cu-ZSM-5 sample, (1) – initial and treated in vacuum at 25 ^{o}C (2) and 150 ^{o}C (3)

Reference

1. K.C.C.Kharas, *Appl. Catal. B; Environ*., 2 (1993) 207
2. R.Gopalakrishnan, P.R.Stafford, J.E.Davidson, et al., *Appl.Catal. B; Environ*., 2 (1993) 165
3. L.T.Tsykoza, S.A. Yashnik, R.A.Shkrabina, Z.R..Ismagilov, E.V.Pluzhnikova, V.V.Kuznetsov, V.A.Sazonov, *3rd European Workshop on Environmental Catalysis 'Environmental catalysis. A Step forward'* (Ed. G.Centi, P.Ciambelli), May 2-5, 2001, Maiori (Italy), p. 173.
4. Z.R.Ismagilov, R.A.Shkrabina, L.T.Tsykoza, et. al., *Kinetics and Catalysis*, 42, 6 (2001) 847
5. V.F. Anufrienko, N.N.Bulgakov, N.T.Vasenin, et. al., *Dokl. RAN* 386 (2002) 770 (in Russian)

METHANATION OF CARBON DIOXIDE IN THE PRESENCE OF SUPPORTED CATALYSTS BASED ON PLATINUM METAL COMPLEXES

Frolov V., Zhilyaeva N., Volnina E., Shuikina L.

Topchiev Institute of Petrochemical Synthesis RAS, Moscow, Russia
Fax: (095) 230-22-24; E-mail: frolov@ips.ac.ru

The advantages of metal complex catalysts that exhibit high activity under much milder conditions compared to traditional heterogeneous catalysts are well known and cause their wide application in liquid-phase processes of various types. At the same time, the attention of researchers have recently been drawn to the use of metal complexes as precursors of catalysts capable of operating at temperatures which are higher than those of the synthesis of the complexes but lower than temperatures at which conventional heterogeneous catalysts are employed. One of the gas-phase reactions, for which a search of novel catalysts based on metal-complex precursors is of importance, is the hydrogenation of carbon dioxide into methane, or the methanation reaction.

Among the reasons for interest in this reaction, a possibility of its usage as a means of production of highly energetic fuel in countries where there are no sources of natural gas should be mentioned, as well as its employment for the purpose of removing carbon dioxide from inhabited closed spaces, such as space vessels or submarines.

The aim of the present paper is to prepare highly active and highly selective catalysts of methanation of carbon dioxide on the basis of platinum metal complexes with higher aliphatic amines. Previously, these complexes were shown to be exclusively active in the liquid-phase hydrogenation of unsaturated organic compounds [1] being used as homogeneous or supported catalysts.

Complexes of ruthenium, rhodium, and platinum with trioctylamine supported on mineral carriers, such as γ-alumina and silica, were used as precursors of hydrogenation catalysts that displayed high activity and selectivity (into methane) under relatively mild conditions (at 403-472 K and atmospheric pressure).

Kinetics of methanation was studied in pulse and flow operation modes. Kinetic orders with respect to reagents (H_2, CO_2) and apparent activation energies were determined.

It was established that, in spite of considerable degradation of the initial complexes during preliminary reduction with hydrogen, their composition and structure affect the activity and selectivity of the resultant catalysts. For example, the catalyst prepared from the complex of rhodium trichloride with trioctylamine in a ratio of 2:1 (“complex II”) displayed a

much greater activity than the complex characterized by a ratio of 1:1 ("complex I"). The selectivity was 100 % in the former case compared to 45 % in the latter case.

In the 80th years, the kinetics of methanation of carbon dioxide on supported ruthenium and rhodium catalysts prepared by impregnation of the carrier with chloride salts followed by a subsequent rigorous thermal treatment was studied in detail by Solymosi and his co-workers [2, 3]. It was expedient to compare our results obtained with catalysts prepared from metal complexes under relatively mild conditions (the temperature of reduction in hydrogen did not exceed 200 ºC) with those obtained by Solymosi et al. The main distinction of our results consists in a substantially greater turnover frequencies (see the Table) and in a lower temperature of the onset of the methanation reaction (by 40-50 K) at 548 K.

Table. Comparison of the results obtained with literature data

System	Operation Mode	E, kcal/mol	n_{H_2}	n_{CO_2}	Turnover Frequency, s^{-1}	Selectivity in CH_4, %
Our data						
0.4% Ru on Al_2O_3 from the complex	Pulse of CO_2 in H_2	12.1 ± 1.4	-	-	-	100
0.4% Rh on Al_2O_3 from complex II	Pulse of CO_2 in H_2	20.0 ± 1.9	-	-	-	100
0.4% Rh on Al_2O_3 from complex II	Flow of stoichiometric mixture	19.2 ± 1.6	0.85	0.38	0.75	100
0.4% Rh on Al_2O_3 from complex I	Flow of stoichiometric mixture	-	-	-	-	45 (55% CO)
Data of work [3]						
5% Ru (from the salt) on Al_2O_3	Pulse of stoichiometric mixture	16.1	1.0	0.47	0.194	100
5% Rh (from the salt) on Al_2O_3	Pulse of stoichiometric mixture	16.2	0.62	0.26	0.113	100

This activity gain seems to be even greater because in our work the turnover frequency values were calculated using the overall number of metal atoms whereas the number of metal atoms at the surface was used in [3].

Thus, it was shown that supported methanation catalysts prepared from complexes of ruthenium and rhodium with trioctylamine are much more active than conventional catalysts prepared by the impregnation technique followed by a subsequent rigorous thermal treatment of the catalysts. The activity and selectivity of the catalysts are sensitive to the composition and structure of the initial complexes.

A mechanism of formation of the active species was put forward on the basis of IR spectroscopy analysis.

References:

[1] Frolov V. M., *Platinum Metals Rev.*, 40, (1996) 8
[2] Solymosi F., Erdöhelyi A., *J. Mol. Catal.*, 8 (1980) 471
[3] Solymosi F., Erdöhelyi A., and Kocsis M., *J. Chem. Soc. Faraday Trans.*, 77 (1981) 1003

CALIXARENE-INORGANIC OXIDE COMPOSITES AS SCAFFOLDS FOR CATALYTIC STRUCTURES

Notestein J.M., Katz A., Iglesia E.

Department of Chemical Engineering, University of California at Berkeley, Berkeley, California, USA
E-mail: katz@cchem.berkeley.edu

Introduction

The growing societal demand for fine chemicals, such as pharmaceuticals, agrochemicals, liquid crystals and chiral monomers, requires development of new catalysts with unprecedented chemical and enantiomeric selectivity. These attributes have been a hallmark of biological catalysts, but there are significant advantages associated with the use of synthetic enzyme mimics without the stability and containment concerns associated with biological moieties. Calixarene-based hosts have been conceptually related to cyclodextrins, and they are capable of selective molecular recognition, which can be designed rationally via functionalization of their upper rim.[1] These compounds are much easier to manipulate synthetically than their natural counterparts. However, the low solubility of calixarenes and their conformational flexibility have limited their use as selective pockets for molecular adsorption and catalysis.[2] Recently, we have developed and implemented methods for the anchoring of rigid calixarene structures onto inorganic supports and used them as adsorbents for molecules dissolved in previously inaccessible solvents, including in the gas-phase and polar solvents such as water. The resulting new class of hybrid organic-inorganic composite materials permits the design of catalyst scaffolds consisting of a highly dense monolayer of isolated calix-[4]-arenes immobilized on the surface of silica. Here, we also show how the upper rim functionality of immobilized calixarene hosts in this new class of materials imparts selectivity to the binding of neutral molecules; we also illustrate how cations of potential catalytic interest can bind onto the shape-selective pockets in rigidly anchored calixarenes.

Results and Discussion

Recently, we have reported a general single-step approach for calixarene immobilization onto silica surfaces. We have applied this approach to the synthesis of **1**, (Figure 1) in order to create materials with unprecedented surface densities of rigidly immobilized calixarenes.[3] Our approach circumvents the need for laborious calixarene derivatization, which had been previously required for calixarene immobilization, and which leads to undesired flexibility in anchoring the calixarene to porous supports.

We have probed the use of the lipophilic calixarene pockets in 1 as adsorbents for neutral organic molecules.[3] At cryogenic temperatures, nitrogen pore-filling experiments with 1 unequivocally show microporosity arising due the size of the calixarene pockets. At room temperature, our experimental results have shown that 1 adsorbs stoichiometric amounts (1:1 complexes) of organics, such as toluene, benzene, nitrobenzene, and phenol, from aqueous solution. Adsorption isotherms over a temperature range were used to estimate an interaction energy of 5.6 kcal/mol between nitrobenzene and a calixarene binding pocket; these binding energies are comparable with values reported for α-cyclodextrins in aqueous solutions. We have also explored the influence of upper rim substitution in controlling the selectivity of binding of organic guest molecules within this class of materials. For example, changing the upper rim substituents from protons to *tert*-butyl groups in calixarene 1 increased the binding constant for nitrobenzene by a factor of ~ 2.5. In all cases investigated, desorption of guest from the calixarene host was reversible, indicating the non-covalent nature of the interactions between the calixarenes and the guest molecules.

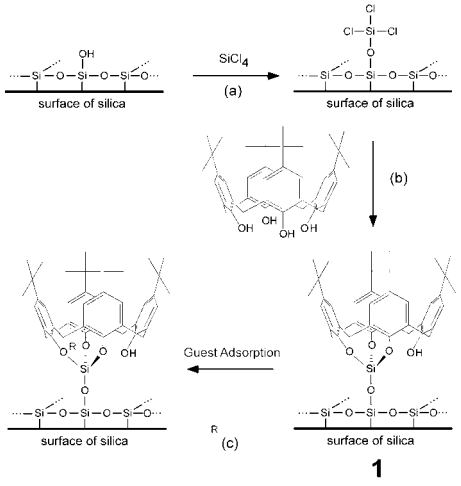

Figure 1. Schematic illustration of the immobilization of *tert*-butylcalix-[4]-arene onto silica and subsequent use of anchored site for small-molecule adsorption comprising (a) activation of silica surface with silicon tetrachloride, (b) reaction of material in (a) with calixarene, and (c) adsorption of small-molecule guest onto immobilized host.

We have conducted initial studies of metal binding using Cu^{2+} and the isolated and the unbound phenolic moiety of **1**. Structure **1** was treated with one equivalent of Cu(II) acetate, with the expectation that phenolate-copper(II) complexes would form. Such interactions were previously detected by a charge transfer band in the UV/Visible spectrum.[4] The diffuse reflectance UV/Vis spectrum of the Cu(II)-treated material indeed showed an intense band at 430 nm, arising from phenoxide-Cu(II) charge transfer on the calixarene lower rim. Thus, it

is possible to bind transition metals to these immobilized calixarenes. We are currently extending the capability to bind metal cations using this class of materials to other types of immobilized calixarene structures possessing specific ligands as part of the macrocyclic scaffold. The rigidly immobilized calixarenes in these materials organize the metal cations in the immediate vicinity of their shape-selective interior pockets and can impart catalytic selectivity, including enantioselectivity, by virture of their upper rim structure. We will discuss the use of these novel hybrid materials as robust single-site microporous supports for anchoring catalytically active metal cations.

References

1. V. Böhmer, D. Kraft, and M. Tabatabai, J. Inclus. Phenom. Mol., 19 (1994), 17.
2. L. J. Bauer and C. D. Gutsche, J. Am. Chem. Soc., 107 (1985), 6063.
3. A. Katz, P. Da Costa, A. Lam, and J. M. Notestein, Chem. Mater., 14 (2002), 3364.
4. G. Arena, R. Bonomo, A. Contino, F. Gulino, A. Magri, and D. Sciotto, J. Inclus. Phenom. Mol., 29 (1997), 347.

STRUCTURE AND PROPERTIES OF PALLADIUM CATALYSTS ON POROUS SUPPORTS PREPARED FROM CHEMICALLY MODIFIED ANTHRACITE AND EXFOLIATED GRAPHITE

Kuznetsov B.N.[1], Chesnokov N.V.[1], Mikova N.M[1], Lubchik S.B.[2], Shendrik T.G.[2], Savos'kin M.V.[2], Yaroshenko A.P.[2]

[1]Institute of Chemistry and Chemical Technology SB RAS, Krasnoyarsk, Russia
Fax: +7(3912)439342; E-mail: bnk@icct.ru
[2]Institute of Physical-Organic and Coal Chemistry NAS, Donetsk, Ukraine

Introduction

Rather high cost of commercial carbon supports restricts the range of their using in the industrial catalysis. Therefore the urgent problem is the development of novel methods for producing porous carbon materials with demanded properties from cheap natural raw materials like anthracite and graphite.

The paper describes results of the study of structure, textural characteristics and catalytic properties in model reaction of liquid phase cyclohexene hydrogenation of palladium catalysts supported on porous materials prepared from chemically modified anthracite and exfoliated natural graphite.

Experimental

Carbon supports from Donetsky anthracite (Progress mine) were prepared by consecutive steps of demineralization, chemical modification by $HClO_4$ and final activation by CO_2 or water-steam at temperature 1123^oC. Depending on conditions of modification and activation the porosity of carbon products ranges from microporous to mesoporous types and their specific surface area from 400 to 1000 m^2/g. The other carbon supports were prepared by a high rate heating of intercalated natural graphite from Zavalevsky pit (Ukraine). Three types of intercalated graphites were used: G-CA – obtained by graphite oxidation with CrO_3 in concentrated sulphuric acid; G-NA – by treatment of graphite with concentrated nitric acid; G-NAA – by consecutive treatment of graphite with concentrated nitric acid and glacial acetic acid. Thermal treatment (exfoliation) of intercalated graphites was carried out in fixed bed reactor at temperature 1173^oK during 30 s. Powder-like exfoliated graphites have very low density (0.01-0.005 cm^3/g).

Catalysts were prepared by impregnation of carbon supports with water-alcohol solution of H_2PdCl_4, subsequent drying at 423 K and reduction in flow of hydrogen at 373-423 K. Palladium concentration in all catalyst was near 1 % wt.

Data on structural and textural characteristics of carbon supports were obtained by SEM method and from isotherms of N_2 adsorption at 77 K and CO_2 adsorption at 273 K. Size, structure and distribution of supported palladium particles were defined with HREM method.

Catalytic activity measurements in model reaction of cyclohexene liquid phase hydrogenation were carried out in a static reactor at atmospheric pressure and temperature 323 K.

Results and discussion

Structure of initial, chemically modified and thermally treated samples of anthracite and graphite was investigated by SEM and TEM methods. Initial graphite particles consists of thin laminas with thickness of few tens of nm. These laminas have a high degree of crystallinity. All samples of intercalated graphites have the same morphology as an initial graphite. But the more intensive periodical background probably connected with the splitting of graphite laminas on more thin layers was observed for intercalated samples. The more pronounced effect of laminas splitting is observed in the case of exfoliated graphite samples. They have more structural defects than samples of intercalated graphite connected with erroneous superposition of graphite layers.

In samples of demineralized anthracite the carbon particles with rough surface are presented. They have irregular microstructure formed by distorted fragments of graphite plane (002). Microstructure of modified by $HClO_4$ and activated by CO_2 (at 1123 K, 24 h) sample is the same as that of an initial anthracite. But modified and activated anthracite has the more developed mesoporosity.

According to presented in Table 1 data the method of intercalation makes the significant influence on textural characteristics of exfoliated graphite.

Table 1. Textural characteristics of different samples of exfoliated graphite calculated from isotherms of N_2 adsorption at 77 K

Sample	S_{BET}, m^2/g (P/Po = 0.005-0.2)	V_{ads}, cc/g (P/Po = 0.996)	D_{pore}, nm ($4V_{ads} / S_{BET}$)	V_{micro}, cc/g
G-CA	53.0	0.241	18.2	0.028
G-NA	12.3	0.083	27.0	0.006
G-NAA	33.3	0.138	16.6	0.013

The volume of micropores was defined from isotherms of CO_2 adsorption (Table 2).

Table 2. Textural characteristics of exfoliated graphite samples calculated from isotherms of CO_2 adsorption at 273 K

Sample	V_{micro}, cc/g	S_{micro}, m^2/g	E_o, kJ/mol	W_{micro}, nm
G-CA	0.330	850	25.4	0.77
G-NA	0.114	300	23.7	0.88
G-NAA	0.199	521	23.2	0.92

Obtained data show that exfoliated graphite samples have a developed microtexture of slit-like micropores with predominant width 0.77-0.92 nm. Total volume of micropores is varied between 0.114 and 0.330 cm^3/g depending on the method of carbon material preparation.

The method of carbon support synthesis influences significantly on catalytic activity of supported palladium in reaction of cyclohexene liquid phase hydrogenation (Table 3).

Table 3. Catalytic activity of samples 1% Pd/graphite in reaction of cyclohexene liquid phase hydrogenation at 323 K

Catalyst	Temperature of reduction, K	Catalytic activity, mmol H_2/mmol Pd×min
1%Pd/ G-NAA	non-reduced	10.7
	373	18.0
	423	21.8
	523	5.1
1%Pd/G-NA	non-reduced	non-active
	373	6.2
	423	7.1
	523	6.9
1%Pd/ G-CA	non-reduced	non-active
	423	0.3

The comparison of catalytic measurements and microscopic study data allow to make some possible explanations of observed differences in catalytic behavior of palladium catalysts on different carbon supports. The sample 1% Pd/G-NAA demonstrates the highest catalytic activity in reaction of cyclohexene hydrogenation. But it has rather big size of palladium particles with dendrite type structure (100 nm and more). Distinctive feature of reduced catalyst 1% Pd/G-NA is the presence of small palladium particles with a predominant size 2 nm which have homogeneously distribution on carbon support surface. Nevertheless this sample has lower than catalyst 1% Pd/G-NAA activity in cyclohexene hydrogenation.

The formation of flat metal particles with size near 5 nm and needle-like particles with a length of few tens of nm and a width near 5 nm was detected for reduced catalyst

1%Pd/G-NA. HREM pictures demonstrate clearly the crystal lattice of metallic palladium with parameters d_{111} = 0.225 and d_{225} = 0.195. Because of a low contrast of TEM image they can be considered as two-dimension particles. The two-dimension morphology of particles indicates the strong interaction of palladium with graphite support of G-NA type. This effect is known to be the reason for reducing the specific catalytic activity of supported metal. Another possible reason of decreased catalytic activity of dispersed palladium on G-NA support is the localization of small metal particles inside micropores inaccessible for reagent molecules.

Since in the preparation of exfoliated graphite the sulphuric acid was used for graphite intercalation one should expect that the low catalytic activity of sample 1% Pd/G-CA is probably connected with palladium poisoning by sulphur impurities producing during thermal treatment of intercalated graphite at 1173 K.

Palladium supported on demineralized anthracite with low BET surface area is not active in cyclohexene hydrogenation at 323 K. Palladium catalyst prepared by supporting H_2PdCl_4 on anthracite modified by $HClO_4$ and activated by water steam at 1123 K during 24 h (BET surface area 425 m^2/g) contains metallic palladium particles with sizes near 2 nm. The treatment of catalyst in hydrogen flow at 423 K results in an increase of average particles size to 3 nm. Some part of supported metal in reduced catalyst has needle-like shape or form clusters consists of 2-4 particles. Reduced and non-reduced catalysts have the same activity in cyclohexene hydrogenation at 323 K (1.6-1.7 mmol H_2/mmol Pd×min).

Conclusion

Strategy of palladium catalyst synthesis with the use of porous carbon supports from Donetsky anthracite and Zavalevsky graphite was optimized taking into account their application in reactions of liquid phase hydrogenation. It was established that the activity of catalysts Pd/graphite and Pd/anthracite is varied in the wide limits depending on size, structure and surface distribution of palladium particles and carbon support porous texture. All these characteristics are defined by applied method of anthracite and graphite chemical modification in carbon supports preparation.

In some cases the residual intercalation products which are present after thermal treatment of graphite reduce the catalytic activity of supported palladium.

Acknowledgements

Authors are grateful to INTAS program (project INTAS 00-750) for the financial support of this research.

CONCEPT OF "MAGIC" NUMBERS IN CLUSTERS AS A NEW APPROACH TO THE INTERPRETATION OF UNUSUAL KINETICS OF THE HECK REACTION WITH BROMOARENES

Schmidt A.F., Smirnov V.V.

Department of Chemistry, Irkutsk State University, Irkutsk, Russia
E-mail: aschmidt@chem.isu.ru

The low reactive ability of bromoarenes in the stage of the oxidative addition to Pd(0) complexes is the main reason of insufficient activity of the traditional catalytic system in the reaction (I). It results in catalyst withdrawal from the basic catalytic cycle because of the undesirable competitive process of Pd(0) aggregation. Higher individual order with respect to Pd(0) of the aggregation [1] allows one to anticipate that a decrease of catalyst concentration would favor at least an increase of catalytic cycle turnover frequency. It was observed earlier for the Heck reaction with iodoaryls and was corroborated for the reaction (I) in the presence of different catalytic systems. However, in the concentration range $0{,}8\cdot10^{-3}$-$3{,}2\cdot10^{-3}$ mol/l not only the increase of the turnover frequency was observed but the increase of the reaction rate (fig. 1).

$$PhBr + CH_2{=}CHPh \xrightarrow[base]{PdCl_2} PhCH{=}CHPh + HBr \qquad (1)$$

The usual explications of the similar effects (fig.1) are different hypotheses of interaction between the catalyst particles containing different number of the atoms. Taking into account, that formation of the Pd colloidal particles in the Heck reaction with nonactivated bromoarenes was established experimentally [2], a new approach to the interpretation of the observed trends is suggested in this paper. This approach is based on the dependence of the formed colloidal Pd(0) particles size on the initial Pd(II) complex concentration (catalytic reaction proceeds simultaneously). According to the hypothesis of the existence of the stable particles with "magic" atom numbers it means a different degree of saturation of the colloidal particles superficial layer in comparison with maximally possible amount of the superficial atoms which corresponds to "magic" particle with the certain number of layers. Available experimental and theoretical data indicate an energetic inequality of the superficial atoms of the metal particles [3] as well as in the Heck reaction [4]. Based on it, one might assume that under the favorable conditions for the formation of the particles with more unsaturated superficial layer, a raise of their specific catalytic activity would occur.

Note that significant distinction between the stage rates of nuclei formation and their further growth in the wide-range concentration results not only in monodisperse size

distribution of the particles [5, 6] but also in virtually full independence of the colloidal particle common concentration on the initial Pd concentration. Taking into account this assumption, it's possible to carry out a quantitative verification of the hypothesis of an influence of the saturation degree of the superficial layer of the particles on their activity. It's necessary to assume that with the certain concentration of the initial Pd(II) the particles are formed, in the general having the saturated superficial layer and possessing rather low catalytic activity. The concentration 0,0032 mol/l (fig. 1) is the most suitable because in this case minimal catalytic activity for all catalytic systems was observed. Formation, in the general, of the particles with "magic" number of the atoms (i.e. 13, 57, 147 and so on) containing therefore 12, 42, 92 and so on superficial atoms was assumed, and possibility emerged of the calculation of the amount of the superficial atoms and of the corresponding saturation degree of the surface in the formed particles with other concentrations.

As anticipated, a change of the layer number (n) in the formed particles at $[PdCl_2]$=0,0032 mol/l leads to absolutely different relationship between the saturation degree of the particle surface and the concentration of $PdCl_2$. Periodic character of these trends for any layer number (n) in the particles was observed. Note that actually qualitatively, observed trends for every chosen number of the layers (n) are unique. So, determination of the layer number (n) becomes practicable by the analyzing of the experimental dependence of reaction rate on the $PdCl_2$ concentration for any catalytic system (fig.1) according to assumption of the catalytic activity decrease with the increase of the saturation degree of the superficial layer.

Let us consider the catalytic system containing no phosphine (curve 4, fig.1). The activity of that system decreased in the range of concentrations: 0,0008>0,0016>0,016>0,0032 mol/l, in the same range the saturation degree of the superficial layer of the formed particles would increase. However, this trend was only observed when n=2 i.e. when the double-layer "magic" particles containing 55 atoms was formed at the $[PdCl_2]$=0,0032 mol/l.

Meanwhile, dependence of the particles activity (apparent activation energy $E_S = -\frac{E_a}{RT}$) on the saturation degree (S) of the superficial layer can be also depicted by linear function:

$$E_S = E_0 + \rho S$$

where parametr ρ describes a linear energetic inequality as the superficial layer is filled, E_0 – maximally possible activity with $S \rightarrow 0$.

Hence, the rate of catalytic reaction with assumption of pseudo zero order with respect to substratum can be depicted as follow:

$$r = k_0 \exp(E_0 + \rho S) \quad (1)$$

Using the equation (1) a good adequacy was observed between the experimental and calculated reaction rates for all catalytic systems.

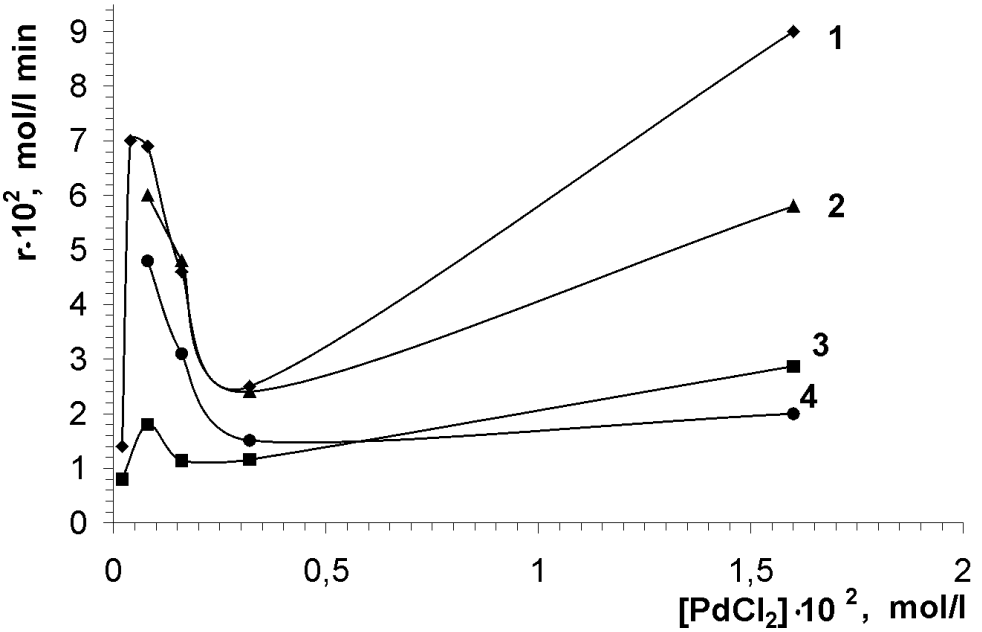

Fig.1. Plot of reaction (I) rate vs. palladium concentration for different catalytic systems (1 – $PdCl_2$ + $2PPh_3$ + NBu_3 + AcONa, 2 – $PdCl_2$ + PPh_3 + NBu_3 + AcONa, 3 – $PdCl_2$ + $2PPh_3$ + AcONa, 4 – $PdCl_2$ + NBu_3 + AcONa)

Acknowledgement: This work is supported by the Russian Foundation for Basic Research (project no. 02-03-32446a).

References:

[1] Shmidt A.F., A.Halaiqa, Kinetics and Catalysis, V. 39, No 6, (1998) 875.
[2] Reetz M.T., Westermann E. Angew. Chem., V. 39, No 1, (2000) 165.
[3] Moiseev I.I., Vargaftik M.N., Zh.Obchej. Chimii., V. 72, No 4 (2002) 550.
[4] Augustine R.L., O'Leary S.T., J. Mol. Catal., V. 72, (1992) 229.
[5] Pomogailo A.D., Rosenberg A.S., Uflyand I.E. Metal nanoparticles in polymers. Moskau: Chimia,2000, 672 p.
[6] Aiken J.D., Finke R.G., J. Am. Chem. Soc., V. 120 (1998) 9545.

SUPPORTED CATALYSTS BASED ON 2,6-BIS(IMINO)PYRIDYL COMPLEXES OF Fe(II): DRIFT STUDY OF THE CATALYST FORMATION AND KINETIC DATA AT ETHYLENE POLYMERIZATION

Semikolenova N.V., Zakharov V.A., Paukshtis E.A., Echevskaya L.G., Bukatov G.D., Barabanov A.A.

Boreskov Institute of Catalysis SB RAS, Novosibirsk, Russia
E-mail: nvsemiko@catalysis.nsk.su

Recently discovered catalysts for olefin polymerization based on iron and cobalt complexes with 2,6-bis(imino)pyridyl ligands[1,2] are of growing academic and industrial interest. Usually these complexes are used as homogeneous catalytic systems with activator – methylalumoxane. The developing of the supported catalysts where the active component - 2,6-bis(imino)pyridyl complex of Fe(II) is anchored on the surface of a solid carrier is the point of extreme interest of the researchers now[3,4,5].

In the present work the supported catalysts prepared by interaction of 2,6-bis[1-(2,6-dimetilphenylimino)-ethyl]pyridineiron(II) ($LFeCl_2$) with oxide supports (SiO_2 and Al_2O_3) are studied. In our earlier publications[5,6] we have shown that aluminium trialkyls ($AlMe_3$, $(i\text{-}Bu)_3Al$, $Al(n\text{-}Oct)_3$) are very effective activators for homogeneous and supported catalysts based on $LFeCl_2$ complexes. Data of NMR spectroscopy evidences that at $LFeCl_2$ interaction with $AlMe_3$ neutral complex of the type $LFe(II)(Me)(\mu\text{-}Me)_2AlMe_2$ is formed[5,6]. Considering these results, we have prepared the series of supported catalysts by interaction of $LFeCl_2$ with oxide supports (SiO_2 and Al_2O_3). Thus prepared catalysts exhibited high and stable activity at ethylene polymerization in presence of $Al(i\text{-}Bu)_3$ as co-catalyst, providing high polymer yield (up to 1000 kg of PE/g Fe).

Catalysts prepared using silica as support were characterized by low iron content (ca. 0.1 wt.%), whereas in case of Al_2O_3 the amount of strongly bounded complex was much higher (ca. 0.5-0.7 wt.%). The values of activities for both supported systems are close.

$LFeCl_2$ interaction with surface functional groups of the oxide supports was studied by means of DRIFT. $LFeCl_2$ adsorbed on the support surface retains its structure. In the catalyst $LFeCl_2/SiO_2$ iron complex is mainly fixed by formation of hydrogen bonds between silica surface OH-groups and the ligand L.

On $LFeCl_2$ interaction with Al_2O_3 the iron complex reacts both with OH- groups and Lewis acidic sites (LAS) of Al_2O_3 . $LFeCl_2$ firstly interacts with the more strong LAS of the support with the increase of $LFeCl_2$ content, more weak LAS are engaged into formation of surface iron compounds. DRIFT data on the state of the surface iron compounds have been

obtained using CO as probe molecule. Some correlation between catalysts composition, surface structures formed and polymerization activity are discussed.

Using the method of polymerization quenching by ^{14}CO the number of active centers and values of constant rate propagation have been determined at ethylene polymerization with supported catalysts $LFeCl_2/SiO_2$, $LFeCl_2/Al_2O_3$ (co-catalyst -$(i\text{-}Bu)_3Al$) and homogeneous system ($LFeCl_2$+$(i\text{-}Bu)_3Al$).

The kinetic data on ethylene polymerization over supported catalysts $LFeCl_2/SiO_2$ and $LFeCl_2/Al_2O_3$ were obtained. The effect of iron content in the catalyst, co-catalyst composition and concentration, polymerization temperature and presence of hydrogen and α-olefin (hexene-1) on catalytic activity and polymer structure were investigated.

References

[1] G. J. P. Britovsek, V. C. Gibson et al. *Chem. Commun*. 1998, 849.
[2] B. L. Small, M. Brookhart et al. *J. Am. Chem. Soc*. 1998, **120**, 4049.
[3] R.Schmidt, M.B.Welch, S.J.Palackal, H.G.Alt *J.Molec.Catal A:Chem.* 2002, **179,** 155-173
[4] F.A.R.Kaul, G.T.Puchta, H.Schneider,F.Bielert et.al. Organometallics, 2002, **21,** 74-82
[5] N.V.Semikolenova, V.A.Zakharov, E.P.Talzi, D.E.Babushkin et.al. *J.Molec.Catal A:Chem.* 2002, **182-183** 283-294
[6] E.P.Talsi, D.E.Babushkin, N.V.Semikolenova, V.N.Zudin, V.N.Panchenko, V.A.Zakharov, *Macromol.Chem.Phys.* 2001, **202**, 1816-1821

POSTER PRESENTATIONS

DESIGN OF NEW CATALYTIC PROCESS OF THE OXIDATIVE ALKOXYLATION OF WHITE PHOSPHORUS

Abdreimova R., Faizova F., Aliev M., Dabeeva A.

Sokolsky Institute of Organic Catalysis and Electrochemistry, Almaty, Kazakhstan
Fax: (+7-3272) 91 57 22; E-mail: abdreimioce@nursat.kz

During the second part of twentieth century, the chemistry of organophosphorus compounds (OPC) has evolved considerably into one of the cornerstones of chemistry and biochemistry. Few other branches of chemistry have a greater influence on chemistry, biology and material sciences and offer greater potential for addressing the future needs and opportunities in far-reaching areas of science and engineering. Nowadays, the chemistry of phosphorus has expanded in many distinct sectors and is almost rivalling in terms of complexity and applications with the chemistry of carbon [1].

From a synthetic point of view, the key-material for the industrial production of organophosphorus compounds is elemental phosphorus in the form of the most reactive and easily accessible white allotrope (P_4). The current technology used in the industrial plants for the synthesis of organophosphorus compounds is largely based on the direct oxidation of white phosphorus by chlorine, followed by phosphorylation of the phosphorus chloride by the appropriate organic substrate. A huge amount of hydrogen chloride is released in the latter reaction with serious corrosion and environmental problems and additional costs for its efficient removal are requested.

The increased commercial and environmental interests have stimulated the search for technical protocols for the direct conversion of the P_4 molecule into useful derivatives, which are alternative to the presently used procedures. We think that a solution to this problem could be the development of a “chlorine-free” metal-mediated catalytic process to synthesize OPC. Our approach was to have both P_4 and organic substrate coordinated to a metal center, which should lead to their activation towards reaction with each other. The scheme below well illustrates the “green chemistry” content related to the development of a catalytic cycle where an OPC is generated by combining P_4 and an organic substrate in the presence of oxygen as cheap and environmentally benign oxidant (on the left). A comparison of the proposed cycle with the currently adopted technology (on the right) is striking if one considers the increased ecoefficiency and the reduction of the associated pollution descending from the new proposed “chlorine free” technology and by the opposite nature of the reaction byproducts: just water in the catalytic process and HCl in the classical procedure.

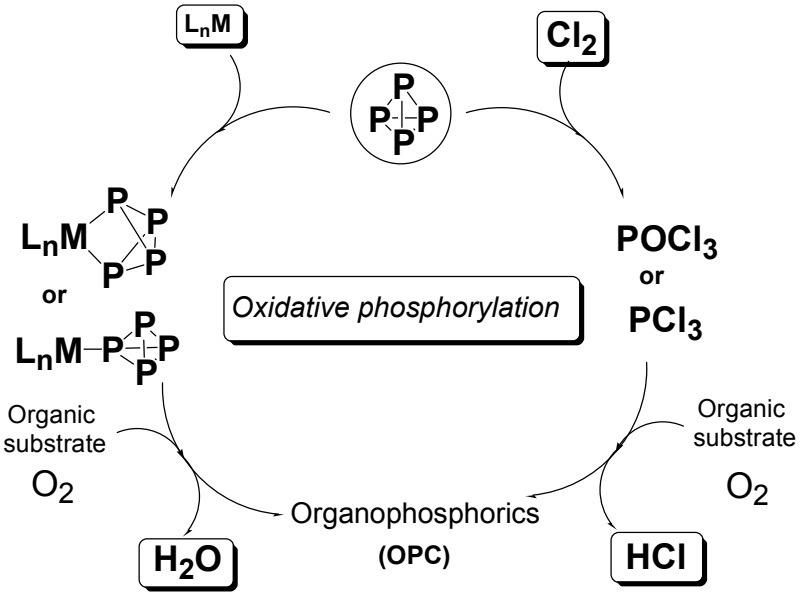

We succeeded in accomplishing the oxidative alkoxylation of P_4 by aliphatic alcohols catalyzed by Cu(II) and Fe(III) acidic complexes under mild reaction conditions [2]. The catalytic reaction yields the esters of phosphoric and phosphorous acids, $P(O)(OR)_3$ and $P(O)H(OR)_2$, which are industrially important in several areas of commercial interest and are broadly employed as extractors of rare and radioactive metals, plastifiers and flame-retardants for plastic materials, additives for lubricants, intermediate substances for further elaboration in pharmaceutical and agricultural industries, *etc*. This new catalytic protocol, allowing incorporate into the catalytic cycle all the advantages of a homogeneous catalytic reaction, may result in development of a new ecoefficient technology for the industrial production of important organophosphorus chemicals from white phosphorus.

Acknowledgement

This work is supported by the INTAS 00-00018 and ISTC K-754p research contracts.

References

[1] Dillon K. B., Mathey F., Nixon J. F. *Phosphorus: The Carbon Copy*, Wiley (1998).
[2] Abdreimova R. R., Faizova F. Kh., Akbayeva D. N., Polimbetova G. S., Aibasova S. M., Borangazieva A. K. and Aliev M. B., *Euras. Chem. -Techn. J.* (2002) 11.

MONTE CARLO/UBI–QEP MODELING OF COVERAGE-DEPENDENT CHEMISORPTION OF ATOMS AND MOLECULES ON METAL SURFACES

Abramova L.A.[1], Baranov S.P.[2], Zeigarnik A.V.[1], Evgeny Shustorovich[3]

[1]Zelinsky Institute of Organic Chemistry RAS, Moscow, Russia
Fax: 1(1-(419)791-0898; E-mail: azeigarn@ioc.ac.ru
[2]Lebedev Institute of Physics RAS, Moscow, Russia
[3]American Scientific Materials Technologies, New York, USA

The unity bond index–quadratic exponential potential (UBI–QEP) method [1–4] has been successfully applied to calculate energetics of various heterogeneous catalytic reactions (such as reforming of methane, methanol synthesis, ammonia synthesis, and Fisher–Tropsch synthesis) on the transition metal surfaces. The analytical UBI–QEP method uses thermodynamic observations only (the binding energies of atomic adsorbates and gas-phase molecular bond energies) to calculate the binding energies of molecular adsorbates and the activation energies of surface reactions (dissociation, recombination and disproportionation), for both low and high local coverages. Under experimental conditions, however, at best the global (but not local) coverage is known. The present work is devoted to determining the binding energies for equilibrium and nonequilibrium overlayer structures at nonzero coverages. Our approach combines the UBI–QEP formalism to calculate the binding energies of atomic and molecular adsorbates in a given local environment and the Monte Carlo (MC) formalism to simulate local situations and then average them into global patterns.

Specifically, we used a MC/UBI–QEP combination to determine the equilibrium coverage-dependent binding energies of atoms adsorbed on fcc (111) and (100) metal surfaces. To do this, we modified the current UBI–QEP formalism to include changes in the total energy of the overlayer during adsorption and desorption of the atoms, which gives a more accurate description of the reaction enthalpy and the activation barrier of desorption. The coverage dependent atomic binding energy $E(\theta)$ was expressed in terms of the binding energy at the zero-coverage limit $E(0)$, namely as $E(\theta) = \sigma E(0)$. The MC simulations were made on the 100×100 lattices. Some representative results are presented in the figure.

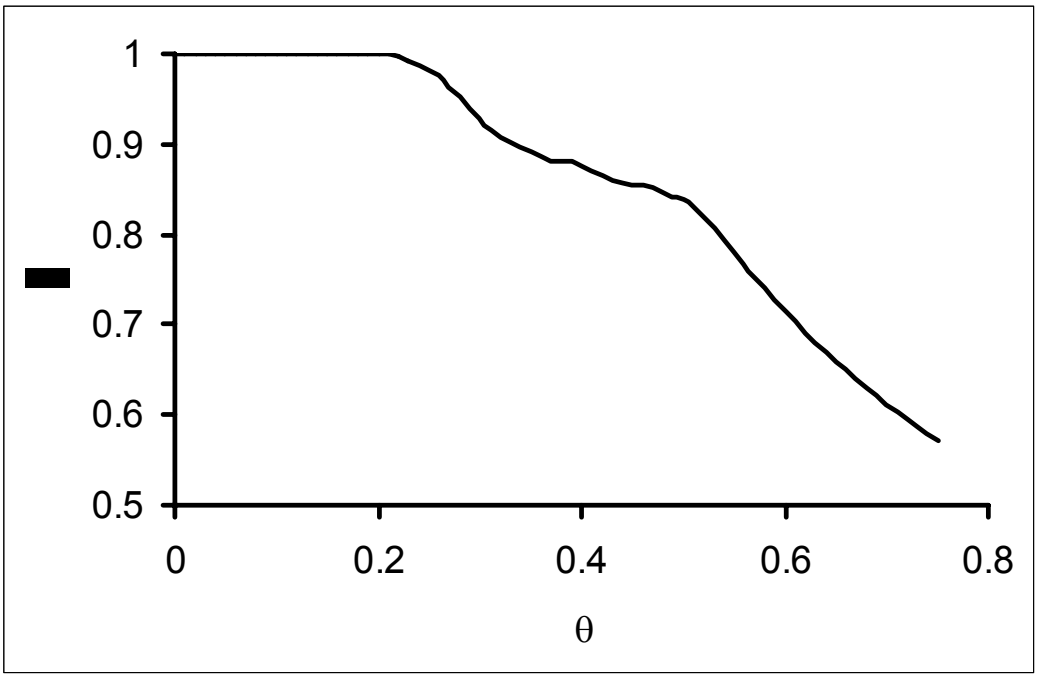

(a)

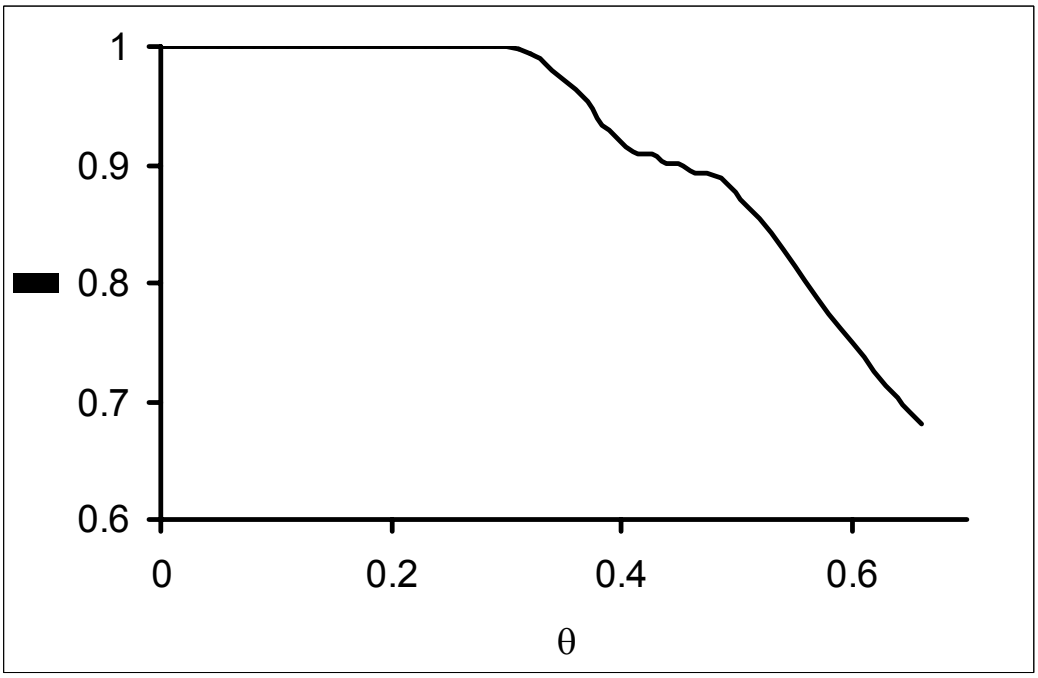

(b)

Dependence of $\sigma = E(\theta)/E(0)$ on the surface coverage θ for (a) fcc (100) and (b) fcc (111)

Microscopic images (snapshots) simulated in this work revealed several typical patterns of occupancy: (a) only hollow sites; (b) hollow and bridge sites with metal coordination remaining equal to unity; (c) bridge sites with mono- and di-coordinated metal atoms. Although hops to the atop sites were allowed, their population was observed only in some diffusion-controlled regimes but never in the equilibrium state at any coverage.

The results obtained by Monte Carlo modeling could be discretely compared with the earlier projections based on UBI–QEP calculations for local cluster configurations. Within the scope of comparability, the agreement was good.

Currently we study a more complex system to model the dynamics of diatomic molecular A_2 (A =H, O, etc.) adsorption on the fcc(111) and (100) surfaces of various metals (Ni, Pd, Pt, Cu, Ag, Au). An MC algorithm has been developed that, by using UBI–QEP energetics, realistically models adsorption, desorption, dissociation, and recombination processes including atomic and molecular diffusion along the surface. Unlike many other known approaches, the new MC program allows the user to vary a metal and an adsorbate (and their geometric characteristics), frequency factors of all events, spatial constraints for adsorbates on the surface, and the reaction temperature. The program provides information on the kinetics of adsorption, coverage-dependent energetics of all elementary events, and the snapshots of the system. As an example, projected patterns of adsorption, dissociation, and desorption of O_2 on typical fcc metal surfaces will be presented and compared with experiment.

References:

[1] Shustorovich E., *Adv. Catal.*, 37 (1990) 101.
[2] Shustorovich E., *Surf. Sci. Rep.*, 6 (1986) 1.
[3] Shustorovich E. and Sellers H., *Surf. Sci. Rep.*, 31 (1998) 1.
[4] Sellers H. and Shustorovich E., *Surf. Sci.*, 504 (2002) 167.

LEWIS ACID DEPENDENT SELECTIVITY USING ZEOLITE H-BETA FOR KETONE REDUCTION

Akata B., Warzywoda J., Weiss A.H., Sacco A., Jr.

Center for Advanced Microgravity Materials Processing, Department of Chemical Engineering, Northeastern University, Boston, USA
E- mail: ahweiss@yahoo.com

Cis/trans structure sensitive selectivity is of critical importance in the fine chemical industry. The effects of Si/Al ratio, and heat treatment (350 vs. 500 °C) of zeolite Beta on the activity and selectivity of gas phase Meerwein-Ponndorf-Verley (MPV) reduction of 4-*tert*-butylcyclohexanone at 100 °C to a mixture of cis- and trans-4-*tert*-butylcyclohexanol (cis-OH and trans-OH) were investigated. The catalysts were heat-treated identically and separately, both in a down-flow reactor and in an FTIR cell. The relative amounts of the tri-coordinated Al species, which are Lewis acid sites and are believed to be the active sites for MPV reduction, were compared using the intensity of IR vibration at 3780 cm^{-1}. FTIR results showed that the intensity of the 3780 cm^{-1} band increased both with increasing Al content and with calcination temperature in all zeolite Beta samples investigated. Catalytic reactions carried out on different Si/Al ratio (75, 22, 12.5) H-Beta catalysts heat-treated at 500 °C showed that the cis-OH yield increased from 14 to 43% at steady state with increasing Al content. Trans-OH stayed nearly constant (~5%). However, calcination of NH_4-Beta (Si/Al=12.5) at 500 °C resulted in a lower yield of trans-OH than did a 350 °C calcination (10 vs. 35 % at steady state). The cis-OH yield did not change in either case (36 %). These results suggest that tri-coordinated Al species are not exclusively responsible for the formation of cis-OH, because samples calcined at 500 °C (more tri-coordinated Al) resulted in the same amount of cis-OH as did samples calcined at 350 °C (less tri-coordinated Al).

FLUORINATED CERAMIC MEMBRANES WITH CATALYTIC PROPERTIES

Amirkhanov D.M., Alexeeva O.K., Alexeev S.Yu., Shapir B.L.

RRC "Kurchatov Institute",
Hydrogen Energy & Plasma Technology Institute, Moscow, Russia
Phone/Fax 196-7314, 196-9549; E-mail: alex@hepti.kiae.ru

One of the perspective directions of preparation of high temperature membranes permselective for gases is the deposition of carbon layers on inorganic membranes with the purpose of their properties modification or for using as temporary carbon barriers in CVD membrane production from organic silicon compounds [1, 2]. It is also necessary to note that modification of alumina supports by carbon coatings creation enhances dehydrogenation activity of some catalysts [3]. Pyrolysis of hydrocarbons is one of the routes of realization of carbonization process. It is interesting to use fluorine-containing compounds which are known to enhance for example alumina activity in cracking and isomerization reactions [4] or $NiW/A1_2O_3$ catalysts activity in hydroisomerization and hydrocracking of n-heptane [5], to decrease pyrolysis temperature.

The objectives of the present study were to select the optimum fluorinating agent and to determine the conditions of initial ceramic membranes modification by gaseous fluorination [6, 7] to induce catalytic properties, for example, for hydrocarbon pyrolysis.

Mesoporous α-$A1_2O_3$-based tube with external diameter of 8 mm, wall thickness of 1 mm, mean surface pore diameter of 0.2 μm was used as initial membrane. Binder material contained impurities of Ca, Si, Fe, K, B mixed oxides.

The following fluorides have been used as modifying agents: gaseous F_2 with 4-8 vol. % HF; vapors of MoF_6, BF_3 and their mixtures. Two modes of modification have been investigated: at room temperature and exposure of 100-200 hours (mode 1) and at the temperature of 60-105 ^oC and exposure of 3-4 hours (mode 2). The partial pressure of the fluorinating agent was 0,01-0,1 MPa.

The samples have been characterized by atomic emission spectroscopy, X-ray diffraction (XRD) (DRON-3, CuK_α radiation), scanning electron microscopy (SEM) (S-570 Hitachi), differential thermal analysis (DTA), (gaseous)permeability testing and quantitative chemical analysis on carbon.

Catalytic activity have been evaluated using gas chromatography method by hydrogen yield and propane-butane conversion degree and also visually by tube blackening. The

efficiency of fluorination has been estimated taking into account mass changes in the sample, visual changes of color, mechanical properties and results of XRD and SEM.

XRD data and average mass changes (Δm) just after fluorination; after exposure at air during 150-1150 hours until weight stabilization; and after heat treatment in air at 550 ^{o}C during 7 hours are given in Table 1.

Table 1

Fluorine - agent / modes of modification	Δm_F, %	Δm_{AIR}, %	Crystal structure (air)	Δm_T, %	Crystal structure (T)
F_2/ mode 1	+4,2	+4,2	α-Al_2O_3 $AlF_3 \bullet 3\ H_2O$	-	-
F_2/ mode 2	-1,5	-0,92	α-Al_2O_3 $CaAl_2Si_2O_8$ α-$AlF_3 \bullet 3\ H_2O$	-3,0	α-Al_2O_3 CaF_2 $CaAl_2Si_2O_8$
BF_3/ mode 1	+0,47	+0,37	α-Al_2O_3 $CaAl_2Si_2O_8$ AlF_3	-0,81	α-Al_2O_3 $CaAl_2Si_2O_8$ AlF_3 traces
BF_3/ mode 2	+0,26	+0,22	α-Al_2O_3 $CaAl_2Si_2O_8$ α-$AlF_3 \bullet 3\ H_2O$ γ-AlF_3	-	-
F_2:BF_3=1:2/ mode 1	+2,30	+1,30	α-Al_2O_3 support amorphization	-1,92	α-Al_2O_3 CaF_2 AlF_3
F_2:BF_3=1:2/ mode 2	+0,16	+0,03	-	-0,73	α-Al_2O_3 $CaAl_2Si_2O_8$
MoF_6/ mode 1	+8,9	+8,9	α-Al_2O_3 AlF_3 γ- AlF_3 $CaAl_2Si_2O_8$ traces	-1,68	α-Al_2O_3 $CaMoO_4$ AlF_3
MoF_6/ mode 2	+5,92	+6,20	α-Al_2O_3 $CaAl_2Si_2O_8$ α-$AlF_3 \bullet 3\ H_2O$ γ-AlF_3	-1,84	α-Al_2O_3 $CaMoO_4$

Fluorination at heating and small exposure produced lower increase in mass. Loss in mass after modification is the evidence of nonselective fluorination process accompanied by

partial removal of binder. In other cases major modifications are in the surface layers of ceramic tubes. XRD data show that depending on the conditions of fluorination aluminium fluorides or hydrofluorides can be formed. The content varies from 0 to 30-40 %. The process can be accompanied by amorphization of alumina support. In the cases when the initial crystal structure does not change fluorine atoms may form surface groups Al-F similar to [8] or are chemisorbed in the pores. After additional heat treatment CaF_2 can be formed due to fluorine interaction with binder components. Intensity of peaks corresponding to support impurity $CaAl_2Si_2O_8$ (main peak $2\Theta=27.9^o$) increased after heat treatment. For the samples modified with MoF_6 additional undefined phase with the most intensive peak at $2\Theta=47^o$ is also present. As a whole we can say that at air heat treatment the main changes take place in the ceramic support. Fluorination with BF_3 influences the crystal ceramic support at the least extent and the modified samples have high stability to air heat treatment.

Catalytic activity of modified membranes has been investigated using propane-butane mixture with flow rate 0.-0.9 l/h and excess input pressure ~ 260-780 Pa in the temperature range of 400-750 ^oC. Unmodified alumina tubular membranes and granular spherical or cylindrical ceramic carriers based on α- or γ-$A1_20_3$ have been used for comparison. $A1_2O_3$ – based ceramic samples modified by MoF_6 fluorination show the highest activity in pyrolysis at the temperature of 580 ^oC. Pyrolysis for 2 hours in the temperature range of 580-605 ^oC leads to carbonization of the samples, carbon content being 0.16-0.23 mass. %. Carbon coatings are not formed on the unfluorinated samples under the same conditions, and at further temperature increase the samples become slightly grayish. Temperature of the process can be reduced by 100-150 ^oC using MoF_6 as the modifying agent and by 50-100 ^oC using BF_3.

XRD patterns of the carbonized samples show the changes in relative intensities of $A1_2O_3$ peaks. Peaks corresponding to carbon are absent which is the evidence of carbon high dispersion in the structure. It is also confirmed by uniform blackening of the tube cross-section and by the absence of marked carbon top layer on micrographs. According to the chromatography data hydrogen yield for the fluorinated tube was enhanced by a factor 1.2-2.5 compared to initial tubes. By comparison, fluorination of granular γ-$A1_2O_3$ –based industrial catalysts under the same conditions allows to enhance hydrogen yield by a factor of 1.5-8.0. Thus, the developed technique of gaseous modification is universal and can be used both for tubular and granular catalysts.

As a result of investigations the conditions for fluorine atoms incorporation by gaseous method into tubular mesoporous ceramic α-Al_2O_3–based supports are determined; interrelation between fluorides, fluorinating agent, content of the fluorine introduced into the sample, temperature and time of fluorination has been revealed. Gaseous method of modification of ceramic mesoporous membranes based on different aluminas has been developed. It includes the preliminary stage of ceramics treatment by volatile fluorides.

References

1. *USA Patent* №5503873 USA, 1994.
2. Jiang S., Yan Y., Gavalas G. R., *J. of Membrane Sci*., 103 (1995) 211.
3. Reddy G.K., Rao K.S.R., Rao P.K., *Cat. Lett.,* 59 (1999) 157.
4. Chernov V.A., Antipina T.V., *Нефтехимия,(in Russia),* 5 (1965) 688.
5. Benitez A., Ramirez J., Cruz-Reyes J., Lopez Agudo A., *J. of Catalysis,* 172 (1997) 137.
6. Amirkhanov D.M., Kotenko A.A., Tulskii M.N., Patin V.G. *RF Patent* №1776195, 1991.
7. Kotenko A.A., Amirkhanov D.M., Tulskii M.N., Patin V.G. *RF Patent* №1776194,1991.
8. Vinokurova E.B., Antipina T.V., *J. Phys.Chem.(in Russia),* 43 (1969), №5,1285.

HETEROGENEOUS CATALYSTS WITH ACTIVITY PROFILE CONTROLLED ON MOLECULAR LEVEL

Andreev V.V.

Chuvash State University, Cheboksary, Russia
E-mail: avv@chuvsu.ru

Optimal control on the chemical reaction proceeding under non-steady-state conditions over heterogeneous catalysts (in particular, on porous catalyst granules) with controlled activity profile allow to make its productivity higher, than under steady-state conditions.

Let us analyse a single reaction of the following type:

$$A_1 \xrightarrow{r_1} products\,. \qquad (1)$$

Here it is supposed that dependency of reaction rate r_1 from concentrations and temperature can have arbitrary functional form.

In a previous study [1] on the base of quasi-homogeneous model [2] we have obtained the necessary conditions of the productivity maximization of a porous catalyst granules with controlled activity profile in the case of a reaction of type (1). These equations are obtained for case of catalytic centres distribution on the internal surface of porous granule as a δ-function at a certain depth from the granule centre. This depth is the function of time. Such distribution of active component for derivation of equations is assumed because previously it was shown [3] that the theoretical effectiveness of the porous catalyst granule reaches a maximum in precisely such a case. In a real case the δ-function can be approximated [4] by a rectangular distribution of an active layer of thickness at most $0.04R_S$ (R_S - is the granule radius).

In a previous studies [1, 5] it is proposed that for obtaining of still more higher productivity of porous catalyst granules the reactions are to be realised on them under artificially created non-steady-state condition) with simultaneous coordinated control by δ-function position in the granule. Such management of activity profile can be achieved with the help of an ultrasound or an electromagnetic field and also with the help of other methods. So, previously [6] the possibility of creation of non-uniform structures on the solid surfaces under laser radiation of comparatively small intensity was shown.

The mechanism of control surface activity can be explained with the help of a Fig.1. After removing from an equilibrium state of one or both particles with masses m_1 and m_2, each of which is located in a potential hole, owing to the presence of connection with rigidity *k* between them after some time mutual synchronization of such system dynamics will come.

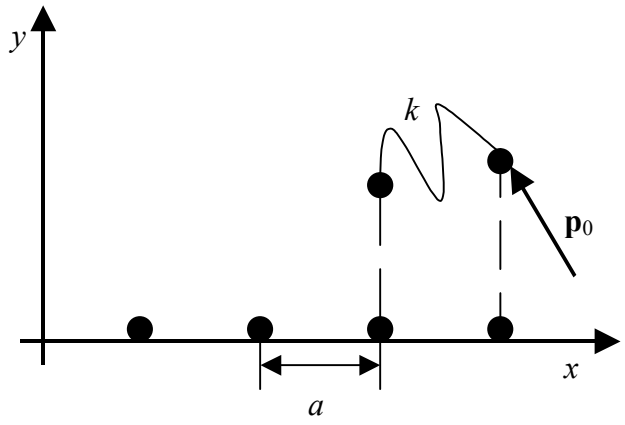

a

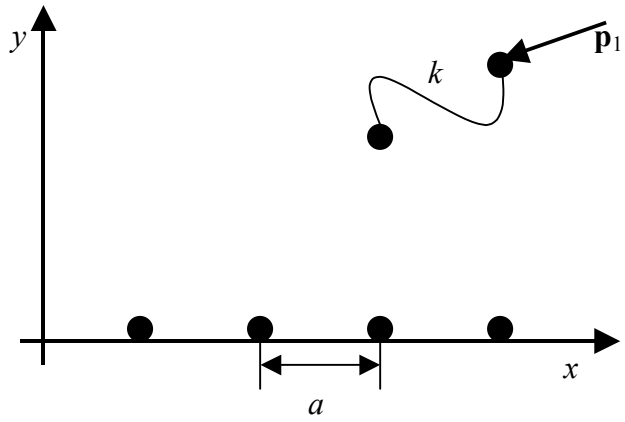

b

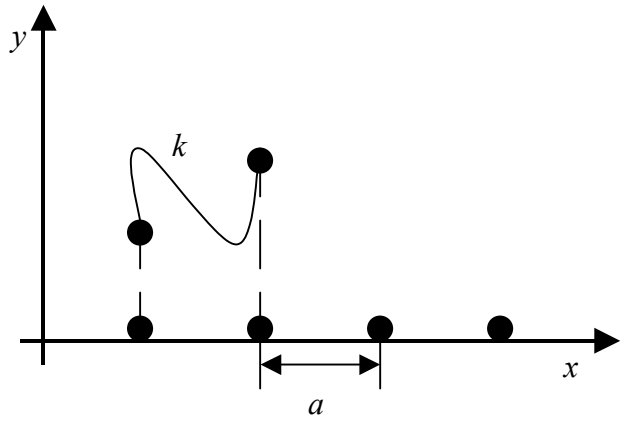

c

Fig. 1

After that the impulse $\mathbf{p_0}$ is transmitted to the given system of particles. This impulse is sufficient to pull up each of these particles from the appropriate potential holes, not breaking

thus connection between them with rigidity k (fig.1*a*). Then the new impulse $\mathbf{p}_1$ (fig.1*b*) is transmitted to particles system, therefore it will be displaced both on an axis x, and on an axis y remaining the structure. As a result the particles system gets into attraction field of new centres on a solid surface (fig. 1*c*).

Necessary conditions of productivity maximization [1] can be represented in the form of equations (2a)- (2e).

$$\frac{R_{1U}}{\Psi(\varphi^2+\sigma I_1)+R_{1\theta}\beta\sigma(B_T^{-1}-B_1^{-1})-1}+\lambda_1=0, \tag{2a}$$

$$\frac{R_{1\theta}}{\Psi(\varphi^2+\sigma I_1)+R_{1\theta}\beta\sigma(B_T^{-1}-B_1^{-1})-1}+\lambda_2=0, \tag{2b}$$

$$\beta-R_{1U}R_{1\theta}^{-1}=0, \tag{2c}$$

$$\theta_1=1+\frac{\overset{)}{T}_0(t)}{\widetilde{T}_0}+\beta(1+\frac{\overset{)}{C}_{01}(t)}{\widetilde{C}_{01}}-U_{11})+R_1\beta\sigma(B_T^{-1}-B_1^{-1}), \tag{2d}$$

$$R_1=\frac{1+\overset{)}{C}_{01}(t)/\widetilde{C}_{01}-U_{11}}{\varphi^2+\sigma I_1}. \tag{2e}$$

Here it is supposed that the concentration C_1 of the substance A_1 and the temperature T in the nucleus of the external reaction mixture stream change with time as follows:

$$C_{01}(t)=\widetilde{C}_{01}+\overset{)}{C}_{01}(t),\quad \int_0^{\tau_1}\overset{)}{C}_{01}(t)dt=0,$$

$$T_0(t)=\widetilde{T}_0+\overset{)}{T}_0(t),\quad \int_0^{\tau_2}\overset{)}{T}_0(t)dt=0,\quad p_1\tau_1=p_2\tau_2=\tau. \tag{3}$$

Here $\widetilde{C}_{01}$ and $\widetilde{T}_0$ do not depend on time; p_1 and p_2 are arbitrary whole positive numbers; τ_1 and τ_2 are the periods of change for the functions $\overset{)}{C}_{01}(t)$ и $\overset{)}{T}_0(t)$. To simplify the analysis it is assumed [7, 8] that the values τ_1 and τ_2 are significantly larger in comparison with the characteristic times of the process proceeding in the porous catalyst granule (quasi-steady-state conditions). The following notations are used in equations (2): $\sigma=\widetilde{r}_{01}g_0R_S^2/\left((\alpha+1)\widetilde{C}_{01}D_1^*\right)$; g_0 - is the catalyst density per unit of porous granule volume when it is distributed uniformly on a granule; D_1^* - is the effective diffusion coefficient of substance A_1 in the pores; α - is a parameter which is determined by a granule geometric form (α=2 for a sphere, α=1 for a cylinder, α=0 for a plate); $\widetilde{r}_{01}=r_1\left(\widetilde{C}_{01},\widetilde{T}_0\right)$; $\beta=D_1^*Q\widetilde{C}_{01}/\left(\lambda^*\widetilde{T}_0\right)$; λ^* is the

effective coefficient of a granule's heat conductivity; Q is the heat effect of the reaction; $B_1 = R_S\beta_1/D_1^*$; β_1 is the coefficient of mass exchange on substance A_1 between a granule and external reaction mixture stream; $B_T = R_S\beta_T/\lambda^*$; β_T is the coefficient of heat exchange between a granule and external reaction mixture stream;$\varphi^2=\delta(I_0+1/B_1)$ is the modified Thiele parameter; $I_0 = \int_{x_{01}}^{1} x^{-\alpha} dx$; $I_1 = \int_{x_1}^{x_{01}} x^{-\alpha} dx$; x_{01} и x_1 are the optimal positions of δ- function in a granule, respectively, at the initial moment of time t_0 and at the moment of time t; $R_1=r_1(C_{11},T_1)/\ \tilde{r}_{01}$; $C_{11}=C_1(x_1)$; $T_1=T(x_1)$; $U_{11}=C_{11}/\tilde{C}_{01}$; $\theta_1 = T_1/\tilde{T}_0$; $R_{1U}=\partial R_1/\partial U_{11}$; $R_{1\theta} = \partial R_1/\partial\theta_1$; $\Psi = \beta R_{1\theta} - R_{1U}$.

System of equations (2) define the extremum of functional (4).

$$\tilde{J}/\tilde{J}_0 = \frac{1}{\tau}\int_0^{\tau} R(U_{11},\theta_1)dt\,. \qquad (4)$$

Here U_{11} и θ_1 are the functions of $\overset{1}{C}_{01}(t)$, $\overset{1}{T}_0(t)$ и $x_1(t)$. In this functional (4) the value $\tilde{J}_0$ is the productivity of a porous catalyst granule calculated in the case when $\overset{1}{C}_{01}(t) = \overset{1}{T}_0(t) = 0$ and in a granule the position x_1 of δ-function do not depend from time t. Thus, the functional (4) is a relation of a porous catalyst granule productivities calculated in assumptions when process is respectively non-steady-state and steady- state.

References

1. Andreev V.V., *Mendeleev Commun.*, (1998), 77.
2. Zel'dovich Ya.B., *Journal of Phys. Chem*., V. 13 (1939), 163 (in Russian).
3. Vayenas C.G., Pavlou S., *Chem. Eng. Sci*., V. 42 (1987), 2633.
4. Morbidelli M., Servida A., Paludetto R. and Carra S., *J. Catal*., V. 87(1984), 116.
5. Andreev V.V., *Ultrasonics Sonochemistry*, V. 6 (1999), 21.
6. Andreev V.V., Ostryakov G.N. and Telegin G.G., *Chem. Phys. Reports*, V. 16/1 (1997), 159.
7. Andreev V.V., Koltsov N.I., Ivanova A.F. and Konstantinova N.V., *Mendeleev Commun.*, (1995), 152.
8. Andreev V.V., *Mendeleev Commun.*, (1997), 35.

THE TEMPERATURE DEPENDENCE OF STICKING COEFFICIENT FOR THE CASE OF THE LINEAR ADSORPTION ISOTHERM

Asnin L.D., Fedorov A.A., Chekryshkin Yu.S.

Institute of Technical Chemistry UB RAS, Perm, Russia
Fax: (3422) 126237; E-mail: cheminst@mpm.ru

The temperature dependence of sticking coefficient for the model of linear adsorption isotherm was obtained by the elementary analysis of correlation between characteristics of adsorption process and adsorption system parameters.

The linear adsorption isotherm is observed when sticking coefficient (s) and residence time (τ) are the functions of only temperature (T). The latter is possible in the case when activation energy for desorption and preexponential factor of Frankel equation are independent from adsorption pressure (p). Taking into account that the adsorption value (a) is the function T and p and on the other hand $a = Ws\tau$ where $W = p/(2\pi mkT)^{1/2}$ is the flux density of impinging molecules one can obtain the expression

$$s(T) = const \cdot T^{(0.5+\Delta C/R)} \cdot \exp\left[-\frac{E_d(0) - q_{st}(0)}{RT}\right]$$

where ΔC is the difference of heat capacities of substance in the adsorption and gaseous phases (ΔC is assumed to be constant), R is gas constant, $E_d(0)$ and $q_{st}(0)$ are activation energy for desorption and isosteric heat of adsorption at 0 K, respectively, *const* is constant of integration.

If the activation energy for adsorption is equal to zero the expression is $s(T) = const \cdot T^{(0.5+\Delta C/R)}$. It is interesting that s greatly depends on ΔC; even value of ΔC of the same order as R changes the function shape of $s(T)$. As a rule, $\Delta C > 0$. In this case s is the unlimited increasing function of T that has no physical sense as s must be less then 1 by definition. This discrepancy is explained by the character of accepted assumptions. So we considered s and τ as continuos functions of T. In fact, these functions are limited by the temperature of existence of a surface. Moreover, the validity of Frankel equation is broken near the melting point. Dissociation or ionization of adsorbate particles is another reason limiting the temperature range of applicability of the obtained expression.

ENHANCING OF THE CATALYTIC ACTIVITY BY MECHANOCHEMICAL ACTIVATION OF Bi-PROMOTED VANADYL PHOSPHATE SYSTEMS

Ayub I.[1], Zazhigalov V.A.[2], Dangsheng Su[1], Willinger M.[1], Kharlamov A.[3], Ushkalov L.[3], Schlögl R.[1]

[1]Fritz-Haber Institute of the Max Planck Society, Berlin, Germany
[2]Ukrainian-Polish Laboratory of Catalysis, Institute for Sorption and Problems of Endoecology, National Academy of Sciences of Ukraine, Kiev, Ukraine
[3]Institute for Problems of Materials Science, Kiev, Ukraine

VPO-Bi catalysts prepared by traditional method in butanol and mechanochemically promoted by Bi (addition of Bi_2O_3 to $VOHPO_4 \cdot 0.5H_2O$) was treated in ethanol, water and air for several times and was studied by means of different characterization techniques such as SEM, TEM, EELS, XPS, BET and XRD.

SEM shows that the initial sample consists mainly of flat smooth needles, that form a blossom secondary morphology. Under mechanochemical treatment the secondary morphology is lost and packages are formed with coin-shape particles. XRD reveals that milling in air for 28 minutes resulted in an amorphous phase. Milling for 30 minutes in air transforms $VOHPO_4 \cdot 0.5H_2O$ to $(VO)_2P_2O_7$. In contrast milling in ethanol for 30 minutes did not induce any phase change. XRD also reveals that milling in water for just 2 minutes hydrates $VOHPO_4 \cdot 0.5H_2O$ to $VOHPO_4 \cdot 4H_2O$.

Catalytic activities of the mechano-activated samples are compared with the conventional thermal-activated VPP. The mechanotreated samples show an enhancement of *n*-butane conversion and an increasing of maleic anhydride selectivity and yield. The sample milled in water for just 2 minutes exhibits an increase in conversion to 91 %. The aim of this work is not only to study the microstructure, but also to get knowledge how different milling conditions change the catalytic properties and how important this method is for catalysis.

THE ALTERNATING COOLIGOMERIZATION OF NORBORNADIENE WITH CARBON MONOXIDE BY HOMOGENEOUS *TRIS*-PYRASOLIL – Pd CATALYTIC COMPLEX

Novikova H.V., Solotnov A.A., Belov G.P.

Institute of Problems of Chemical Physics RAS, Moscow Region, Chernogolovka, Russia
Fax: (096)-515-5420; E-mail: novik@cat.icp.ac.ru

The alternating cooligomerization of norbornadiene with CO in the presence of Pd-catalyst of the following structure:

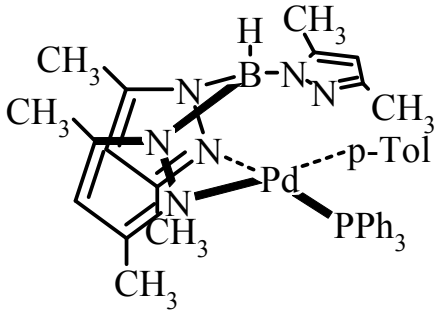

was carried out in different conditions. The cooligomers of keton, spiroketal and keto-enol structure were obtained in dependence of used co-catalysts (CF_3COOH, $C_6H_4O_2$) and solvents (MeOH, CH_2Cl_2). The structure of cooligomers was analyzed by IR-, NMR, GPC and it was supposed that they are formed by coordination of MeOH/co-catalyst to Pd or substitution of p-Tol group by MeO^- or CF_3COO^- upon the cooligomerization process. The new complexes are less stable, but more effective in the processes of alternating cooligomerization of norbornadiene with CO.

Here we report the first experimental observation for above mentioned processes and discuss possible mechanism of the formation of cooligomers with different structure.

We are grateful to Prof. Klauie for providing us with the catalyst. The work was supported by Russian Foundation for Basic Research (project № 01-03-33248).

MAIN PATHWAYS OF ISOPRENE OXIDATION IN AQUEOUS SOLUTIONS IN THE PRESENCE OF THE CATALYTIC SYSTEM $PdCl_2$ – *n*- BENZOQUINONE

Belyaev B.A., Gromova E.V., Krylov A.V., Belov A.P.

Lomonosov Moscow State Academy of Fine Chemical Technology, Moscow, Russia
E-mail: bbelyaev@hotbox.ru

The catalytic oxidation of diens is used for the synthesis of unsaturated polyfunctional compounds of various structures. Unlike 1,3-pentadien the oxidation of which is studied in detail [1, 2], the information on oxidation of isoprene is rather limited.

The objective of this work is the study of oxidation process of isoprene in aqueous solutions of palladium(II) chloride in the presence of *n*-benzoquinon.

The oxidation reaction proceeds via intermediate formation of hydroxo-containing η^3-allyl palladium complex, the subsequent oxidation of which brings about the formation of unsaturated diols of various composition.

The reaction of oxidation can be described by the following stoichiometric equation:

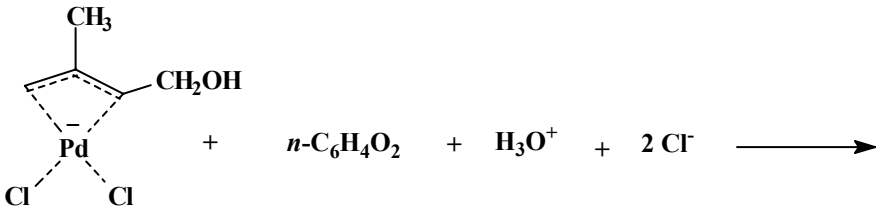

The investigation of the process in question by means of NMR ^1H – spectroscopy revealed that the main oxidation products are 2-methyl-3-butendiol-1,2 and 3-methyl-3-butendiol-1,2 (in 1:1 ratio), the total yield being 70 %. The results allow us to suppose the formation of *cis*- / *trans*- isomers of 2-methyl-2-butendiol-1,4.

In the course of kinetic experiments series the orders to reagents were determined and activation energy of oxidation reaction of η^3-allyl palladium complex was estimated.

The results suggest that the formation of 2-methyl-3-butendiol-1,2 could be associated with the isomerization of primary formed diol-1,4.

References:

1. Belozerov V.E., Finashina E.D., Flid V.R., Belov A.P // Kinetics and Catalysis (in Russian). 1997, V. 38, № 3, P. 387 – 390.
2. Finashina E.D., Flid V.R., Belov A.P // 3-rd World Congress on Oxidation Catalysis. San-Diego, 1997.

^{1}H, ^{13}C NMR AND ETHYLENE POLYMERIZATION STUDY OF THE CATALYSTS $(Cp\text{-}R)_2ZrCl_2$+MAO AND ANZA-ZIRCONOCENES+MAO: EFFECT OF THE LIGAND COMPOSITION ON THE FORMATION OF THE ACTIVE INTERMEDIATES AND POLYMERIZATION KINETICS

Bryliakov K.P., Semikolenova N.V., Yudaev D.V., Zakharov V.A., Talsi E.P.

Boreskov Institute of Catalysis SB RAS, Novosibirsk, Russia
E-mail: talsi@catalysis.nsk.su

Spectroscopic monitoring of the cationic intermediates formed upon activation of metallocenes with methylaluminoxane (MAO) and correlation of their concentration with polymerization activity is crucial for the elucidation of the reaction mechanisms[1-5]. Recent NMR studies[6,7] have provided important information on the structures of 'cation-like' intermediates formed upon activation of Cp_2ZrMe_2 with MAO in toluene. It was shown that complexes $Cp_2MeZr\text{-}Me{\rightarrow}Al{\equiv}MAO$ (**I**) and $[Cp_2ZrMe(\mu\text{-}Me)Cp_2ZrMe]^{+}Me\text{-}MAO^{-}$ (**II**) dominate in the reaction solution at low Al/Zr ratios (20–50), whereas $[Cp_2Zr(\mu\text{-}Me)_2AlMe_2]^{+}Me\text{-}MAO^{-}$ (**III**) and $Cp_2ZrMe^{+}{\leftarrow}Me^{-}\text{-}Al{\equiv}MAO$ (**IV**) are the major species at high Al/Zr ratios (200–4000). It has been proposed[7] that complex $[Cp_2Zr(\mu\text{-}Me)_2AlMe_2]^{+}$ $Me\text{-}MAO^{-}$ (**III**) is the precursor of the active centers for polymerization. In order to elucidate the factors that govern activity of the catalytic systems zirconocene/MAO, it is important to extend such studies to more complex and practically attractive zirconocene catalysts and to correlate the data on the concentrations of species **III** and **IV** at various Al/Zr ratios with the polymerization activity. In this work, we have undertaken a ^{1}H and ^{13}C NMR spectroscopic study of the cationic intermediates formed upon activation of L_2ZrCl_2 with MAO at various Al/Zr ratios. The following catalysts were studied: $(Cp\text{-}R)_2ZrCl_2$ (R= Me, 1,2-Me_2, 1,2,3-Me_3, 1,2,4-Me_3, Me_4, Me_5, *n*Bu, *t*Bu), rac-ethanediyl$(Ind)_2ZrCl_2$, rac-$Me_2Si(Ind)_2ZrCl_2$, rac-Me_2Si(1-Ind-2-Me)$_2ZrCl_2$, rac-ethanediyl(1-Ind-4,5,6,7-$H_4)_2ZrCl_2$, (Ind-2-Me)$_2ZrCl_2$, $Me_2C(Cp)(Flu)ZrCl_2$, Me_2C(Cp-3-Me)$(Flu)ZrCl_2$, $Me_2Si(Flu)_2ZrCl_2$. Correlations between spectroscopic and ethene polymerization data for catalysts $(Cp\text{-}R)_2ZrCl_2$/MAO (R= Me, 1,2-Me_2, 1,2,3-Me_3, 1,2,4-Me_3, Me_4, Me_5, *n*Bu, *t*Bu) were elucidated. The catalysts $(Cp\text{-}R)_2ZrCl_2/AlMe_3/CPh_3^{+}B(C_6F_5)_4^{-}$ (R= Me, 1,2-Me_2, 1,2,3-Me_3, 1,2,4-Me_3, Me_4, Me_5) were also studied for comparison of spectroscopic and polymerization data with MAO based systems. Complexes of type $(Cp\text{-}R)_2ZrMe^{+}{\leftarrow}Me^{-}$-Al≡MAO (**IV**) with different Me-MAO^{-} counter anions have been identified in the $(Cp\text{-}R)_2ZrCl_2$/MAO (R = *n*Bu, *t*Bu) systems at low Al/Zr ratios (Al/Zr = 50-200). At Al/Zr ratios of 200–1000, the complex $[L_2Zr(\mu\text{-}Me)_2AlMe_2]^{+}$ $Me\text{-}MAO^{-}$ (**III**) dominates in all

MAO-based reaction systems studied. Ethene polymerization activity strongly depends on the Al/Zr ratio (Al/Zr = 200-1000) for the systems (Cp-R)$_2$ZrCl$_2$/MAO (R = H, Me, *n*Bu, *t*Bu), while it is virtually constant in the same range of Al/Zr ratios for the catalytic system (Cp-R)$_2$ZrCl$_2$/MAO (R = 1,2-Me$_2$, 1,2,3-Me$_3$, 1,2,4-Me$_3$, Me$_4$, Me$_5$) and rac-Me$_2$Si(Ind)$_2$ZrCl$_2$/MAO. The data obtained are interpreted on assumption that complex **III** is the actual precursor of active centers of polymerization in MAO based systems. The data obtained for the (Cp-R)$_2$ZrCl$_2$/MAO systems correlate with those for the highly active catalytic systems (Cp-R)$_2$ZrCl$_2$/AlMe$_3$CPh$_3^+$B(C$_6$F$_5$)$_4^-$. In the latter, ^{1}H NMR spectroscopy indicates the presence of only the intermediates [(Cp-R)$_2$ZrMe(μ-Me)$_2$AlMe$_2$]$^+$ B(C$_6$F$_5$)$_4^-$ containing the same cations as those in the intermediates **III** in the MAO-based systems, thus confirming the role of complex **III** as the precursor of the crucial catalyst species. The fraction of complex **III** can be increased over that of complex **IV** by Cp ligand substituent patterns which disfavor the anion-cation contacts in complex **IV**, due to steric or electronic effects.

Acknowledgement. The authors thank INTAS for financial support of this work (grant 00-841).

References

[1] E. Chen, T. J. Marks, *Chem. Rev*. 100 (2000) 1391.
[2] W. Kaminsky, Ed., "*Metalorganic Catalysts for Synthesis and Polymerization: Recent Results by Ziegler-Natta and Metallocene Investigations*", Springer-Verlag, Berlin, 1999.
[3] R. F. Jordan Ed., *J. Mol. Catal. A: Chemical*. 128 (1998) 1.
[4] M. Bochmann, *J. Chem. Soc., Dalton Trans*. (1996) 255.
[5] H.-H. Brintzinger, D. Fischer, R. Mülhaupt, B. Rieger, R. M. Waymouth, *Angew. Chem., Int. Ed. Engl*. 34 (1995) 1143.
[6] I. Tritto, R. Donetti, C. Sacchi, P. Locatelli, G. Zannoni, *Macromolecules*, 30 (1997) 1247.
[7] D. E. Babushkin, N. V. Semikolenova, V. A. Zakharov, E. P. Talsi, *Macromol. Chem. Phys*. 201 (2000) 558.

METAL-SALEN CATALYZED ALKENE EPOXIDATIONS: KEY INTERMEDIATES

Bryliakov K.P., Talsi E.P.

Boreskov Institute of Catalysis SB RAS, Novosibirk, Russia
Fax: 7 3832 343766; E-mail: bryliako@catalysis.nsk.su.

Catalytic epoxidation of unfunctionalized olefins was first proposed in achiral versions (Mn(salen) [1] and Cr(salen) [2]). Then, for the most part after the works by Jacobsen [3] and Gilheany [4], chiral manganese- and chromium-salen catalytic systems turned out popular and attractive both from synthetic and mechanistic points of view. The basic distinctions between Mn and Cr series were the lower activity of the high-valence chromium intermediates that allowed to isolate $[Cr^{V}O(salen)]^{+}$ reactive species [2], and the observed higher effectiveness of the Cr systems for *E*- substituted alkenes epoxidation (the Mn(salen) systems demonstrated higher *ee*s with *Z*-alkenes). However, in spite of high interest, the mechanisms (and the nature of reactive intermediates, in particular) remained unclear because of the absence of detailed *in situ* mechanistic studies. Here, we present such a basic work lately done in our group with the aid of EPR and NMR techniques: high-valence Mn and Cr intermediates were detected and identified, their reactivities probed, and donor ligands effect considered.

Recently, it has been shown that two different intermediates operate in the Katsuki-Jacobsen catalytic systems [5]. When PhIO was used as oxidant, $[Mn^{V}O(salen)]^{+}$ complex (**I**) was detected and identified in the catalytic system at -20 °C by ^{1}H NMR, an acylperoxo Mn^{III}(salen) complex (**II**) operating in the catalytic system with meta-chloroperoxybenzoic acid. In the Mn^{III}(salen)Cl/PhIO system, dinuclear [(salen)Mn^{IV}-O-Mn^{IV}(salen)] complexes acting as a reservoir of the intermediates. $Mn^{IV}O$(salen) have also been observed with both oxidants: the latter could affect the yield of practical epoxidations, giving mainly radical-type products on reaction with styrene.

The situation is different for Mukayiama-type catalytic systems Mn^{III}(salen)Cl/aldehyde/O_2 systems [6]. Two high-valence Mn complexes $Mn^{IV}O$(salen) and Mn^{IV}(salen)(OOCOR) were detected and identified, the former being responsible for radical type products, while the latter giving racemic epoxides. Based on the reactivity pattern of the catalytic system, the intermediate can be proposed as a $[Mn^{V}O(salen)]$ type species with *N*-methyl imidazole and Mn^{III}(salen)(OOCOR) (**III**, with pivalaldehyde) without additives.

An EPR and NMR studies of the chromium-salen catalyzed epoxidations revealed that two types of high-valence chromium complexes - possible reactive intermediates exist in

Cr^{III}(salen)Cl/PhIO catalytic systems. One of them is a $[Cr^{V}O(salen)]^{+}$ (**IV**) reactive intermediate, whereas the other one is a mixed valence $[(salen)Cr^{V}OCr^{III}(salen)]^{2+}$ species. The $Cr^{V}OCr^{III}$ dimers display representative EPR spectra of the Cr^{V} moiety and NMR spectra of the Cr^{III}(salen) part. Like $Mn^{IV}OMn^{IV}$ dimers in manganese-salen system, they can be regarded as an active $Cr^{V}O$ reservoir. In dry CH_3CN, dimeric species predominate, equilibrium concentration of $Cr^{V}O$ being very small. The effect of donor ligands is of two kinds: first, they shift the equilibrium into monomeric $Cr^{V}O$(salen), and secondly, they can affect the reactivity of the latter intermediate ('push-effect').

In the course of mechanistic studies, new EPR and NMR spectroscopies of Mn^{III}(salen), Mn^{IV}(salen), Mn^{V}(salen) [5-7], Cr^{III}(salen), Cr^{V}(salen) complexes [8,9] as well as common approaches to probing and understanding of transition metal catalyzed oxidation have been developed.

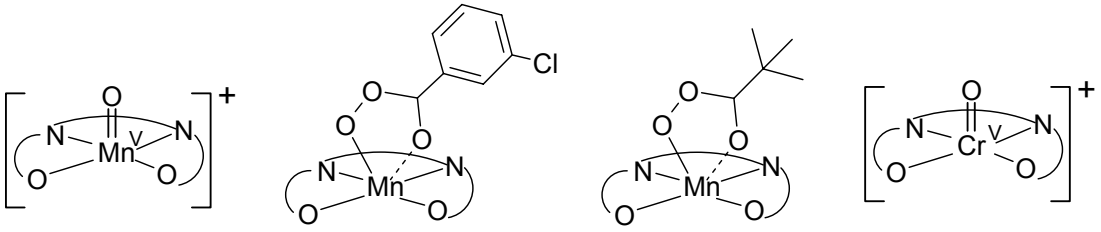

I **II** **III** **IV**

Acknowledgements. The authors thank Russian Foundation for Basic Research for financial support (grants 00-03-32438, 01-03-06384, 02-03-06185).

[1] K. Srinivasan, P. Michaud, J. K. Kochi, *J. Am. Chem. Soc. ,* 108 (1986) 2309.
[2] E. G. Samsel, K. Srinivasan, J. K. Kochi, *J. Am. Chem. Soc. ,* 107 (1985) 7606.
[3] E. N. Jacobsen, W. Zhang, A. R. Muci, J. R. Ecker, L. Deng, *J. Am. Chem. Soc. ,* 113 (1991) 7063.
[4] C. Bosquet, D. G. Gilheany, *Tetrahedron Lett.*, (1995) 7739.
[5] K. P. Bryliakov, D. E. Babushkin, E. P. Talsi, *J. Mol. Catal. A: Chemical*, 158 (2000) 19.
[6] K. P. Bryliakov, O. A. Kholdeeva, M. P. Vanina, E. P. Talsi, *J. Mol. Catal. A: Chemical*, 178 (2002) 47.
[7] K. P. Bryliakov, D. A. Babushkin, E. P. Talsi, *Mendeleev Communications* (1999) 29-32.
[8] K. P. Bryliakov, M. V. Lobanova, E. P. Talsi, *J. Chem. Soc. Dalton Trans.*, 2002, 2263.
[9] K. P. Bryliakov, E. P. Talsi, *submitted*.

SURFACE CARBON IN DRY METHANE REFORMING: INTERMEDIATE AND POISON

Bychkov V.Yu., Korchak V.N.

Semenov Institute of Chemical Physics RAS, Moscow, Russia
E-mail: bychkov@polymer.chph.ras.ru

Dry methane reforming (1) is a promising process for natural gas conversion to synthesis gas.

$$CH_4 + CO_2 \rightarrow 2\ CO + 2\ H_2 \quad (1)$$

Supported platinum group metals, nickel or cobalt are the most active catalysts of this reaction. Under catalytic conditions carbon can form by dissotiative adsorption of methane on metal surface (2):

$$CH_4 \rightarrow C + 2\ H_2 \quad (2)$$

Then surface carbon can react with CO_2 giving CO in direct reaction (3) or via CO_2 decomposition on metallic component (4-5):

$$C + CO_2 \rightarrow 2\ CO \quad (3)$$

$$CO_2 + Me \rightarrow CO + Me\text{-}O \quad (4)$$

$$C + Me\text{-}O \rightarrow CO + Me \quad (5)$$

Surface carbon is the main intermediate in dry methane reforming. At the same time, after the formation carbon can cover metallic surface and prevent further decomposition of methane (2). So surface carbon is also a poison for methane reforming.

We investigated properties of surface carbon, produced on different catalysts (Ni/Al_2O_3, Co/Al_2O_3, and Pt/Al_2O_3) during their interaction with methane and CH_4-CO_2 mixture. It was shown that the rate of CO_2 reaction with surface carbon (3) was much more than the rate of CO_2 reaction with supported metals [1-3]. It means, that just reactivity of carbon with respect to CO_2 determines catalytic activity in dry methane reforming.

Testing of $Ni(Co)/Al_2O_3$ interaction with methane pulses revealed that the rate of methane decomposition (2) in a series of CH_4 pulses depends on time interval between the pulses. The obtained results [1, 2] indicate that carbon species, produced at the methane decomposition, undergo further transformation during some minutes after their formation. This process includes agglomeration of carbon particles and regeneration of metallic surface. It was possible to measure heats of reactions of this surface carbon with CO_2 pulses (reaction (3)) using DSC-111 (Setaram) calorimeter [2]. Measured values of enthalpy of carbon formation ($\Delta H_{f,C}$) are significantly higher than zero (graphite carbon) and close to the

enthalpy of carbide carbon in Co_3C. It was observed, that measured $\Delta H_{f,C}$ values decreased with a "lifetime" of the produced carbon, that indicates gradual transformation of metastable carbon state into more stable one. High reactivity with respect to CO_2 allows keeping stable catalytic activity under the reaction conditions (700 °C).

Similar experiments with Pt/Al_2O_3 catalyst showed that another state of surface carbon was formed from methane on this catalyst [3]. It demonstrated lower "mobility" and reactivity with respect to CO_2 than the carbon formed on $Ni(Co)/Al_2O_3$. Measured on Pt/Al_2O_3 $\Delta H_{f,C}$ values are close to zero that is typical for graphite carbon. It was shown that carbon cover all platinum surfaces after 2-3 min in methane flow at 700 °C. Average covering depends on sample history and platinum dispersity. Respectively low reactivity of surface carbon to CO_2 on Pt/Al_2O_3 leads to gradual coking of platinum particles during catalysis at 700 °C and decrease of catalytic activity.

Acknowledgement: This work was supported by Russian Foundation for Basic Research (grant 01-03-32554).

References:

[1] Bychkov V.Yu., Krylov O.V., Korchak V.N., Russian Kinetics and Catalysis, 2002, **43** (1), 86–94.
[2] Bychkov V.Yu., Tyulenin Yu.P., Krylov O.V., Korchak V.N., Russian Kinetics and Catalysis, 2002, **43** (5) 724–730.
[3] Bychkov V.Yu., Tyulenin Yu.P., Korchak V.N., Russian Kinetics and Catalysis, in press.

SIMULATION OF SURFACE WAVES DURING OSCILLATORY CARBON MONOXIDE OXIDATION OVER PALLADIUM AND PLATINUM SINGLE CRYSTALS CAUSED BY "SUBSURFACE OXYGEN FORMATION" AND "SURFACE STRUCTURE TRANSFORMATION" MECHANISMS

Elokhin V.I., Latkin E.I., Matveev A.V., Gorodetskii V.V.

Boreskov Institute of Catalysis SB RAS, Novosibirsk, Russia
E-mail: elokhin@catalysis.nsk.su

The kinetics and mechanism of CO oxidation on a noble metals (Pt, Pd) was the object of extended research. The fascinating kinetic phenomena were discovered: oscillations of the reaction rate, moving of the concentration chemical waves over the surface of metal. This complex dynamic behaviour in oxidation reaction over platinum metals can be directed by the structure of the detailed reaction mechanism, specifically by the laws of physicochemical processes in the «reaction medium - catalyst» system. The types and properties of mathematical models describing the critical effects are naturally dependent on those physicochemical prerequisites that these models are often based on.

In the oscillating regime, the reaction mixture periodically affects the properties of metal surfaces. Mechanisms of oscillations are connected usually either with the surface structure reconstruction (Pt(100): hex $\Leftrightarrow$ 1×1) or associated with subsurface oxygen formation (Pd(110): $O_{ads} \Leftrightarrow O_{sub}$) [1]. The aim of this contribution is to compare the specific features of the statistical lattice models for imitating the oscillatory and autowave dynamics in the adsorbed layer during carbon monoxide oxidation over Pt(100) and Pd(110) single crystals differing by the structural properties of catalytic surfaces. It is well-known that Pt(100) undergoes the reversible adsorbate-induced surface structure transformation (Pt(100): hex $\leftrightarrow$ 1×1) depending on CO coverage. The lifting of the hex $\rightarrow$ 1×1 reconstruction is accompanied by increase in the oxygen sticking coefficient from ≈ 0.001 (hex) to ≈ 0.3 (1×1) thus inducing a transition from a catalytic inactive state into an active state with high sticking coefficient for oxygen. The competition of the O_2 and CO adsorption in combination with the processes of the surface structure transition hex $\leftrightarrow$ 1×1 is a driving force for self-oscillations. Contrary to Pt(100) the surface of Pd(110) single crystal does not reconstruct in the course of reaction. In this case the oscillatory behaviour of the CO + O_2 reaction can be attributed to the periodic formation and decomposition of subsurface oxygen (Pd(110): $O_{ad} \Leftrightarrow O_{ss}$) Detailed mechanism of this reaction has been established [2] by means of FEM, TPR and XPS studies. The subsurface oxygen modifies the catalytic properties of the surface, e.g., the heat of CO adsorption on the modified surface is less than that on the initial one. The O_{ss} layer blocks the

oxygen adsorption simultaneously with the growth of CO_{ads} layer and the surface reaction is poisoned (low rate of CO_2 formation). The slow CO_{ads} reaction with O_{ss} removes the subsurface oxygen and O_2 adsorption is again possible (high rate of CO_2 formation). The subsurface oxygen layer is formed again and the cycle repeats. In both cases oscillations exist only in the quite narrow range of the reaction parameters.

Based on the available experimental information the following detailed reaction mechanisms has been used for simulations:

1) Carbon monoxide oxidation reaction over Pt(100) [3].

1) $CO + * \rightarrow CO_{ads}$;

2) $CO_{ads}^{hex} \rightarrow CO + *_{hex}$;

3) (hex) $\rightarrow$ (1×1): $4CO_{ads} \rightarrow 4CO_{ads}^{1\times1}$;

4) (1×1)$\rightarrow$ (hex): $*_{1\times1} \rightarrow *_{hex}$;

5) $O_2 + 2*_{1\times1} \rightarrow 2O_{ads}^{1\times1}$;

6) $O_{ads}^{1\times1} + CO_{ads} \rightarrow CO_2 + *_{1\times1} + *$;

7) $CO_{ads}^{1\times1} \rightarrow CO + *_{1\times1}$

8) $CO_{ads} + * \rightarrow * + CO_{ads}$.

2) Carbon monoxide oxidation reaction over Pd(110) [2].

1) $O_{2(gas)} + 2* \rightarrow 2O_{ads}$;

2) $CO_{gas} + * \leftrightarrow CO_{ads}$;

3) $CO_{ads} + O_{ads} \rightarrow CO_{2(gas)} + 2*$;

4) $CO_{ads} + * \rightarrow * + CO_{ads}$;

5) $O_{ads} + {}_{v} \rightarrow [O_{ss}]$;

6) $CO_{ads} + [*O_{ss}] \rightarrow CO_{2(gas)} + 2* + *_v$;

7) $CO_{gas} + [*O_{ss}] \leftrightarrow [CO_{ads}*O_{ss}]$;

8) $[CO_{ads}*O_{ss}] + [*O_{ss}] \rightarrow [*O_{ss}] + [CO_{ads}*O_{ss}]$

9) $[CO_{ads}\ O_{ss}] \rightarrow CO_{2(gas)} + * + *_v$ - «cork-screw» reaction

The model catalyst surface was represented by the square lattice N×N (N = 400 – 1600) with periodic boundary conditions. States of the lattice cells are determined according to the rules prescribed by the detailed reaction mechanisms used in the cases under study. So-called Monte Carlo step (MCS) consisting from N×N elementary actions was used as a time unit. During the MCS each cell is tested on the average once. By elementary action it is meant a trial to change a state of the randomly chosen centre in such a manner, as it will with the substances taking part in the elementary processes (steps) constitute the detailed reaction mechanism. The probability of the particular process w_i is determined by a ratio between the rate coefficients, therewith the rate coefficients for the adsorption processes are multiplied by the relevant partial pressures. The rate coefficients of the elementary processes were partially taken from the available literature. During the MCS after each of N×N trial to carry out one of the elementary action the inner cycle of CO_{ads} diffusion has been arranged (usually M = 50-100 attempts of diffusion). The diffusion is necessary for the spatio-temporal processes synchronisation occurring on the different regions of the model surface. The

reaction rate and surface coverages were calculated after each MCS as a number of CO_2 molecules formed (or the number of cells in the corresponding state) divided by the total number of the lattice cells.

In both cases the synchronous oscillations of the reaction rate and surface coverages are exhibited within the range of the suggested model parameters under the conditions very close to the experimental observations [3, 4]. These oscillations are accompanied by the autowave behaviour of surface phases and adsorbates coverages. The intensity of CO_2 formation in the CO_{ads} layer is low, inside oxygen island it is intermediate and the highest intensity of CO_2 formation is related to a narrow zone between the moving O_{ads} island and surrounding CO_{ads} layer («reaction zone», characterised by the elevated concentration of the free active centres). The presence of the narrow reaction zone was found experimentally by means of the field ion probe-hole microscopy technique with 5 Å resolution [5]. The important role of the diffusion rate and of the lattice size on the synchronisation and stabilisation of surface oscillations has been demonstrated. The boundaries of oscillatory behaviour and hysteresis effects have been revealed. The possibility for the appearance of the target and turbulent patterns, spiral and elliptic waves on the surface in the cases under study has been shown [3, 4, 6, 7]. The results obtained make possible to interpret the surface processes on the atomic scale.

Acknowledgement. This work was supported by Russian Fund for Basic Research (RFBR Grants # 02-03-32568 and # 03-03-89013) and partly by NWO Grant # 047.015.002.

References

[1] G. Ertl. *Surface Sci.,* 1994, **299/300**, 742-754, and references therein.
[2] V.V. Gorodetskii, A.V. Matveev, A.V. Kalinkin, B.E. Niewenhuys. *Chemistry for Sustainable Development,* 2003, **11**, 67-74.
[3] E.I. Latkin, V.I. Elokhin, V.V. Gorodetskii. *J. Molec. Catal. A, Chem.*, 2001, **166**, 23-30.
[4] E.I. Latkin, V.I. Elokhin, A.V. Matveev, V.V. Gorodetskii. *J. Molec. Catal. A, Chem.*, 2000, **158**, 161-166.
[5] V.V. Gorodetskii, W. Drachsel. *Appl. Catal. A: General,* 1999, **188**, 267-275.
[6] E.I. Latkin, V.I. Elokhin, V.V. Gorodetskii. *Chem. Eng. Journal,* 2003, **91**, 123-131.
[7] A.V. Matveev, E.I. Latkin, V.I. Elokhin, V.V. Gorodetskii. *Chemistry for Sustainable Development,* 2003, **11**, 173-180.

KINETIC AND QUANTUM-CHEMICAL EXAMINATION OF SULPHOOXIDATION OF AROMATIC SUBSTANCES IN THE PRESENCE OF IONS, ANCHORED ON THE COBALT COMPLEXES WITH POLYETHYLENEIMINE

Emelyanova V., Yuldasheva G., Zhubanov K., Baysalbaeva A.

Research Institute of New Chemical Technologies and Material, Almaty, Kazakhstan
E-mail: ohtn@mail.ru

The sulphoacids are valuable raw material for synthesis of various organic substances, and also are used in production of organic dyes, medicinal drugs. The sulfur dioxide, which is one of the most toxic components of an atmosphere, is applied as the sulphurizing agent in the process of sulphooxidation, therefore this process can be used for salvaging of sulfur dioxide. At dissolution in water the sulfur dioxide forms weak acid H_2SO_4.

$$ArH + 2SO_2 + O_2 \xleftrightarrow{H_2O} ArSO_3H + H_2SO_4 \quad (1)$$

The kinetic equation featuring the basic experimental kinetic results looks like:

$$W_{O_2} = \frac{k \cdot C^2_{Co^{2+}} \sum_{m=1}^{2} \alpha_m \cdot C^m_{ArH} \cdot \sum_{n=2}^{3} \gamma_n \cdot C^n_{ПЭИ} \cdot \sum_{p=1}^{3} \sigma_p \cdot C_{SO_3^{2-}} \cdot \delta \cdot P_{O_2}}{\sum_{m=0}^{2} \alpha_m \cdot C^m_{ArH} \cdot \sum_{n=0}^{3} \gamma_n \cdot C^n_{ПЭИ} \cdot \sum_{p=0}^{3} \sigma_p \cdot C_{SO_3^{2-}} \cdot (1 + \delta \cdot P_{O_2})} \quad (2)$$

α_m, γ_m, σ_p , δ - are constants of formation of binuclear complex of cobalt with ArH, PEI, H_2SO_3, O_2, k - partial constant of the rate of ArH sulphooxidation with cobalt complexes of different structure. The kinetic studies allow to offer the mechanism of reaction:

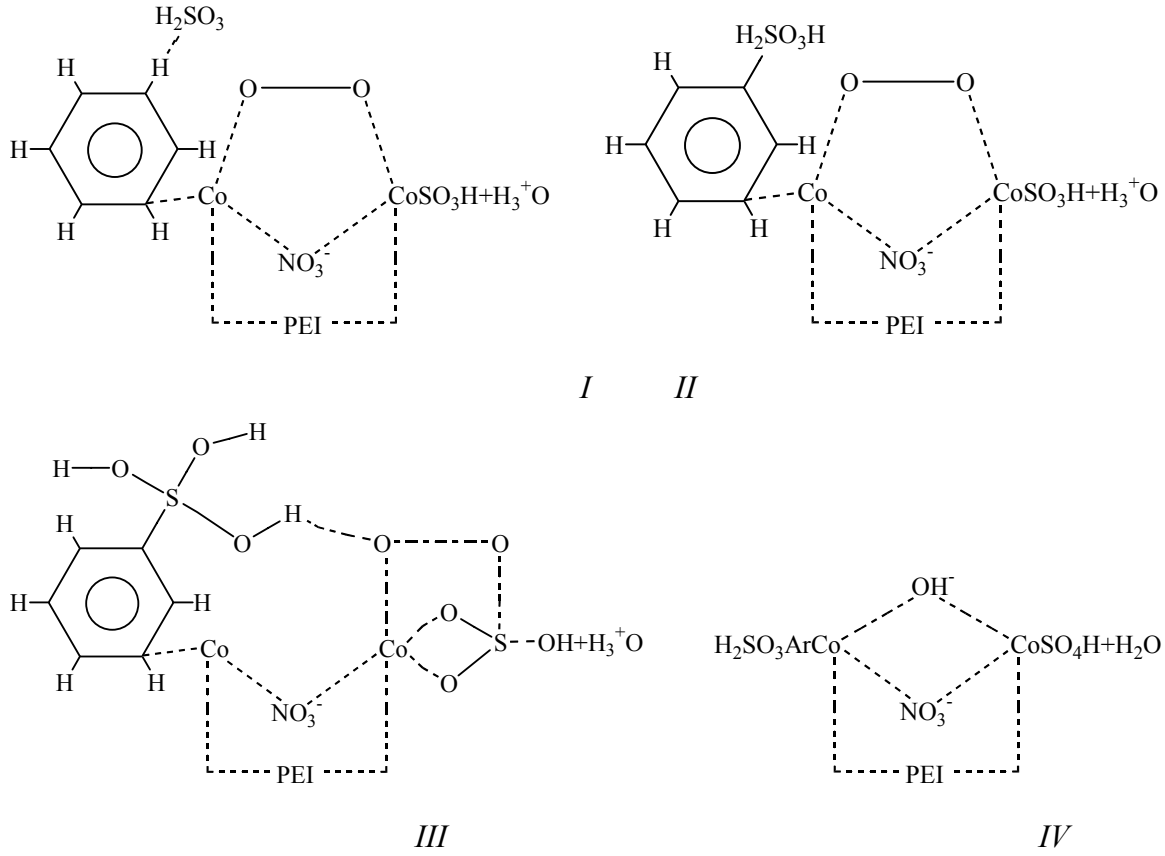

Fig. 1

Within the framework of a quantum-chemical method PM3 [1] the calculation of dimensional and electronic complexes I-IV is carried out.

On an initial stage of reaction an oxygenal complex I and hydroxonium ion are formed. In I the transition of π-electronic density of a benzene ring on ions of a cobalt and on atoms of an oxygen molecule is observed, therefore the positive charge on atoms of hydrogen of a benzene ring is considerably increased, and the bond O-O is weakened. At the following stage of reaction the promoted transition of hydroion from a benzene ring to one of the atoms of oxygen of H_2SO_3, and then formation of more stable structure $ArSO_3H_3^{2+}$ is possible (II). It was established experimentally, that formation of oxygenal complexes is accompanied by heat evolution [2]. In structure II the major negative charge is focused on oxygen atoms, and on atom of sulfur of HSO_3^- – considerable positive charge, probably, the energy oxygenal can transfer partially in intrinsic energy, which will be consumed on rotational displacement of O-O bond and formation of structure III. At the following stage of reaction the bond O-O is broken and HSO_3^- acidifies up to HSO_4^-. At this stage of reaction the transition of hydrion with $ArSO_3H_3^{2+}$ + on HSO_4^- is observed also, the second atom of oxygen is reduced up to OH^-

by hydroxonium ion, more stable structure IV is formed. At the last stage the reversible reaction $ArSO_3H_2^+ + H_2O \leftrightarrow ArSO_3H + H_3O^+$ with shift of equilibrium to direct reaction is possible.

The calculations are carried with the help of the package HyperChem, Release 5.0 for Windows (HyperCube Inc., 1996).

References:

[1] Stewart J.J.P., J.Comp.Chem. 12(1991) 320.
[2] Bratushko Y.,i., Coordination Compounds of 3d-Transition Metals with Molecular Oxygen. Kiev,1987.

HIGH-LOADED NICKEL-SILICA CATALYSTS FOR HYDROGENATION, PREPARED BY SOL-GEL ROUTE: STRUCTURE AND CATALYTIC BEHAVIOR

Ermakova M.A., Ermakov D.Yu.

Boreskov Institute of Catalysis SB RAS, Novosibirsk, Russia
E-mail: erm@catalysis.nsk.su

Ni-SiO_2 catalysts containing nickel in amount of 50 wt % and more often are used for industrial hydrogenation processes. An only available method for preparation of these catalysts is precipitation of nickel hydroxocomplexes on silica suspension. An improved version of this method developed and patented by Geus in 1967 is deposition-precipitation (homogeneous precipitation) [1]. The method allows nickel silicates of optimal composition to be obtained under controlled conditions; the nickel silicates can be reduced to form the dispersed metal phase (3-4 nm in particle size). The deposition-precipitation method underlay development of the standard European Ni/SiO_2 catalyst EuroNi-1 in 1980s [2]. The said method is complex enough that makes it of importance to develop other methods for synthesis of high-loaded Ni/SiO_2 catalysts. Among very promising methods is simple and ecologically friendly sol-gel synthesis based on alcoxysilanes.

Colloidal silica of high purity can be obtained by sol-gel synthesis at the entire absence of harmful wastes. The large-scale production of alcoxysilanes allows the current price for these products to be considerably reduced and partially hydrolyzed technical tetraethoxysilane (ethyl silicate as the trade name) becomes widely used as a binding and hydrophobizing agent. As a result, the silica produced from ethyl silicate is comparable in cost to commercial alumina.

Progress in the sol-gel technology for synthesis of catalysts is restrained due to impossibility to synthesize dispersed metal particles (<10 nm) at the amount of metal more than 15 wt % in the catalyst by the commonly employed methods based on the use of metal salt solutions as the metal precursor. It has been demonstrated before [3-5] that the problem can be resolved if dispersed hydroxide or oxide is used as the metal precursor, and alcosol obtained by partial hydrolysis of tetraethoxysilane in an acidic medium as the SiO_2 precursor. Hydrated nickel oxide is a pseudomorphose with respect to the initial hydroxide (Fig. 1). The loss of water and hydroxyl groups results in weakening of bonds between flakes in the secondary aggregates and the structure is partly destroyed. The micrograph demonstrates individual flakes in a large amount and fine nickel oxide crystals, while the secondary aggregates are shaped indistinctly. Specific surface area of hydrated nickel oxide equals

400 m^2/g. Ni/SiO_2 catalysts (from 50 to 95 wt% of nickel) were prepared by the heterophase sol-gel method through impregnation of dispersed hydrated nickel oxide with commercial ethyl silicate-32. Impregnation of a porous metal precursor with alcoholic solution of the ethyl silicate followed by drying makes it condensed to form polysiloxane films directly on the precursor surface. The next steps of calcination and reduction lead to formation of a silica matrix with metal nanoparticles confined in its pores.

The proposed method is in essence the reverse of impregnation of a porous support by the metal salt solution. The sol-gel procedure followed by drying of the gel coating the dispersed metal precursor results in formation of a silicate-silica net on the surface which prevents sintering of the metal particles during reduction and thermal treatments.

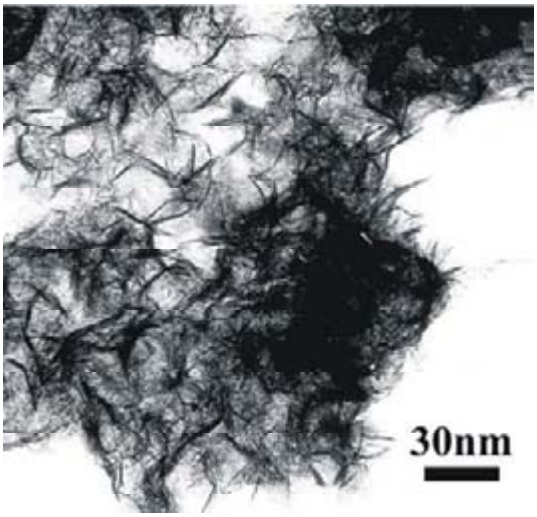

Figure 1. TEM image of hydrated nickel oxide

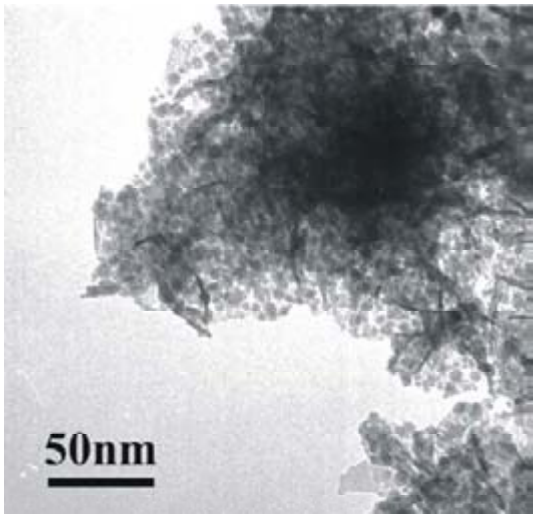

Figure 2. TEM image of reduced catalyst Cat34red

We shall refer to catalysts as CatXn, where X is silica percentage in the sample and index **n** indicates the nickel state in the sample at the measurement (**ox** for oxidized and **red** for reduced states).

The present work deals with sol-gel preparation of high-loaded nickel-silica systems (to 95% of Ni) and with characterization of physicochemical properties of the systems. ^{29}Si NMR, IR spectroscopy, Differentiating Dissolution, TPR, XRD and TEM techniques were used for studies of the precursors and catalysts. It was shown that silicate species favoring formation of fine nickel particles under reduction were produced by interaction of hydrated NiO with ethyl silicate. As the silica content increased from 0 to 52%, the nickel particles decreased in size from 44 to 4 nm (**Tabl. 1**, **Fig. 2**).

Table 1. Dependence of the reduction temperature of the nickel-silica systems and average size of nickel crystallites on the component ratio. Reduction temperature was determined from TPR data. Reduction degree of the samples was not lower than 98 %.

Ni/SiO_2, wt % in reduced systems	Reduction temperature, °C	Mean XRD size of nickel crystallites, nm
100 / 0	250	44
95 / 5	400	10-11
90 / 10	500	7
80 / 20	550	5-6
66 / 34	550	3-4
48 / 52	550	4

The sol-gel catalysts were tested in the reaction of benzene hydrogenation to show that the nickel surface was not blocked by silica but exposed to reactants (**Tabl. 2**).

Table 2. Catalytic reactivity of sol-gel $Ni-SiO_2$ systems to benzene hydrogenation at 120 ^oC

% Ni	d, Å	mmol benzene/g Ni·min	S_{Ni}, m^2/g	μmol/m^2·min
100	440	0.164	15,3	10.7
95	105	0.678	64,0	10.6
90	75	0.728	90,0	8.1
80	55	0,999	122	8.2
66	40	1.210	169	7.2
48	40	1.210	169	7.2

$S_{Ni}=6\times10^4/8.9\cdot d$, where 8.9 g/$cm^3$ is the nickel density

The data show that the hydrogenation rate is always in good agreement with the average size of nickel particles in the catalyst, i.e. the rate increases with decreasing average size of nickel crystallites. Close values of specific activity are characteristic of all the catalysts and silica-free nickel powder.

Characteristics of several nickel catalysts used for large-scale hydrogenation of edible oils are given in **Table 3**. It seems suitable to use this catalysts from leading producer companies for comparison because of the high surface area (150-180 m^2/g) characteristic of them and the most advanced technologies employed for their manufacturing. They are compared with the sol-gel catalyst with respect to their activity to benzene hydrogenation.

Table 3. Characteristics of some commercial Ni-containing catalysts used for comparison.

Commercial catalysts	Nickel content, %	Support	Application: liquid phase hydrogenation of edible oil, T ~ 200 ^{o}C
1. H-222 (Engelhard)	>60	SiO_2 + MgO	
2. Pricat-9910 (Synetix)	>60	SiO_2	
3. GM-3 (PRP-Ufa)	50	SiO_2	

As a result, the observed catalytic activity was higher than the activity of commercial nickel catalysts (Fig. 4)

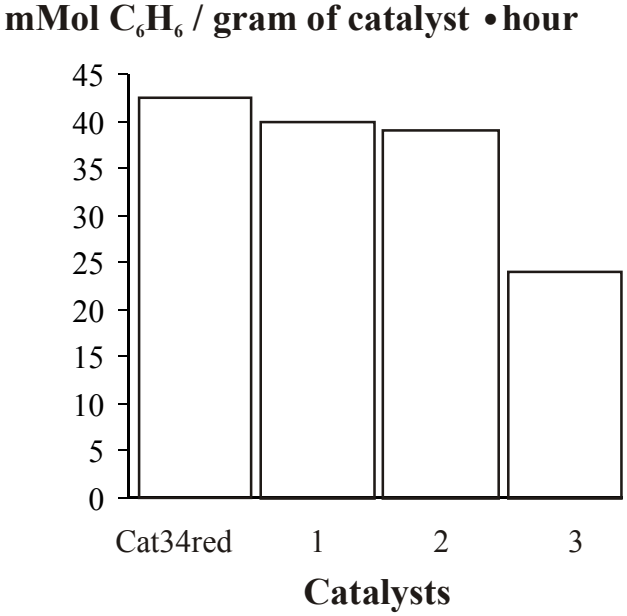

Figure 4. Comparative activities of some commercial nickel catalysts (see **Table 3**) and catalyst Cat34red for benzene hydrogenation

References

[1] J. W. Geus, Neth. Pat. Appl. 6705259, 1967 and 6813236, 1968.
[2] J. W. E. Coenen, Appl. Catal. A, 54 (1989) 59.
[3] G. G. Kuvshinov, D. Yu. Ermakov, M. A. Ermakova, Patent Russia 2126718 (1999), Boreskov Institute of Catalysis.
[4] M. A. Ermakova, D. Yu. Ermakov, L. M. Plyasova, and G. G. Kuvshinov, Russian J. Phys. Chem., 76 (2002) 665.
[5] M. A. Ermakova, D. Yu. Ermakov, Appl Catal, in press.

INFLUENCE OF CATALYTIC COPPER-BEARING SALINE SYSTEM STRUCTURE ON THE SIDE REACTION OF CARBON OXIDES FORMATION DURING ETHYLENE OXIDATIVE CHLORINATION

Flid M.R., Kurlyandskaya I.I., Babotina M.V., Treger Ju.A.

Federal State Unitary Enterprise "Research Institute "Synthez" with Design Office",
Moscow, Russia
Fax: 7 (095) 883-9243; E-mail: mflid@newmail.ru

Carbon mono- and dioxides are the by-products of ethylene oxidative chlorination proceeding in a fluidized copper-chloride ($CuCl_2/\gamma$-Al_2O_3) catalyst bed. Formation conditions of each of these oxides are the important factors of the process proceeding using concentrated oxygen and recycle of the reaction gas. Carbon oxide content in the steady-state reaction gas may achieve 65-70 %.

It might be supposed that such concentration of carbon oxides and CO/CO_2 ratio significantly influence upon the indications of the "oxygen" in oxidative chlorination of ethylene.

The purpose of this work is to study the interrelation between copper-bearing phases of catalytic systems for oxidative ethylene chlorination and its parameters, and selectivity and product formation routes of deep oxidation.

Establishment of such interrelation allows to test purposefully the catalysts for oxidative ethylene chlorination from the process selectivity point of view.

The studies of deep oxidation products formation were carried out over K1 and K2 catalysts differing by saline copper-bearing phases and their distribution across the surface of γ-Al_2O_3. The samples were subjected to radiographic examination using DRON-2 unit (CuKα, Ni-filter) with subsequent diffractogram phases referring to the JCPDS index. Upon X-ray phase analysis, K1 sample includes a number of copper-bearing phases – $CuCl_2$, $Cu_2(OH)_3Cl$ and other hydroxochlorides with excess of the saline component content at the surface. As for the K2 sample, the saline component exists preferably as a superfine fraction. This catalyst has relatively large part of the surface free of saline phases and as well, as areas where copper is located in the matrix lattice as aluminate structures.

The conditions of formation of deep oxidation products at ethylene oxychlorination has been studied in flow reactor (diameter of 42 mm) in a fluidized catalyst bed at the temperature range of 210-230 °C, dwell time of 1-20 sec., and the reagent ratio of $C_2H_4 : HCl : O_2 = 1{,}05 \div 1{,}07 : 2 : 0{,}6 \div 0{,}7$.

It was stated during the work that carbon oxides were formed as a result of both ethylene and 1,2-dichloroethane oxidation. Carbon dioxide is CO oxidation product, i.e. CO

and CO_2 are formed subsequently. General scheme of carbon oxide formation during the process is following:

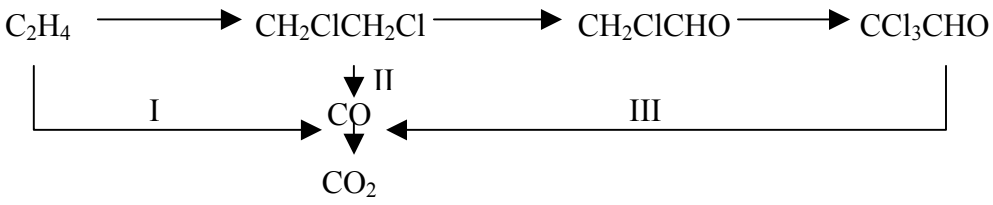

Rate ratio for COx formation routes is as follows: $r_1 : r_2 : r_3 = 1 : 2 : 0,3$

Active centers of K1 and K2 catalysts behave differently in the dichloroethane oxidation and chloroacetaldehyde chlorination reactions from the one hand, and in the reactions of chloral oxidation to CO and CO oxidation to CO_2, from the other hand, that explains different K1 and K2 catalyst activities in these reactions.

In particular, in the conditions of ethylene oxychlorination process, K2 catalyst is more active in the CO oxidation reaction in comparison with K1 one. This is an evidence of the fact that such active centers as Cu^{2+} ions in the saline clusters or in the matrix lattice are more active in such reaction than Cu^{2+} ions in the excess copper-bearing phases weakly bounded with the matrix surface.

It is essentially that if CO content in the reaction mixture exceeds 3 %, it results in fluidization mode impairment and in the catalyst activity and selectivity reduction.

It is the K2 catalyst that is preferable for this process due to its higher activity both in the main reaction of dichloroethane formation, and in CO oxidation into CO_2 that provides selectivity growth.

Upon the available experimental data the composition has been estimated of the recycle gas for industrial ethylene oxychlorination using oxygen as an oxidizer. These estimations showed that if the K2 catalyst is used, steady state gas contains 60-65 % (mol.) of CO_2 and 2-3 % (mol.) of CO. Gas of such composition has a positive influence upon fluidizing character and process selectivity. Dichloroethane content in raw material is 99,5-99,6 % (mol.) in chloral absence.

So, the recommendations for the catalytic copper-bearing saline system based on aluminum oxide of the certain structure may be applied for the efficient testing of catalytic systems for the high-selective process of “oxygen” chlorination of ethylene.

MECHANISM OF 1,1-DIMETHYLHYDRAZINE OXIDATION OVER SOLID CATALYSTS: KINETIC AND FTIR SPECTROSCOPIC STUDY

Ismagilov I.Z.[1], Kuznetsov V.V.[1], Kerzhentsev M.A.[1], Ismagilov Z.R.[1], Garin F.[2], Veringa H.J.[3], Heywood A.C.[4]

[1]Boreskov Institute of Catalysis SB RAS, Novosibirsk, Russia
[2]Louis Pasteur University, Strasbourg, France
[3]Netherlands Energy Research Foundation, Petten, The Netherlands
[4]Lawrence Livermore National Laboratory, Livermore, USA
Fax: 7 (3832) 39-73-52; E-mail: iismagil@catalysis.nsk.su

The kinetic study of 1,1-dimethylhydrazine $(CH_3)_2N–NH_2$ (or unsymmetrical dimethylhydrazine – UDMH) oxidation by air has been performed over the several types of solid catalysts, with the goal to reveal reaction mechanism through the temperature dependencies of all product concentrations. This study is an important part of big international project dedicated to the development of safe and efficient technologies for the neutralization of UDMH, which is a hazardous liquid rocket fuel [1]. In this communication we present the results of experiments with commercial catalysts IC-12-73 ($20\%Cu_xMg_{1-x}Cr_2O_4/\gamma\text{-}Al_2O_3$), IC-12-74 ($2\%Fe_2O_3/\gamma\text{-}Al_2O_3$), AP-64 ($0.64\%Pt/\gamma\text{-}Al_2O_3$) and modified zeolite $Cu/(ZSM\text{-}5+TiO_2+Al_2O_3)/Al_2O_3\text{-}SiO_2$ (further – "Cu/zeolite"). These experiments were conducted in the flow setup with vibro-fluidized catalyst bed in the glass reactor under the following conditions: catalyst temperature 200–400 ^oC, initial C(UDMH) in the reaction mixture with air 0.55 ± 0.05 mmol/L (1.2 ± 0.1 vol.%), catalyst loading 1 cm^3, catalyst fraction 0.5–1 mm, reaction mixture gas hourly space velocity (GHSV) 7200 h^{-1}, vibration frequency 50 Hz; the on-line GC and selective gas analyzer were used to monitor the product concentrations.

The above range of reaction temperatures was selected in the preliminary experiments [1], so that it would be possible to observe the transition between the regimes of partial and deep UDMH oxidation. It was found that the most active catalysts for deep oxidation to CO_2 in this temperature range are IC-12-73 and AP-64, while catalysts IC-12-74 and "Cu/zeolite" can be effectively used for deep oxidation only at temperatures above 400 ^oC (Fig. 1a). In the case of IC-12-73, whose activity is slightly higher than AP-64, noticeable increase of conversion to CO_2 begins already at 260 ^oC, and at the temperatures above 300 ^oC almost complete UDMH transformation into the deep oxidation products CO_2, H_2O and N_2 is observed.

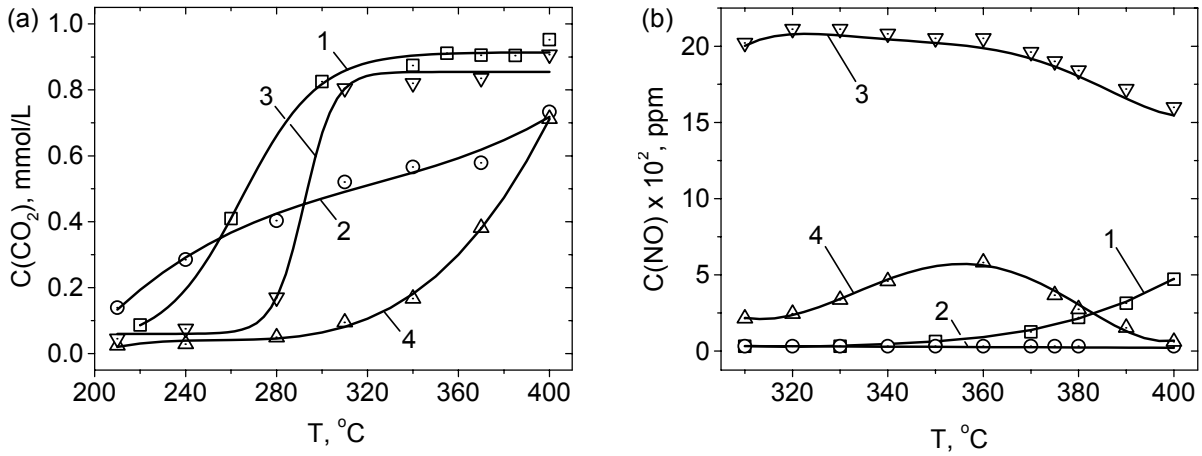

Fig. 1. Comparison of the temperature dependencies of CO_2 (a) and NO (b) concentrations upon UDMH oxidation over different catalysts. Initial C(UDMH) = 0.55 ± 0.05 mmol/L, GHSV = 7200 h^{-1}, 1 – IC-12-73, 2 – IC-12-74, 3 – AP-64, 4 – "Cu/zeolite".

The acquired dependencies correspond to the general concept, that noble metal catalysts are typically more active in deep oxidation, than oxide or zeolite catalysts [2]. For all the studied catalysts, at 200–300 °C along with the products of deep oxidation, a number of intermediate products forming from UDMH were revealed on the chromatograms, with CH_4, dimethylamine $(CH_3)_2NH$ (DMA), methylenedimethylhydrazine $(CH_3)_2N–N=CH_2$ (MDMH) dominating among them. Additional identification using the GC/MS technique showed, that other products, having lower concentrations, are C_2H_6, NH_3, dimethyl ether $(CH_3)_2O$, 1,1-dimethyldiazene $(CH_3)_2N=N$, methanol CH_3OH, acetonitrile $CH_3–C\equiv N$, acetone $(CH_3)_2CO$, dimethylformamide $(CH_3)_2N–COH$, nitrosodimethylamine $(CH_3)_2N–N=O$. All the product concentrations show good match with respect to initial C(UDMH) in the material balance by carbon and nitrogen. It was determined, that the most toxic product nitrosodimethylamine is usually formed only at the temperatures below 240 °C, and is absent near 400 °C.

As it can be seen from Fig. 1b, the highest concentrations of NO, as the one dominating among NO_x in our data, are formed on AP-64 catalyst, while the lowest – on IC-12-74 and IC-12-73 catalysts. In the vicinity of 360°C "Cu/zeolite" catalyst demonstrates rather high C(NO), which then decreases with temperature. Here the highest C(NO) for noble metal was expected again due to its high oxidation activity, while the oxides and "Cu/zeolite" show lower C(NO) [2]. For "Cu/zeolite", the decrease of C(NO) at high temperatures can be resulting from the process, similar to the well-known SCR of NO_x by hydrocarbons over Cu-ZSM-5 catalysts [3]. In our case, some of the intermediate UDMH oxidation products, like CH_4, C_2H_6, NH_3 can become the reducing agents. In summary, among all the perspective

catalysts tested by us (total of 14 samples), IC-12-73 demonstrated the cleanest neutralization of UDMH: high activity in deep oxidation to CO_2, and low selectivity of NO_x formation. Therefore, this catalyst was chosen to be employed in the fluidized catalyst bed (FCB) reactor of the technological scheme for UDMH neutralization [1].

Temperature dependencies of all the intermediate UDMH oxidation product concentrations for different studied catalysts allow to refine the tentative UDMH oxidation mechanism, that was proposed in [1]. The most important initial stages are oxidative dehydrogenation of adsorbed UDMH to form 1,1-dimethyldiazene (1), and interaction of two 1,1-dimethyldiazene molecules to form MDMH (2):

$$[(CH_3)_2N–NH_2]_{ads} + [O]_{ads} \rightarrow [(CH_3)_2N=N]_{ads} + [H_2O]_{ads} \quad (1)$$

$$2[(CH_3)_2N=N]_{ads} \rightarrow [(CH_3)_2N–N=CH_2]_{ads} + [CH_3N=NH]_{ads} \quad (2)$$

Several new stages were included. One of them is formation of acetonitrile, which can take place due to either decomposition of 1,1-dimethyldiazene with accompanying NH_3 formation (3), or oxidative ammonolysis of C_2H_6 (4):

$$[(CH_3)_2N=N]_{ads} \rightarrow [CH_3–C\equiv N]_{ads} + [NH_3]_{ads} \quad (3)$$

$$[C_2H_6]_{ads} + [NH_3]_{ads} + 3[O]_{ads} \rightarrow [CH_3–C\equiv N]_{ads} + 3[H_2O]_{ads} \quad (4)$$

Results of the study of UDMH adsorption and oxidation over IC-12-73 catalyst in the temperature range 100–300 ^oC using the FTIR spectroscopy, which also suggest the possible routes of intermediate products formation, will be discussed. Spectra of UDMH adsorbed in the absence of oxygen on IC-12-73 show, that at 100 ^oC the initial molecule is physisorbed on the surface, while temperature increase to 200 and 300 ^oC leads to the UDMH decomposition. In the presence of oxygen, spectra of adsorbed UDMH oxidation products indicate, that in the temperature range 100–200 ^oC some of the intermediate products remain on the surface, then at 300 ^oC the interaction of adsorbed species with oxygen results in almost complete conversion of UDMH into the deep oxidation products. Spectra of UDMH oxidation products in the gas phase correlate well with the spectra of adsorbed oxidation products, taken at the same temperatures, and with the results of GC analysis.

Acknowledgements

Support of this work by INTAS Grant 99–01044 and ISTC Project # 959–99 is gratefully acknowledged. The authors would like to thank Dr. L.T. Tsykoza for the preparation of "Cu/zeolite" catalyst, and Drs. Yu.V. Patrushev, V.A. Utkin, V.A. Rogov for their contribution into the identification of some partial UDMH oxidation products.

References

[1] Ismagilov Z.R., Kerzhentsev M.A., Ismagilov I.Z., Sazonov V.A., Parmon V.N., Elizarova G.L., Pestunova O.P., Shandakov V.A., Zuev Yu.L., Eryomin V.N., Pestereva N.V., Garin F., Veringa H.J., *Catal. Today*, 75 (2002) 277.

[2] Ismagilov Z.R., Kerzhentsev M.A., *Catal. Rev. Sci. Eng.*, 32 (1990) 51.

[3] Parmon V.N., Ismagilov Z.R., Kerzhentsev M.A., Catalysis in Energy Production, in: Perspectives in Catalysis, Chemistry for the 21st Century (J.M. Thomas, K.I. Zamaraev, Eds.), Oxford, Blackwell Sci. Publ. (1992) 337.

RARE EARTH PROMOTED CATALYSTS FOR SULFUR DIOXIDE OXIDATION

Jumabaeva A.[1], Zhubanov K.[1], Lebedeva O.[1], Yudaev I.[2], Lapina O.[2]

[1]al-Faraby Kazakh National University, Almaty, Kazakhstan
E-mail: olga@lorton.com
[2]Boreskov Institute of Catalysis SB RAS, Novosibirsk, Russia

Sulfur dioxide is formed both by the oxidation of sulfur contained in fossil fuels and the industrial processes that involve sulfur-containing compounds. Catalytic oxidation of environmentally undesirable SO_2 emissions is widely investigated and different catalysts being tested for this purpose.

In the present investigation the catalytic activity of several ternary and quaternary oxide catalysts in sulfur dioxide oxidation reaction was examined. Rare earth promoted aluminum and chromium oxides were used as the active components. Silica, clays and diatomite have been examined as a support for such catalysts. To reveal the molecular structure and the effect of rare earth oxide addition the NMR study of the catalysts was performed.

Catalytic activity determination experiments were carried out in a flow fixed-bed reactor under atmospheric pressure. Sulfur content in the reaction mixture varied in the range 0,6-1 vol. %. A pronounced effect of rare earth metal oxide promotion was revealed. Enhancement of SO_2 conversion depends both on the nature of the promoter and on its content (vide infra). A certain positive effect of CeO_2 and Y_2O_3 promotion is observed under the optimal conditions (1 vol. % SO_2, WHSV = 4000 h^{-1}).

Conversion of SO_2 over catalysts promoted with rare earth oxides

promoter	promoter content		conversion of SO_2 into SO_3, %			
	oxide, wt. %	metal cation, mmole·g^{-1}	673 K	773 K	873 K	973 K
-	-	-	30	50	57	67
CeO_2	1	0,06	30	55	63	67
CeO_2	5	0,29	40	67	80	81
Sc_2O_3	5	0,72	19	44	52	59
Y_2O_3	5	0,44	16	34	68	72

The ^{27}Al MAS NMR spectra were recorded at room temperature on a Bruker MSL-400 spectrometer operating at 104,2 MHz. Deconvolution of the spectra of the catalysts shows resonance lines at 57-61, 1-10 and 22-37 ppm attributed to fourfold (tetrahedral), sixfold (octahedral) and pentacoordinated (non framework) aluminum respectively. In the spectrum of the support Al^{IV} resonance contains about 50 % of the total intensity, whereas Al^{VI} and Al^{V}

lines intensities are nearly equal. Tetrahedral/octahedral aluminum ratio in the catalysts spectra was also found to be unusual compared to conventional aluminas. Addition of a small amount of rare earth metal as a promoter leads to dramatic changes in catalysts spectra, e.g. addition of cerium gives rise to a sharp signal at 2 ppm, which could be due to formation of highly symmetrical structure. The same signal appears for the samples containing scandium while addition of yttrium or lanthanum does not cause these effects. Moreover catalytic systems of this type exhibit substantial sensitivity to the promoter quantity since examination of catalysts with different content of cerium showed that only for 5 % of CeO_2 the above-mentioned changes have taken place.

It is likely that the increase of the catalytic activity for the samples promoted with rare earth oxides is connected with the formation of the highly symmetrical octahedrally coordinated aluminum observed in NMR spectra. The most active sample does display the most intense signal at 2 ppm, but for the elements other than cerium the correlation seems to be more complex since the activity strongly depends on the reaction temperature.

STRONG METAL-SUPPORT INTERACTION IN THE Ni-CONTAINING CATALYSTS OBTAINED FROM Si-CONTAINING LAYERED PRECURSORS

Khassin A.A., Kaichev V.V., Simentsova I.I., Baronskaya N.A., Plyasova L.M., Kovalenko A.S., Itenberg I.Sh., Yurieva T.M., Bukhtiyarov V.I., Parmon V.N.

Boreskov Institute of Catalysis SB RAS, Novosibirsk, Russia
E-mail: a.a.khassin@catalysis.nsk.su

The surface chemical composition and adsorption properties of Ni-containing catalysts otained from several Si-containing layered precursors, like nepouite, $Ni_3[Si_2O_5](OH)_4$, and amesite $(Ni,Mg,Al)_3[(Al,Si)_2O_5](OH)_4$ were studied using XPS, TPD of hydrogen, and adsorption of oxygen during the N_2O decomposition. After the reduction of the samples in a H_2 flow at 650-700 ^oC, both Ni^0 and Ni^{2+} species are detected by XPS on the surface, despite the TPR-TPO thermogravimetric data evidence in more than 95 % extent of the nickel cations reduction. For the amesite-derived samples, almost all nickel species on the surface remain to be Ni^{2+}. Sputtering the sample by Ar^+ ions for 5 min removes the Ni^{2+} signal from the Ni2p XP-spectra and increases significantly the intensity of the Ni^0 signal. The [Si]/[Ni] atomic ratio determined from the XPS data is decreased dramatically as a result of the sputtering.

On the other hand, the reduced sample adsorption capacity with respect to hydrogen appears to correlate well with the sample dispersion estimated from the XRD line broadening. Contrary to that, the adsorption capacity with respect to oxygen is much less and correlates well with concentration of Ni^0 species on the catalyst surface. These observations lead to a supposition that the surface Ni^{2+} species are not forming the nickel oxide film, but relate to some silicon- and oxygen-containing clusters on the surface of metallic particles.

The above hypothesis is supported by the catalyst tests in methane steam reforming and in carbon formation from CO (the Boudouard reaction) as well as from methane. The specific activities in the methane converion reactions appears to be close to those of a standard Ni/MgO catalyst, while the catalytic activity in CO disproportionation is much lower for the silicon-containing samples and correlates with the surface concentration of Ni^0 species.

Thus, the metallic nickel particles in the studied systems interact strongly with the silicon-containing support. The nature of this interaction is under discussion.

The research was supported in part by NATO grant SFP-972557 and by INTAS fellowship YSF 2002-282.

THE PREPARATION AND THE PHASE EVOLUTION OF THE LAYERED ALUMINOSILICATE OF Ni-Mg-Al WITH AMESITE STRUCTURE

Khassin A.A., Yurieva T.M., Kustova G.N., Demeshkina M.P., Plyasova L.M., Kaichev V.V., Larina T.V., Anufrienko V.F.

Boreskov Institute of Catalysis SB RAS, Novosibirsk, Russia
E-mail: a.a.khassin@catalysis.nsk.su

Synthetic TO (1 tetrahedron layer : 1 octahedral layer) phylloaluminosilicates of Ni-Mg-Al, $(Ni,Mg,Al)_3[(Al,Si)_2O_5](OH)_4$, with amesite (septochlorite) structure were synthesized and their evolution in the inert and hydrogen medium was studied. The initial structure was characterized by FTIR and XRD. According to these methods as well as to the Si2p XPS spectra, the samples do not contain SiO_2. Nickel, and magnesium cations are randomly distributed in octahedral positions.

The calcination of the amesites in the inert gas flow results in the polymorphic transition to the chlorite strusture, $(Ni,Mg,Al)_3[(Al,Si)_4O_{10}](OH)_2*(Ni,Mg)_3(OH)_6$. UV-VIS DRS data show the appearance the intence absorption in the range above 30000 cm^{-1}, which is related to (-Ni-O-Ni-) charge transfer. Thus, it evidences in enrichment of the brucite like layers, $(Ni,Mg)_3(OH)_6$, by the nickel cations. The chlorite structure is stable upto 850 ^oC in the inert gas medium.

The reduction of the samples at 600-750 ^oC is accompanied by the formation of Ni^0 phase with the mean particle size of 17-25 nm which occurs simultaneously to the gradual transformation of chlorite structure to the vermiculite one. $(Mg,Al)_3[(Al,Si)_4O_{10}](OH)_2$. The nickel reduction extent exceeds 95 %. No silica is formed during the reduction in the hydrogen medium till 850^oC, as it was proved by XPS of the reduced samples. The stability of the support at the water vapors pressure upto 0.6 MPa and temperature upto 650 ^oC was also proved experimentally. The samples exhibit high activity in the methane steam reforming.

The research was supported in part by NATO grant SFP-972557 and by INTAS fellowship YSF 2002-282.

References

T.M. Yurieva, I.Sh. Itenberg, G.N. Kustova, M.P. Demeshkina, I.I. Bobrova, I.A. Zolotarskii, T.P. Minyukova, V.N. Parmon, A.A. Khassin. WO 02/077125A3 (03.10.2002).

NOVEL STATISTICAL LATTICE MODEL FOR THE PHYSICOCHEMICAL PROCESSES PROCEEDING OVER THE SUPPORTED NANOPARTICLE

Kovalyov E., Elokhin V., Myshlyavtsev A.

Boreskov Institute of Catalysis SB RAS, Novosibirsk, Russia
Fax: (7-3832) 34 30 56; E-mail: kovalev@catalysis.nsk.su

The aim of the study is to reveal the mutual influence of the shape and of the surface morphology of the supported nanoparticles on the reaction kinetics. The analysis has been provided by means of the novel statistical lattice model, which imitates the physicochemical processes that proceed over the supported catalytic particles. To simulate the active metal particle the finite Kossel crystal located on the inert support has been chosen. The surface morphology of the particle is defined by distribution of heights of the metal atom columns. The metal atoms attract the nearest neighbor metal atom and the atoms of support. The attraction is characterized by interaction energies between the nearest neighbor metal atoms and between the metal atom and the support underneath. The change of morphology is caused by the thermal diffusion of the surface atoms. To simulate the diffusion of the metal atoms over the metal and support surfaces the standard the Metropolis algorithm [1] has been used. As a result the equilibrium shapes of the particle has been observed to depend on the temperature and the relative ratio of "metal-metal" and "metal-support" energies. At temperatures ~ 700-900 K the initial cubic shape of the metal crystal move to hemisphere. Increasing the temperature up to 1100 K result in dispersed shape of the particle, if such particles are located close enough, the coalescence of particles is possible.

The model reaction $A+B_2$ has been studied (monomolecular adsorption of A, dissociative adsorption of B_2 and reaction between A_{ads} and B_{ads}) taking into account the roughening of the particle surface and the spillover phenomena of the adsorbed A_{ads} species over the support. The influence of the adsorption and the reaction processes on the equilibrium shape of the nm-sized particles was also investigated. The following propositions has been made to model the reaction proceeding on the supported catalyst particle: 1) the reaction starts on the equilibrium shape of the particle at a particular temperature; 2) B_2 molecule can adsorb with subsequent dissociation only on the two neighboring active sites of the catalyst particle situated at the same level; 3) A molecule can adsorb and diffuse both on the metal and support surface (spillover); 4) desorption of A_{ads} and B_{ads} is neglected; 5) the reaction between A_{ads} and B_{ads} proceeds immediately when they are brought into contact due to adsorption, or A_{ads} diffusion into the two neighboring active sites situated at the same level;

6) the probabilities of adsorbed species A_{ads} diffusion are governed by the above-mentioned Metropolis algorithm; 7) the simulation procedure makes provision for taking account of the lateral interactions both of A_{ads} and B_{ads} with each other and with near neighboring metal atoms with corresponding energies, although in the case considered below they are not taken into account. After each attempt to adsorb A or B_2 molecule several attempts of diffusion of metal atoms and A_{ads} species were performed to equilibrate both the surface of the catalyst particle and the adsorbed layer.

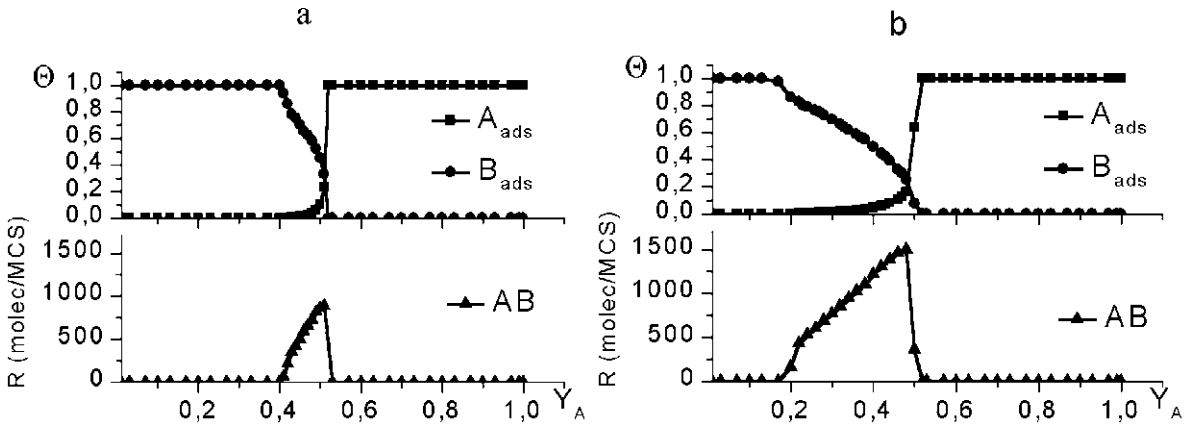

Fig. 1. The dependencies of A_{ads} and B_{ads} coverages (upper graph) and reaction rate (absolute value of formed AB molecules of product per one MCS - lower graph) *versus* molar ratio Y_A in the case of the flat surface of the particle. (a) The absence of A_{ads} diffusion; (b) A_{ads} diffusion over the support and the particle surfaces.

The kinetic dependencies of A_{ads} and B_{ads} coverages normalized on the number of the active sites of the catalyst particle *versus* molar ratio $Y_A = P_A/(P_A+P_{B2})$ (P_i are the partial pressures of the reagents in the gas phase) obtained at different variants of the model reaction performance (with or without A_{ads} species and/or metal atoms diffusion, various ratios of interaction energies, etc.) has been compared with ones of the well-known Ziff-Gulari-Barshad model [2]. In our case ZGB-model corresponds to the performance of the reaction only on the initial flat uniform surface of the catalyst particle without any diffusion of adsorbates and metal atoms (Fig 1a). Introducing into the model the A_{ads} molecules diffusion over the metal and support surface leads to the considerable decrease of the unit B_{ads} coverage region observed in ZGB-model and to a minor shift (from 0.51 to 0.48) of the reaction rate maximum to the smaller values of Y_A [3,4] (Fig 1b) (in contrast to the behavior of ZGB-model with A_{ads} diffusion). This effect is connected with additional source of A_{ads} molecules due to the spillover from the support to the active particle. In that way, the spillover effect leads to the effective increasing of the A reagent partial pressure. Two reaction channels exist in this case. The first channel is the diffusion one. The reaction occurs via the adsorption

of ***A***-molecules on the support followed by diffusion to the particle and proceeds on the boundaries of the B_{ads} atoms island with the dense core. The diffusion channel takes place at all values of Y_A starting from very low Y_A. The second channel is an adsorption one that leads to the rarefaction of the dense core of adsorbed B_{ads} island. When the reaction proceeds on the non-regular roughened surfaces all the regions with sharp stepwise changing of adsorbates coverage disappear (in this case the number of active sites convenient for B_2 adsorption is restricted) (Fig2 a-c).

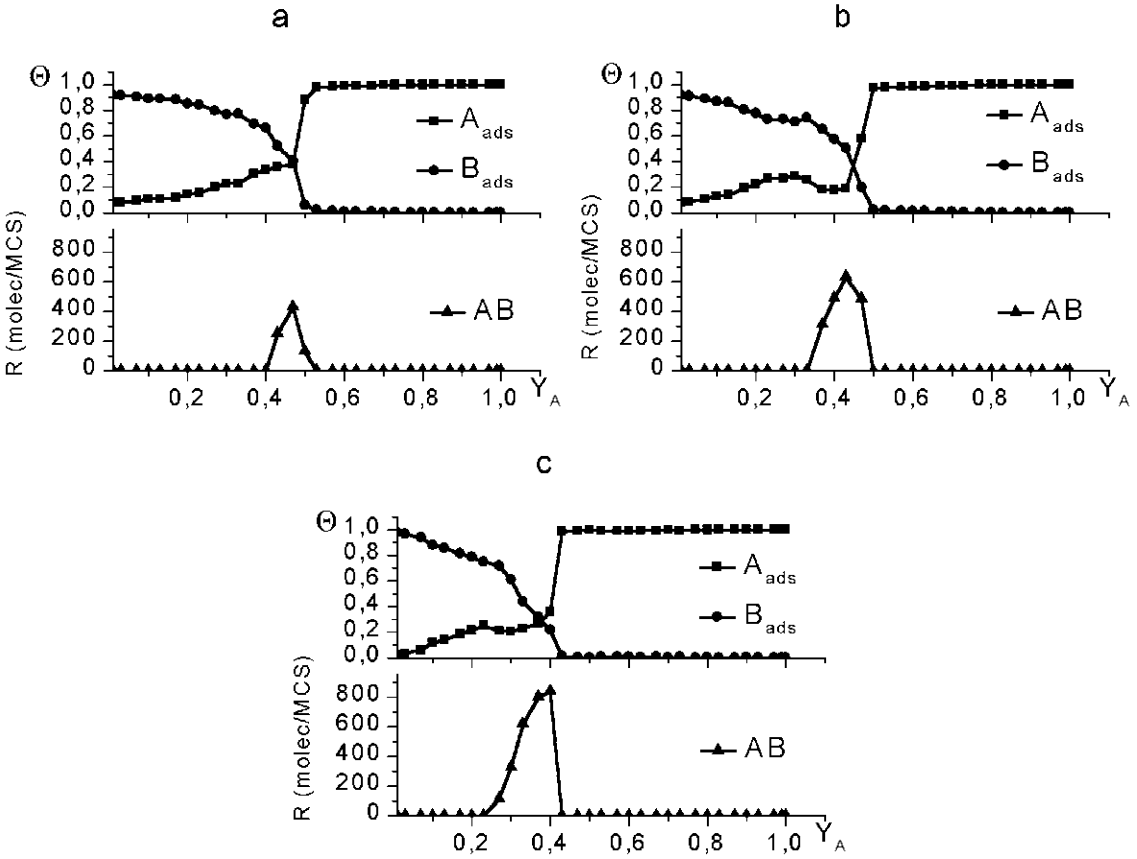

Fig. 2. The dependencies of A_{ads} and B_{ads} coverages (upper graph) and reaction rate (absolute value of formed AB molecules of product per one MCS - lower graph) *versus* molar ratio Y_A in the case of the roughened surface of the particle, T = 500 K. (a) - rigid surface, the absence of metal atoms and A_{ads} diffusion; (b) - rigid surface, A_{ads} diffusion over the support and the particle surfaces; (c) - dynamic surface, metal atoms and A_{ads} diffusion over the support and the particle surfaces.

Introduction of the diffusion channel leads, as earlier, to the shift of the reaction window to the smaller values of Y_A. In this case (Fig. 2b) we can observe, again as earlier, the preferred occurrence of the reaction at the boundaries of the dense core of adsorbed B_{ads} island at low values of Y_A. Introduction into the model the diffusion of surface metal atoms results in the further change of the kinetic dependencies (Fig. 2c) which is connected with the

dynamic change of the surface morphology determining the geometric impediments for B_2 adsorption.

Thus it has been shown (in the frames of the proposed model) that the shape of the active particle can change under the influence of the adsorbed layer, even in the absence of the "adsorbate-metal" interactions and that the kinetics on the nanometer-size particle can be remarkably different from those corresponding to the infinite surface.

Also it has been shown that the shape of the active particle change in the presence of the "adsorbate-metal" interaction too.

References:

[1] Metropolis N., Rosenbluth A.V., Rosenbluth M.N., Teller A.H. and Teller E., *J. Chem. Phys.,* **21 (**1953) 1087.

[2] Ziff R.M., Gulari E. and Barshad Y., *Phys. Rev. Lett.,* **56 (**1986) 2553.

[3] Kaukonen H.-P. and Nieminen R.M., *J. Chem. Phys.,* **91 (**1989) 4380.

[4] Ehsasi M., Matloch M., Frank O., Block J.H., Christmann K., Rys F.S. and Hirschwald W., *J. Chem. Phys.,* **91 (**1989) 4949.

SYNTHESIS OF NANODISPERSED HYDROXIDE Co^{2+} PARTICLES CONTAINING CATIONS IN THE TETRAHEDRAL COORDINATION

Krivoruchko O.P., Larina T.V., Anufrienko V.F., Kolomiichuk V.N., Paukshtis E.A.

Boreskov Institute of Catalysis SB RAS, Novosibirsk, Russia
E-mail: opkriv@catalysis.nsk.su

Co^{2+} hydroxides have found a wide use as precursors in the synthesis of industrial catalysts (selective and deep oxidation, hydrogenation etc.) and high-tech materials for other fields of application. Physicochemical properties of materials significantly change as one proceeds to particles smaller than 10 nm [1-5]. Compared to bulk phases, such particles in the above nano dimension range have quite different surface and bulk properties, providing their unusual structural, optical and magnetic properties. Such nanodispersed systems are likely to exhibit unusual performance in the reactions of adsorption and catalysis [1-5].

In this paper we report for the first time data for Co^{2+} cations in tetrahedral oxygen coordination (Co^{2+}_{Td}) in nanodispersible $Co(OH)_2$ hydroxides synthesized by our technique.

The structural modifications of α-$Co(OH)_2$ and β-$Co(OH)_2$ are known for the Co^{2+} hydroxide [7-17]. The β-$Co(OH)_2$ is a relatively stable hydroxide which contains hexagonal plate crystals of several hundreds nm in size. It has a $Mg(OH)_2$ brucite-like lattice and Co^{2+} cations are located only in the octahedral oxygen coordination. α-$Co(OH)_2$ hydroxide is metastable and has a strongly disordered layered structure. The coordination of Co^{2+} in this hydroxide structure has not been elucidated. According to earlier publications [7-14], the structural model of α-$Co(OH)_2$ is formed by four brucite-like layers (Co^{2+}ions are located in the octahedral oxygen coordination) and one disordered $Co(OH)_2$ layer which presumably contains Co^{2+} cations in the tetrahedral oxygen coordination. The latter suggestion have not been experimentally supported. Among the five models suggested for α-$Co(OH)_2$ [15-17], the model based on the $Mg_6Al_2(OH)_{16}CO_3 \bullet 4\,H_2O$ hydrotalcite-like structure (however, which does not contain M^{3+}cations in the hydroxide layer) has been experimentally substantiated. Note that in the hydrotalcite-like structures, M^{2+} and M^{3+} cations are situated only in the octahedral oxygen coordination. Partial protonation of the hydroxyl groups by $M(OH)_2+xH \rightarrow [M(OH)_{2-x}(H_2O)_x]^{x+}$ reaction provides the uncompensated positive charge of the hydroxide layer needed for α-$Co(OH)_2$ hydrotalcite-like structure [17]. The positive charge of this layer is compensated at the expense of anions which incorporate into the interlayer area of α-$Co(OH)_2$. So, the protonation can distort the Co^{2+} octahedral.

Co^{2+} cations in the tetrahedron oxygen coordination in the cobalt hydroxides we observed by UV-VIS DR spectroscopy. The principles of attribution of absorption bands (a.b.) in the UV-VIS DR spectra to different cobalt states and regarding the coordination surrounding were considered in ref. [18]. Typical absorption bands associated with Co^{2+} or Co^{3+} in different crystalline fields of the oxide nature have been recently systematized [19]. It should be briefly noted that in the octahedral oxygen crystalline field, Co^{3+} ions (the electron configuration is d^6, the ground term of free ion is ^5D) exist in the low-spin state and the UV-VIS DR spectra could exhibit two a.b. at 16500-25000 cm^{-1} that are determined by transitions: $^1A_{1g}\rightarrow{}^1T_{1g}$ and $^1A_{1g}\rightarrow{}^1T_{2g}$ [14]. For Co^{2+} ions (the electron configuration is d^7, the ground term of free ion is ^4F) in the octahedral coordination, the following transitions are probable: $^4T_{1g}\rightarrow{}^4T_{2g}$, $^4T_{1g}\rightarrow{}^4A_{2g}$ and $^4T_{1g}(F)\rightarrow{}^4T_{1g}(P)$. However, one observes only one band at 19000-20500 cm^{-1} associated with $^4T_{1g}(F)\rightarrow{}^4T_{1g}(P)$ transition. Note that the first transition lies in the far IR region and we do not observe it. The second is a two-electron transition whose intensity is considerably lower than that of the third transition. For Co^{2+} ions in the tetrahedral oxygen coordination, one can also observe three transitions: $^4A_2\rightarrow{}^4T_2$, $^4A_2\rightarrow{}^4T_1(F)$, and $^4A_2(F)\rightarrow{}^4T_1(P)$, the splitting being much lower. For the same reasons, we have observed only one typical $^4A_2\rightarrow{}^4T_1(P)$ transition manifesting itself as a multiplet at 15000-17000 cm^{-1} [18]. The important difference between $Co^{2+}{}_{Td}$ and $Co^{2+}{}_{Oh}$ is high intensity (10-100 fold) of absorption bands of the Co^{2+} tetrahedral ions.

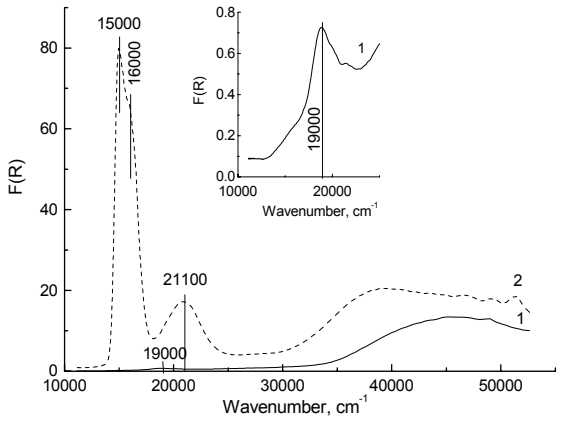

Fig.1. UV-VIS DR spectra.
1: sample β-$Co(OH)_2$, 2: freshly precipitated sample 1 of $Co(OH)_2$ hydroxide.

To demonstrate the observed by us effect, we present from the first the UV-VIS DR spectrum (Fig.1, curve 1) of the β-$Co(OH)_2$ usual coarse-dispersible with size of particles about 100 nm. One clearly sees a.b. at 19000 cm^{-1} associated with $^4T_{1g}(F)\rightarrow{}^4T_{1g}(P)$ transition which is typical of Co^{2+} ions in the octahedral oxygen surrounding, which is in complete agreement with the reference data [18]. It is apparent that low intensity of this band is due to almost perfect octahedral oxygen coordination around Co^{2+} ions, which results in the almost complete the spin-forbidden

adsorption bands of d-d-transitions. In the UV region (above 30000 cm^{-1}), the bands of L→M transition of Co^{2+} ions are most likely observed.

Fig.1 (curve 2) gives UV-VIS DRS of the nanodispersed $Co(OH)_2$ synthesized by us, the size of particles being ~1.5 nm. Fig.2 shows size particles distribution of the prepared sample. Two important features characterize this UV-VIS DR spectrum. First, it does not contain any absorption bands of hydroxide structure containing Co^{3+} ions (as CoOOH [19], providing an a.b. at 25000 cm^{-1}). Second, absorption bands of high intensity are unexpectedly registered about 15000-16000 cm^{-1}. These bands are conditioned by a multiple nature of $^4A_2(F) \rightarrow {}^4T_1(P)$ transition for Co^{2+} ions in the tetrahedral oxygen coordination [18]. The fact that the spectrum exhibits some multiplicity provides evidence [18] of the ideal tetrahedral coordination of Co^{2+}. A shift of a.b. of Co^{2+}_{Oh} ions to 21100 cm^{-1} for involved in the nanodispersed cobalt hydroxide (compared to a.b. at 19000 cm^{-1} belonging to β-Co(OH) coarse-dispersible) and its high relative intensity suggest strengthening of the oxygen octahedron crystalline field and its distortion in the synthesized nanodispersed cobalt hydroxide, which is also accompanied by broadening of the absorption band. Note that the absorption band of Co^{2+}_{Oh} involved in the nanodispersed hydroxide (Fig.1, curve 2) is much more intense than that in β-$Co(OH)_2$ (Fig.1, curve 1). It is evident that an increase in the 21100 cm^{-1} absorption band intensity is associated with weakening of the spin-forbidden absorption bands for the distorted octahedral coordination of Co^{2+} in this structure as compared to β-$Co(OH)_2$.

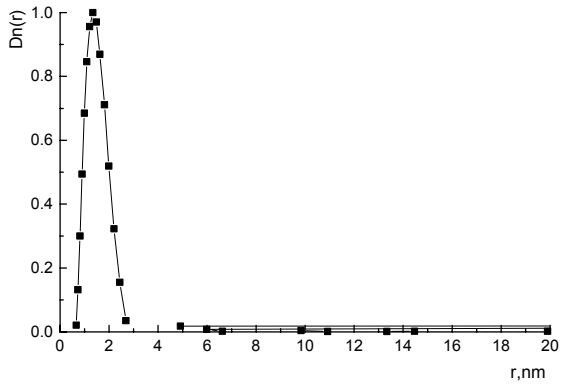

Fig.2. Particle size distribution freshly precipitated sample 1 of $Co(OH)_2$ hydroxide.

The presence of Co^{2+}_{Td} and Co^{2+}_{Oh} ions in our samples can be explained by two ways: (i) sample of the nanodispersed hydroxide cobalt is monophase and contains Co^{2+} ions in both coordination states and (ii) the sample consists of two phases, one phase contains only Co^{2+}_{Td} ions, the other, only Co^{2+}_{Oh} ions. The latter phase can be formed, for example, by thin plate crystals β-$Co(OH)_2$ that could probably exhibit distortion in the Co^{2+} octahedral coordination in the subsurface layers. We think that we have synthesized a new modification of Co^{2+} hydroxide whose particles range from 1.0 to 2.0 nm and the cations are predominantly located

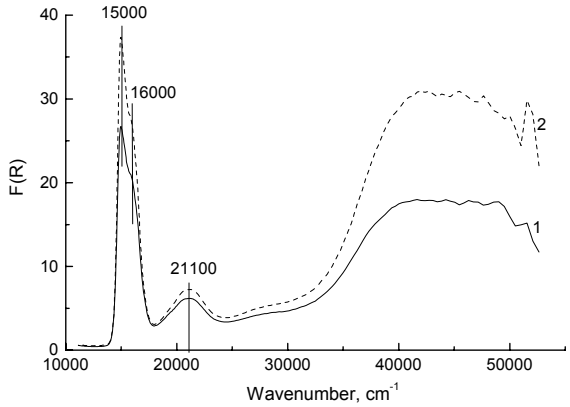

Fig.3. UV-VIS DR spectra.
1: freshly precipitated sample 2 of $Co(OH)_2$ hydroxide, 2: sample 2 of $Co(OH)_2$ hydroxide aged in the mother solution for 6 hours.

in the tetrahedral oxygen coordination (γ-$Co(OH)_2$). Fig.1 (curve 2) shows the typical UV-VIS DR spectrum of this hydroxide. From the crystal-chemical standpoint the tetrahedral oxygen coordination of Co^{2+} ions in nanodispersed Co^{2+} hydroxides is energetically preferable as compared to the octahedral coordination.

Note that for some hydroxide samples we have registered clearly shaped absorption bands of $Co^{2+}{}_{Oh}$ (Fig.4) corresponding to tetragonal distortion of the oxygen octahedron around Co^{2+} ions. This distortion is accompanied by appearance of absorption bands determined by d-d-transitions such as $^4E_g \rightarrow {}^4B_{1g}$ (18500 cm^{-1}), $^4E_g \rightarrow {}^4E_g(^4T_{1g}(P))$ (20100 cm^{-1}) and $^4E_g \rightarrow {}^4A_{2g}(^4T_{1g}(P))$ (21100 cm^{-1}) [18]. For the sample in Fig.4, this distortion of the octahedron is more pronounced than that of sample in Fig.1 (curve 2). A multiplet of spectrum produced by $Co^{2+}{}_{Oh}$ ions in the UV-VIS DR spectrum can be attributed to α-$Co(OH)_2$ phase (Fig.4) which probably contains Co^{2+} cations in the strongly distorted octahedral oxygen surrounding. This conclusion is in agreement with the hydrotalcite-like structure of α-$Co(OH)_2$ discussed in [15-17]. The absorption band of $Co^{2+}{}_{Td}$ suggests that the samples also contain the admixture of the γ-$Co(OH)_2$ nanodispersed phase (i.e. the samples are multiphase).

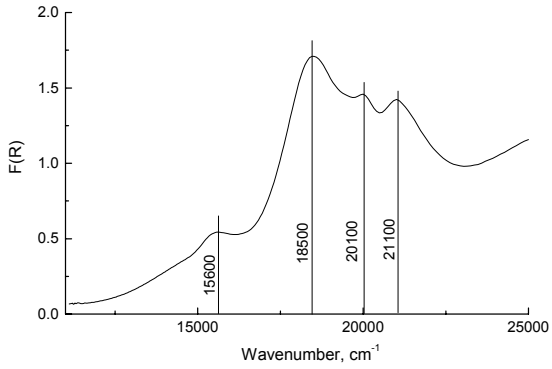

Fig.4. UV-VIS DR spectra of sample 3 of $Co(OH)_2$ hydroxide.

Note that the $Co^{2+}{}_{Td}$ nonadispersed hydroxides are stable at least for two-three months in the mother solutions excluding the reactions of oxidation of Co^{2+} to Co^{3+} or/and dehydration.

So, the synthesis of the nanodispersed $Co(OH)_2$ samples by our method provided evidence for stabilization of Co^{2+}_{Td} ions which is not complicated by the presence of oxide phases and other cobalt oxidation states such as Co^{3+}. There is no doubt that the pronounced tetrahedral oxygen coordination of Co^{2+} ions in the nanodispersed $Co(OH)_2$ hydroxides is of much interest for researchers.

References

[1] A.I. Gusev, A.A. Rempel, Nanocrystalline Materials, FIZMATLIT, Moscow, 2000, 224 p.
[2] G.B. Sergeev, Usp. Khim., 2001, 70, No 10, p. 915.
[3] N.F. Uvarov, V.V. Boldyrev, Usp. Khim., 2001, 70, No 4, p. 307.
[4] N.R. Suzdalev, P.I. Suzdalev, Usp. Khim., 2001, 70, No 3, p. 203.
[5] V.I. Bukhtiyarov, M.G. Slin'ko, Usp. Khim., 2001, 70, No 2, p. 167.
[6] A.Grimer, G.Fournet, Small-angle scattering of X-rays, N-Y.:J.Wiley, Sons Inc., 1955.
[7] W.Feitknecht, Helv. Chem. Acta, 1938, 21, 766.
[8] H.B.Weiser, W.O.Milligan, J. Phys. Chem., 1932, 36, 722.
[9] W.Feitknecht, Kolloid Z., 1940, 92, 257.
[10] W.Feitknecht, Kolloid Z., 1940, 93, 66.
[11] W.Feitknecht, Angew. Chem., 1939, 52, 202.
[12] W.Feitknecht and W. Bedernt, Helv. Chem. Acta, 1941, 24, 676.
[13] W.Lotmar and W.Feitknecht, Z.Krist, 1936, 93, 368.
[14] C.W.F.T.Pistorius, Z. Phys. Chem. New Folge, 1962, 34, 287.
[15] J.T.Sampanthar and H.C.Zeng, J. Am. Chem. Soc., 2002, 124, 6668.
[16] Y.Zhn, N.Li, Y.Koltypin and Gedanken, J. Mater. Chem., 2002, 12, 729.
[17] V.P.Kamath, A.H.G.Therese, J.Gopalakrishnan, J. Solid State Ghem., 1997, 128,38.
[18] A.B.P. Lever, *Inorganic Electronic Spectroscopy,* 2nd ed.; Elsevier: Amsterdam – Oxford – New York – Tokyo, 1987.
[19] A.A.Khassin, V.F.Anufrienko, V.N.Ikorskii, L.M.Plyasova, G.N.Kustova, T.V.Larina, I.Yu.Molina, V.N.Parmon, Phys. Chem. Chem. Phys., 2002, 4, 4236.

FLUCTUATION-INDUCED TRANSITIONS AND KINETIC OSCILLATIONS IN THE LATTICE-GAS MODEL OF $CO+O_2$ REACTION OVER SMALL SCALE CATALYSTS

Kurkina E., Semendyaeva N.

Computational Mathematics and Cybernetics Department;
Lomonosov Moscow State University, Moscow, Russia
Fax: +(7) (095) 939-25-96; E-mail: kurkina@cs.msu.su

The present work is aimed to study different driving mechanisms for oscillations in the catalytic $CO+O_2$ reaction. Experimental investigations over palladium catalysts revealed that the mechanism of kinetic oscillations in the rate of CO oxidation is related to the ability of a metal surface to be oxidized and reduced. In this work the dynamic Monte Carlo (MC) algorithms with correct time dependence based on multi-component lattice-gas (LG) model and the macroscopic mean-field (MF) model of the reaction under consideration have been suggested. The simulation results showed that a small scale system undergoes a strong influence of intrinsic fluctuations and can demonstrate the behavior not predicted by macroscopic MF model. Namely, three essentially different types of oscillatory–like behavior in LG model of $CO+O_2$ reaction have been found instead of one type in MF model.

Two types of fluctuation-induced oscillatory behavior in LG model have been investigated. Oscillatory-like behavior of the **first type** take place in the region of bistability of macroscopic model and represent the fluctuation-driven transitions between two steady states. The simulated fluctuation-induced oscillations of the **second type** occur in monostable region of the MF model in consequence of the excitable nature of the stable steady state characterized by a special arrangement of the nullclines. They correspond to travelling pulses in the reaction-diffusion model described by partial differential equations. The analysis of the power spectrum of times series reveals an obvious peak, which indicates the occurrence of oscillations. The oscillations in LG model of the **third type** are the kinetic ones. They take place in oscillation region of the MF model.

The influence of the lattice size and the diffusion rate on the reaction dynamics for all types of oscillations has been studied.

The obtained results are useful for prediction and explanation of the behavior of small scale systems (facets of a field emitter tip, nanostructured composite surfaces, etc.) which have many applications in modern chemistry and biochemistry.

Acknowledgment: This work has been supported by the Russian Fund of Fundamental Researches (Grant № 03-01-00872).

STUDIES OF CATALYST FORMATION UNDER ELECTROHYDRAULIC TREATMENT

Kuzmina R.I., Dogadina N.V., Liventsev V.T., Rakitin S.A.

Saratov State University, Saratov, Russia
E-mail: kuzminaraisa@mail.ru

Catalytic reforming is a traditional basis of large-tonnage production of motor fuels and aromatic hydrocarbons, the principal raw materials of organic synthesis and petrochemistry. The further development of reforming is directed to creating new effective and inexpensive catalysts and widening source of raw materials through lower hydrocarbons [1].

Under reforming, paraffin hydrocarbons undergo reactions of dehydrogenation, dehydrocyclization, isomerization, and hydrocracking. The above reactions are predetermined by bifunctional character of reforming catalysts realizing both acid and hydrogenant-dehydrogenant functions.

In order to increase catalytic activity, at the stage of catalyst preparation different methods of surface modification are applied: mechano-chemical activation, microwave and UV-wave emission, ultrasound, low-temperature plasma of glow discharge etc.

Almost all of the above factors take place during electrohydraulic blow described in details by Yutkin [2]. The essence of the effect is in high-voltage (scores of kilovolts) very short (few microseconds) electrical pulse in dense liquid media (mainly water). In this paper, electrohydraulic blow (EHB) was used to modify copper-containing heterogeneous catalytic systems demonstrating high activity in *n*-hexane conversion.

Catalysts of paraffin hydrocarbons conversion are prepared by impregnation method. γ-Al_2O_3 (mark A-1) annealed at air (550 °C) is used as a carrier. Copper (1.0-5.0 % wt) is deposited from aqueous copper acetate solution, platinum (0.1 %) – from platinum hydrochloric acid. Catalysts are dried at 100 °C and activated at 500 °C for 2 hours.

Influence of EHB on activity of aluminum-platinum-copper catalyst (2.5 % Cu + 0.1 % Pt/Al_2O_3) is studied during platinum deposition by impregnation method from solution of platinum hydrochloric acid. EHB treatment is applied to heterogeneous system consisting of 2.5 % Cu/Al_2O_3 and aqueous solution of H_2PtCl_6.

Obtained samples of aluminum-platinum-copper catalyst with varying copper content are investigated by electron microscopy. Computation of interplanar distances shows presence of metallic phase (Cu^0) and copper spinel ($CuAl_2O_4$) on (2.5 % Cu + 0.1 % Pt/Al_2O_3)-catalyst surface (fig. 1). Surface of (2.5 % Cu + 0.1 % Pt/Al_2O_3)-catalyst contains spinel structures.

This catalyst demonstrates distinct hydrocracking properties that decrease benzene yield (fig. 2).

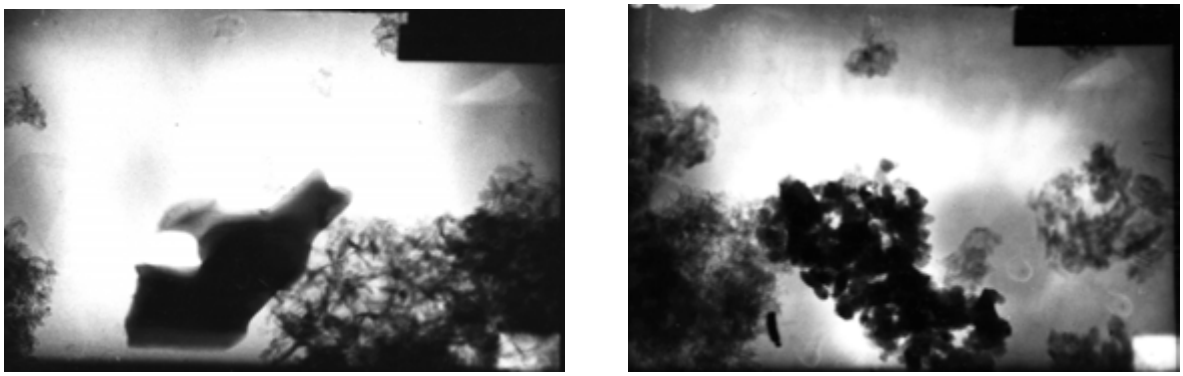

a b

Figure 1. Photographs of aluminum-platinum-copper (2.5 % Cu, 0.1 % Pt) catalyst surface: a – Cu^0 particle; b – $CuAl_2O_4$ particle

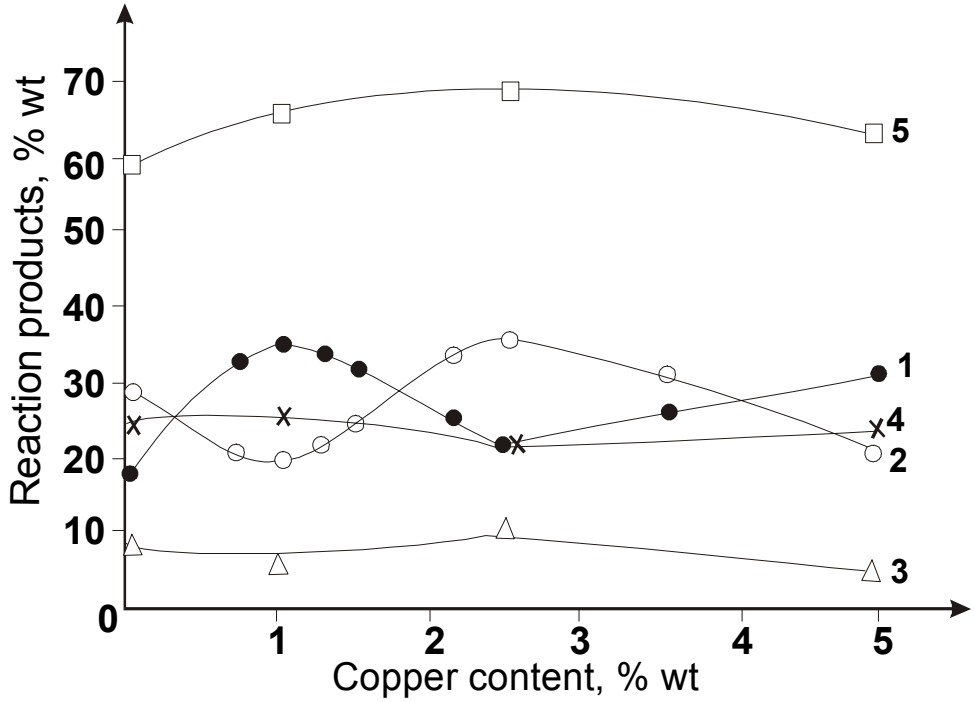

Figure 2. Influence of copper content in aluminum-platinum-copper catalyst on distribution of *n*-hexane conversion: *1* – $\sum C_1$-C_5; *2* – benzene; *3* – methylcyclopentane; *4* – isohexanes; *5* – conversion level

Results of n-hexane conversion in presence of $Cu,Pt/Al_2O_3$ (EHB treated) are presented in Table 1. It is found that preliminary treatment of source catalytic system by EHB on the impregnation stage results in increasing benzene yield (from 30.8 to 64.1 % wt, t = 550 °C) in comparison with traditional method of impregnation by platinum hydrochloric acid.

Table 1. Results of *n*-hexane conversion on (2.5 % Cu + 0.1 % Pt/Al_2O_3)-catalyst: prepared by traditional method (numerator) and EHB treated (denominator)

t, °C	$V_{vol.}$, h^{-1}	Conversion products, % wt					
		$\sum C_1$-C_2	$\sum C_1$-C_5	i-C_7	C_5-DHC	C_6H_6	C_6H_{14}
450	2.1	1.4 / 0.1	6.8 / 0.2	9.9 / -	23.9 / 0.3	22.4 / 36.3	37.0 / 63.2
500	2.4	3.3 / 0.2	10.7 / 0.4	9.5 / -	22.8 / 0.5	24.9 / 50.1	32.1 / 49.0
550	2.2	6.0 / 1.2	18.8 / 4.0	4.9 / -	13.8 / 0,9	33.2 / 64.8	29.3 / 30.3

It is necessary to note change of mechanism of n-hexane to benzene conversion in presence of EHB treated aluminum-platinum-copper catalyst. Catalyzate contains almost no products of C_5-dehydrocyclisation (C_5-DHC) whereas traditionally prepared catalyst provides 20 % wt yield of the above products. It points to synthesis of aromatic hydrocarbons from *n*-paraffins in presence of the developed catalysts by direct C_6-dehydrocyclization avoiding intermediate stages of C_5-DHC and isomerization.

Feature of the developed catalyst is decreasing hydrocracking reaction that gains selectivity of *n*-hexane reforming via aromatization.

In order to determine role of EHB treatment in the process of catalyst preparation, additional experiment concerning conversion of platinum hydrochloric acid were carried out. So, EHB treatment of H_2PtCl_6 aqueous solution leads to formation of metallic platinum detected by mass-spectroscopy.

Thus, it is shown that ultrasonic waves, cavitational and blast waves, hard UV-rays which accompany electrohydraulic blow stimulate reduction of H_2PtCl_6 up to metallic platinum already on the impregnation stage. This causes formation of active centers on the catalyst surface which provide significant yield of aromatic compounds via dehydrocyclization of *n*-hexane.

References:

[1] Kuzmina R.I. *Catalytic Reforming of Hydrocarbons*. Saratov, 2002 [in Russian].
[2] Sevostyanov V.P., Rakitin S.A., *Extreme Physical Treatment in Technology of Display Device Production*. Saratov, 1999 [in Russian].

SOME REGULARITIES OF WOOD DELIGNIFICATION BY CH_3COOH/H_2O_2 IN THE PRESENCE OF TiO_2 AND MOLYBDENUM CATALYSTS

Kuznetsov B.N.[1], Danilov V.G.[2], Kuznetsova S.A.[2], Yatsenkova O.V.[2], Ivanchenko N.M.[2]

[1]Krasnoyarsk State University, Krasnoyarsk, Russia
[2]Institute of Chemistry and Chemical Technology SB RAS, Krasnoyarsk, Russia
Fax +7(3912)439342; E-mail: bnk@icct.ru

Introduction

The conventional sulfate and sulfite processes of cellulose production negatively influence on an environment since they use the sulfur and chlorine containing reagents for removing lignin from a wood biomass. New methods of wood delignification in organic solvents use sulphur-free reagents and allow to utilize the side-products from lignin and hemicelluloses into valuable chemicals and to decrease the energy expenses in solvent regeneration as compared to conventional pulping technologies. In our previous study the intensive oxidation of wood-lignin was observed in acetic acid/hydrogen peroxide mixture in the presence of sulphuric acid catalyst. This paper describes some regularities of abies-wood and birch-wood delignification by CH_3COOH/H_2O_2 mixture in the presence of TiO_2 and dissoluble molybdenum catalysts.

Experimental

Sawdust of abies wood, larch wood and birch wood (fraction 2-5 mm) was used as starting raw material. Abies wood composition (% wt. on a.d.w.): cellulose 50.3, lignin 27.7, hemicelluloses 15.4, extractive substances 6.8. Birch wood composition (% wt. on a.d.w.): cellulose 41.3, lignin 19.9, hemicelluloses 30.3, extractive substances 8.4. Larch wood composition (% wt. on a.d.w.): cellulose 34.5, lignin 26.1, hemicelluloses 27.2, extractive substances 13.0.

The concentrations of CH_3COOH and H_2O_2 in delignification liquor were varied between 22.3-28.6 % and 1.5-8.2 % respectively. Molar ratio CH_3COOH/H_2O_2 was varied in the range 0.1-0.7. The delignification process was carried out in a static reactor made from titanium with volume 200 cm^3 at temperatures 100-140 ^oC and liquor ratios 7.5:1, 10:1, 15:1, 20:1 during 1-3 hours. TiO_2 powder and dissoluble $Fe_2(MoO_4)_3$ and H_2MoO_4 were used as catalysts in amount 0.5-2.0 % wt. on a.d.wood.

In some cases, before the beginning of delignification process the reaction mixture with TiO_2 catalyst was pre-treated by UV-irradiation in a quartz reactor during 10 min. The main components of cellulosic product obtained were analyzed by conventional chemical methods.

Results and discussion

Abies and birch wood delignification with TiO_2 catalysts. The influence of temperature and process time on the yield and composition of cellulosic product from abies wood was investigated. According to obtained results the optimum temperature of delignification in the presence of 2 % wt. TiO_2 is 120-130 ^oC and time of pulping 2-3 hours. At these conditions the cellulosic products with low content of lignin (2.7-0.8 %) were obtained. The yield of cellulosic product with low lignin content increased with the decrease of TiO_2 concentration to 0.5 % wt. (Table 1).

Table 1. Influence of TiO_2 concentration and time of abies wood delignification at 130 ^oC on the yield and composition of cellulosic product (liquor composition: 24.5 % CH_3COOH and 6.4 % H_2O_2, liquor ratio 15:1)

Parameters	TiO_2 catalyst concentration, % wt. on a.d.w.							
	0.5		1.0		1.5		2.0	
	2h	3h	2h	3h	2h	3h	2h	3h
Yield of cellulosic product, %*	53.6	48.4	42.6	39.8	40.1	35.8	36.5	34.0
Product composition, %**:								
cellulose	83.5	89.5	84.7	83.9	78.1	86.9	84.6	87.9
lignin	4.4	0.8	4.5	1.8	12.0	7.2	5.3	4.8
Delignification degree, %	91.8	98.7	93.7	97.3	83.1	90.9	93.7	94.1

* relative to mass of a.d.w.; ** relative to mass of product.

The most pronounced catalytic effects were observed at high liquor ratios (1:15 and 1:20) when the diffusion limitations play the lesser role as compared to wood delignification at low liquor ratios (1:5 and 1:10).

Delignification properties of pulping liquor can be improved by optimizing the concentrations of CH_3COOH, H_2O_2 and liquor ratio. In order to obtain cellulosic product with the sufficient yield and low content of lignin the next conditions of abies wood delignification have to be used: temperature 130 ^oC, molar ratio H_2O_2/CH_3COOH 0.5, liquor ratio 1:15, process time 2-3 h. The optimum parameters for birch wood delignification are: temperature 120 ^oC, H_2O_2/CH_3COOH ratio 0.3, TiO_2 concentration 0.5 %, liquor ratio 1:10, pulping time 3 h.

Delignification of abies wood pre-treated by UV-irradiation. It is well known that TiO_2 can act as a photocatalyst. Results of delignification of UV-activated mixture of abies sawdust, CH_3COOH, H_2O_2 and TiO_2 catalyst are presented in Table 2.

The increase of H_2O_2 concentration in reaction mixture from 1.5 % to 8.2 % promotes the lignin removal from wood (Fig. 1). Residual lignin is practically absent in cellulosic product obtained at H_2O_2 concentrations 6.4 % (3 h) and 8.4 % (2 h). But the high concentrations of H_2O_2 (8.2 %) reduce significantly the cellulosic product yield at time of delignification 3 h.

Table 2. The influence of delignification process temperature and time on the yield of cellulosic product from UV activated pulp (activation time 10 min, liquor ratio 15:1, molar ratio H_2O_2/CH_3COOH 0.5, TiO_2 catalyst 0.5 % wt. on a.d.w.)

Temperature, °C	Process time, h	Cellulosic product yield, %*	Cellulose content, %**	Lignin content, %**	Delignification degree, %
110	2	88,0	49,3	24,1	23,1
110	3	59,1	76,2	2,8	93,9
110***	3	58,3	74,2	3,4	92,8
120	2	72,0	63,2	20,1	47,5
120	3	43,9	85,5	less 0,04	>99,9
120***	3	52,3	81,7	2,1	96,0
130	2	43,5	82,9	0,32	99,6
130***	2	53,6	83,5	4,4	91,8
130	3	40,3	85,7	less 0,04	>99,9
140	2	47,8	84,4	less 0,04	>99,9
140***	2	45,6	84,3	0,90	98,5
140	3	41,1	85,6	less 0,04	>99,9

* - relative to mass of a.d.w.; ** - relative to mass of cellulosic product; *** without UV activation

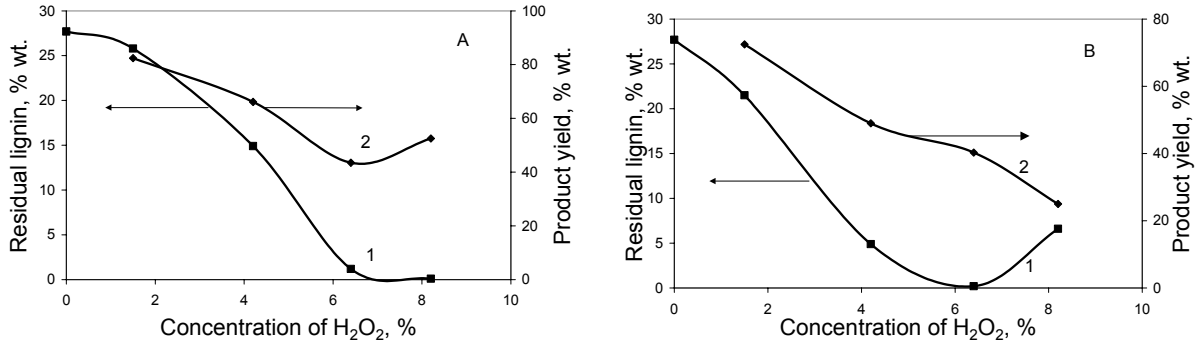

Fig. 1. Influence of H_2O_2 concentration on the residual lignin content (1) and on the yield of cellulosic product (2) from photochemically activated pulp (delignification parameters are the same as in table 2. A – process time 2 h, B – process time 3 h).

It was found that liquor ratio value influences considerably on the yield of cellulosic product from UV-activated pulp and on residual lignin content in the product. Diffusion limitations at liquor ratio 7.5:1 restrict the dissolvation of lignin destruction fragments and the cellulosic product with high yield (to 62.9 % wt.) and with residual lignin content 16.5-15.6 % wt. was obtained. The higher liquor ratios improve the mass transfer conditions. Therefore the cellulosic products with residual

lignin content 6.8-5.8 % wt. were obtained at liquor ratio 1-:10. Liquor ratios 15:1 and 20:1 allow to produce the pure cellulose with lignin content less than 0.04 % wt.

Wood delignification with dissoluble molybdenum catalysts. In an acidic medium H_2O_2 generates hydroxyl cations HO^+, which initiate the lignin depolymerization reactions. Some transition metal ions capable of peroxycomplexes formation can promote the formation of acetic peracid:

$H_2O_2 + Cat \leftrightarrow CatO + H_2O$; $AcOH + CatO \leftrightarrow AcOOH + Cat$.

Acetic peracid intensifies the lignin oxidative delignification via generation of hydroxy-radicals $O^{\bullet}H$. The influence of molybdenum catalysts on larch wood delignification by CH_3COOH/H_2O_2 mixture was studied (Table 3).

Table 3. Influence of catalyst nature on the process of larch wood delignification by CH_3COOH/H_2O_2 mixture (24.5 % CH_3COOH + 6.4 % H_2O_2) at 130 ^oC, liquor ratio 15:1 and time of pulping 2 h.

Parameters	Catalyst nature and concentration*		
	H_2SO_4 (2 %)	H_2MoO_4 (0.5 %)	$Fe_2(MoO_4)_3$(0.5 %)
Yield of cellulosic product, %*	38.6	40.0	39.2
Product composition, %**:			
cellulose	80.3	83.4	76.4
lignin	3.8	<0.04	2.0
Delignification degree, %	94.4	>99.9	97.0

* relative to mass of a.d.w.; ** relative to mass of product

The most active delignification catalysts H_2MoO_4 allow to produce pure cellulose with the yield 40 % wt. The comparison of delignification activity of H_2MoO_4 and H_2SO_4 catalysts makes it possible to draw some conclusions about the role of hydrolytic and homolytic mechanisms of lignin destruction in CH_3COOH/H_2O_2 medium. The first mechanism dominates in the presence of strong acid catalyst H_2SO_4. The second one takes place in the case of H_2MoO_4 catalyst promoting the formation of acetic peracid. According to the data of Table 3 the homolytic rote of lignin destruction is more effective than heterolytic one.

Conclusion

Advantages of the use of oxidation-reduction catalysts for the ecologically pure process of wood deep delignification in CH_3COOH/H_2O_2 medium are demonstrated. Data about the influence of catalyst nature on their activity in oxidative depolymerization of lignin were obtained. Possibility of the significant increase of delignification activity by photochemical activation of reaction mixture with TiO_2 catalyst was established.

The optimum parameters of catalytic delignification process with TiO_2 catalyst supplying the production of cellulosic product with demanded properties (high yield cellulose, conventional cellulosic product, cellulose for chemical processing) were established.

Acknowledgements

Authors are grateful to program “University of Russia” (grant UR.05.01.021) for financial support of this research.

STUDY OF RUTHENIUM CATALYSTS OF LOW TEMPERATURE AMMONIA SYNTHESIS

Larichev Y.V., Moroz B.L., Prosvirin I.P., Zaikovskii V.I., Bukhtiyarov V.I.

Boreskov Institute of Catalysis SB RAS, Novosibirsk, Russia
Fax. (+7-3832)342453; E-mail: vib@catalysis.nsk.su

Ru/support catalysts promoted with salts of alkali metals are promising catalysts allowing decrease in temperature of the ammonia synthesis compared to the commercially used iron catalysts [1]. The activity of non-promoted Ru/support catalysts in the low-temperature synthesis of ammonia increases in the row: Ru/C ≈ zeolite < Al_2O_3 < MgO [2, 3]. The promoting strength of alkali metals increases from Na^+ to Cs^+, i.e. with the increase in their basicity [4, 5]. However, the reasons of these effects are not clear yet.

This work presents the data of XPS and TEM studies of the electronic state of ruthenium as result of its interaction with a support (MgO) and with a promoter (salts of Cs^+). The obtained data were compared with the data for Ru/C(sibunit) and Ru-Cs/C(sibunit) samples.

4 %Ru/MgO catalyst was prepared by incipient wetness impregnation of MgO (surface area of 135 m^2/g) with an acetone solution of $Ru(OH)Cl_3$ at room temperature. The reduction of $Ru(OH)Cl_3$/MgO precursor was carried out in flowing H_2 (80 ml/min) by heating the sample up to 450 °C during 2 h and keeping at this temperature in a H_2 flow for another 6 h. The reduced Ru/MgO sample was impregnated with an ethanol solution of cesium carbonate followed by drying and reduction at the same conditions as the non-promoted sample. According to TEM, the mean size of the Ru particles in the Ru/MgO sample was 30-40 Å and did not change during promotion. The activity of the non-promoted catalyst in the synthesis of ammonia was very low, whereas after the promotion, the NH_3 content was almost equilibrium at temperature of 350 ^oC.

XPS data indicates that in full agreement with literature both the Ru/MgO and the Ru-Cs/MgO samples are characterized by lower binding energies of an $Ru3d_{5/2}$ spectrum (279.5 and 279.2 eV, respectively) than that of metallic Ru (280.2 eV). To elaborate the reasons of this negative shift we have measured RuMNN Auger spectra and calculate the Auger parameter – $\alpha = E_{св}(Ru3d) + E_{кин}(RuMNN)$. The choice of this parameter is explained by its insensitivity to the differential charging effect. It is known [6] that this effect can cause the negative shifts in the systems of a metal on a dielectric support when the method of internal standard is used to take into account total charging of the non-conductive sample. It

has been shown that namely the differential charging effect is responsible for the BE negative shift of the non-promoted sample. Correction of the binding energy to the value of the differential charging, which has been determined from the XPS spectra of ruthenium valence band, leads to the binding energy value of 280.5 eV. In the case of the promoted sample, not only the differential charging, but also the relaxation effect contributes to the observed shift of the Ru3d spectrum. The true binding energy value (after correction by both the final state effects) is equal to 279.8 eV.

The observed variation of BE value from 280.5 eV for the non-promoted sample to 279.8 eV for the promoted one (i.e. higher and lower than the metallic value) seems to be of great importance, since it correlates with the catalytic properties – low activity for the Ru/MgO and high activity for the Ru-Cs/MgO. Two reasons could be applied for explanation of this observation: variation of the charge on Ru particles and variation of their work function. The former reason is well-known to be a basement of the core-level shift XPS or ESCA, whereas the latter one is discussed more rarely. At the same time, it is known that small metallic particles exhibits usually higher work function than bulk metal. On the other hand, the work function of metal surface (f.e. silver) decreases under influence of an alkali metal that is applied in photocathodes (f.e. S1). To select these effects the obtained data were compared with the data for sibunit-supported catalysts. The preparation procedure and their catalytic properties were described in details in [7]. The choice of these samples is explained by the conductive nature of the carbon support that provides the electrochemical equilibrium between the catalyst surface and spectrometer. As consequence, the variation in the work function of the sample surface does not exhibit in the XPS spectra. Contrary to this, variation of the charge should not depend on nature of a support.

It has been shown that binding energies of the $Ru3d_{5/2}$ spectra for both the Ru/sibunit and the Ru-Cs/sibunit catalysts coincide with the value of metallic ruthenium (280.2 eV). This allows us to conclude that the charge on ruthenium is similar in both cases. It should be however noted that the catalytic activity of the sibunit-originated catalysts exhibits the same tendency as the catalysts on MgO – the promoted sample is much more active that the non-promoted one. In other words, it can be suggested that in both cases, the promotion of Ru particles consists in a decrease in the work function of metal particles. However, due to different conductivity of the supports, the negative shift appears in one case and does not appear in the other.

It has been also shown that the Ru-Cs/MgO and Cs/MgO systems pretreated with hydrogen at 450 ^{o}C contain cesium in the form of a thin film of Cs_2O oxide

(BE($Cs3d_{5/2}$) = 724.8 eV). In the samples exposed to air, the promoter exists in the form of peroxide ($E_bCs3d_{5/2}$= 724.0 eV). The oxide layer covers not only some part of the support surface, but also Ru particles, that confirm a possibility of the decrease in the ruthenium work function under influence of the cesium compounds.

The change in the work function of a metal may be related to the change in its catalytic activity. In papers by Roginsky [8], it was shown that changes in the activation energy of adsorption can correlate with changes in the work function that were induced by promotion. In other words, the decrease in the work function due to promotion facilitates chemisorption of nitrogen, and consequently the whole process, since the N_2 chemisorption is a controlling step of the synthesis of ammonia.

This study was supported by RFBR grants, No. 00-15-99335 and 02-03-32681, as well as by an integration project of the Russian Academy of Sciences, No 10.4.

References

1. Anastasiadi et al, Low-temperature ruthenium-containing catalysts for ammonia synthesis, NIITKhIM, M., 1988 (in Russian).
2. F. Rosowski, A. Hornung, O. Hinrichsen, D. Herein, M. Muhler and G. Ertl, Appl. Catal. A 151 (1997) 443.
3. A. Ozaki Acc. Chem. Res. 14 (1981) 16.
4. K. Aika, K. Shimazaki, Y. Hattori, A. Ohya A., S. Ohshima, K. Shirota and A. Ozaki, J. Catal. 92 (1985) 296.
5. W. Rarog, Z. Kowalczyk, J. Sentek, D. Skladanowski and J. Zielinski, Catal. Lett. 68 (2000) 163.
6. T.L. Barr, Critical Rev.in Anal. Chem. 22(1991) 229.
7. N.B. Shitova, N.M. Dobrynkin, A.S. Noskov, I.P. Prosvirin, V.I. Bukhtiyarov, D.I. Kochubey, P.G. Tsyrul'nikov, D.A. Shlyapin., Kinetics and Catalysis in Russian (in press)
8. S.Z. Roginsky., Kinetics and Catalysis in Russian v.1,1,1960.

INVESTIGATION AND APPLICATION OF Mo AND Ti CATALYSTS FOR EPOXIDATION OF LOW REACTIVE OLEFINS

Leonov V.N., Stozhkova G.A., Bobylev B.N.

ZAO "RaSlav", Yaroslavl, Russia
Tel.: 7(0852)733170,275695; Fax: 7(0852)733170; E-mail: Leonov_RSAn@rambler.ru

MOLYBDENUM CATALYSTS

Cumene hydroperoxide (CHP) epoxidation of low reactive olefins (e.g. propylene) catalyzed by usual molybdenum complexes such as $MoO_2(diol)_2$ is characterized by a low selectivity on hydroperoxide (CHP conversion (CHP_c) 83 %, selectivity (CHP_s) 32 %). At the same time it is known that styrene epoxidation gives a low selectivity on olefin (CHP_c 64 %, CHP_s 67 %, polymers yield based on styrene 20 %).

Experimental (typical run conditions)*:* The catalytic activity was measured in *CHP epoxidation of propylene* (t=120 ^oC, concentrations, mol/l : $[CHP]_o$ 0,9; $[Mo]_o$ $6*10^{-4}$; $[C_3H_6]_o$ 4,5; solvent – cumene) and *styrene* (St) (t=100 ^oC, concentrations, mol/l : $[CHP]_o$ 1.6; $[Mo]_o$ $4.8*10^{-4}$; $[St]_o$ 3.2; solvent – toluene).

We claim that catalytic properties of molybdenum catalyst depend on ligands in coordination sphere of central atom. Therefore, a catalyst active and selective during the whole epoxidation process may be reached by purposeful exchange of ligand nature.

The ligands for modification of Mo catalysts may be divided into some groups:

- **Ph_3X, Ph_3XO ligands (where X - P, As, Sb) or diphosphine oxides**

It was established that Ph_3XO is an active ligand form. In the presence of Ph_3XO the CHP catalytic decomposition is inhibited and the propylene epoxidation is activated, Consequently, selectivity increases from 32 up to 70-90 %. The effect of Ph_3XO correlates with ligand basicity which decreases in order Ph_3SbO > Ph_3AsO > Ph_3PO.

The correlation between basicity ($NMR^{31}P$), chelate cycle stability of diphosphine oxides and epoxidation rate was found.

The effect of Ph_3X, Ph_3XO ligands (where X - P, As, Sb), diphosphine oxides and $Cp(CO)_2MoPh_3XHlg$ (Hlg – Cl, Br, I) catalytic activity don't confirm the traditional epoxidation mechanism.

- **Boron-containing ligands**

In the presence of boron-containing substance $(RO)_3B$ styrene epoxidation is characterized by CHP_c 85 – 90 %, CHP_s 85-87 % . The yield of polymers decrease up to 5...9 %. The investigation of boron-containing substance effect on the activity of molybdenum

catalytic systems in styrene epoxidation (by CHP), on catalytic CHP decomposition and on styrene polymerization have been made. It was established that boron compounds play a role of modifier, but not co-catalyst.

- **R_3SiOH, $R_2Si(OH)_2$ ligands**

The activity of Mo–Si catalytic systems significantly depends on (i) nature of silica compounds; (ii) molar ratio Mo:Si. Propylene epoxidation is characterized by CHP_c ~90 %, CHP_s ~ 70 %. Changes in differential selectivity show that stable catalytic centre containing Mo-O-Si unit exists during the reaction time. That's why polymolybdoorganosiloxanes was used. The results obtained are follows: CHP_c ~96 %, CHP_s ~ 80 %.

- **N,O-contaning ligands**

The introduction of nitroxyle ligand is accompanied by an increase of activity and selectivity of propylene epoxidation which are the greater the higher the additive content: at molar ratio $MoO_2(diol)_2$: $RNO^{\cdot}$ = 1:2 CHP_c 87,5 %, CHP_s 70 %, at 1:10 97 % and 83 % respectively.

Catalytic activity of $MoO_2[N(CH_2CH_2O)_2(CH_2CH_2OH)]$ was determined. Modification of Mo leads to increase both of activity and of selectivity to 95 % and 72 % respectively.

- **ROH compounds**

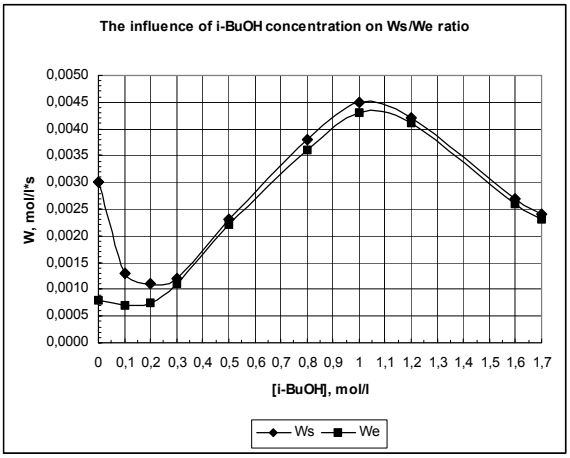

High results in CHP propylene epoxidation were achieved by addition of ROH into reaction media (CHP_c up to 98 %, CHP_s up to 92 %). Among n-, i-, s- and t-ROH 2-propanol give the best results.

Epoxidation of octene-1 by CHP served us as model reaction which allow to characterise ROH effect both on epoxidation itself and on side reaction of catalytic CHP decomposition. Basing on kinetic studies (see fig.) we consider that ROH effect is more difficult than suggested earlier.

Strong inhibition of catalytic CHP decomposition by ROH was founded. The correlations of donor properties of oxygen in n-ROH vs. decomposition rate, donor properties of oxygen in s-,t-ROH and steric effect of radical R vs. decomposition rate were established. The reaction scheme was proposed. It includes [Mo*CHP] and [ROH*Mo*CHP] complexes which are an active species in CHP decomposition on phenol-acetone and 2-phenylpropanol-2

respectively and [Mo*ROH], [Mo*2ROH] complexes which are responsible for inhibition (non-competitive and competitive respectively).

The experimental data mentioned above (see Fig.) give some information about dual ROH function in epoxidation: ROH is activator or inhibitor in dependence of concentration. At the same time for n-ROH inhibition effect decreases when the carbon chain in radical R becomes longer and correlates with changes in H-acidity. For s- and t-ROH inhibition effect determines by O-donor properties and steric influence of radical R.

TITANIUM CATALYSTS

With respect to the epoxidation reaction of unsaturated hydrocarbons the titanium compounds are inferior in their activities to molybdenum catalysts. Thus, cumene hydroperoxide epoxidation of propylene catalyzed by usual $Ti(OBu)_4$ is characterized by CHP conversion 49% and selectivity 61 % (t=120 ^oC, concentrations, mol/l : $[CHP]_o$ 0,9; $[Ti]_o$ $3*10^{-3}$; $[C_3H_6]_o$ 4,5; solvent – cumene).

The combination of Ti(IV) with silica provides a unique homogeneous catalyst which appears to possess the results comparable with molybdenum catalyses.

Really, using $Ti(OBu)_4$ + $(C_6H_5)_2Si(OH)_2$ (Ti:Si = 1:10) we obtain CHP_c ~85 %, CHP_s ~ 90 %.

Previously prepared homogeneous catalyst containing Ti-O-Si bonds gives more remarkable results: CHP conversion 98 % and selectivity 93 %.

CHP decomposition catalyzed by $Ti(OBu)_4$ + $(C_6H_5)_2Si(OH)_2$ was investigated. It was shown that $(C_6H_5)_2Si(OH)_2$ inhibits the reaction. At the same time a new coordination sphere is carried out.

The siloxane ligands activate Ti and promote the formation of Ti=O group which play a key role in oxygen transfer to the olefin.

COMMERCIAL USE

The results mentioned above were used for development of commercial technologies such as:

- propylene oxide (leading organisazion – VNIIOS);
- styrene oxide (leading organization – YARSYNTEZ);
- 1,2-epoxypentane and pentanediol-1.2 (leading organization – VNIIOS);
- cyclohexane oxide and guaiacol (leading organization – YARSYNTEZ).

SOME APPROACHES TO DESIGN NEW HETEROGENEOUS CATALYSTS FOR OLEFINE POLYMERIZATION

Mushina E.[1], Podolsky Yu.[1], Frolov V.[2], Gabutdinov M.[2], Kudryashov V.[2], Bobrov B.[2], Khasanshin R.[2]

[1]Topchiev Institute of Petrochemical Synthesis RAS, Moscow, Russia
[2] "Kazanorgsintez" Stock Company, Kazan, Russia
Fax: (095)230 2224; E-mail: mushina@ips.ac.ru

The development of new catalytic systems in combination with the new polymerization technologies makes the basis for elaboration of perspective modern environmentally friendly and energy saving processes for production of polymers with new and unusual properties.

The work, which is aimed at creation of new catalytic systems for manufacturing of polyethylene (PE) of various grade has been performed by the group of researchers from the Topchiev Institute of Petrochemical Synthesis together with the central laboratory of the stock company "KAZANORGSINTEZ". The investigation results in the creation of original catalytic systems based on the titanium-magnesium and chromium containing compounds modified with oligodienyl complexes of nickel and zirconium. These systems are distinguished from traditional catalysts by their universality as they can be used for polymerization not only of olefins, but dienes as well. Besides these systems display high activity, that means the decreasing of the consumption of heavy metals and therefore enhancement of the environmental safety of the process. The third main feature of the catalysts in question is their ability to display (due to the presence of two active centers in one system) the bifunctional action. It appeared, in particular, that some of the catalysts can perform simultaneously oligomerization and polymerization of olefins, combine such functions as *cis*- and *trans*-polymerization of dienes, and so on.

It is well known that $MgCl_2$ is – due to high electronegativity of Mg atom - a preferable carrier for preparation of effective Ziegler-Natta catalysts in the olefin polymerization. On the other hand, such inorganic oxides as Al_2O_3 or SiO_2 can also be used as carriers of catalysts because of their good morphology and porosity. Using both types of carriers opens an opportunity to combine the advantages of each of them. This approach have been used in this investigation and the following three types of catalysts have been created and studied: (1) titanium-magnesium catalysts (TMC) and the same catalysts deposited on the surface of silica gel; (2) TMC deposited on the surface of silica gel, which was beforehand treated by the oligodienyl complex of nickel or zirconium; (3) mixed catalysts, prepared by the mixing of two portions of carrier, one of which contains TMC and the other - oligodienyl complex of

nickel or zirconium. Moreover, the chromium-containing catalysts (triphenylsilylchromate and CrO_3 deposited on silica gel and treated with diethylaluminumethoxide) have been studied as well.

The TMC have been prepared by interaction of $TiCl_4$ with the freshly obtained $MgCl_2$. The oligodienyl complex of nickel or zirconium has been synthesized by the reaction between $NiCl_2$ (or $ZrCl_4$) and triisobutylaluminum (TIBA) in the presence of isoprene. The structure of the synthesized complexes has been studied by means of IR-spectroscopy and it was shown that the oligodienyl complexes are a mixture of complexes containing the oligomeric ligands of various chain length, di-, tri- and tetramers of isoprene being the major part of them.

It was established that when the polymerization of ethylene is performed using the catalyst prepared according to the second method, the catalyst manifests the maximum activity in a very narrow range of Ni/Ti ratio (about 0.5). In this case, the attempts to control the molecular mass of polymer by increasing the hydrogen concentration appeared to be unsuccessful, leading to a sharp decrease in the activity of catalyst. On the contrary, when the mixed catalysts are used (the third method of catalyst preparation), catalytic activity remains high at Ni/Ti ratio varying from 1 to 6 in spite of changing in the hydrogen concentration from 10 to 30 vol. %.

It was also shown that using these catalysts one can obtain PE with various MMD – from the narrow (M_w/M_n=6-7 in the case of Ti/Mg catalyst) to the broad one (M_w/M_n=17 – 20 in the case of Cr-containing catalyst). The same catalysts, modified with olygodienyl complexes, can produce PE with a bimodal MMD.

It was shown for the first time that the TMC prepared according to the proposed method in combination with TIBA are effective in diene (butadiene and isoprene) *trans*-polymerization with the formation of polymers containing about 96 – 98 % of *trans*-units. The catalysts are active in a very broad range of Al/Ti ratio (from 20 to 100), indicating the high stability of catalytic centers responsible for the *trans*-polymerization of dienes as compared to the homogeneous catalysts $TiCl_4/AlR_3$. When the oligodienyl complex of Ni is added to the catalytic system the formation of polymer containing 28 – 96 % of *cis*-units is observed. It means that usage of the bifunctional catalysts permits one to obtain polymer blends with virtually any *cis*- to *trans*-units ratio.

The financial support of the Russian Foundation for Basic Research (grants No. 02-03-32975 and 02-03-08117-inno) is gratefully acknowledged.

THE PRODUCTION IN BULK OF ELASTOMERIC POLYPROPYLENE WITH *ANSA*-METALLOCENE C_1 -SYMMETRY

Nedorezova P.[1], Solntseva E.[1], Veksler E.[1], Optov V.[1], Aladyshev A.[1], Tsvetkova V.[1], Lemenovskii D.[2]

[1]Semenov Institute of Chemical Physics RAS, Moscow, Russia
[2]Department of Chemistry, Lomonosov Moscow State University, Moscow, Russia
Fax: (095) 137-82-84; E-mail: pned@chph.ras.ru

The discovery of highly effective homogeneous metallocene (MC) catalytic systems opened new opportunities for synthesis of different polymer materials with unique properties. C_1- symmetric metallocene species are excellent tools for the design of polymer with different properties by introduction of substituents in key position of the ligands. Those structure also proved to be excellent for studying of the polymerization mechanism, due to two different coordination sites available for migratory polyinsertion reaction of olefins. According to Chien [1] and Collins [2] for a number C_1 symmetric metallocenes one coordination site is aspecific and the other one is isospecific. The elastic properties of materials, producing upon these systems, were shown to be provided by blocklike structures composed of isotactic and atactic sequences. New type catalytic systems on the base of C_1 symmetric metallocenes were proposed by Rieger [3, 4]. Two different coordination sites of these "dual-side" catalysts lead to isotactic polypropylene (PP) with variable amounts of stereoerrors, depending on the monomer concentration.

In our work *ansa*-metallocene with C_1 symmetry of Rieger-type ethylene-bridged fluorenyl/(5,6cyclopenta-2-methyl-indenyl)zirconocene dichloride was synthesized. Composition, structure and properties of zirconocene were studied by element analysis methods, ^{13}C and ^{1}H NMR spectroscopy.

This MC was studied in the processes of propylene polymerization in a medium of liquid propylene. An original method was used for investigation of the kinetics of a propylene polymerization in bulk. Polymerization was carried at 30-70 ^{o}C using different cocatalysts, mainly polymethylalumoxane (MAO) or partly exchange MAO on (*iso*-$C_4H_9)_3Al$. The influence of the ways of catalytic complex activation, the polymerization temperature, monomer concentration on the activity, molecular weight characteristics, stereoregularity, thermophysical and mechanical properties of producing polymers were studied.

Depending on polymerization conditions the activity changes from 15 to 160 kgPP/mmolZr h, the content of "mm" triads from 50 to 78 % and "rr" triads from 7 to

21 %. The molecular weight of PP, producing at polymerization temperature 50 ^{o}C, changes from 48000 g/mol ([C_3]=1,9mol/l) [4] to 146000 g/mol ([C_3]=11 mol/l).

It was established that monomer concentration and temperature variation is an efficient tool to make an influence on the polymer microstructure and to achieve defined material properties.

Comparison with the data obtained for the catalytic systems of Waymouth-type on the base of "oscillating" catalysts [5-8] was done. For "oscillating" metallocene catalysts during the growth of the polymer chain, reversible isomerization from isospecific *rac*-form to the aspecific *meso*-form takes place repeatedly and as a result stereoblock isotactic-atactic PP are produced. For used MC of C_1-symmetry and MC of "oscillating" type at the increasing polymerization temperature one can see increasing of the degree of isotacticity, the degree of crystallinity and decreasing of PP molecular weight. For MC of C_1-symmetry and MC of Waymouth-type increasing of propylene concentration lead to increasing of PP molecular weights, at the same time for MC of C_1-symmetry it leads to decreasing and for MC of "oscillating" type to increasing of PP stereoregularity. Different models of elastomeric PP producing are discussed.

It was shown that for polypropylene produced with metallocene catalytic systems mechanical properties are determined by molecular weight, the stereoregularity and the crystallinity of the materials. Depending on the polymerization conditions one may produce polymers from amorphous to the samples that have 35 % of crystallinity. The produced PP possesses good elastomeric properties: elongation at break 800 –1100 %, the elongation set 15-30 % after elongation sample PP to 300 %. Varying the polymerization conditions one may produce PP with widely varied properties ranging from crystalline thermoplastics to thermoelastoplast.

So, 5,6-cyclopentyl substitution by the indenyl ligand of *ansa*- metallocene catalyst plays an important role in obtaining a good balance between activity, molecular weight and a sufficient amount of stereoerros for the design of thermoplastic elastomers. Polymerization in a medium of liquid propylene leads to producing of PP with high molecular weight. For the production of elastomeric PP, studied type of MC catalytic system have a unique possibilities for the design of new PP materials.

References

[1] Chien J.C.W., Llinas G.H., Rausch M.D., Lin Y.G., Winter H.H., Attwood J.L., Bott S.G. *J.Polym. Sci., Part A*, 30, (1992), 2601

[2] Gautier W.J., Corrigan J.F., Taylor N.J., Collins S., *Macromolecules,* 28, (1995), 3771

[3] Kukral J., Rieger B., *Macromol. Symp.* 177, (2002), 71

[4] Dietrich U., Hackmann M., Rieger B., Klinga M., Leskela M., *J.Am.Chem.Soc.*, 121, (1999), 4348

[5] Bruce M.D., Coates G.W., Hauptmann E., Waymouth. R.M., *J. Am. Chem. Soc.*, 119, (1997), 11174

[6] Bravaya N.M., Nedorezova P.M., Tsvetkova V.I., *Russian Chemical Reviews*, 71, 1, (2002), 49.

[7] Tsvetkova V.I., Nedorezova P.M., Bravaya N.M., Savinov D.V., Dubnikoba I.L., Optov V.A., *Vysokomol. Soedin., Ser. A*, 39, (1997), 1.

[8] Nedorezova P.M., Tsvetkova V.I., Bravaya N.M., Savinov D.V., Optov V.A., *Vysokomol. Soedin., Ser. A*, 42, (2000), 901

DISPLAY THE EFFECTS OF SURFACE SEGREGATION OF SUPPORTED ALLOYS DURING THE DEHYDROGENATION OF THE LOWEST PARAFFINS IN VARIOUS REACTION MEDIA

Pakhomov N. A., Buyanov R.A.

Boreskov Institute of Catalysis SB RAS, Novosibirsk, Russia
E-mail: pakhomov@catalysis.nsk.su

Elucidation of the mechanism of modifying action of various additives including inactive in target reaction on catalytic and structural properties of active metal is one of the fundamental problems in the field of catalysis of supported bimetallic alloys.

Studying of the contribution of the phenomenon of a surface segregation of alloys to their catalytic properties takes a special place in the common list of problems and questions, which are included in this problem. It is known that the surface segregation of alloys results in a considerable difference in the bulk and surface composition [1, 2].

The surface enrichment with an alloy component depends on the nature of these components, the treatment temperature, and the composition of a gas medium. In a vacuum, the surface is enriched in a metal with a lower heat of sublimation or with a lower melting temperature. As for the bimetallic systems under consideration, their surface in a vacuum is enriched in an inactive metal modifier. The surface enrichment with a particular component in a gas medium depends on the chemical affinity of the gas to either of the two alloy components.

Though the theoretical and experimental aspects of superficial segregation are wide enough considered in the literature plan [2], a role of this phenomenon during transformation of hydrocarbons, catalyzed by the supported alloys was investigated insufficiently.

In this context, the dehydrogenation of lower C_3-C_5 paraffins on spinels supported Pt-Sn, Pt-Cu, Pt-In and Pt-Zn alloys is a very convenient model reaction for studying the effects of surface segregation because the process can be performed either in a purely reductive medium or on diluting the feed with steam, used for decrease the partial pressure and increases of the dehydrogenation depth [3].

In the first case, the enrichment of alloy surfaces with platinum should be expected. In the steam medium, which carries an oxidizer function, the surface may be enriched by inactive metal with formation of its superficial oxide [1].

In the present message results of studying of catalytic properties of Pt-Sn, Pt-Cu, Pt-In and Pt-Zn alloys supported on $ZnAl_2O_4$ and $MgAl_2O_4$ in reaction of dehydrogenation of n-butane and isopentane in various reaction media are submitted. Spinel-

supported bimetallic catalysts were prepared by co-impregnation method. Synthesis of alloys of various composition and structure was carried out by change of a ratio of supported components and the pretreatment conditions according to approaches described by us earlier [4-7]. Alloys were characterized by X-ray and NGR-spectroscopy methods.

From the data represented in the Table 1 we can see that catalytic properties of the investigated systems essentially depend both on crystal structure and a chemical compound of the supported alloys, and contents of the reaction medium.

Table 1.

Influence of reaction mixture compositions on the catalytic properties of spinel supported bimetallic alloys

Catalyst			Active component composition		Catalytic characteristics *)			
	Pt wt.%	Me/Pt atom.	Phase	Particle size nm	Dilution **) mol.	X %	S mol.%	C_4H_6 yield mol.%
Pt-Sn/$ZnAl_2O_4$	0.55	1.5	PtSn	28	Steam	0	0	0
					H_2	44	97	2.5
Pt/$ZnAl_2O_4$+ZnO	0.5		δ-PtZn	35	Steam	0	0	0
Pt-In/$MgAl_2O_4$	1.0	2	PtIn	20	Steam	0	0	0
Pt-Sn/$ZnAl_2O_4$	0.55	1.5	Pt-Sn alloy f.c.c.	12	Steam	75	83	11.6
Pt/$ZnAl_2O_4$+ZnO	0.5		Pt-Zn alloy f.c.c.	10	Steam	43	69	1.8
Pt-Sn/$MgAl_2O_4$	1.0	1.8	Pt-Sn f.c.c. + Pt_3Sn	10	Steam	63	87	16.1
					H_2	65	83	3.9
Pt-Cu/$ZnAl_2O_4$	1.3	1.6	$Pt_{70}Cu_{30}$	17	Steam	39	63	9.4
					H_2	57	90	6.5
Pt-Cu/$ZnAl_2O_4$	1.04	3.6	$Pt_{10}Cu_{90}$ $Pt_{32}Cu_{68}$ (trace)	3	Steam	0	0	0
					H_2	37	88	2.0
Pt-In/$MgAl_2O_4$	**1.0**	**2.5**	Pt-In alloy f.c.c.	8	**Steam**	**63**	**62**	**12.5**
					H_2	**61**	**90**	**3/6**

*) X – n-butane conversion, S – n-C_4H_8+C_4H_6 selectivity, T – 575 °C, time – 5 min.

**) Delution: C_4H_{10} : H_2O(Steam) = 1 : 10; C_4H_{10} : H_2 = 1 : 0.25

The highest catalytic activity and selectivity at a dehydrogenation in the water vapor medium are achieved on solid solutions with the face-centered cubic (f.c.c.) arrangement with the maintenance of inactive metal no more than 25 ат. % and intermetallic compounds such as Pt_3Sn, Pt_3In. Solid solutions with a higher content of the second element (Pt-Cu) and alloys with other crystalline structures (PtSn, δ-PtZn, PtSn, PtPb, etc.) are inactive during dehydrogenation under same conditions. Probably in the presence of steam the surface of alloys can be enriched in an inactive metal. At replacement the steam by hydrogen should occur return diffusion of platinum to superficial layers of an alloy. Such change of structure of a surface is responsible for a noticeable increase in the dehydrogenation activity on PtSn-type alloys in pure hydrogen atmosphere (see Table 1).

The effect of the reaction medium on f.c.c. alloys depends on the nature of a modifying element. Thus, a solid solution of tin in platinum ($Pt_{92}Sn_8$) and the Pt_3Sn alloy exhibit comparatively low sensitivity to steam exposure. Because of this, the Pt–Sn catalyst can be used in the single-step process of paraffin dehydrogenation to dienes [3]. The catalytic activity and selectivity of Pt–Cu solid solutions decrease on feed dilution with steam. The higher the copper content of the alloy, the more sensitive is the system to the poisoning effect of steam. In steam dehydrogenation, catalysts containing Pt–In solid solutions are highly selective in cracking and deep oxidation reactions.

In general, the catalytic activity and selectivity of catalysts containing f.c.c. alloys in dehydrogenation in a steam medium decrease in the order

Pt–Sn > Pt–In > Pt–Zn > Pt > Pt–Cu.

If the process is performed in a hydrogen medium, the overall conversion decreases, and the selectivity increases, whereas the order of activity undergoes considerable changes:

Pt–In ≅ Pt–Sn > Pt–Cu > Pt–Zn > Pt.

The effect of surface segregation in supported fcc alloys can also be explained by the experimentally observed dependence of the catalytic properties of a P̃tSn catalyst on the composition of a pretreatment medium. Figure 1 illustrates the effect of additional reduction (before measuring the catalytic activity) of an oxidized (or regenerated) sample on the rate of isopentane dehydrogenation in a water vapor medium. It can be seen (Fig. 1, curve *1*) that the preliminary treatment in a hydrogen atmosphere dramatically decreased the initial activity of the catalyst in dehydrogenation and simultaneously increased the activity in side reactions of cracking and deep oxidation with steam. In other words, the pretreatment with hydrogen decreased the selectivity for dehydrogenation products. The oxidized sample, which was not

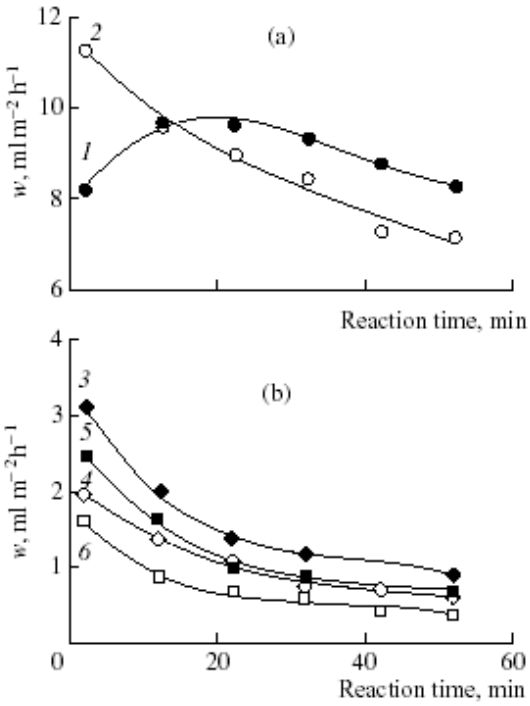

Fig. 1. Dependence of the rates of isopentane (*1*, *2*) dehydrogenation, (*3*, *4*) cracking, and (*5*, *6*) deep oxidation with steam on the reaction time on (*2*, *4*, *6*) oxidized and (*1*, *3*, *5*) additionally reduced Pt–Sn/$ZnAl_2O_4$ catalysts. Catalyst composition: Pt, 0.56 wt %; Sn, 0.45 wt %. Reaction conditions: T = 582°C; *i*-C_5H_{12} : H_2 : H_2O = 1 : 1 : 10; space velocity, $v_{i-C_5H_{12}}$ = 225 h^{-1}. Conditions of reduction: T = 580°C; time, 1 h.

subjected to additional reduction, exhibited a higher initial activity in the target reaction (curve *2*) and a lower activity in side reactions (curves *4*, *6*). It is believed that, in the reduction of the sample in hydrogen, the surface of the Pt–Sn alloy, which was formed before the contact of the sample with the reaction medium, was enriched in platinum. As mentioned above, pure unmodified platinum exhibits very low selectivity in the target reaction of dehydrogenation. The surface composition of a Pt–Sn solid solu tion is subsequently changed under exposure to steam, which is a constituent of the reaction medium. The activity of the catalyst in dehydrogenation increases because of an increase in the modifying effect of tin atoms. The rate of dehydrogenation is an extremum function of reaction time because a side reaction of coke formation occurs.

Note that all changes in the catalytic properties depending on the compositions of a reaction medium and a pretreatment medium, which can be relevant to the surface segregation of alloys, are reversible.

Acknowledgements

This work has been supported by the Russian Foundation for Basic Research (Grants 00-15-97440).

Reference

1. Bauman R., Toneman L.H., Holscher A.A. *Surface science.* 1973. V.35. P.8.
2. Foger K. *Catalysis Science and Technology (J.R.Anderson and M.Boudart Editors). Berlin - Heidelberg- New York -Tokyo: Springer-Verlag*. 1984. V. 6. P. 227.
3. Buyanov R. A. and Pakhomov N. A. *Kinetics and Catalysis, 2001. V. 42. No. 1. P. 64.*
4. N.A.Pakhomov, R.A.Buaynov, E.N.Yurchenko et al., React. Kinet. Catal. Lett., 14 (1980) 329.
5. N.A.Pakhomov, R.A.Buaynov, E.M.Moroz, E.N.Yurchenko et al., Kinetika i Kataliz, 22 (1981) 488 (in Russian).
6. N.A.Pakhomov, N.A.Zaytceva and E.M.Moroz, Kinetika i Kataliz, 33 (1992) 426 (in Russian).
7. Pakhomov N.A., Buyanov R.A., and Zolotovskii B.P. *Stud. Surf. Sci. Catal.* 1998. V. 118. P. 185.

FT-IRS STUDY OF THE SURFACE ZIRCONOCENE COMPLEXES IN SUPPORTED CATALYST FOR ETHYLENE POLYMERIZATION

Panchenko V.N., Danilova I.G., Zakharov V.A., Paukshtis E.A.

Boreskov Institute of Catalysis SB RAS, Novosibirsk, Russia
Fax: 7 (383 2) 344687; E-mail: Panchenko@catalysis.nsk.su

The homogeneous catalysts for olefin polymerization obtained from metallocene compounds and methylaluminoxane (MAO) have been intensively investigated in the last years. Nevertheless data on composition and structure of the surface zirconium compounds in the supported catalysts are very limited.

Earlier we have studied the interaction of SiO_2 with MAO by means of FT-IRS and presented the data on Lewis acidic sites (LAS) in the support SiO_2(MAO) and interaction of zirconocene with LAS of this support [1-2].

In the present work we have studied by means of FT-IRS (adsorption of CO) the surface zirconium compounds formed in the supported catalysts Cp_2ZrMe_2/SiO_2 (I), Cp_2ZrMe_2/SiO_2(MAO) (II), Cp_2ZrMe_2/Al_2O_3 (III).

It was shown by FT-IRS study that Cp_2ZrMe_2 interacts with surface hydroxyl groups and LAS of supports (SiO_2, SiO_2(MAO) and Al_2O_3) and forms various kinds of surface zirconium compounds.

Not long ago the stable non-classical σ-carbonyl zirconium complex $[Cp_3Zr(CO)]^+[MeB(C_6F_5)_3]^-$ was synthesized [3]. On account of these data it was shown that CO interacts at 77 K with zirconocene catalysts Cp_2ZrMe_2/SiO_2 (I), Cp_2ZrMe_2/SiO_2(MAO) (II), Cp_2ZrMe_2/Al_2O_3 (III) and formed the carbonyl adducts $[Cp_2ZrMe(CO)]^{\delta+}[Me\text{-}Support]^{\delta-}$ (Tab. 1).

Table 1. Position of absorbance bands in carbonyl zirconium complexes.

№	Carbonyl zirconium complexes	Oxidation state of Zr	ν_{CO}, cm^{-1}	T, K	Reference
1	$[Cp_3Zr(CO)]^+[MeB(C_6F_5)_3]^-$	IV	2150	273	3
2	$[Cp_2ZrMe\leftarrow(CO)]^{\delta+}[Me\text{-}MAO]^{\delta-}/SiO_2$	IV	2123, 2146	77	the present work
3	$[Cp_2ZrMe\leftarrow(CO)]^{\delta+}[Me\text{-}Al_2O_3(700)]^{\delta-}$	IV	2125, 2135	77	the present work

FT-IR spectroscopic studies of CO interaction with surface zirconium alkyl compounds of SiO_2/Cp_2ZrMe_2, $SiO_2/MAO/Cp_2ZrMe_2$ and Al_2O_3/Cp_2ZrMe_2 have revealed that it proceeds through a step of CO adsorption on these surface zirconium alkyl compounds at 77 K with subsequent insertion of CO into the zirconium-alkyl bonds producing various surface acyl compounds (ν_{CO} 1500-1750 cm^{-1}) at 298K.

It was shown that only small part of surface zirconium compounds may be considered as active cationic species. It is proposed that the surface active species are formed at zirconocene interaction with the definite types of LAS.

[1] V.N. Panchenko, N.V. Semikolenova, I.G. Danilova, E.A. Paukshtis, V.A. Zakharov, J. Molec. Catal. A: Chemical 142(1999)27-37.
[2] V.A. Zakharov, V.N. Panchenko, N.V. Semikolenova, I.G. Danilova, E.A. Paukshtis, Polym. Bull. 43(1999)87-92.
[3] Marsella J.A., Curtis C.J., Bercaw J.E., Caulton K.G.//J. Am. Chem. Soc. ,1980, v.102, p.7244-7246
[4] Manzinger J., McAlister D., Sanner R., Bercaw J.// J. Am. Chem. Soc., 1978, v.100, p.2716.
[5] Brackemeyer T., Erker G., Frohlich R.// Organometallics, 1997, v.16, p.531.

CHEMILUMINESCENCE TECHNIQUES IN THE INVESTIGATION OF COBALT-BROMIDE CATALYTIC OXIDATION OF METHYLBENZENES

Paskhin A.I., Gavrichkov A.A., Zakharov I.V.

Moscow Institute of Physics and Technology
Dolgoprudny, Moscow Region, Russia
Fax: 7 (095) 408-56-77; E-mail: bio@pop3.mipt.ru

The cobalt-manganese-bromide catalyzed oxidation of alkylaromatic hydrocarbons to the corresponding carboxylic acids (also known as MC-Amoco process) constitutes a basis for several large-scale industrial processes – manufacturing of terephthalic, isophthalic, and trimellitic acids.

MC Oxidation

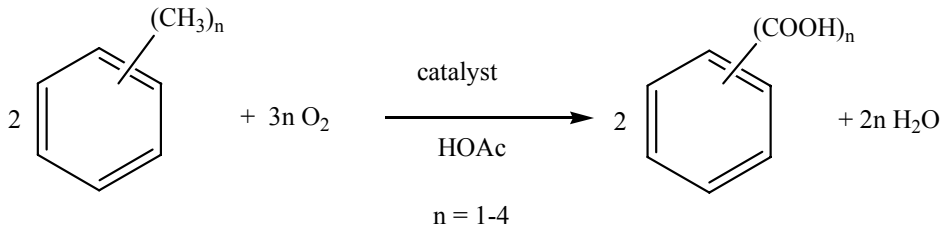

catalyst = $Co(OAc)_2$ /HBr / $Mn(OAc)_2$

Application of chemiluminescent (CL) techniques to the studies of metal-bromide catalyzed hydrocarbon oxidation systems allows one to obtain key kinetic information, which is not otherwise available.

Liquid-phase oxidation of alkylaromatic hydrocarbons is accompanied by the weak CL, which is caused by the recombination of peroxide radicals formed during oxidation. Energy released during this recombination is enough to excite a carbonyl product, subsequent fluorescence of which is responsible for the emission in the visible part of the spectrum with a maximum at approximately 450 nm.

$$\mathbf{RO_2^\bullet + RO_2^\bullet \rightarrow R'CO^* + ROH + O_2} \quad (1)$$

$$\mathbf{R'CO^* \rightarrow R'CO + h\nu} \quad (2)$$

$$\mathbf{R'CO^* \rightarrow R'CO + heat} \quad (3)$$

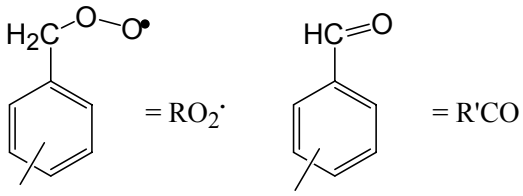

CL intensity is proportional to the rate of recombination of peroxo radicals, which, at a steady-state condition, is equal to the rate of their initiation.

$$\mathbf{I = \eta \cdot 2k_6[RO_2^{\bullet}]^2 = \eta W_i} \qquad (4)$$

$$\mathbf{\eta = \eta_1 \bullet \eta_2}$$

Where η - quantum yield of CL, which ranges between 10^{-15} to 10^{-8}, η_1 is a quantum yield of excitation (10^{-5} -10^{-6}), η_2 - quantum yield of fluorescence.

We have demonstrated earlier that, in the case of cobalt-bromide catalysis, intensity of CL, concentration of peroxo radicals and the rate of oxidation (defined as the rate of oxygen consumption) are related as shown in equations below.

$$\sqrt{I} \approx [RO_2^{\bullet}] = \frac{k_4[Co^{2+}]}{k_6}$$

$$W_{o_2} = \frac{2k_4^2[Co^{2+}]^2}{k_6} \qquad W_i = 2k_6[RO_2^{\bullet}]^2 = \frac{2k_4^2[Co^{2+}]^2}{k_6} \qquad W_i \cong W_{o_2}$$

This set of key relationships allowed us to develop several CL methods that we use for the mechanistic studies of metal-bromide catalysis.

This poster shows the examples of the CL methods and the type of information that can be obtained from CL measurements. The modified CL setup and our measurements of CL yield in cobalt-bromide catalyzed oxidation are also discussed. Implementation of a new photon-counting CL detector allowed us to obtain new, more precise values for the quantum yields of CL for toluene, p-xylene, and pseudocumene.

Acknowledgement. This work is sponsored by BP Chemicals.

PHENOL AQUEOUS PHASE OXIDATION IN THE PRESENCE OF SOLID CATALYSTS. THE ROLE OF SURFACE OF CATALYST

Pestunova O.P., Ogorodnikova O.L., Parmon V.N.

Boreskov Institute of Catalysis, SB RAS Novosibirsk, Russia
Tel. : +7 3832 34-25-63; Fax: +7 3832 34-30-56; E-mail: oxanap@catalysis.nsk.su

Aqueous effluents from some industries such as chemical, petrochemical, pharmaceutical etc. contain toxic organic pollutants in concentration too high to be treated through biological oxidation. Catalytic wet oxidation (CWO) employing oxygen (CWAO), ozone or hydrogen peroxide appears to be more effective and more economical, because it allows to reduce significantly the temperature and pressure [1].

Homogeneous catalysts such as transition metal's cations and complexes (Fe and Cu are usually used) are very effective catalysts in processes of CWAO and CWPO [2, 3]. However the heterogeneous catalysts allow to avoid the processes of the catalyst regeneration. There are two groups of the heterogeneous catalysts. The first group consists of oxides and mixed oxides of transition metals (usually Cu, Fe, Mn, Co) or oxides supported on oxide carriers [3, 4]. These catalysts are sufficiently effective, but they have essential imperfection. Active component can be leached under reaction conditions. Second group is noble metals supported over either oxides or carbon [4]. In contrast to oxide catalysts, these catalyst are usually stable, but much more expensive.

In our study we are comparing activity and stability of wide range of oxide catalysts and graphite like catalyst Sibunit in model reaction of phenol oxidation with the hydrogen peroxide.

We have tested following catalysts: Cu, Fe and Mn-oxides supported on such stable carriers as α-Al_2O_3, TiO_2 and CeO_2, mixed oxide MnO_2/CeO_2 prepared via co-precipitation and porous graphite-like carbon Sibunit.

The phenol oxidation was carried out in a batch reactor with a reflux condenser at atmospheric pressure and temperature 368 K. Concentration of phenol and hydrogen peroxide was 0.01 mol/l and 0.1 mol/l, respectively.

Concentrations of phenol and some products of its oxidation were detected by HPLC. Concentration of hydrogen peroxide was determined by UV-Vis spectroscopy via reaction with Ti.

Metals leaches were detected with atomic absorptive analyzer.

Conversion of phenol and hydrogen peroxide after 30 minutes and 3 hours of reaction and TOC abatement after 3 hour are shown in the Table. The same Table presents amounts of active metals found in solution after reaction and pH of the solution.

Blank experiment (No.1) showed that phenol can be oxidized with hydrogen peroxide at 368 K without catalysts, but conversion after 3 hours was only 44 % and TOC abatement 12 %. The solution after reaction has dark brown color.

The catalysts containing ceric dioxide (Nos. 2, 6, 8, 9) and manganese dioxide (Nos. 8, 9) (except of the 2%Mn/α-Al_2O_3) were found to be very active in hydrogen peroxide decomposition but inactive in phenol oxidation. Cu-containing catalysts (Nos. 4-6) and 2% Mn/α-Al_2O_3 (No. 7) are extremely unstable under reaction conditions. The most part of copper and manganese leaches into solution, and it seems to act like a homogeneous catalyst. The sample 2%Fe/α-Al_2O_3 (No. 3) was found to be the most stable under reaction conditions and sufficiently active in phenol oxidation. Moreover, it was much more stable at the reuse (only 4% of iron was leached and 90 % of phenol was oxidized). The influence of the surface area of support was revealed. The sample No. 4 on γ-Al_2O_3 (S_{BET}= 270 m^2/g) turned out to be much more effective than No.3 on α-Al_2O_3 (S_{BET}= 5 m^2/g).

Comparative tests of homogeneous catalyst $Fe(NO)_3$ were carried out (No. 14). The amount of Fe^{3+} was 100 μM. It is approximately equal to the amount of Fe^{3+} usually leached into solutions. Phenol conversion was 100 % already after 30 min, but TOC abatement was very low (only 18 %).

Table. Catalytic behavior of the different catalysts in the phenol oxidation by hydrogen peroxide

No.	Catalyst	Phenol conversion, %		H_2O_2 conversion, %		TOC abate-ment, % 3 hrs	Active metal leaching, %	Final pH
		0.5 hour	3 hrs	0.5 h	3 hrs			
1	none	5	44	15	33	12	-	3.7
2	2%Fe/CeO_2	0	0	100	100	0	0.3	4.0
3	2%Fe/α-Al_2O_3	46	100	15	100	26	21	2.9
4	1.9%Fe/γ-Al_2O_3	100	100	100	100	80	15.7	4.4
5	1%Cu/α-Al_2O_3	100	100	100	100	48	65	3.0
6	1%Cu/TiO_2	100	100	100	100	39	80	3.0
7	1%Cu/CeO_2	5	6	100	100	0	27	4.0
8	2%Mn/α-Al_2O_3	41	81	31	59	14	60	3.5
9	2%Mn/CeO_2	0	0	100	100	0	39	5.1
10	MnO_2/CeO_2	14	35	100	100	41	6.2	5.5
11	Sibunit-4	50	86	21	76	50	-	2.7
12	Sibunit-4 + Fe^{3+} + Cu^{2+}<0.1μM	27	35	51	97	35	-	5.3
13	1.6%Fe/Sibunit-4	99	100	100	100	58	27	3.8
14	100 μM $Fe(NO)_3$	100	100	100	100	18	-	4.0

However, the most interesting result was obtained in the presence of Sibunit based samples. The conversion of phenol was 86% and TOC abatement was 50% (No.11) but after reaction, we detected in the solution the traces of Fe^{3+} and Cu^{2+} (~1-5 μM). When the content of metals was reduced (No.12) the activity of sample reduced too. The content of iron in different samples of Sibunit was about 0.02 weight %. The catalyst 1.6%Fe/Sibunit-4 turned out to be very effective.

Hydroquinone and pyrocatechol were found to be the intermediate products in all cases. However, the final solution had deep brown color without a catalyst and in presence in Fe^{3+}. That could be explained by formation of polymeric products from hydroquinone and pyrocatehol. More deep oxidation occurs when the catalysts supported on high surface area supports Sibunit and γ-Al_2O_3 are used. The solutions were colorless in these cases.

Acknowledgement

The authors gratefully acknowledged INTAS (grant 00-129) for financial support.

Reference

1 F.Luck, Chem.Biochem. Q., 1996, 27, 195.
2 V.S.Mishra, V.V.Mahajani, J.B.Joshi, Ind. Eng. Chem. Res., 1995, 34, 2.
3 J.Barrault, M.Abdellaoui, C.Bouchoule, at al., Appl. Cat. B., 2000, 27, 225.
4 Yu.I.Matatov-Meytal, M.Sheintuch, Ind. Eng. Chem. Res., 1998, 37, 309.

FROM STUDY OF THE MECHANISM TO MODELING THE SYNTHESIS OF THE N-PENTANE ISOMERIZATION CATALYST WITH THE SUPPORTED LEWIS DIMERIC SPECIES

Pikersky I.E., Polubentseva M.F.

Oil and Coal Based Chemical Synthesis Institute at ISU, Irkutsk, Russia
Fax: (3952) 46 22 00; E-mail: Pikersky@mail.ru

Long-standing labeled atom studies on the mechanism of n-pentane isomerization transformations for different catalysts showed that the registered quantitative distribution of a radioactive marker cannot be ascribed to only the rearrangements covered in the literature. Analysis of the obtained results confirmed the earlier assumptions that the actually registered rearrangement of a radioactive marker was a superposition of several mechanisms and suggested the following:

1. the isomerization process has an individual set of mechanisms for every particular catalyst;
2. reaction mechanisms are closely allied and comparable for the processes with the same type catalysts;
3. the marker $1C^{14}$ is for testing the mechanism of the n-pentane isomerization;
4. there exists one more, at least, mechanism which in conjunction with those already known can clarify the experimental data adequately.

To explain the fourth item one should consult the table comparing the experimental data and the theoretical calculations for the n-pentane -1^{14}C isomerization.

According to the mechanisms previously reported in the published works (alkyl transferring, protonation of C-C and C-H bonds, and formation of methylcyclobutane complex) less than 25 % of the marker might become the central atoms (C-2 and C-3) of the formed 2-methylbutane molecule, whereas data of some experiments afforded the values close to 100 %.

As a consequence, considering electronic and structural parameters of the hydrocarbon and the catalyst, we proposed a new mechanism, with a reactive transition complex of dicyclopropane structure being formed at the dimeric Lewis species at the first step. The example of this complex on Al_2Cl_6 is given on the diagram. After the isomerization the initial marker may completely transfer to the center of the 2-methylbutane molecule according to one of three routes (three end lines in the table).

Comparison of the isomerizing activity of the catalysts with data of the radiometric analysis allows revealing some regularities. A significant concentration of the initial marker at

Experimental distribution of the radioactive marker in the 2-methylbutanes formed in the course of the n-pentane -1^{14}C isomerization compared with theoretical calculations

EXPERIMENT									
Catalyst	Registered distribution of the marker in the atoms of 2-methylbutane, %						η yield of 2-methyl-butane, %	M= η·Σ	**Y=M/47.51**
	C-I	C-2	C-3	C-4	C-2^{I}	Σ (C-2+C-3)			
0.55%Pt-Al_2O_3-3.5%F (ИП-62)	2.6	33.9	59.0	1.9	2.6	92.9	47.0	4361	91.8
WS_2	6.7	41.0	38.3	7.2	6.7	79.3	35.9	2846	59.9
$AlCl_3$	10.2	37.3	30.0	12.3	10.2	67.3	70.6	4751	100
SbF_5-HSO_3F	17.1	33.3	19.5	13.0	17.1	52.8	45.2	2386	50.2
SbF_5-HF	20.0	28.0	12.1	19.8	20.0	40.1	54.2	2173	45.7
$AlBr_3$	23.3	15.2	16.5	21.7	23.3	31.7	59.5	1892	39.8
0.62%Pt-Al_2O_3-0.7%Cl (АП-64)	24.5	3.0	31.0	17.0	24.5	34.0	30.4	1003	21.1
1.7%Pt-Al_2O_3 (обр.766)	24.0	4.7	16.6	30.7	24.0	21.3	20.4	434	9.1
0.69%Pt-Al_2O_3 (обр.635)	26.5	0.6	10.7	35.7	26.5	11.3	21.2	240	5.1
THEORY									
Mechanism	Calculated distribution of the marker in the atoms of 2-methylbutane, %								
	C-I	C-2	C-3	C-4	C-2^{I}	Σ (C-2+C-3)			
~CH_3-transfer [1]	33.3	0	0	33.3	33.3	0			
~C_2H_5- transfer [1]	33.3	0	0	33.3	33.3	0			
Protonation C_1-C_3 [2,3]	33.3	0	0	33.3	33.3	0			
Protonation C_2-C_4 [2,3]	33.3	0	0	33.3	33.3	0			
Protonation C-H [4]	33.3	0	0	33.3	33.3	0			
Methylcyclobutane complex [5,6]	25	0	25	25	25	25			
Dicyclopropane complex (route A)	0	50	50	0	0	100			
Dicyclopropane complex (route B)	16.6	50	0	16.6	16.6	50			
Dicyclopropane complex (route C) [7]	16.6	0	50	16.6	16.6	50			

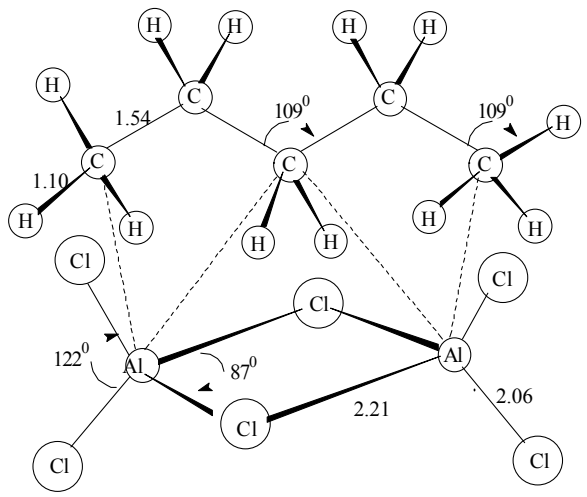

the C-2 and C-3 carbon atoms of 2-methylbutane takes place for highly active catalysts that can be explained via revealing the role of the dimeric Lewis species in the n-pentane isomerization. All the catalysts highly active in the isomerization have the high concentrations of the species but the low active ones, on the contrary, have the very low concentrations. A relationship between the yield of 2-methylbutane and the amount of the radioactive marker in the center of the molecule is illustrated by their product (column M in the table) normalized to 100 % (column Y=M/47.51 in the table). The catalysts having the factor more than 40 % are classified as with the catalytic systems highly active in the isomerization. Hence it is safe to say that the dimeric Lewis species are the most reactive ones in the n-pentane isomerization.

This gave rise to the idea to synthesize a new catalyst capable of conducting the isomerization via the dicyclopropane mechanism but having no drawbacks of its precursors. Thus, aluminum chloride being a highly active mid-temperature catalyst fits the required conditions in terms of its geometrical and electronic parameters but, unfortunately, it is not recyclable and besides requires quite a long reaction time – 24 hours. The latter drawback is explained by the fact that aluminum chloride exists in the monomer form – $AlCl_3$ in the conventional conditions, but the catalytically active phase – the dimeric Al_2Cl_6 is formed as a result of transformation of the catalyst into gaseous phase in the course of the isomerization.

In our view to overcome both of the drawbacks the active catalytic phase had to be supported. To realize the idea the way of condensation of aluminum chloride in the dimeric form with surface silicagel hydroxyl groups was chosen. To synthesize the catalyst successfully one should to do the following:

a) to fulfill calculations on comparing the Al_2Cl_6 dimeric dimensions and the silicagel interhydroxyl distances in order to find the amount of the SiO_2 surface residual hydroxyl groups required for supporting a particular structure complex;

b) to find the support treatment optimal temperature leaving at the surface the residual hydroxyl groups in the required amount determined previously;

c) to find which of the ways to support aluminum chloride on the prepared carrier – penetration by a solution or condensation from gaseous phase gives the catalyst active in the n-pentane isomerization.

It would be fair to note that quests for the catalytic systems via supporting the active phase also took place previously, but in general they were of a quite occasional, unsystematic character. That is the reason why our method – from the reaction mechanism toward the catalyst synthesis with regard to different factors and calculations seems to be useful for design of different systems with predictable catalytic properties.

References

[1] Whitmore F.C., Ind. Eng. Chem. 1948. Vol. 26. P. 668.
[2] Roberts J.D., Lee C., Saunders W., J. Am. Chem. Sos. 1954. Vol. 76. P. 4501 – 4510.
[3] Brouwer D.M., Rec. trav. chim. 1968. Vol. 87. P. 1435 –1444.
[4] Ola G.A., Usp. Khimii, 1975. T. 44. № 5. P. 793 – 867.
[5] Muller J.M., Gault F.G., J.Catal. 1972. Vol. 24. P. 361 – 364.
[6] A.G., Laad J.R., Weeks J., 6-th International Congress of Catalysis. London. 1976. A22. P. 1 – 6.
[7] Lipovich V.G., Khvan K.S., Polubentseva M.F., Pikerskii I.E., Kaletchits I.V., Dokladu USSR. 1978. T.240. P.1119-1120

SYNTHESIS AND ESTIMATION OF THE N-PENTANE ISOMERIZATION CATALYST

Pikersky I.E., Polubentseva M.F.

Oil and Coal Based Chemical Synthesis Institute at ISU, Irkutsk, Russia
Fax: (3952) 46 22 00; E-mail: Pikersky@mail.ru

Experiments showed that the dimeric Lewis species are the most reactive ones in n-pentane isomerization. It gave rise to the idea to synthesize a new catalyst possessing the properties required to realized the dicyclopropane mechanism. To do this an active catalytic phase had to be supported, the support geometrical and electronic parameters being able to make the reaction afford the dicyclopropane complexes.

To embody the idea the way of condensation of aluminum chloride with silicagel surface hydroxyl groups was chosen. The aluminum chloride molecule reacts in a dimeric form, so comparison of its dimensions with the interhydroxyl distances allows for finding the optimal amount of hydroxyl groups to fix a particular structure complex on the surface.

Some papers [1] report about a dependence of the silanolic group concentration on the thermal treatment in vacuum. It was calculated that the preparation of an effective catalyst for the n-pentane isomerization by the silicagel surface anhydrous aluminum chloride condensation technique requires the hydroxyl concentration to be within 1.5 ÷ 4 OH-groups per 1 nm^2. It follows from the data in [2] that evacuation of silicagel at 350 - 400 °C results in the required hydroxyl concentration.

Vacuum dehydration of KCK silicagel at 350 °C during 2.5 h gave the support with specific surface of 408 $m^2 \cdot g^{-1}$. Aluminum chloride was supported by different ways.

Four samples of the catalyst obtained through saturation of the prepared silicagel with aluminum chloride solutions in diethyl ether, ethyl acetate, acetone, and ethyl chloride were inactive in alkane isomerization.

Study [3] on the silicagel adsorption of Al, Cu, Zn, and Ti chlorides from binary solutions in hexachlorodisilane as well as the adsorption of these chlorides from a system of five components at 20 ^oC revealed that the adsorption was physical. So, the condensation of aluminum chloride with the surface hydroxyls did not take place at 20 ^oC; this was in line with the fact that no HCl was formed. The surface held the physically adsorbed monomeric $A1Cl_3$ incapable of the n-pentane isomerization activation.

In this connection another way to support aluminum chloride was chosen – the gas condensation technique at 200°C. Three samples of KCK silicagel were prepared by

evacuation at 200, 350 and 500 ^{o}C during 2.5 h. $AlCl_3$ and SiO_2 were placed in a glass ampoule, evacuated, sealed, and heated at 200 °C during 2 h followed by cooling to room temperature.

On unsealing the ampoule the evolved HC1 was an indication of the condensation between aluminum chloride and the silanolic groups. The prepared catalyst was in the form of light-yellow spheres of 3-5 mm in diameter with specific surface of 278 $m^2 \cdot g^{-1}$. N-pentane isomerization tests (20 ^{o}C, τ = 1h) exhibited a high catalytic activity of sample 2 confirming the foregoing theoretical preconditions on the support treatment:

Sample	Evacuation temperature, ^{o}C	Residual amount of OH-groups according to [1]	General conversion of n-pentane, %	Yield of 2-methyl-butane, %
1	200	6 -12	1.0	0.6
2	350	3 - 5	14.7	8.5
3	500	1 - 2	2.1	1.2

Detailed study of the properties of the synthesized $AlCl_3/SiO_2$ catalyst established that the isomerization of n-pentane with a minor addition of ethyl chloride as a promoter proceeded at low temperatures for short times of the contact:

Isomerization of n-pentane for $AlCl_3/SiO_2$ with 0,01% C_2H_5Cl added

t,°C	τ, h.	Chromatographic analysis data, %				
		General conversion	Products boiling below 28 °C	2-methyl-butane	n -pentane	Products boiling above 36 °C
20	0.25	3.0	1.0	1.8	97.0	0.2
20	0.5	17.5	4.8	9.5	82.5	3.2
20	0.75	23.0	5.6	14.6	76.7	3.1
20	1.0	30.0	7.3	17.0	70.0	5.7
20	1.25	36.5	9.4	19.1	63.5	8.0
20	3.0	55.7	23.5	19.8	44.3	12.4
36	0.167	16.6	8.1	6.8	83.1	1.7
50	0.167	28.0	14.4	8.2	72.0	5.4
80	0.167	38.5	18.5	13.4	61.5	6.6
100	0.167	41.2	22.7	11.7	58.8	7.2

Analysis of the change in the general conversion and yield of 2-methylbutane in the course of time established that the reaction rate constants for the n-pentane transformation for both of the reactions have equations of the first order and have the following values.

General conversion of n-pentane: $k_{\Sigma} = 0.359 \pm 0.012$ h^{-1} (R = 99.72 %, $S_o = 2.9 \cdot 10^{-2}$)

Formation of 2-methylbytane: $k_i = 0.170 \pm 0{,}0095$ $ч^{-1}$ (R = 99.22 %, $S_o = 2.3 \cdot 10^{-2}$)

Activation energies were determined on the basis of the temperature dependence.

General conversion of n-pentane: $E_a^{\Sigma} = 66.1$ kJ·mole^{-1} (R = 97.45 %, $k = 1.22 \cdot 10^{11}$)

Formation of 2-methylbytane: $E_a^{i} = 44.8$ kJ·mole^{-1} (R = 93.92 %, $k = 1.125 \cdot 10^{11}$)

The values of the reaction rate constants and the activation energies are in agreement with the results of the n-pentane isomerization for the solid superacidic catalysts $AlCl_3/Al_2O_3$ (E_a=41.8 kJ·mole^{-1}) [4] and $A1Cl_3$/polystyrene – divinylbenzene sulfated (E_a=34.8 ± 3.8 kJ·mole^{-1}) [5] as well as with the data on the low temperature n-pentane isomerization for the $AlCl_3$-$CuCl_2$ mixture having superacidic properties ($k = 0.073$ $ч^{-1}$, $E_a = 57$ kJ·mole^{-1}) [6].

Hence the obtained experimental data testify that $AlCl_3/SiO_2$ is an active low temperature superacidic catalyst for the n-pentane isomerization. The assumption that the supported catalysts contain the fixed catalytically active Al_2Cl_6 is confirmed by Drago and Getty's data [7] on the presence of aluminum with coordination number 4 at the surface of the systems prepared by the treatment of silicagel with aluminum chloride.

To enhance the yield of 2-methylbutane both the reaction temperature and hydrogen pressure were risen as a rise in temperature solely decreases the target product yield because of a decrease in the selectivity.

The done tests on n-pentane isomerization at 125 ^{o}C under 10 MPa of hydrogen pressure during 6 hours confirmed a high catalytic activity of the sample 2:

Sample	Evacuation temperature, ^{o}C	Residual amount of OH-groups according to [1]	General conversion of n-pentane, %	Yield of 2-methyl-butane, %
1	200	6 -12	8.3	6.3
2	350	3 - 5	51.8	48.3
3	500	1 - 2	15.7	14.4

It was of utmost interest to compare the catalytic activities of the synthesized chloroaluminum silicagel catalyst and pure aluminum chloride. The comparative data on the isomerization activities of $AlCl_3$ and $AlCl_3/SiO_2$ showed the undoubted advantage of the latter.

Isomerization of n-pentane for $AlCl_3$ and for $AlCl_3/SiO_2$

Catalyst	t,°C	τ, h.	P_{H_2} MPa	Chromatographic analysis data, %			
				Products boiling below 28°C	2-methyl-butane	n -pentane	Products boiling above 36°C
$AlCl_3$	125	24	10.0	0.1	19.0	80.7	0.2
$AlCl_3/SiO_2$	50	1.5	1.0	2.2	19.2	76.8	1.9
$AlCl_3/SiO_2$	80	1.5	1.0	11.6	19.0	52.4	17.0
$AlCl_3/SiO_2$	125	1.0	10.0	0.1	14.0	85.8	0.1
$AlCl_3/SiO_2$	125	3.0	10.0	0.1	26.4	73.2	0.3
$AlCl_3/SiO_2$	125	6.0	10.0	2.1	48.3	48.2	1.4

The presented data evidence that the n-pentane conversion degree for the $AlCl_3/SiO_2$ catalyst runs to the same values as for $AlCl_3$ but at 50 °C and for 1.5 h. A rise in the temperature enhances the n-pentane conversion, for 6 h at 125 °C the yield of 2-methylbutane reaches one half the possible yield for the thermodynamical equilibrium. Kinetic parameters of the n-pentane isomerization show that the reaction rate constants differ from each other by over ten-fold:

$$k_{AlCl_3} = (1.07 \pm 0.06) \cdot 10^{-2}\ h^{-1}$$

$$k_{AlCl_3/SiO_2} = (15.1 \pm 0.9)1 \cdot 0^{-2}\ h^{-1}$$

and indicate that the higher activity of $AlCl_3/SiO_2$ is achieved due to a decrease in the activation energy:

$$E_{aAlCl_3} = 72\ kJ \cdot mole^{-1}$$

$$E_{aAlCl_3/SiO_2} = 30\ kJ \cdot mole^{-1}$$

References.

[1] Boem H.P., Angew.Chem., 1966. Bd.78. №12. S.617-628.
[2] Peri J.B., Hensley A.L., J.Phys.Chem., 1968. Vol.72. № 8. P. 2926-2933.
[3] A.P. Dyakiv, Yu.A. Padzerskii, V.F. Kochubei, Preparation and Analysis of Pure Substances. Gorkii, 1982, pp. 97-99
[4] Marczewski M., Bull.Sos.Chim.Fr., 1986. № 5. P.750-755.
[5] Fuentes G.A., Boegel J.V., Gates B.C., J.Catal. 1982. V.78. №2. P.436-444.
[6] Ono Y., Tanabe T., Kitaima N., J.Catal. 1979. V.56. №1. P.47-51.
[7] Drago R.S., Getty E.E., J.Amer.Chem.Sos., 1988. V.110. №10. P.3311-3312.

N-PENTANE ISOMERIZATION CATALYST SYNTHESIS MODELING

Pikersky I.E., Polubentseva M.F.

Oil and Coal Based Chemical Synthesis Institute at ISU, Irkutsk, Russia
Fax: (3952) 46 22 00; E-mail: Pikersky@mail.ru

The labeled atom study of the mechanism of n-pentane isomerization transformations for different catalysts showed that the registered quantitative distribution of a radioactive marker in 2-methylbutanes cannot be ascribed to only the rearrangements covered in the literature. It is most likely that there is at least one more mechanism which in conjunction with the known ones will explain the experimental data adequately. Based on electronic and structural parameters of the hydrocarbon and the catalyst we proposed a new mechanism achievable for the dimeric Lewis species [1]. Experiments showed that the latter is the most reactive ones in the n-pentane isomerization.

This gave rise to the idea to prepare a new more active catalyst with the dimeric Lewis species and capable of realizing the dicyclopropane mechanism. To do this it is necessary to support the active catalytic phase capable of conducting the reaction via the dicyclopropane complexes formation with the help of geometrical and electronic parameters of the phase.

To realize the idea the way of condensation of the aluminum chloride dimer with the silicagel surface hydroxyl groups was chosen. It is known that the untreated silicagel surface is saturated with hydroxyls and adsorbed water. Vacuum heating allows removing the water and a part of the hydroxyls, a sufficiently large amount of the chemically active silanolic groups being unchanged on the surface [2]. Thus, the condensation with anhydrous aluminum chloride gives the oxychlorides chemically bonded with silicon, the concentration of the hydroxyl groups governing the mechanism of the condensation of the hydroxyls with the reagent to be supported. The ratio Al:Cl increases from 1 to 1.99 depending on the change in the thermal pretreatment between 200 °C and 700 °C. It was determined that the surface had the (-$AlCl_2$) groups as well as (>AlCl) groups suggesting that two reactions of condensation took place. The measured contribution of the (-$AlCl_2$) content to the general ratio of the dichloride and monochloride ranged up to 99 % [3].

Considering that the molecule of aluminum chloride reacts as a dimer, comparison of its dimensions and the distances between the hydroxyls allows for determining the optimal amount of the hydroxyl groups able to fix the complex of a particular structure on the surface.

Generally 1 nm^2 of the silicagel surface bears between 1.3 and 12 OH-groups depending on the temperature of the pretreatment [4]. Taking into account that every hydroxyl takes the surface S =1/n, nm^2, the distance between two hydroxyls can be calculated, it is equal to the twofold radius

$\delta L_{OH} = 2R = 2\sqrt{\frac{1}{n\pi}}$. Besides it is necessary to take into account the length of two Si-O bonds as the reacting hydroxyls may be spaced at these distances. The length of the Si-O bond is 0.163 nm, it follows that the possible distances between the hydroxyls vary within: $\lambda_1 \div \lambda_2 = \delta L_{OH} \pm 2L_{Si\text{-}O} = \delta L_{OH} \pm 0.326$. The δL_{OH} values for different amounts of hydroxyls are listed in the table.

The length of the Al_2Cl_6 molecule was calculated regarding the fact that the atom of aluminum lay in the distorted tetrahedral coordination with the angel of 122^o between the geminal atoms of chlorine in Cl-Al-Cl: $L_\Sigma = L_{Al\text{-}Al} + 2\, L_{Cl\text{-}Cl} \cdot \sin 29^o = 0.341 + 2 \cdot 0.1 = 0.541$nm.

Besides the molecular dimensions of aluminum chloride the length of two Si-O bonds has to be taken into account. The zone of aluminum chloride adsorption with the end chlorine atoms ranges $\Lambda_1 \div \Lambda_2 = L_\Sigma \pm 2L_{Si\text{-}O} = 0.541 \pm 0.326$ nm.

The upper limit of the absorption zone boundary is the sum of the Al_2Cl_6 molecule length and two Si-O bonds: $L_{ads.max.} = L_\Sigma + 2L_{Si\text{-}0} = 0.541 + 2 \cdot 0.163 = 0.867$ nm.

However to prepare selectively the aluminum chloride dimer supported via two its atoms it is necessary to rule out the interaction between both of the geminal chlorine atoms, their separation being equal to: $L_{hem.C1\text{-}C1} = L_{Al\text{-}Cl} \cdot 2\sin 61^o = 0.206 \cdot 2 \cdot 0.8746 = 0.36$ nm. The inclusion of two Si-O bonds gives the value of the lower limit of the Al_2Cl_6 absorption zone boundary: $L_{ads.min} = L_{Cl\text{-}Cl} + 2L_{Si\text{-}O} = 0.36 + 2 \cdot 0.163 = 0.686$ nm. The whole zone of the aluminum chloride adsorption via the end chlorine atoms is symbolized by the indexes A_1 and A_2 at the diagram and lies within 0.686-0.867 nm. Comparison of it with the variations in the interhydroxyl distances $\lambda_1 \div \lambda_2$ allows for finding the optimal amount of the hydroxyl groups on the silicagel surface. The presented diagram illustrates the shaded part of the zone A_1-A_2 realizing the 100 % compliance of the interhydroxyl distances for the selective adsorption of aluminum chloride via two end chlorine atoms at the concentration of 1.5 ÷ 4 hydroxyls per 1 nm^2 of the silicagel surface.

However after the adsorption the condensation reaction results in formation of oxychloride, with its geometrical parameters differing from those of Al_2Cl_6. As the bond Al-O equal to 0.178 nm is shorter than the Al-Cl bond, the length of the $Al_2Cl_4O_2$ molecule reduces correspondingly as well as the distance between the heminal chlorine and oxygen atoms situated at the aluminum atom. Consequently, as to the forming oxychloride the foregoing calculations would require a correction. The upper limit of the boundary of the zone of the reaction interhydroxyl distances is equal to the sum of the $Al_2Cl_4O_2$ molecule length, estimated at 0.513 nm, and two Si-O bonds: $L_{react.max.} = L_{Al2Cl4O2} + 2L_{Si\text{-}O} = 0.513 + 2 \cdot 0.163 = 0.839$ nm.

For the calculation of the boundary lower limit it was assumed that the aluminum oxychloride molecule had two geminal oxygen atoms at the aluminum atom with the 120° angle between them in place of the end chlorine atoms. The calculation of this hypothetical molecule rules out completely the simultaneous interaction of the two end chlorine atoms with the surface hydroxyls. Assuming the intergemoxygen distance equal to 0.308 nm and two siloxane bonds gives the value of the lower limit of the zone boundary: $L_{react.min.} = L_{hem.O\text{-}O} + 2L_{Si\text{-}O} = 0.308 + 2 \cdot 0.163 = 0.634$ nm.

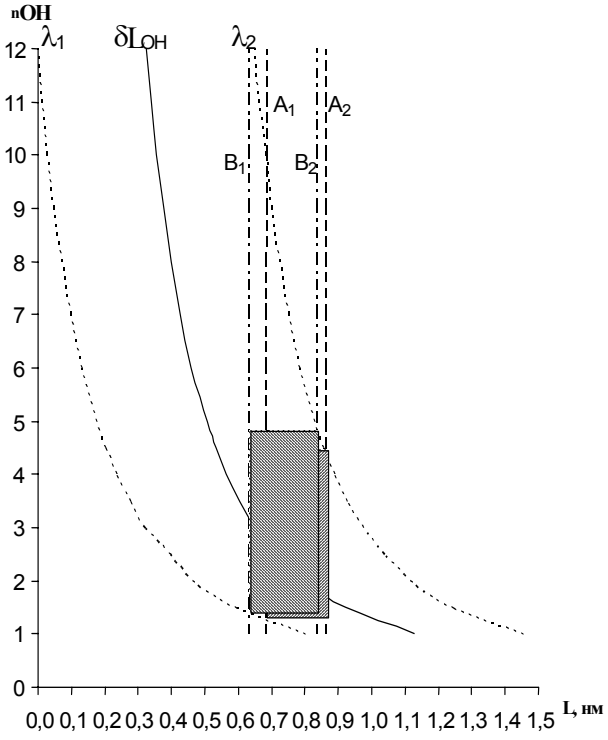

Calculation of the interhydroxyl distances and variations $\lambda_1 \div \lambda_2 = \delta L_{OH} \pm 0.326$ nm depending on the hydroxyl concentration

OH/nm^2	δL_{OH} nm	λ_1 nm	λ_2 nm
1	1.128	1.454	0.802
1.5	0.922	1.248	0.596
2	0.798	1.124	0.472
2.5	0.714	1.040	0.398
3	0.650	0.976	0.324
3.5	0.604	0.930	0.278
4	0.564	0.890	0.238
4.5	0.532	0.858	0.206
5	0.506	0.832	0.180
6	0.460	0.786	0.134
7	0.426	0.752	0.100
8	0.400	0.726	0.074
9	0.376	0.702	0.050
10	0.356	0.686	0.030
11	0.340	0.666	0.014
12	0.326	0.652	0

The formation zone for the aluminum oxychloride supported via two its atoms is symbolized by the indexes B_1 - B_2 at the diagram and lies within 0.634 – 0.839 nm. Comparison of the zone with the variations of the interhydroxyl distances $\lambda_1 \div \lambda_2$ allows for finding the optimal amount of the residual hydroxyl groups on the silicagel surface affording the reaction product formation. It follows from the diagram that the completely shaded part of the zone B_1–B_2 realizes the 100% compliance of the interhydroxyl distances at the concentration of

1.5 ÷ 4.5 hydroxyls per 1 nm^2 of the silicagel surface. As a consequence of this the aluminum oxychloride supported via two bonds is the single product of the adsorbed Al_2Cl_6 reaction.

Considering that the selective adsorption needs less amount of hydroxyls – 1.5÷4 OH-groups per 1 nm^2, it may be concluded that in the assumed selective reaction of the condensation the limiting step is the adsorption of aluminum chloride.

When less than 1.5 OH-groups per 1 nm^2 are left on the silicagel surface it makes aluminum chloride react with only one silanolic group to give the dimer supported via one its atom which is most likely to decompose similarly to aluminum chloride after the completion of the reaction.

When more than 4.5 OH-groups per 1 nm^2 are left on the silicagel surface more than two chlorine atoms of the Al_2Cl_6 molecule are involved in the reaction, and the reaction products are the oxychlorides, supported via three and four its atoms, having the dimer structure in which the Al_2Cl_2 bridge rhomb plane is upright relative to the surface (considering that coordination number of aluminum is 4 and the atoms surrounding it are in tetrahedral configuration). In this connection there are no conditions for the n-pentane 1,3,5-chemosorption required for realization of the dicyclopropane mechanism. It is suggested that these compounds as well as the $AlCl_3$ are not active catalysts of n-pentane isomerization.

The chloride supported via two its atoms has, on the contrary, the Al_2Cl_2 rhomb plane parallel with the silicagel surface making favorable conditions for the 1,3,5 – chemosorption of n-pentane.

So, to prepare an effective catalyst for the n-pentane isomerization by the technique of the condensation of anhydrous aluminum chloride on the silicagel surface the concentration of hydroxyls is bound to be between 1.5 ÷ 4 OH-groups per 1 nm^2.

Several samples of the catalyst were tested in the n-pentane isomerization (20 ^oC, τ=1h.) and sample 2 showed a high catalytic activity confirming the foregoing theoretical preconditions of the support treatment:

Sample	Temperature of evacuation ^oC	Residual amount of OH-groups according to [4]	General conversion of n-pentane, %	Yield of 2-methyl-butane, %
1	200	6 -12	1.0	0.6
2	350	3 - 5	14.7	8.5
3	500	1 - 2	2.1	1.2

References.

[1] Lipovich V.G., Khvan K.S., Polubentseva M.F., Pikerskii I.E., Kaletchits I.V., Dokladu USSR 1978. T.240. P. 1119-1120

[2] Peri J.B., Hensley A.L., J.Phys.Chem., 1968. Vol.72. № 8. P. 2926-2933.

[3] Kopylov V.B., Koltsov S.I., Volkova A.N., Aleskovskii V.B., Izvestia, Khimia i Khimicheskaya Tekhnologia, 1973. T.16. № 10. P.1475-1477.

[4] Boem H.P., Angew.Chem., 1966. Bd.78. №12. S.617-628

IONIC COORDINATION MECHANISM FOR TRANSFORMATIONS OF UNSATURATED HYDROCARBONS BY CATIONIC Ni(I) COMPLEXES

Saraev V.V., Kraikivskii P.B., Ratovskii G.V., Matveev D.A., Vilms A.I.

Irkutsk State University, Irkutsk, Russia
E-mail: saraev@chem.isu.ru

It is known that phosphine complexes of zero-valent nickel in combination with Lewis acids effectively catalyze the oligomerization of unsaturated hydrocarbons [1]. The formation of nickel catalysts is accompanied by quantitative oxidation of Ni(0) to Ni(I). The resulting coordinatively unsaturated cationic Ni(I) complexes are highly reactive in the oligomerization of unsaturated hydrocarbons [1].

In this study, the reactions of the individual cationic Ni(I) complex $[(PPh_3)_3Ni]BF_4$ with unsaturated hydrocarbons (ethene, propene, and styrene) were examined using EPR, UV, and NMR spectroscopy.

The starting cationic complex $[(PPh_3)_3Ni]BF_4$, which was discharged from a catalytic system $(PPh_3)_4Ni$ – $BF_3{\cdot}OEt_2$, in toluene (77 K) gives an EPR signal characteristic of tricoordinate structures [10]. After addition of styrene to $[(PPh_3)_3Ni]BF_4$ in nearly equimolar quantities (C_2H_3Ph : Ni = 1.5 : 1) the EPR signal from the starting Ni(I) complex disappears, the solution turns bright crimson, and no EPR signal is detected for a long period of time (~ 4 h). If triethyl phosphite is added to the system within this period (P : Ni = 2 : 1), an intense signal from the heteroligand tetracoordinate complex $[(PPh_3)_2Ni(P(OEt)_3)_2]BF_4$ immediately appears. Therefore, the reaction of styrene with the cationic Ni(I) complex initially gives an EPR-undetectable stable alkene Ni(I) complex, which can decompose upon replacement of alkene by phosphite.

To reveal the nature of the metal-styrene bond in the Ni(I) complex, the process of complexation was studied using UV spectroscopy. It was found that addition of styrene to the starting cationic Ni(I) complex (C_2H_3Ph : Ni = 1.5 : 1) gives rise to an intense band at 30 000 cm^{-1} and a weak band at 21 000 cm^{-1}, which are characteristic of a benzene ring conjugated with a carbocation. These data suggest the formation of a carbocationic σ-alkyl Ni(I) complex $(PPh_3)_2Ni\text{-}CH_2CH^+Ph$, in which the positive charge is transferred from the nickel ion to styrene. The carbocationic σ-alkyl Ni(I) complex is in a dimer state in solution.

The addition of excess styrene to $[(PPh_3)_3Ni]BF_4$ initiates, after a short induction period (two to four minutes), a vigorous reaction of styrene oligomerization. The induction period is probably due to slow replacement of the second triphenylphosphine ligand by styrene. The

carbocationic form of styrene in the σ-alkyl Ni(I) complex is supported by the NMR detection of styrene telomers with ethanol among the products obtained from styrene and ethanol on the individual cationic complex $[(PPh_3)_3Ni]BF_4$.

Ethene and propene are less active in complexation. For example, when exposed to gaseous ethene or propene, $[(PPh_3)_3Ni]BF_4$ in toluene remains unchanged as long as it is desired. However, if boron trifluoride etherate is added to $[(PPh_3)_3Ni]BF_4$ (B : Ni > 7) in an atmosphere of these gases, the EPR spectrum no longer shows signal from the starting complex (as with styrene) and there is an oligomerization of gaseous hydrocarbons. Therefore, in the case of ethene and propene, dimeric carbocationic σ-alkyl Ni(I) complexes are also formed, suggesting that the transition metal is coordinatively unsaturated in the presence of the Lewis acid $BF_3 \cdot OEt_2$. It should be noted that the catalyzed oligomerization of gaseous hydrocarbons for the ratio B : Ni > 7 stops upon adding triethyl phosphite (P : Ni = 2 : 1) to give the mononuclear heteroligand complex $[(PPh_3)_2Ni(P(OEt)_3)_2]BF_4$.

Based on the aggregate of the data presented in this paper, one can propose, with ethene as an example, the following ionic coordination mechanism of activation and transformations of olefinic hydrocarbons:

- ethene in the presence of $BF_3 \cdot OEt_2$ replaces one phosphine ligand in $[(PPh_3)_3Ni]BF_4$ to form a π-complex, which is rapidly transformed into a carbocationic σ-alkyl complex stabilized in solution by dimerization;
- the replacement of the second phosphine ligand by ethene gives an organonickel(I) compound containing both π- and σ-bonded carbon atoms;
- the insertion of π-coordinated ethene into the Ni-C σ-bond lengthens the carbon chain, thus eliminating the positive charge from the Ni atom;
- subsequent transformations of the metal-carbon bonds follow the classic mechanism of a β-hydride shift;
- after σ-π rearrangement and elimination of the dimer closing the catalytic cycle of ethene dimerization.

References:

[1]. Saraev V. V., Kraikivskii P. B., Zelinskii S. N., *et al., Russ. J. Coord. Chem. 27 (2001) 757.*

THEORETICAL MODELING OF HYDROGENE SHIFTS IN THE WACKER PROCESS

Shamsiev R.S., Belov A.P.

Lomonosov State Academy of Fine Chemical Technology, Moscow, Russia
E-mail: shamsiev@pisem.net

Selective oxidation of ethylene to acetaldehyde, catalyzed by palladium chloride in water is the industrially important reaction, generally known as the Wacker process. This process was intensively studied by experimental [1, 2] and quantum-chemical methods [3, 4]. But one of key step of this multistage reaction – 1,2 hydrogen shift was not studied in details.

The purpose of this work was the determination of a series of hydrogen transfers and the detection of all intermediates and transition states. The calculations based on the density functional theory in approximation PBE [5] have been performed using the program written by D.N. Laikov [6]. Large orbital basis sets of contracted Gaussian-type function were used in conjunction with the effective core potential SBK [7] and density-fitting basis sets of uncontracted Gaussian-type function. The technique of intrinsic reaction coordinate was used for studying in detail the elementary steps.

As a result of the calculations, the stationary points on the PES of system were found, values of activation and thermodynamics parameters were defined. It was established, that 1,2 hydrogen shift proceed through a formation of vinyl alcohol π–complex, which afterwards transfers in palladium-β-agostic hydrogen complex. It was shown by the modeling that hydrogen shift without palladium participation is characterized by considerably higher activation barriers than with Pd-assisted shift.

References:

[1] P.M. Henry, *Palladium-Catalyzed Oxidation of Hydrocarbons*, D. Reidel, Dordrecht, 1980
[2] Moiseev I.I. *π – Complexes in liquid phase oxidation of olefins*, Nauka, Moscow, 1970 (in Russian)
[3] P.E.M. Siegbahn, *J. Phys. Chem.*, 1996, 100, 14672
[4] D.D. Kragten, R.A. van Santen, *J. Phys. Chem. A*, 1999, 103, 80
[5] J.P. Perdew, K. Burke, and M. Ernzerhof, *Phys. Rev. Lett.*, 1996, 77, 3865.
[6] D.N. Laikov, *Chem. Phys. Lett.*, 1997, 281, 151.
[7] W.J. Stevens, M. Krauss, H. Basch and P.G. Jasien, *Can. J. Chem.*, 1992, 70, 612.

QUANTUM-CHEMICAL MODELLING OF THE CLUSTERS IN Co-CONTAINING CATALYSTS FOR THE SYNTHESIS ON CO_2 BASE

Shapovalova L.B., Shlygina U.A., Shyrtbaeva A.A., Zakumbaeva G.D., Gabdrakipov A.V.

Sokolsky Institute of Organic Catalysis & Electrochemistry, Almaty, Kazakstan
Fax: (007) 3272 915722; E- mail: orgcat@nursat.kz

The application of polycomponent metallic systems opens the wide opportunities for the chemical synthesis on the CO_2 base. As a rule selection of the components for polymetallic catalysts is carried out empirically. Using of the quantum-chemical methods allows the calculation of the cluster's stability, their structure and adsorption ability for the reaction components. These calculations can lighten the catalyst choice and allow to predict their behavior.

In this paper we tried to connect the theoretical quantum chemical calculations with the experimental studies of the state and structures of Ru-Co an Rh-Co-catalysts, their catalytic activity and selectivity in the CO_2+ C_3H_6 reaction.

Quantum-chemical calculations have been made on the basis of extended Huckel method complemented with Anderson core-core repulsions as an item of total electron energy. Cluster approximation was used for calculations. Minimal quantity of metal atoms (2-7-13) was taken into account. This approach seams to be reasonable, because, as it is known, chemisorption is highly localizated phenomenon.

The quantum chemical calculations showed that cobalt may interact with ruthenium or rhodium with the formation of stable cluster structures. The formation of bimetallic clusters is more energetically favorable than monometallic ones. The stability of 2,4,7, or 13 atomic Co-Ru and Co-Rh-clusters depends on the ratio Co:M (M= Ru, Rh), the locations of Co and M in the clusters and the nature of metals. It was shown that cobalt and ruthenium (both are crystallized in hexagonal type) are able to form bimetallic Ru-Co-clusters more stable than monometallic Ru- or Co-systems. Rhodium crystallizes in cubic type, but it is able to form bimetallic Rh-Co-cluster stronger then Ru-Co ones. The full binding energy and stability of Co-M- clusters are changed in the series:

$12Co\text{-}Rh_2 > 12Co\text{-}Rh_1 > 12Co\text{-}Ru_2 > 12Co\text{-}Ru_1 > 13Co > 3Co_{4.6.12}\text{-}10Ru > 3Co_{3.4.5}\text{-}10Ru \approx 1Co_{11}\text{-}12Ru \approx 3Co_{1.2.3.}\text{-}10Ru > 2Co_{2.3}\text{-}11Ru > 1Co_2\text{-}12Ru > 1Co_5\text{-}12Ru > 13Ru > 3Co_{1.2.5}\text{-}10Rh > 3Co_{1.4.7}\text{-}10Rh > 3\ Co_{1.7.8}\text{-}10Rh = 3Co_{1.4.5}\text{-}10Rh > 2Co_{1.7}\text{-}11Rh > 1Co_1\text{-}12Rh > 1Co_5\text{-}12Rh > 13Rh.$

Quantum-chemical calculation are conformed with experimental data. It was shown that the structure, surface state of metals of the active phase for Co-Ru-catalysts differs from that for Co-Rh catalysts. At the ratio Co/M= 0.19, rhodium is mainly in Rh^0 form with E_{bind} $Rh3p_{3/2}$ = 307.6 eV ($Rh^0 3p_{3/2}$=307.1 eV), while ruthenium is in the forms of Ru^0 and RuO_2 with $Ru3p_{3/2}$ =461.8 eV, ($Ru^0 3p_{3/2}$ =461.0 eV). Cobalt is in oxidized forms with E_{bind} $Co2p_{3/2}$= 780.6 eV (Co-Rh-system) and 777.8 eV (Co-Ru-system). Ruthenium forms the agglomeration of highly dispersed particles (≤ 5Å) of Ru^0. The middle size of these agglomerations depends on the Co:Ru ratio and is equal to 80-60 Å (Co/Ru=0.19) and 80-100 Å (Co/Ru=0.24). There are dense particles of Rh^0 on the surface of Co-Ru-catalysts. The size of these particles is reduced with cobalt concentration from 90-100 Å (Co/Rh=0.19) to 15-20 Å (Co/Rh=16.6). Also the clusters formation of Co-Rh and Co-Ru are revealed on the surface of Co-Rh and Co-Ru catalysts. The amount of Co-Ru-clusters increased with the increasing of Co concentration and reached maximum at ratio Co/Ru=1,60. Simultaneously α-Co and $CoRuO_4$ appeared. The $CoRuO_4$ may turn into Co-Ru-clusters under the reaction conditions. The amount of Co-Ru-clusters decreased at the content of Co > 70% in the metallic phase of catalyst. Maximum quantity Co-Rh cluster's structures is typical for bimetallic catalyst with Co/Rh ratio=4.0. Rhodium cluster's structures with higher cobalt content are more stable then Ru-Co ones.

The adsorption of carbon dioxide and propylene on mono- and bimetallic clusters of Ru, Rh and Co has been investigated using quantum-chemical and experimental methods. The quantum-chemical calculations showed, that depending on Co:M ratio in clusters and initial orientation of CO_2 molecule either associative or dissociative carbon dioxide adsorption can take place. It had been examined two positions of CO_2 molecule: vertical and horizontal. For example, the transfer of CO_2 molecule parallel to 7Ru or 7Co-monometallic clusters plane is accompanied with complete destruction of CO_2 molecule according to equation:

$$CO_{2ads} \rightarrow C_{ads} + 2O_{ads.}$$

At vertical approach of adsorbed molecule to monometallic 7Ru or 7Co plane clusters plane or bimetallic plane clusters containing one atom of second metal (6Co1Ru or 1Co6Ru) the associative adsorption occurs. It must be noted, that axis deflection of CO_2 molecules from vertical position (up to value of angle between normal to surface and axis of molecule CO_{2ads} close to 90^0) is accompanied with the increase of total energy of the systems to ~1 eV. The complete optimization of the CO_2 geometry from initial position at < 45^0 to surface brings to vertical reorientation of molecule. As follows from these results the approaching of CO_2

adsorbed molecule to plane part of the surface must cause its vertical (linear) orientation. The associative CO_2 adsorption was realized without energy barrier on mono- and bimetallic clusters of cobalt and ruthenium. Moreover in this case the adsorption processes via oxygen atom. However, if content of second metal was >30% and there was no local symmetry in the sample the dissociative adsorption was observed according to the scheme:

$$CO_{2ads} \rightarrow CO_{ads} + O_{ads.}$$

The presence of defects on the surface and small sizes of Co-Ru clusters lead to dissociative adsorption. IR-data of CO_2 adsorption on Co-Ru-catalysts are conformed with quantum-chemical calculations. Adsorption bands of CO_2^{gas} (2350 sm^{-1}), CO_{2ads} (1580 and 1440 sm^{-1}). CO_{ads} (1950 sm^{-1}, 2020 sm^{-1}) is present in IR-spectra of adsorbed CO_2.

Quantum- chemical calculations showed that Co and Ru in the clusters have different affinity to CO_2, CO and O_2-molecules. Ru is characterized by lower affinity to CO_{ads} than Co, but higher affinity to oxygen. So it may be suggested that during the CO_2 dissociation on the Co-Ru-clusters the preferable formation of new bond Co-CO_{ads} and Ru-O_{ads} metal has positive charge and could activate the olefin molecule (the typical donor of the electron).

To clarify the mechanism of propylene adsorption on Ru-Co-catalysts the quantum-chemical calculation of interaction between these catalysts and mono- and bimetallic Ru- and Co-containing clusters were carried out. It was assumed that atoms of C=C- bond are situated parallel to metal-metal bond. The distance at which the cluster and absorbable molecule begin to interact is characterized by the nature of active center. Full optimization of C_3H_6 molecule geometry confirms that propylene adsorbs associatively on Co-Co clusters and form π- type complex. The presence of Ru atom provides significant electron density transfer from olefin molecule orbitals to d-orbital of ruthenium in bimetallic Ru-Co- or monometallic Ru-Ru-clusters (independently on either the tertiary carbon atom is located on ruthenium or cobalt atom). At the same time the olefin C=C- bond is weaken substantially down to their break. The degree of rhodium reduction in Co-Rh- catalyst is higher, than ruthenium in Ru-Co-systems. The difference of Ru and Rh states determines the CO_2 and C_3H_6 adsorption characteristics and the trends of CO_2+ C_3H_6 interaction.

The mixture of C_1-C_6- hydrocarbons and oxygen containing products are formed by the interaction CO_2+ C_3H_6 on Co-M-catalysts (M=Ru or Rh). The product composition and the propylene conversion depend from the catalysts nature. At T=523 K and P =1,5 MPa the propylene conversion is 49.3%, when the Co/Ru = 0.24 catalyst is used. The products consist of methanol (2.3 %), iso-propanol (1.9 %), propanol(9.0 %), butanol (8.1 %),

iso-butanol (2.0 %), acetic acid (4.6 %), pronionic acid (5.2 %), butyric acid (11.2 %), formic acid (3.7 %), butiraldehyde(3.5 %), C_{5+}-oxigenates(15,0 %) and C_1-C_6- hydrocarbons (34.0 %). In these condition on Rh-Co (Co/Rh=0.24)- catalyst the propylene conversion is 8.3 %; the products consist of methanol (22.7 %), aceton (5.0 %), iso-propanol (31.9 %), butanol (1.8 %), butyric acid (20.3 %), C_{5+}-oxigenates (6.8 %), the traces of C_1-C_6-hydrocarbons. The formation of C_1-C_6- hydrocarbons shows that the main reaction is accompanied with the side process of propylene destruction and dimerization with participation of CH_x-species and hydrogen, which are formed upon the propylene decomposition. Besides these products the traces of O_2 and CO (~ 1.0 %) are present in product formed by the interaction CO_2+C_3H_6 on Co-M-catalysts. Carbon dioxide and oxygen are formed due to the dissociation $CO_2 \rightarrow CO_{ads}+O_{ads}$.

Analysis of experimental data and quantum-chemical calculation show that the direction of interaction of propylene and CO_2 or fragments of its dissociation is determined by the mechanism of CO_2 and propylene adsorption on the clusters of different nature and composition.

HYDROGENOLYSIS OF ORGANOHALOGEN COMPOUNDS OVER BIMETALLIC CATALYSTS

Simagina V.I., Stoyanova I.V., Gentsler A.G., Tayban E.S.

Boreskov Institute of Catalysis SB RAS, Novosibirsk, Russia
E-mail: simagina@catalysis.nsk.su

Halogenated organic compounds have been used on a large scale in the chemical, petrochemical and electronic industries. The disposal of organic wastes containing halogen has become a major environmental problem, because most of them are toxic and thermally stable, and are accumulated in surroundings for the long periods of time. Catalytic hydrodehalogenation, also called hydrogenolysis, with heterogeneous catalysts is recognized as a facile and efficient procedure. However, the practical application of catalysts to the dehalogenation of organic halides is always accompanied by the problem of the deactivation of the catalysts. The addition of a second metal in the catalysts may affect their catalytic properties, stability and activity.

Thus, the goal of this study is the preparation and investigation of nanodispersed bimetallic supported catalysts, which has high activity, stability and selectivity in the reaction of hydrogenolysis of halogenated organic compounds in gas and liquid phases.

The reaction products were analyzed by gas chromatography and IR-Fourier spectroscopy. Catalysts were studied by transmission electron microscopy and X-ray analysis.

Nanodispersed bimetallic supported palladium-based catalysts, which contain Pd with Pt, Fe, Ni or Co were prepared by precipitation of metal salts from their solution with subsequent low-temperature reduction by $NaBH_4$. We used a carbonaceous material, called "Sibunit", as the support. Activity and stability of the catalysts was investigated in the reactions of the gas phase hydrodechlorination of carbon tetrachloride at 250 ^{0}C and in the reactions of the liquid phase hydrodechlorination of chlorobenzene and hexachlorobenzene at 55 ^{0}C, hydrogen pressure 1 atm .

It was shown, that chloroform, methane and his homologues $C_2 - C_5$, ethylene and propylene were obtained in the reaction of hydrogenolysis of CCl_4. Reactions proceeded to full conversion of chlorobenzene and hexaclorobenzene to benzene in the presence of the bimetallic catalysts. The row of activity and stability of the catalysts in this liquid phase is: 1% $Pd_{90}Pt_{10}$/C > 1% Pd/C >1% $Pd_{50}Pt_{50}$/C > 1% $Pd_{20}Co_{80}$/C. Catalysts modification (base addition, phase-transfer addition, second metal addition) as well as its transformation during the hydrogenolysis (deactivation) are discussed.

INTERACTION OF ACETONE OXIME WITH H-ZSM-5 AND Cu-ZSM-5 ACCORDING TO FTIR DATA

Simakov A.V.[1,2], Stoyanov E.S.[1], Rebrov E.V.[3], Sazonova N.N.[1]

[1]Boreskov Institute of Catalysis SB RAS, Novosibirsk, Russia
E-mail: asimakov@catalysis.nsk.su
[2]CCMC-UNAM, Apdo Postal 2681, Ensenada 22800, B.C., Mexico
E-mail: andrey@ccmc.unam.mx
[3]TUE, Eindhoven, The Netherlands,
E-mail: rebrov@tue.nl

Introduction

The various studies involving catalytic activity measurements often coupled with different spectroscopic techniques and temperature programmed desorption (TPD) technique have yielded important information about the conversion, kinetics and surface species of the NO_x SCR-HC reaction over Cu-ZSM-5 catalysts. Nevertheless many aspects, such as the surface species or fragments formed in the process of SCR-HC of NO, need to be further explored.

Many efforts were devoted to the study of acetone oxime formation/decomposition and its reaction with NO. So, the formation of acetone oxime at propane interaction with NO and oxygen was shown by FTIR [[1]], interaction of which with NO was studied by NMR on ^{13}C and ^{15}N nuclei [[2]]. The study of kinetics of the individual reaction steps (2-nitrosopropane isomerization into acetone oxime and reaction of adsorbed acetone oxime with NO) with FTIR *in situ*, TPD and transient kinetic technique has shown that NO reaction with acetone oxime is the rate determining step in the whole chain of transformations leading to formation of molecular nitrogen at temperatures below 300 ^oC over Cu-ZSM-5 catalyst [[3]].

In this work main attention was paid to the peculiarities of acetone oxime coordination over surface of H-ZSM-5 zeolite and that doped with Cu^{2+} and Cu^{+}-cations.

Experimental

Catalyst preparation and pretreatment

Cu-ZSM-5 was prepared by traditional ion-exchange at 20^oC described in [1]. Elemental analysis gave the following data: Cu/Al = 0.28 and Si/Al=19.5. BET surface area was 412 m^2g^{-1}. Prior to adsorption/desorption experiments the catalyst was treated in a flow of oxygen for 1 h, followed by a helium one for 1 h at 500^oC repeatedly (about 10 cycles).

1. Rebrov E.V., Simakov A.V., Sazonova N.N., Stoyanov E.S. Catal. Lett. 58 (1999) 107-118.
2. J. Wu, S.C. Larsen, J.Catal. 182 (1999) 244.; J.Wu, S.C.Larsen, Catal.Lett. 70 (2000) 43-50.
3. Rebrov E.V., Simakov A.V., Sazonova N.N., Stoyanov E.S. Catal.Lett. 64 (2000) 129-134.

FTIR measurements

Two types of the zeolite samples after pretreatment before IR spectra recording were used: (1) treatment in He flow at 500 ^{o}C for 1 h followed by the cooling in He to the adsorption temperature; (2) treatment in oxygen at 500 ^{o}C for 1 h followed by the cooling in the atmosphere of O_2, and then, the sample was purged with He flow at the adsorption temperature for 5 min to remove oxygen from the gas phase. The samples are termed as "reduced sample" and "oxidized sample", respectively.

The IR spectra of AO dissolved in CCl_4 (from highly diluted 0.005M to saturated solutions), in solid state and adsorbed on zeolites were recorded using a BOMEM MB-102 FT-IR spectrometer (Hartmann&Braun). Spectra were taken in transmittance with 10 scans accumulated at a spectral resolution of 4 cm^{-1}. The data were processed with a computer program. The spectra from the adsorbed species were obtained by subtracting the spectrum of the wafer from the spectrum determined after adsorption. Background corrected spectra are only discussed in the paper.

Results and discussion

The intensity of band $\delta(H_2O)$=1630 cm^{-1} of water molecules adsorbed on the zeolite surface decreases during adsorption of acetone oxime (AO) at 120 ^{o}C both over H-ZSM-5 and Cu-ZSM-5 due to replacement of water molecules by AO adsorbed.

The spectrum of acetone oxime adsorbed on H-ZSM-5 zeolite includes (i) non symmetrical band at 1710 cm^{-1} which could be referred to AO strongly bounded with zeolite surface through H-bond, keeping nitrogen atom of AO free; (ii) band ν(C=N), frequency of which (1648 cm^{-1}) is lower then that for AO in CCl_4 solutions (1664 cm^{-1}). This band is characteristic for AO which is bounded with zeolite surface centers through H-bond of OH group and nitrogen atom. Adsorbed AO molecules do not interact with each other, since the spectrum doesn't developed the bands of self-associated AO similar to those observed for CCl_4 solutions of AO.

When AO is absorbed by reduced Cu-ZSM-5 catalyst, IR spectra developed in the ν(C=N) frequency region two bands at 1700-1706 and 1664 cm^{-1} (the spectra are similar to that shown in Fig. 1, curve 5). The first one is very strong and belongs to AO molecules bounded via OH groups both with Cu^{+} and O-atoms of the zeolite surface, as it is shown in the Scheme I. The second one can be attributed to AO molecules bounded with Cu^{+} via nitrogen atoms (Scheme II), since only in this case the ν(C=N) frequency can decrease significantly. The stretching OH vibrations of the both types of coordination are located at ca.

2850 cm^{-1} and belong to the OH groups forming strong hydrogen bonds with the surface oxygen atoms.

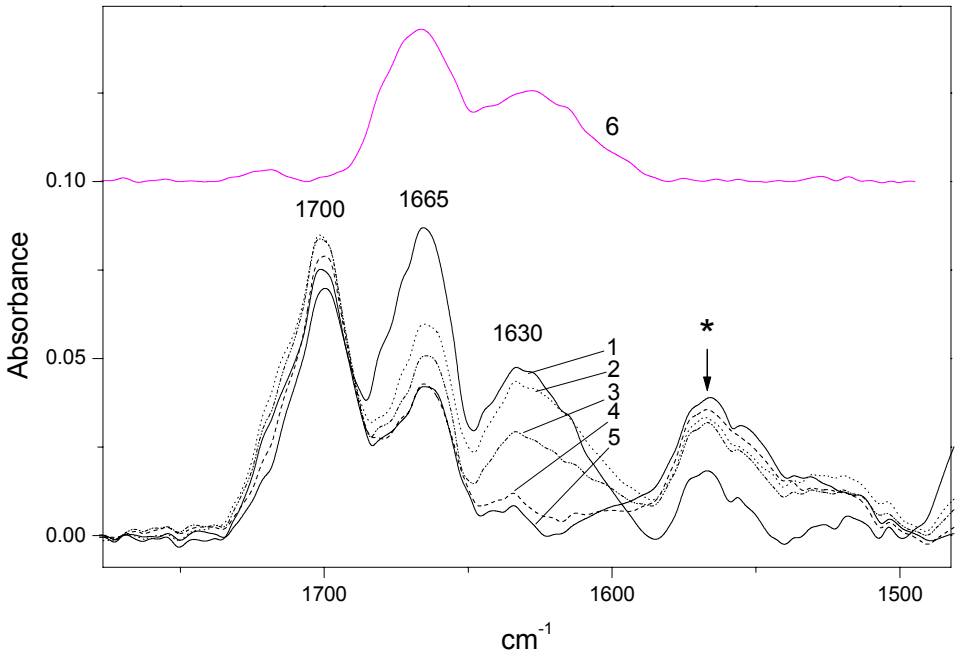

Figure 1. FTIR spectra of AO adsorbed after 1 (1), 2 (2), 3 (3), 9 (4) and 14 min (5) at 120 °C on oxidized Cu-ZSM-5. Spectrum 6 was obtained by subtraction of spectrum 1 with spectrum 5.

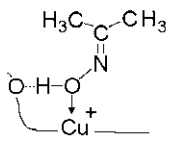

Scheme I.

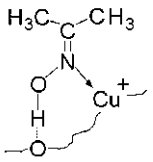

Scheme II.

In the IR spectra of absorbed AO molecules on oxidized Cu-ZSM-5, when copper ions are mainly in bivalent state (2+), three ν(C=N) bands developed with the time dependence intensities: at 1700 and 1665 cm^{-1} related to AO surface complexes I and II, respectively, and new one at ca. 1630 cm^{-1}. Intensities of complex II and the band at 1630 cm^{-1} of the new complex III decreases rapidly during first few minutes of AO adsorption. After 10 min the ν(C=N) band of III fully disappeared and that for complex II reaching some low value in intensity becomes then timely independent. As a result, the spectrum transforms to that known for AO adsorbed on reduced Cu-ZSM-5 with surface complexes I and II.

One could expect that the reason of quickly degradation of surface complex III is based on the fact that complex III is formed by AO molecules bounded with Cu^{2+} ions. Indeed, AO mixed with CuO oxide decomposed completely for a few minutes due to AO - Cu^{2+} interaction. The spectrum of complex III was isolated by subtracting of spectrum recorded after first minute with that after 10 minutes. Resulting spectrum (Fig. 1, curve 6) includes in addition to the ν(C=N) band of the complex III, the new one at 1665 cm^{-1} also referred to AO bounded with Cu^{2+} ions (complex IV). The band at 1665 cm^{-1} could be assigned to AO bounded with Cu^{2+} through oxygen atom similar for Cu^{+} in Scheme I. The lower frequency band at 1630 cm^{-1} of complex III seems to correspond to AO bounded with Cu^{2+} ions via nitrogen atom as on Scheme II for Cu^{+} ions. Note, that difference between two couples of ν(C=N) frequencies corresponding to coordination types I-II / III-IV is about 37 cm^{-1} both for Cu^{+} and for Cu^{2+}. The coincidence of these two values is circumstantial evidence that our assignment was performed correctly.

Thus, there are four AO adspecies on zeolite with two different types of AO coordination to Cu^{+} or to Cu^{2+} ions: one with participation of O atom and another one with N atom. Note, that complexes of AO with Cu^{+} ions are much more stable then those with Cu^{2+} ions.

STUDYING OF VERBENOL INTO ISOPIPERITENOL ISOMERIZATION FOR DEVELOPMENT OF THE METHOD OF *p*-MENTHOL SYNTHESIS

Simakova I.L., Maksimchuk N.V., Semikolenov V.A.

Boreskov Institute of Catalysis SB RAS, Novosibirsk, Russia
Tel.: (3832) 341222 Fax: (3832) 343056, E-mail: simakova@catalysis.nsk.su

Introduction

Selective conversion of α-pinene derivatives represents an interesting route to utilize these cheap natural products and synthesize the valuable materials for medicines, fragrances, cosmetic stuffs and vitamins (A, E, K_1). Verbenol, the secondary unsaturated bicyclic monoterpene alcohol, prepared by α-pinene oxidation [1] is the attractive precursor for synthesis of the valuable organic compounds. Thus, hydrogenation of verbenol over Pd/C catalysts to form controlled verbanol isomers distribution is the first explored step of perspective route of verbenol conversion into fragrances 3,4,6-trimethylhept-5-enal (lemon aroma) and *o*-menthol (sweet mild cloves odor) [2].

In continuation of this approach another promising way of verbenol utilization is to produce isopiperitenol that can be converted into *p*-menthol (strong mint aroma) by simple saturation of C=C double bonds. The scheme of isopiperitenol synthesis is based on the termal isomerization of verbenol; valuable citral isomers (strong lemon grass aroma) being occurred occasionally [3, 4]. According to [4] verbenol is converted consecutively into isopiperitenol and then into citral and desirable product can be produced by realization of the process in optimal reaction conditions. Unfortunately, kinetic study of verbenol thermal isomerization process hasn't been considered in literature. Earlier studying of the pinan-2-ol isomerization process has shown that reagent pressure, temperature and contact time determine the yield and selectivity of the aimed linalool [5].

The aim of this work is to study the kinetics and factors determining the selectivity of isopiperitenol and citral formation in the thermal isomerization of verbenol under vacuum for a very short contact time.

Experimental

Experiments on verbenol isomerization (*cis*-/*trans*-verbenol isomer mixture in *n*-octan (10 % mol.)) were carried out in flow reactor (stainless steel capillary with carbon deposited on the inside surface: length = 80.0 cm, diameter = 2 mm) at feed rate 0.5 ml/min under products outlet pressure 5 Torr and in temperature range from 480 to 620°C for contact time $10^{-4} \div 10^{-3}$ min.

Reaction mixture was condensed in a trap cooled by liquid nitrogen and identified by VG-7070 GC/MS using a 25 m x 0.2 quartz capillary column (Silicone SE-30). Product contents in reaction mixture were determined chromatographically using capillary column, Silicone SE-30.

Results and discussion

According to GLC analysis three aimed products of verbenol thermal isomerization: isopiperitenol and two isomers of citral as well as unreacted verbenol and side products unsaturated hydrocarbons (molecular formula $C_{10}H_{14}$ and $C_{10}H_{16}$) were found in reaction mixture.

Effect of contact time on isopiperitenol and two citral isomers content was studied at temperature 480÷580°C. The portion of reaction mixture was passed with a constant feed rate through the reactor heated to a fixed temperature. Reaction mixture was analysed by GLC method and then passed again through reactor under the same conditions and this procedure was repeated many times. With contact time growth verbenol content was decreased, whereas isopiperitenol and citral isomers content increase and come to plateau at verbenol conversion more than 60% (Fig. 1a). The time for plateau achievement decreases from $\tau = 3 \cdot 10^{-4}$ to $\tau = 1{,}5 \cdot 10^{-4}$ min with reaction temperature growth from 480 °C to 580 °C.

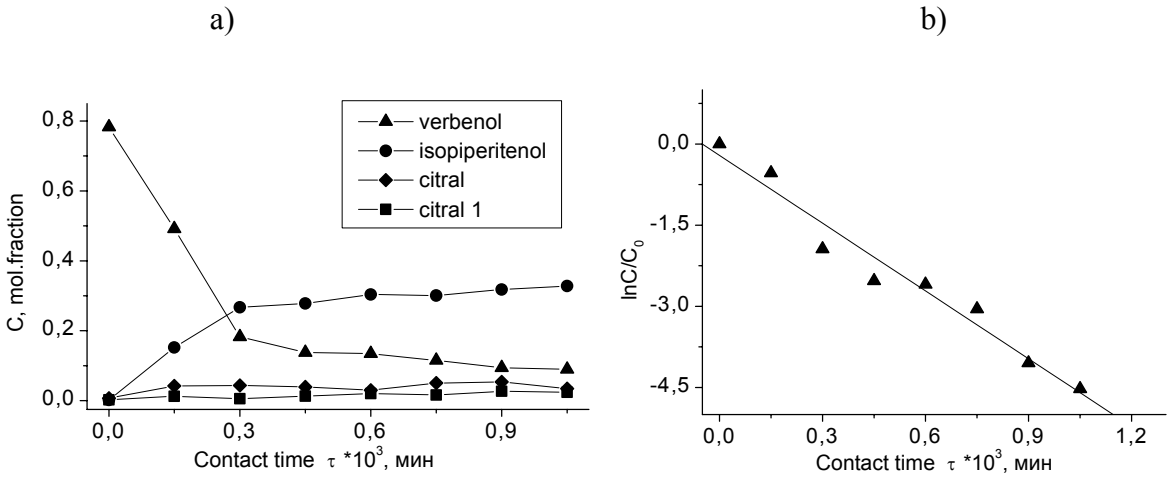

Fig. 1. Effect of contact time on contents of verbenol isomerization products (a), in semi-logarithmic coordinates (b), T = 480 °C.

Relative verbenol concentration dependence versus contact time in semi-logarithmic coordinates is linear (Fig. 1b). It indicates that reaction rate of verbenol thermal isomerization is of the first order on verbenol concentration.

Dependence of selectivity versus contact time indicates that isopiperitenol and citral isomers are formed in parallel routes. The ratio between reaction constants observed is about $k_1:k_2:k_3 \sim 16:4:1$ (Fig. 2a).

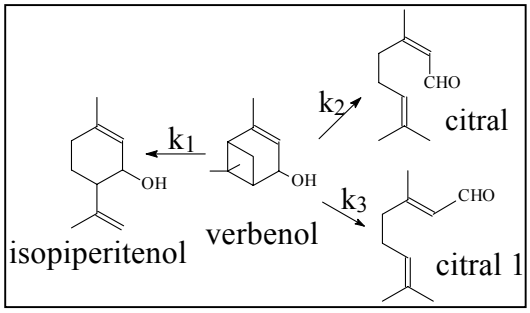

The effect of temperature on selecivity of isopiperitenol and citral isomers formation have been studied at temperature from 480 to 620 ^oC (Fig 2b).

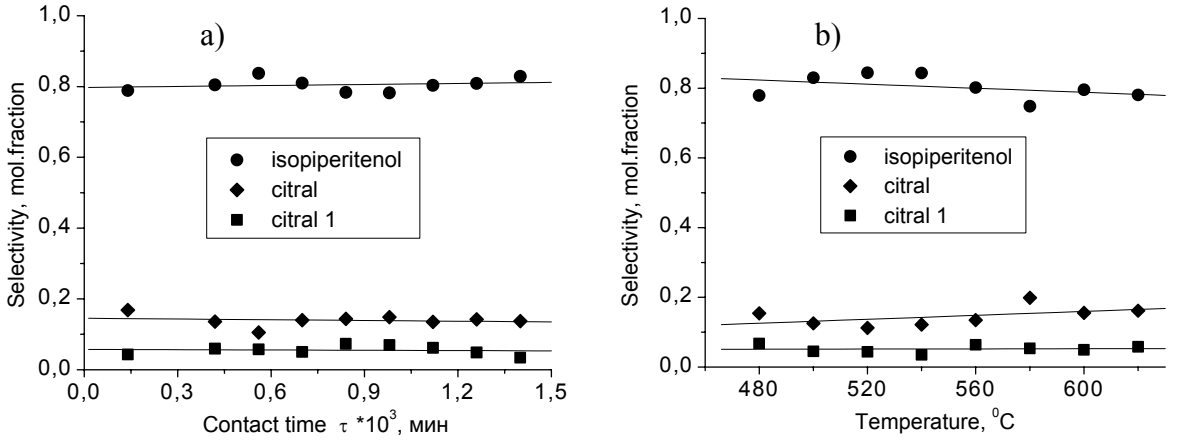

Fig. 2. Effect of (a) contact time (T = 520 ^oC) and (b) temperature (contact time = $1.5 \cdot 10^{-4}$ min) on selectivity of product formation.

It was found that product distribution doesn't depend on temperature. The activation energy 97.8 kJ/mol of verbenol isomerization was determined from Arrhenius plot. Weak temperature dependence of k_1, k_2, k_3 indicates that corresponding reaction activation energies have close values. Obviously the aimed products formation proceeds via common step of 4-membered ring opening followed by biradical conversion into stable molecules by different rearrangement of the radical bonds. Note, that the activation energy of verbenol isomerization is less than that for pinan-2-ol isomers to linalool isomerization (E_{act} = 190÷215 kJ/mol) [5]. Obviously π -electrons of C=C double bond of unsaturated molecule of verbenol take part in the electron distribution of biradical to stabilize its formation. Besides, availability of C=C double bond brings an additional stress in verbenol framework that favors 4-membered ring cleavage.

Conclusion

1. The method of verbenol thermal isomerization as selective synthesis of isopiperitenol has been proposed.

2. The kinetics of verbenol pyrolysis at vacuum, different contact time and temperature range from 480 to 620 ^{o}C have been studied. Three parallel routes of isopiperitenol and citral isomers formation were revealed. The ratio of isopiperitenol/citral is close to 4 and doesn't change within the temperature range 480÷620 ^{o}C.
3. The maximum isopiperitenol selectivity 49,1 % can be achieved at verbenol conversion 83,5 % at temperature 520 ^{o}C and contact time $\tau \sim 2{,}8 \cdot 10^{-4}$ min.
4. The results obtained permit to develop the promising way for *p*-menthol synthesis by verbenol conversion into isopiperitenol.

Acknowledgements

Authors are grateful to Ytkin V.A. for GC/MS data registration.

The research described in this publication was made possible in part by Award No. REC-008 of the U.S. CRDF.

References

[1] Harry Schmidt, *Bericht der Schimmel & Co. Aktiengesellschaft,* (1940) 38
[2] I.L. Simakova, V.A. Semikolenov, *Chemistry for Sustainable Development*, 11 (2003)
[3] Pat. USA № 2815383, 1957
[4] Pat. GB № 755667, 1956
[5] V.A. Semikolenov, I.I. Ilyna, I.L. Simakova, *J. Mol. Cat., A: Chem*, 182-183 (2002) 383

SYNTHESIS OF NANOMATERIALS VIA LASER VAPOR DEPOSITION (LVD) AND THEIR STUDY VIA LASER-INDUCED LUMINESCENCE (LIF)

Snytnikov V.N. , Stoyanovsky V.O. , Snytnikov Vlad. N. , Parmon V.N.

Boreskov Institute of Catalysis SB RAS, Novosibirsk, Russia
E-mail: Stoyn@Catalysis.nsk.su

Catalytic and optical properties of pure and activated nanoparticles are presently of special interest.

A laser vapor deposition (LVD) unit has been developed at the Institute of Catalysis to synthesize nanodispersed catalyst samples. The unit applies 10.6 μm radiation of continuous-wave CO_2 laser of 120 watts power. The controllable atmosphere with pressure $P=10^{-7}$ –3 atm and a special system of gas leek-in and particles collection allowed us to obtain the oxide samples of controlled average particle size from 2 to 100 nm. Al, Zr, Ti, V and Si oxide samples of average particle size 2–4 nm have been prepared. For the first time nanodispersed catalyst samples of complex composition supported over SiO_2-MgO-FeO-Al_2O_3 from the samples of natural origin with characteristic size 5 nm have been produced. The samples were studied using the X-ray phase analysis and electron microscopy. We also employed the method of laser-induced luminescence with ultraviolet radiation of ArF-laser to study the obtained nanoparticle samples.

Luminescence spectra of the initial bulky and nanodispersed samples were recorded in a wide range from 200 to 800 nm. A distinctive feature of the spectra is the presence of broad luminescence bands at 260 and 530 nm, along with the presence of typical lines of individual elements. These bands are typical of SiO_2, FeO and Al_2O_3 nanoparticles. Potentialities of the laser-induced luminescence method using ultraviolet radiation of ArF-laser in some cases allows concurrent recording the catalyst luminescence spectra and spectral elemental analysis of a substance ablated layer by layer from the catalyst surface by laser radiation.

LASER-INDUCED LUMINESCENCE OF OXIDE CATALYSTS

Snytnikov V.N., Stoyanovsky V.O., Parmon V.N.

Boreskov Institute of Catalysis SB RAS, Novosibirsk, Russia
E-mail: snyt@catalysis.nsk.su

Luminescence of inorganic crystal substances may be caused by metal ions — activators located in the phosphor crystal lattice, by the defects of crystal lattice, in particular, F-centers, or by excitation of the lattice oxygen of oxocomplexes supported over the surface. It seems important that both metals and surface oxocomplexes and F-centers can act as active sites of catalytic reactions.

The aim of the work was to reveal potentialities of the method of laser-induced luminescence excited by radiation of ArF-laser (wavelength 193 nm and pulse energy up to 200 mJ) for studying the surface layers of bulky and finely dispersed catalysts, nanoparticles, and molecules adsorbed on their surfaces.

Using of high-power pulse radiation in narrow line 193 nm for luminescence excitation has the following features:

1. Most materials effectively adsorb the radiation contiguous to the vacuum UV-light, and the emission spectra provide a great body of information in a broad spectral range from high-frequency UV to IR.

2. High adsorption of radiation allows obtaining the luminescence spectrum of a thin surface layer, e.g., with Al_2O_3, the layer depth is 100 nm at I = 1 J/cm^2.

It was shown experimentally that:

1. Layer-by-layer ablation of the surface layers by laser radiation allows recording the luminescence spectra from various depths of the sample under study. With aluminum oxide, the representative depth of the layer evaporated by ArF-laser per impulse is $\delta \approx 5$ nm.

2. Luminescence spectra can be taken in a wide temperature range 77–800 K without heating the sample, under the real gas pressures.

3. High energy of the initial light quantum 6.45 eV and two-photon adsorption processes at high power densities cause a high excitation efficiency of sublimated substance and don't prevent the luminescence of the sample itself. In the case of plasma formation, no shielding of laser radiation from the sample surface occurs.

4. The luminescence spectra of aluminum oxide powders of various phase composition studied at room temperature and radiation power density Q ≈ 100 MW/cm^2 have the lines of atomic Al an Na. α-Al_2O_3 samples have 629.9 and 694.1 nm lines of ruby luminescence. The

θ-Al_2O_3 spectra, in addition to the "α" lines, have two strong lines at 683.6 and 687.0 nm.

5. The spectra of laser-induced luminescence of the catalyst samples based on glass cloth with Pt content up to 0.01–0.05% are characterized by a broad luminescence band of a support, typical lines of Al_2O_3-SiO_2 structures and line spectrum of atoms. Among metals, only the lines of platinum, iron, sodium, aluminum and calcium are identified. The measurement of Pt and Fe lines intensity vs. the number of radiation impulse allows estimation of the impurities and Pt concentrations distribution in the near-the-surface catalyst layer with $\delta \approx 100$ nm.

Thus, using the radiation of high-power ArF-laser with wavelength 193 nm allows simultaneous studying the structure of the catalyst surface layers and spectral elemental analysis of a substance ablated layer by layer from the catalyst surface by laser radiation.

OXIDATIVE DEHYDROGENATION OF ETHANE ON PROMOTED VPO CATALYSTS

Solsona B.[1], Zazhigalov V.A.[2], López Nieto J.M. [1], Bacherikova I.V.[2], Diyuk E.A.[2]

[1]Instituto de Tecnología Química, UPV-CSIC, Valencia, Spain
[2]Institute for Sorption and Problems of Endoecology,
National Academy of Sciences of Ukraine, Kiev, Ukraine
E-mail: zazhigal@ispe.kiev.ua

VPO catalysts doped with different amounts of Bi, Bi-La and Zr were synthesized in conditions that had allowed achieve samples with most intense reflexes of plane perpendicular to vanadyl one. The samples were characterized by means of XRD, UV-VIS, XPS, TPD NH_3, transformation of 2-methyl-3-butyn-2-ol methods and tested in the oxidation of ethane.

Most of these catalysts possess high selectivity in the oxidative dehydrogenation of ethane to ethene. The addition of Bi or Zr to VPO leads to a sufficient increase in both catalytic activity and selectivity to ethene, especially in the case of Zr-containing catalysts. However, the addition of La results in a decrease of both catalytic activity and selectivity to ethene. $(VO)_2P_2O_7$ is the main crystalline phase observed in the structure of the most selective catalysts, in the meanwhile the appearance of β-$VOPO_4$ is related to a drop in the selectivity to ethene. The addition of Bi or Zr to VPO catalysts results in an increase of the specific surface area and a decrease of the O 1s-electron binding energy, which probably lead to the improvement of the catalytic performance. The modification of acid-base characteristics of the surface, in particular, the decrease of Lewis centers strength, increases the selectivity to ethylene.

THE MECHANISM OF OXYGEN ADSORPTION AND FORMATION OF THE OXIDE RECONSTRUCTIVE LAYERS ON Pd(110) SURFACE

Titkov A.I., Salanov A.N.

Boreskov Institute of Catalysis SB RAS, Novosibirsk, Russia
E-mail: Titkov@catalysis.nsk.su

Palladium is one of the main active components of the catalysts for neutralization of automotive exhaust gases to abate ecological damage, which is now the most severe problem worldwide [1]. Palladium is used in catalysis because it is very active in the reaction of CO oxidation and NO reduction. That is why thorough studies both of interactions of CO, NO and O_2 with palladium and of regularities of CO oxidation and NO reduction are of vital interest. Adsorption of O_2, CO and NO on the Pd(110) single crystal induce the surface reconstruction and the formation of reconstructive structures [2, 3].

Reconstructive structures are known to be formed at low oxygen pressure ($<10^{-7}$ Torr) during oxygen chemisorption on the Pd(110) surface. These structures consist of chains in certain direction with distance between neighboring chains of two rows at oxygen coverage θ = 0,3 and of the one row at θ = 0,5 [4, 5]. At high oxygen pressure more significant reconstruction occurs including both surface and subsurface layers of Pd(110). As it is follows from the analysis of the literature data [2-8], experimental and theoretical studies of the reconstruction mechanism of palladium surface mainly have aimed to determine the structures formed during gas chemisorption. Unfortunately, the mechanism of the surface reconstruction of Pd(110) induced by oxygen chemisorption is not clear till now. At high oxygen pressures $O_2 \geq$ (0,1-10 Pa) and temperatures T $\geq$ 300 K, i.e. close to real catalytic conditions for neutralization of automotive exhaust gases, the interaction of oxygen with Pd(110) practically has not been investigated.

The present work aimed to study the mechanism of Pd(110) surface reconstruction during interaction with oxygen over wide ranges of pressures (10^{-8} - 10^{-2} Torr) and temperatures (400 - 1200 K). The mass spectrometry technique to take TPD spectra was installed on vacuum chamber LEED-240 (Varian). The numeric simulation of the adsorption process was also used in this work.

Adsorption and desorption data have been obtained at 400 -700 K и $Po_2=10^{-7}$ – 10 Pa, in the interval of oxygen exposure 0 - 7 $*10^6$ L. From the analysis of these data it was established that at low exposure 0 – 3 L ($(2*10^{-6} – 1*10^{-5}$ Pa) oxygen adsorbs on the surface of Pd(110) with constant rate (S_0 = 0.4-0.8), so the saturated adsorption layer is formed with

θo ~ 0.5. As Bennett et al. reported [4] at this coverage a reconstructive chains structures are formed. According to our data these structures are formed with a constant rate. It can point to formation of these structures through oxygen precursor state. On heating the sample, these structures are decomposed and oxygen desorbs by β_2 peak with T_p=885 K, as it is shown on fig. 1. Then, with increasing of O_2 exposure (> 3L) and the surface oxygen coverage the rate of oxygen adsorption noticeably decreases. It can point to gradual diffusion of oxygen atoms to the subsurface palladium layer or the formation of the surface oxide.

On heating the sample after oxygen exposure 3 – 600 L a low temperature peak β_1 appears in thermal desorption spectra (TDS) (fig.1). The dynamics of the desorption process appears to be consistent with the first order kinetics. The β_1 peak can be associated with a decomposition of the surface oxide islands. Further features of TDS spectra of oxygen from Pd(110) after high exposures are associated with oxygen penetrated both to the subsurface and bulk layers of the metal. It has been determined with increasing of the exposure temperature the amount of absorbed oxygen noticeably increases. As it follows from fig. 2, at T< 550 K and oxygen pressures 0,1 –10 Pa the maximum total coverage is ~ 7 ML, while at T≥ 550 K the picture changes. At Po_2 > 0,1 Pa oxygen penetrates to the bulk of palladium more actively. At T = 700 K and Po_2 = 1 Pa the amount of O_2 absorbed by palladium is about 80-90 ML, and at Po_2 = 10 Pa is about 550 – 600 ML of O_2.

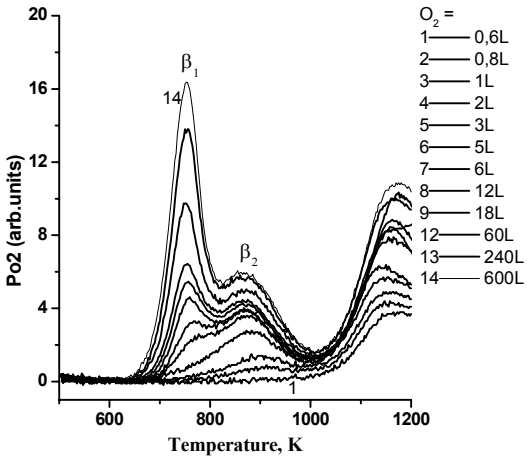

Fig. 1. TPD spectra of oxygen from Pd(110), Po_2 increase from $2*10^{-8}$ Torr to $1*10^{-6}$ Torr, T = 500 K

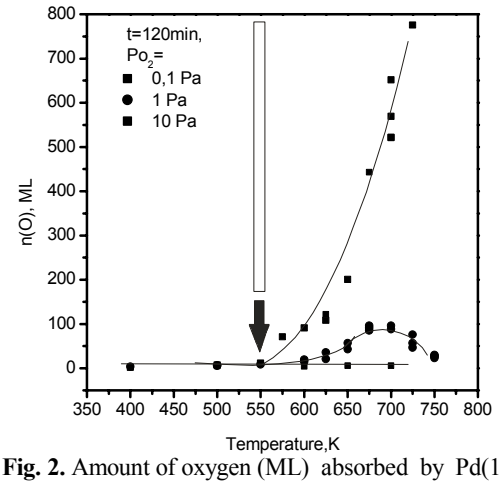

Fig. 2. Amount of oxygen (ML) absorbed by Pd(110) after interaction with O_2 at different temperatures, Po_2 = 0.1, 1 and 10 Pa, t =120 min

Thus, by the detailed analysis of the literature data [2-8] and our data we have established general behavior of the formation of the reconstructive and the oxide layers during interaction of oxygen with Pd(110).

During oxygen interaction with Pd(110) adsorbed metal atoms generated by steps diffuse on terraces and interact with chemisorbed oxygen atoms, so only short fragments of reconstructive chains are formed. Then, these fragments of chains grow through oxygen precursor state. The chains interact between each other and as result a reconstructive chain structures are formed in which chains are situated in one direction with equal distance between neighboring two. With increasing of oxygen surface coverage the distance between the chains decreases. At θ_o = 0,5 ML reconstructive chain structure (1×2) is formed with distance between neighboring chains of the one row palladium atoms. During further oxygen adsorption the reconstructive chain structure (1×2) is reconstructed, and islands of surface oxide are formed. Then, these islands grow and cover all the surface. After that the thin film of surface oxide about 6 –7 ML is formed. When oxygen exposure and temperature of the sample are further increased the film of oxide is decomposed and oxygen penetrates to the bulk of palladium.

We acknowledge financial support from CRDF REC 008.

References:

1. R. M. Heck, R. J. Farrauto, Catalytic Air Pollution Control : commercial technology, Van Nostrand Reinhold, 1995.
2. G.A.Somorjai, Cat.Lett. 7(1990)169; Cat.Lett. 12(1992)17; Langmuir 7(1991)3176; Ann. Rev. Phys. Chem., 45(1994)721.
3. S. Titmuss, A. Wander, and D. A. King, Chem. Rev., 1996**,** 96, 1291-1305
4. R.A.Bennett, S.Poulston, I.Z.Jones, M.Bowker, Surf. Sci., 401 (1998) 72.
5. H.Tanaka, J. Yoshinobu and M. Kawai, Surf. Sci., **327**(1995) L505-L509.
6. V. A. Bondzie, P. Kleban, D. J. Dwyer, Surf. Sci., 347 (1996) 319
7. M.Peuckert, J.Phys.Chem., 89(1985)2481
8. J.-W. He and P .R. Norton, Surf. Sci., 204(1988) 26

DFT INVESTIGATION OF σ-DONATING AND π-ACCEPTING LIGANDS INFLUENCE ON THE STRUCTURE OF (η^3-ALLYL)PALLADIUM COMPLEXES

Tkatchenko O.Yu., Kuvardina E.V., Morozova T.A., Belov A.P.

Lomonosov Moscow State Academy of Fine Chemical Technology, Moscow, Russia
E-mail: out@pochtamt.ru

(η^3-Allyl)palladium complexes play an important role in the catalytic synthesis of organic compounds. Theoretical investigation is able to give information about the influence of coordination sphere composition on the complex structure. This information is important to evaluate reactivity of the complex.

The series of anionic and neutral complexes of general formula [η^3-C_3H_5PdClL], containing the row of σ-donating and π-accepting ligands (L=Cl^-, H^-, OH^-, NH_3, Py, PH_3, CO, NO …), were theoretically studied. DFT calculations with PBE functional [1] in the large orbital basis set with pseudopotential SBK [2] were carried out. Program kindly submitted by the author D.N.Laikov (Moscow State University) [3] was used.

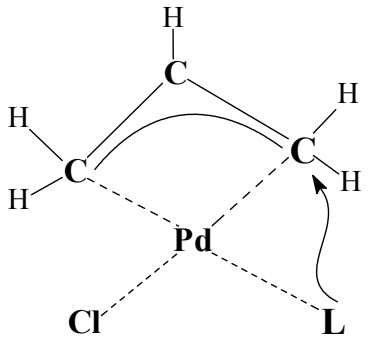

Structural characteristics of the complexes were analyzed. The influence of regulating ligand L on *cis*- and *trans*-Pd-C bonds was revealed. The mechanism of intraspheric transformations was studied: activation parameters of the nucleophilic attack on the terminal carbon atom of the allyl ligand were established.

References:

[1] *Perdew J.P., Burke K., Ernzerhof M.* Phys. Rev. Lett. 1996. V.77. P.3865.
[2] *Stevens W.J., Basch H., Krauss M.* J.Chem. Phys. 1984.V.81 P.6026.
Stevens W.J., Basch H., Krauss M., Jasien P. Can. J. Chem. 1992. V70.P.612.
Cundari T.R., Stevens W.J. J.Chem. Phys. 1993. V.98. P.5555.
[3] *Laikov D.N.* Chem. Phys. Lett. 1997. V.281. P.151.

DESIGN AND CHARACTERIZATION OF OXIDE CATALYSTS FOR NOx SELECTIVE REDUCTION BY HYDROCARBONS IN THE OXYGEN EXCESS

Tretyakov V.[1], Burdeynaya T.[1], Matyshak V.[2], Zakorchevnaya Yu.[2], Zakirova A.[1], Berezina L.[1]

[1]Topchiev Institute of Petrochemical Synthesis RAS, Moscow, Russia
E-mail: Tretjakov@ips.ac.ru
[2]Semenov Institute of Chemical Physics RAS, Moscow, Russia

Introduction

Nitrogen oxides are one of the major pollutants in the atmosphere and their removal from exhaust gases is of great need. In this connection, considerable attention has been paid to the development of new catalysts for selective NOx reduction by hydrocarbons in the presence of oxygen excess. Several publications have reported the enhancement of NO reduction activity by combination of two active catalytic species. Consequently, the catalysts have become more and more complex in the course of catalyst development. At present time great interest arises to multi-component, particularly multi-phase catalysts, which provide high activity and selectivity due to special separation of the process where each catalysis step proceeds on separate phase. Special separation of active centers is the common rule for complex catalytic processes. In such systems interphase diffusion of adsorbed species, including spillover, plays significant role. Synergistic effect is one of the ways to increase the efficiency of catalytic systems [1-6].

It is suggested that the selective catalytic reduction (SCR) of NO by hydrocarbons under oxygen-rich or lean conditions proceeds via a series of sequential and/or parallel reaction steps, probably catalyzed by different catalytically active species. There are many factors affecting the catalytic activity, including NO adsorption capability, and oxidation activity of NO or hydrocarbons. Most researchers propose reaction mechanisms in which some kind of intermediate, such as NO_2, partially oxidized hydrocarbons, carbonaceous materials and nitrogen-containing compounds leading to the formation of N_2, are formed during the reaction pathway. It is expected from the reaction mechanism that adequate combinations of catalytic species may give high-performance catalysts. In order to obtain new concepts for the future catalyst design the reaction mechanism should be studied in detail.

Because the increase in the number of catalyst phases leads to the increase in selectivity, we employed mechanical mixing of components as the method to obtain the multiphase catalytic system for NOx SCR by hydrocarbons in the oxygen excess. We have used in our

research original catalytic compositions obtained as mechanical mixtures of commercial oxide catalysts which are widely used in petrochemical processes and which contain neither zeolites nor noble metals. Mechanical binary mixtures of the commercial catalysts STK, NTK were found to have synergistic properties in the NO SCR by methane and propane [1, 2].

Therefore, the goal of this work was to study synergistic phenomenon and the detail mechanism of SCR process over the separate components (STK and NTK catalysts) of mechanical mixture.

Experimental

The composition and properties of oxide catalysts were elucidated using X-ray structural analysis, temperature-programmed desorption (TPD) and *in situ* spectrokinetic measurements. Catalytic properties of these systems were characterized in the reactions of NO_x selective reduction in the excess of oxygen by propane. Spectrokinetic measurements in stationary and non-stationary modes allow to determine the rate of surface species transformation by means of IR spectroscopy and to compare it with the rate of reaction. The use of two modes of IR spectroscopy (recording of transition spectra, possessing higher sensitivity in lower frequency range, < 1400 cm^{-1}, and diffusive reflection, better for use in higher frequency range, > 1800 cm^{-1}) has given the fullest overall picture.

Results and discussion

According to the X-ray diffraction data and X-ray structural analysis, the catalyst NTK-10-1 has various oxides in its composition: ZnO, CuO, NiO, $ZnAl_2O_3$, $Cu_2Al_2O_4$, and $CaCO_3$. The catalyst STK consists of Fe_2O_3 and Cr_2O_3. The results of temperature-programmed reduction have shown that the surface of NTK-10-1 loses oxygen quite easily. CuO can be reduced into the metal state easily and to a larger degree (34-36 %) than others. On the opposite side only 2.7 % of NiO can be reduced.

Maximum of reduction for STK was observed at T_{max} = 250 ^oC, which corresponds to reduction of Cr_2O_3 into CrO. Degree of reduction for this process fell during three redox cycles from 14.1 % to 7.6 %. Also reduction of Fe_2O_3 into Fe was observed with peak at 360 ^oC and degree of reduction 7.0 % which remained unchanged with new redox cycles.

Quantitative spectroscopic measurements have shown that over NTK and STK catalysts nitrite and nitrate surface complexes formation was observed. With temperature increase, nitrates transform into nitrites; this process is inhibited when propane is present in the gas phase. Oxygen, found to be non-adsorptive over studied catalysts, nevertheless plays an

important role in propane adsorption. Nitrate complex is the intermediate in SCR over 150 °C. It transforms into a nitro-organic compound, which in oxidative media is able either to give end products or to be oxidized with release of NO_x into the gas phase.

At temperatures lower than 150 °C, nitrite complex was found to become an intermediate. It allows to explain the unexpectedly high activity at low temperatures.

The key role of nitrates in SCR process is attributed to NO_2 formation during decomposition of nitrates in amount exceeding an equilibrium one. This NO_2, formed directly in reaction zone, is highly active in reaction with hydrocarbons.

Quantitative comparison of adsorption characteristics and properties of surface complexes under SCR conditions over STK and NTK catalysts has allowed to explain the synergistic effect observed for the mechanical mixture of these catalysts. Over STK catalyst, propane is oxidized into a complex, a product of partial oxidation. Propane cannot be oxidized fully over this component of catalytic system because it is void of NO in its high-temperature adsorption form, so the complex formed from propane is oxidized over NTK catalyst, which surface is covered with activated NO molecules, after the diffusion through the gas phase.

Additional facts favoring this mechanism were found during a series of experiments where behavior of individual catalysts (NTK), (STK) and their mixtures was investigated in gas media of the following composition: NO - 0.1 vol.%, C_3H_8 - 0.5 vol.%, O_2 - 2.5 vol.% (Table 1).

Table 1. Catalytic reduction of NO by propane at 450 °C
(NO - 0.1 %, C_3H_8 - 0.5 %, O_2 - 2.5 %)

Catalyst	NO conversion to N_2, %	C_3H_8 conversion, %
0.8 cm^3(NTK)	27	80
0.4 cm^3(NTK) + 0.4 cm^3 SiO_2	0	16
0.8 cm^3 (STK)	48	70
0.4 cm^3 (STK) + 0.4 cm^3 SiO_2	20	24
0.4 cm^3 (NTK) + 0.4 cm^3 (STK) (mechanically mixed)	75	50
0.4 cm^3 (NTK)(first layer) + 0.1 cm^3 SiO_2 (second) + 0.4 cm^3(STK) (third)	79	-
0.4 cm^3 (STK) (first layer) + 0.1 cm^3 SiO_2 (second) + 0.4 cm^3(NTK) (third)	100	-

The loading of components into reactor was performed in different orders. Quartz, which was used as one of the components of catalytic compositions, was not found to possess catalytic properties in this reaction. When the catalysts were loaded layer by layer, NO

conversion in the case where catalyst (NTK) was the first layer, closest to the entrance of the gas flow, was about the same (79 %) as that for mechanical mixture of catalysts (NTK) + (STK). When catalyst (STK) was the first layer contacting with the gas, complete conversion of NO was observed, and it remained the same even when the amount of quartz dividing the catalysts (NTK) and (STK) was increased. When the volume of quartz reached 0.4 $см^3$, the height of quartz layer became 5 mm. These data give evidence that the product of propane oxidation on catalyst (STK) is stable enough to reach the surface of catalyst (NTK) through 5 mm of quartz layer and to interact with adsorbed NO molecules. When catalyst (STK), on which the products of propane partial oxidation are formed, is the first layer to contact with entering gas flow, SCR of nitric oxide proceeds with greater efficiency than in the case of mechanical mixture of catalysts or in the case when catalyst (NTK) is the first contacting layer. Obtained experimental data allow to conclude that the known mechanism of "remote control" or synergistic strengthening of catalysis in mixtures of catalysts [7] takes place. It also becomes evident that it would be expedient in our case to load the catalyst layer by layer in definitive order.

Thus the concept of the cooperation effect of two catalytic species or bifunctional catalysis will certainly provide the possibility of better catalyst design for the selective reduction of NO by hydrocarbons.

Acknowledgments Financial support by RFFI under 02-03-33161 project is gratefully acknowledged.

References

1. Tret'yakov, V.F., Burdeinaya, T.N., Matyshak, V.A., Uharskii, A.A., Mokrushin, O.S., Glebov, L.S., *Kinet. Katal*., 41 (2000) 261.
2. Burdeinaya, T.N., Matyshak, V.A., Tret'yakov, V.F., Mokrushin, O.S., Glebov, L.S., *Kinet. Katal*., 41 (2000) 415.
3. Yokoyama, C., Misono, M., *Catal. Lett,* 29 (1994) 1.
4. Shipiro, E.S., Joyner, R.W., *et al., Stud. Surf. Sci. Catal.*, 84 (1994) 1483.
5. Bethke, K.A., and Kung, H.H., *J. Catal.*, 171 (1997) 1.
6. Yan, J-C., Kung, H.H., Sachtler, W.M.H., and Kung, M.C., *J. Catal.*, 175 (1998) 294.
7. Delmon B., Froment G. F., *Catal. Rev.,* 38 (1996) 69.

SYNTHESIS OF MESOPORIUS TITANIUM SILICATES FOR CATALYST PREPARATION

Trusova E.A., Korolev Yu.M., Slivinsky E.V.

Topchiev Institute of Petrochemical Synthesis RAS, Moscow, Russia
E-mail: trusova@ips.ac.ru

The research of nanomaterials on the basis of pure and modified silicates began 10-15 years ago. During this short period, mesoporous silicates and their metal- (Ni, Fe, Pt, and Al), sulfur- and phosphorous-modified forms were extended to almost all fields of application of zeolites surpassing them by many parameters. Micro (3-20 Å) and mesoporous (up to 100 Å) silicates can be used as acid or oxidation-reduction catalysts or as gas separating materials (molecular sieves and membranes).

The difficulties of synthesis of mesoporous metal-modified silicates are caused by the fact that temperature changes in the course of synthesis and crystallization by 10-15 ºC can affect the porosity, initiate phase transitions and lead to formation of nonsingle phases. The medium pH, solvents, concentrations and ratios of initial components, the length and the structure of hydrocarbon chains of the template, the volume and nature of a ligand in an initial derivative of the modifier metal, as well as the mode of drying (temperature, supercritical conditions) play extraordinarily important role in the synthesis, crystallization, and the phase formation.

Here, we report the technique of creating highly porous titanium-silicate systems whose modification with transition metal ions allows us to obtain a broad spectrum of catalysts for various petrochemical processes. We present results of the differential selection of synthesis conditions for highly porous materials based on silica with a low bulk weight (0.2-0.4 g/cm^3), both crystalline and amorphous.

Titanium tetrabutoxide and H_2SiO_3 (dissolved in 32 % NaOH water solution with ratio Si/Ti about 20) were used as initial reactants. The syntheses were carried out using monoethanolamine and ammonium chloride as structure-directing agents. Toluene, acetylacetone, and water–alcohol mixtures were used as cosolvents. The preparation was performed at a temperature range of 65 –100 ºC.

The effect of the initial pH (11 – 14) and the temperature of the washing water on the yield, phase composition, and the porosity of the systems obtained were also established. The gel was dried at 100 ºC during 10 – 12 hrs at atmospheric pressure in air. Then the gel was calcined in air at temperature 300–600 ºC. The changes in the phase composition, crystallinity

degree, and thermal stability were determined using a computerized DRON-2 X-ray diffractometer with Cu Kα radiation and an accessory registrating reflections >70 Å. Two series of Ti silicates, crystalline and amorphous, were obtained.

The investigation of surface area and porosity was carried out applying an ASAP 2010 instrument (adsorption – desorption of nitrogen).

The first series of experiments was carried out in a flask with a reflux condenser at 65º C. The second series was performed in an autoclave equipped with a magnetic stirrer. The effect of temperature on the yield and crystallinity of the product was investigated in a temperature range of 70 – 100 ºC at an excess autogenic pressure of 2.0 – 2.5 bars.

In the first case, the product was a brown gel with a greenish tinge whose bulk weight did not exceed 0.20 – 0.23 g/cm^3. In the course of further thermal treatment (drying and calcination), an XRD control of crystalline structure changes was carried out. The X-ray patterns of the gel dried at 100 ºC had a set of reflections that are characteristic of the monoclinic cell with parameters a=47.07, b=4.81, c=18.71, β=103.58º, V=4115.3 Å^3. The size of crystallites was 280 - 350 Å. The calcination of the gel at temperature 300 ºC resulted in a decrease in the size of crystallites down to 280-300 Å and in a partial degradation of the monoclinic structure with the formation of a second, amorphous phase having a broad halo of 4.4 Å and a particle size of 40 Å. As the calcination temperature rose up to 400 ºC, the size of the crystallites decreased to 270 Å, the interplanar distances remaining the same, and the fraction of the amorphous phase reduced.

The calcination of the gel at temperature 500 ºC led to an origination of a new phase with a crystallite size of 445 Å and an appearance of an intense reflection of 5.31 Å. Almost total amorphization was observed at temperature 600 ºC. The analysis of X-ray patterns showed that the set of reflections did not correspond to any crystalline form of titanium or its oxides.

In the second series of experiments, the initial pH of the medium and the temperature of the synthesis were changed. Amorphous mesoporous titanium silicates were obtained with which the effect of temperature on the amount of the gel and the size of its particles was established.

According to the porosimetry and XRD data, the mesoporous silicates obtained (35 – 70 Å) contain 94 – 97 % of the amorphous phase. The impurities of crystalline phases do not exceed 3 – 6 %. In both cases the X-ray patterns do not allow the assignment of the impurities to any forms of titanium or its oxides. The size of the particles of the amorphous phase is 10 – 18 Å. The size of crystallites of impurity phases changes from 170 – 260 Å at

synthesis temperature 100 ºC to 170 – 300 Å at synthesis temperature 90 ºC. It was shown that the titanium silicate gel prepared at temperature 100 ºC has a BET surface area of 115 – 132 m^2/g with a specific volume of mesopores being 0.20 – 0.23 cm^3/g and their diameter of 69 – 70 Å.

Thus, a method of the synthesis of mesoporous titanium silicate gels is proposed which can be used to obtain a broad variety of catalysts by means of the targetted molecular design.

The authors express gratitude to E.E. Knyazeva and I.I. Ivanova for their help in sorption measurement.

COMPARISON OF GOLD AND SILVER SPECIES SUPPORTED AND INCORPORATED INTO MORDENITES

Tuzovskaya I.[1,2], Bogdanchikova N.[2], Pestryakov A.[1,3], Gurin V.[4], Simakov A.[2,6], Lunin V.[5]

[1]Tomsk Polytechnic University, Tomsk, Russia
[2]CCMC-UNAM, Apdo Postal 2681, Ensenada, B.C., Mexico
E-mail: nina@omega.ccmc.unam.mx
[3]Fritz Haber Institute, Dept. of Inorganic Chemistry, Berlin, Germany
[4]Physico-Chemical Research Institute, BSU, Minsk, Belarus
[5]Lomonosov Moscow State University, Department of Chemistry, Moscow, Russia
[6]Boreskov Institute of Catalysis SB RAS, Novosibirsk, Russia

Introduction

The unique properties of zeolites including transition metal ions within the zeolite framework or cavities have opened new possibilities for many applications including catalysis. The transition metal ions incorporated in zeolites are considered to be highly dispersed at the atomic level and well defined, existing in a specific structure of the zeolite framework. This phenomenon is of great significance in the design of highly dispersed transition metal. Fundamental understanding of the coordination structure and electronic state of the active species is important in the design and development of applicable catalysts having high activity and selectivity [1].

UV-Visible spectroscopy could be very informative to clarify the nature of active species in the case of Ag, Au and Cu incorporated into zeolites. Optical properties of these metals are well studied but these results are not intensively applied to characterization of catalysts [2]. However the formation of different Ag species including clusters was investigated in mordenite by UV-Visible reflectance spectroscopy [3].

In this work investigation for gold and the comparison of the optical spectra of gold and silver species in mordenites had been performed.

Catalysts preparation and characterization

Mordenites in protonated form with SiO_2/Al_2O_3 molar ratio (MR) from 10 (M10) to 206 (M206) supplied by TOSOH corporation (Tokyo, Japan) were used for the ion exchange of the gold and silver cations. Metal containing samples were obtained by ion exchange in aqueous solution of $AgNO_3$ [3] and of $[Au(NH_3)_4](NO_3)_3$. The last complex was prepared by reaction of $HAuCl_4$ with NH_4OH and NH_4NO_3 [4]. After ion exchange the samples were dried and reduced by H_2 at different temperatures during 4 and 2.5 hs for Ag and Au samples, respectively. The silver content measured using X-ray Fluorescence Spectrometer SEA 2010 was 0.4-2.3 wt. %. The gold content evaluated by

energy dispersive spectroscopy was within 0.5-2 wt. %. UV-Visible diffuse reflectance spectra were measured at room temperature on a CARY 300 SCAN (VARIAN) spectrophotometer with a standard diffuse reflectance unit. The spectra are presented after subtraction of spectrum of pure zeolite from the spectra of metal containing samples.

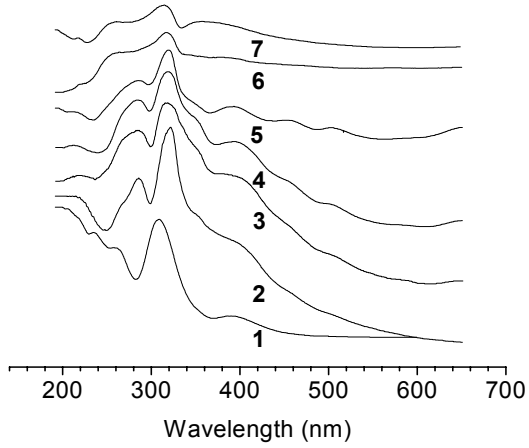

Fig. 1. UV-Visible spectra of Ag M15 reduced by hydrogen at: 1-25 ^{o}C, 2-50 ^{o}C, 3 –100 ^{o}C, 4- 200 ^{o}C, 5-300 ^{o}C, 6-400 ^{o}C, 7-500^{o}C (curves were translated in vertical direction for clear observation).

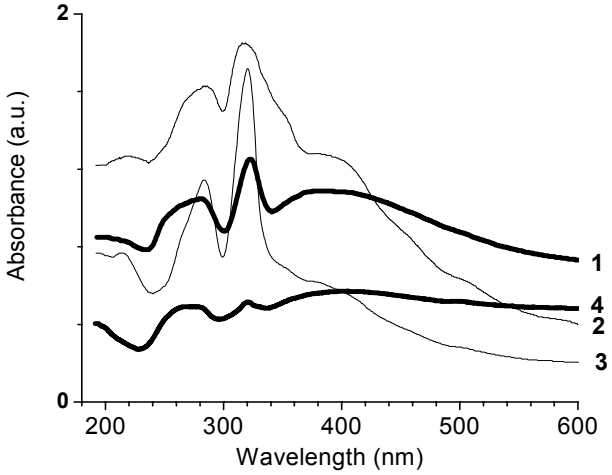

Fig. 2. UV-Visible spectra of Ag samples reduced at 100 ^{o}C with various MR: 1-Ag M10, 2-Ag M15, 3-Ag M20, 4-Ag M 206

Results and discussion

The diffuse reflectance spectra of Ag-mordenites with various SiO_2/Al_2O_3 molar ratios registered immediately after sample reduction are represented in the Figs. 1 and 2. For all samples the absorption bands at 320 and 285 nm (typical for absorption of neutral Ag_8 and charged $Ag_8^{\delta+}$ clusters, respectively) with shoulder at 265 nm (Ag_4^{2+} clusters) were observed in UV region. Identical positions of peaks indicate that mordenites stabilize selectively the same silver cluster types independently on SiO_2/Al_2O_3 molar ratio. In the spectra of all studied samples, peaks in the wavelength regions 370-400 nm and higher than 400 nm were also observed (Fig. 2). These peaks were assigned to quasi-metal colloidal particles and larger silver particles, respectively [3].

UV-Visible spectra of Au samples are presented on Figs. 3 and 4. The spectra of Au samples show three characteristic absorption bands. The absorption band at 195 nm was assigned to the gold cations Au^+ [5]. It implies that precursor $[Au(NH_3)_4]^{3+}$ complex was at least partially reduced to Au^+ just after ion exchange. The reliable interpretation of two other absorption bands in the regions 250-260 and 320-340 nm we could not find in literature. In reference [2] it was suggested that the absorption bands in this spectra region could be due to the gold clusters. It should be noticed that

relative intensity of absorption bands in the region of clusters correlates with the concentration of Brønsted acid centres in mordenites measured in [3] (Fig. 4).

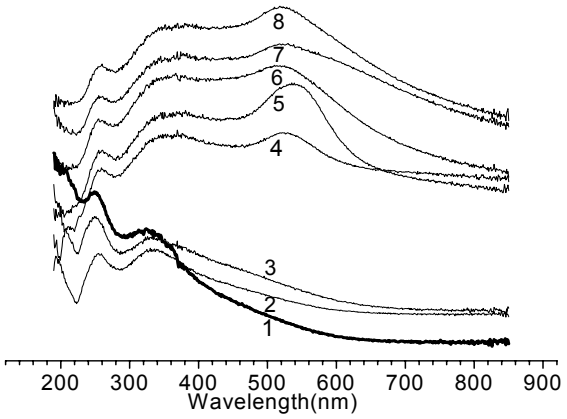

Fig. 3. UV-Visible spectra of Au/M15 samples 1- no reduced, 2- reduced at: 25 °C, 3- 50 °C, 4- 100 °C, 5-200 °C, 6-300 °C, 7-400 °C, 8-500 °C (curves were translated in vertical direction for clear observation).

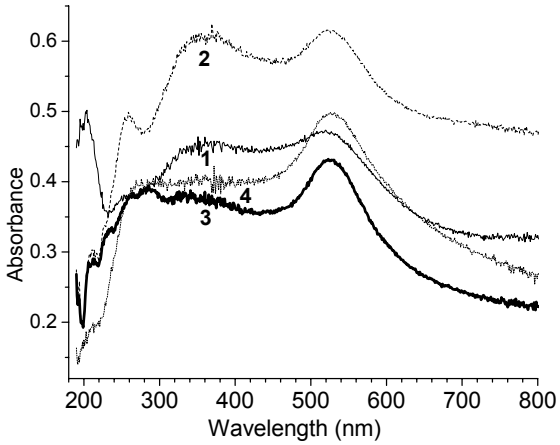

Fig. 4. UV-Visible spectra of samples reduced at 100 °C: 1-Au M10 (1), Au M15 (2), Au M24 (3), Au M206 (4).

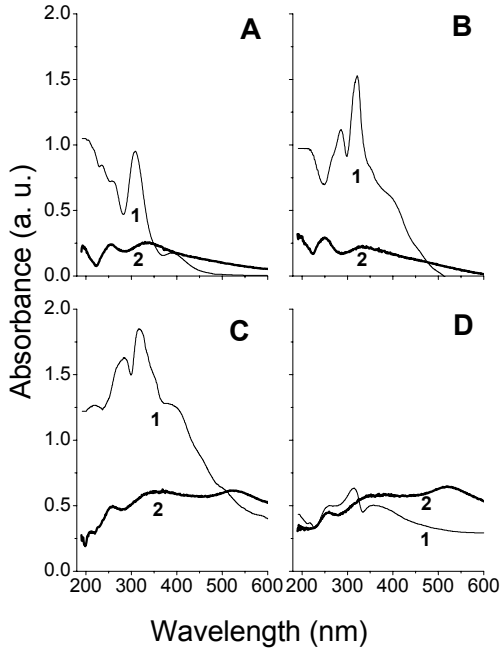

Fig. 5. UV-Visible spectra of 1-Ag M15 and 2- Au/M15 reduced at: A- 25 °C, B- 50°C, C- 100°C, D- 500°C.

The maximum at λ=530 nm in the spectra presented in Figs. 3 and 4 is attributed to the surface plasmon resonance for Au nanoparticles [5] located on external surface of zeolite microcrystals. Increase of reduction temperature (Fig. 3) leads to decrease of relative intensity of the peak assigned to cations and to rise of relative intensity of the plasmon resonance of nanoparticles. Thus, with increase of reduction temperature the contribution of gold cations decreases and the features of reduced species are developed.

The spectra of silver and gold supported samples are illustrated in Fig. 5. The peaks at 250 and 320 nm assigned preliminary to gold clusters are much broader than those for silver clusters that can be due to the fact that a set of clusters in the silver samples is more uniform then in gold samples. In the spectra for both metals the absorbance at > 400 nm assigned to the nanoparticles grows significantly after reduction at the temperatures ≥100 °C.

Thus, UV-Visible data show the presence of silver and gold species in the supported mordenites in similar spectra region. The reduction treatment increases the amount of reduced species for both

metals. The contribution of species attributed to clusters can be varied with variation of reduction temperature and with SiO_2/Al_2O_3 molar ratio for both Ag and Au. The revealed difference between Ag and Au samples is suggested to be due to uniform set of Ag clusters and not uniform set of Au clusters.

References:

[1] Masaya Matsuoka, Masakazu Anpo., *Journal of Photochemistry and Photobiology C: Photochemistry Reviews* 3 (2003) 225.
[2] Pestryakov A.N., Lunin, V.V. etc., *Journal of Molecular Structure* 642 (2002) 129.
[3] Bogdanchikova N., Petranovskii V., Fuentes S. etc., *Materials Sci. and Ing,.* A276 (2000) 236.
[4] Skibsted L.H., Bjerrum J., *Acta Chemica Scandinavica* A28 (1974) 740.
[5] Kang Y., Wan B., *Catalysis Today* 26 (1995) 59.

PROMOTED COPPER CATALYST OF PARTIAL ALCOHOL OXIDATION

Knyazeva A.[1], Shmotin V.[1], Vodyankina O.[1], Stoyanov E.[2], Odegova G.[2], Chesalov Yu.[2], Salanov A.[2], Kurina L.[1]

[1]Tomsk State University, Tomsk, Russia
[2]Boreskov Institute of Catalysis SB RAS, Novosibirsk, Russia
Fax: (3822)426195; E-mail: vodyankina_o@mail.ru,

It is known that addition of such volatile compounds as chlorine, bromine, iodine and phosphorous into the reaction mixture increase yield of carbonyl compounds in partial oxidation of alcohols on the IB subgroup catalysts and the yield of glyoxal in ethylene glycol oxidation. However, at high temperature (823 – 923 K) halogen containing compounds, being added into oxygen-containing reaction mixture lead to apparatus corrosion, the latter been a serious draw back. Copper likewise silver is one of the main catalysts of monoatom alcohol oxidation into carbonyl compounds and also the ethylene glycol oxidation into glyoxal. Promotion of copper surface by P-containing compounds was assumed to increase the catalyst activity and selectivity. From the economic point of view and the simplicity of operation the promotion of the catalyst surface is more preferable then the volatile compounds addition into reaction mixture. Activity of P-modified copper catalyst is studied in both the ethylene glycol and ethanol oxidation processes in dependence on oxygen content in reaction mixture.

Copper catalyst has been prepared by electrolytic deposition of copper on the polymer support. The promotion of the catalyst surface has been carried out by the interaction of copper with the phosphoric acid solution, the sample being dried in the air at room temperature and activated in nitrogen atmosphere at 873 K during 3 h. The morphology investigations have been performed with the use of scanning electron microscope (SEM), the chemical composition of the samples has been investigated by X-ray diffraction (XRD) and IR-spectroscopy.

SEM data showed that the treatment of the copper catalyst with the promoter followed by drying in the air at 298 K leads to the formation of agglomerates consisting of thin plates of about 0.1 μm thick, which are perpendicularly oriented to the catalyst surface. Annealing of the phosphorus-containing copper catalyst in nitrogen at 873 K leads to the melting of the agglomerates forming a film, which covers the catalyst surface. Under the action of the oxygen-containing reaction mixture on the unpromoted sample the formation of carbon deposits, which remind a filaments, is observed. In the case of P-containing catalyst the promoter film on the copper cakes up resulting in the island like structure under the reaction

mixture action. As a consequence a certain part of copper surface remains uncovered by promoter film.

According to XRD data copper monoxide (Cu_2O) and traces of copper oxide (CuO) are found on the surfaces of P-doped catalyst samples (dried in the air, annealed in nitrogen and taken after catalytic experiments). This method did not register the P-compounds. After drying and annealing, XRD-spectra of samples have a peak, which is attributed to the amorphous phase whose film covers the copper catalyst surface.

IR spectroscopy data are showed that copper phosphates ($Cu_3(PO_4)_2 \cdot 3H_2O$) are present on the surface of P-content copper catalyst dried in the air. After annealing of promoted sample of Cu catalyst in nitrogen the $Cu_2P_2O_7$ phase is formed. After treatment by $N_2/EG/H_2O$ reaction mixture in the IR spectra the intensive absorption bands relating to copper carbonate and Cu_2O are appeared on the promoted catalyst surface. Appearance of 911, 1141 cm^{-1} bonds is probably connected with the transformation of phosphates into condensed state. Varying of the O_2 / EG molar ratio in reaction mixture is accompanied by a change of the promoted copper surface state. The oxygen partial pressure growth in the reaction mixture leads to formation of the state of copper (+1).

The oxygen-content in the reaction mixture is one of the important parameters affecting the process of alcohols oxidation. Varying the O_2 / alcohol molar ratio the carbonyl compounds yield curves pass through a maximum. On the promoted catalyst in comparison with unpromoted the carbonyl compounds yield is 10 – 15 % higher both for ethanol and ethylene glycol while the alcohol conversion remains the same. The content of carbon dioxide and monoxide on the promoted catalyst is less then that on the unpromoted one. It may be explained by the decrease of the active centers which are responsible for the heterogeneous way of CO_2 formation on the P-containing catalyst surface.

Thus the P-promoted catalysts are characterized by an elevated selectivity in attitude to carbonyl compounds. It may be connected with the formation of refractory phosphorus-containing film which protects the copper surface from the formation of copper oxide (II) which is responsible for the deep alcohol oxidation processes.

NO MOLECULE AND SPIN DESIGN OF IRON COMPLEXES ON FeZSM-5 ZEOLITES

Volodin A.M., Dubkov K.A., Starokon E.V.

Boreskov Institute of Catalysis SB RAS, Novosibirsk, Russia
E-mail: volodin@catalysis.nsk.su

FeZSM-5 zeolites are efficient catalysts for oxidation of organic compounds with nitrous oxide. Fe(II) ions are the most likely candidates for the role of active sites in one-step oxidation of benzene to phenol using nitrous oxide as the oxidation agent [1, 2]. In oxide systems such complexes usually have even spin (S=2) and are not observed by ESR. Earlier we have shown that [Fe(II)-NO] complexes with intermediate spin (S=3/2) can be formed due to NO adsorption from the gas phase to yield surface nitrosyl complexes [3]:

$$[Fe^{2+}]\ (\mathbf{S=2}) + NO \rightleftharpoons [Fe^{3+} \ldots NO^{-}]\ (\mathbf{S=3/2}) \qquad (1)$$

In current communication we shall demonstrate new capabilities of "in situ" ESR for investigation of the state of Fe ions in zeolites. We use adsorption of various molecules from the gas phase for alteration of the spin state in iron complexes.

The reaction of the active sites of FeZSM-5 zeolites (α sites) with N_2O is known to result in stabilization of an active oxygen form (O_α) that accounts for selective oxidation of benzene into phenol.

$$(\ )_\alpha + N_2O \longrightarrow (O_\alpha) + N_2 \qquad (2)$$

Most probably, this reaction involves Fe(II) ions and does not result in a change of the total spin:

$$[Fe^{2+}]\ (\mathbf{S=2}) + N_2O \longrightarrow [Fe^{3+} \ldots O^{-}]\ (\mathbf{S=2}) + N_2\ , \qquad (3)$$

Therefore, neither initial paramagnetic ions $[Fe^{2+}]$ nor their complexes with oxygen $[Fe^{3+} \ldots O^{-}]$ can be registered by ESR. However, ESR reliably detects high-spin paramagnetic complexes resulting from the reaction of α oxygen with organic molecules:

$$[Fe^{3+} - O^{-}]\ (\mathbf{S=2}) + H_2 \longrightarrow [Fe^{3+} - OH^{-}]\ (\mathbf{S=5/2}) \qquad (4)$$

$$[Fe^{3+} - O^{-}]\ (\mathbf{S=2}) + NO \longrightarrow [Fe^{3+} - NO_2^{-}]\ (\mathbf{S=5/2}) \qquad (5)$$

NO adsorption on studied zeolites allowed us to distinguish two types of low spin (S=1/2) nitrosyl complexes of Fe ions with different spectral parameters. Most likely, their formation is due to the presence of binuclear low-valence iron complexes and can be described as follows:

$$[Fe^{2+}\text{-}\ Fe^{2+}]\ (\mathbf{S=0}) + nNO \rightleftharpoons [Fe^{2+}\text{-}\ Fe^{2+}\ ...\ (NO)_n]\ (\mathbf{S=1/2}) \qquad (6)$$

The role of different iron sites in FeZSM-5 zeolites in the formation of α oxygen from N_2O will be discussed. The applicability of the suggested approach for investigation of the state of iron ions in different types of zeolites by ESR will be shown.

Financial support of the Russian Foundation for Basic Research (grant 03-03-33178) and NWO (project 047.015.001) acknowledged with gratitude.

References

1. Dubkov, K.A., Ovanesyan, N.S. Shteinman, A.A., Starokon, E.V., Panov, G.I., *J. Catal.,* **207** (2002) 341.
2. Panov, G.I. *CATTECH*, **4** (2000) 18.
3. Volodin, A.M., Dubkov, K.A., Lund, A., *Chem. Phys. Lett*., **333** (2001) 41.

NON-OXIDATIVE METHANE CONVERSION TO AROMATIC HYDROCARBONS ON Mo/HZSM-5 CATALYSTS

Vosmerikov A.V.[1], Korobitsyna L.L.[1], Echevskii G.V.[2], Zhuravkova M.F.[1], Kodenev Ye.G.[2], Barbashin Ya.Ye.[1]

[1]Institute of Petroleum Chemistry SB RAS, Tomsk, Russia
Fax: (3822) 258457; E-mail: pika@ipc.tsc.ru
[2]Boreskov Institute of Catalysis SB RAS, Novosibirsk, Russia

Methane is the major component of natural gas as well as of associate gas, its annual production amounts to billions of cubic meters. Nevertheless, methane inertia conditioned by C–H bond strength and a high symmetry of CH_4 molecules is major obstacle for a wide application of these gases as the feedstock for chemical industry [1]. Despite of the existing methods for methane processing that are characterized by a multistage process and large expenses for feedstock and energy, the problem of selective methane activation and directed synthesis of valuable chemicals is a great challenge, it is both of fundamental and applied importance. In recent years the research connected with the non-oxidative CH_4 dehydrocondensation into aromatics in the presence of Mo/HZSM catalysts or to a direct conversion of methane to the compounds of applied interest attracted considerable attention [2-4].

The present work represents the results of the study of CH_4 conversion on Mo-modified high-silica zeolites of ZSM-5 type. We have studied how the ratio of the concentration of the framework atoms, the method of Mo introduction, Mo concentration, the reaction conditions and catalysts pretreatments effect their catalytic activity, selectivity and stability. The acidic properties of the catalysts obtained, the concentrations and the strength of acidic sites of different types have been studied using ammonia thermodesorption method. The nature of the compaction products and the influence of the catalyst composition and the conditions of methane conversion on the parameters of coke formed on the surface of Mo-containing catalysts have been revealed using differential thermal analysis.

The conversion of methane precleaned from the admixtures was carried out at atmospheric pressure in a flow fused silica reactor mode (5 mm i.d.) The volume of the catalyst charge was 1.0 cm^3, the dimensions of the catalysts particles were 0.25-0.5 mm. Before and after each experiment the reactor with the sample studied was blown off with an inert gas at the reaction temperature changed from 500 to 750 ^oC. The space velocity of methane was within 250-2500 h^{-1}. To prevent the possible condensation or strong adsorption of the higher hydrocarbons formed, the pipe at the outlet of the reactor and the sample injector

were kept at a temperature above 200 ^{o}C. To analyse the products of CH_4 conversion, we used gas chromatographs equipped with thermal conductivity detectors. The analysis of non-volatile compounds such as benzene, naphthalene and their derivatives, as well as of hydrogen, methane, ethane and ethylene was carried out simultaneously on two packed columns.

The study of the effect of zeolite composition has shown that with the increase in silica modulus from 30 to 80 the activity and selectivity of a modified catalyst in the formation of the aromatic hydrocarbons decreases. The highest selectivity of arenes formation (90 %) was observed for the samples with silica modulus of 30-40. The degree of methane conversion over the catalysts increases with the volumetric feed rate and reaches maximum values (>10 %) at 750 h^{-1}. At a short contact time (~1.5 s) the conversion does not exceed 3%. At the increase in the reaction temperature from 650 to 750 ^{o}C at 750 h^{-1} the aromatizing activity of the catalysts increases, reaching maximum values at 720-750 ^{o}C. Benzene and naphthalene are major reaction products, and gaseous products, along with methane that did not entered into the reaction, contain hydrogen, ethane, ethylene and CO and CO_2 traces. The selectivity of benzene and naphthalene formation significantly depends on the process conditions. The study of the influence of the reaction time on the degree of CH_4 conversion over 3-6 % Mo/HZSM-5 (Si_2O_3/Al_2O_3=30-80) has shown that over all the samples in the first 15-20 min a maximum methane conversion degree is observed within all the range of the space velocities studied, then it gradually decreases and after 8 hours of operation does not exceed 3-4 %. It should be noted that the drop in the catalyst activity during the operation occurs faster at shorter contact times. The decrease in conversion degree of CH_4 is connected to an intensive coke formation on the catalyst surface under the reaction conditions, which leads to its deactivation. The studies performed have lead us to the conclusion that the most effective methods for zeolite modification by molybdenum are the impregnation by a solution of Mo salt and solid-phase interaction of Mo oxide with zeolite matrix during thermal treatment of their mixture under different conditions.

References:

[1] Usachev N.Ya., Minachev X.M., *Petroleum Chemistry,* 33 (1993) 387
[2] Jun-Zhong Zhang, Mervyn A. Long, Russell F. Howe, *Catalysis Today,* 44 (1998) 293
[3] Yide Xu, Liwu Lin, *Appl. Catalysis,* A 188 (1999) 53
[4] Meriaudeau P., Tiep Le V., Ha Vu T.T., Naccache C., Szabo G., *J. Mol. Catalysis,* A 144 (1999) 469

THE MOLECULAR APPROACH TO DESIGN OF SUPERACIDIC CATALYSTS

Yatsimirsky V.K., Gut I.N., Boldyreva O.Yu., Lisnyak V.V., Stus N.V., Slobodyanik M.S.

Chemical Department National Taras Shevchenko University, Kyiv, Ukraine,
Fax: 380442346166; E-mail address: yats@univ.kiev.ua

The modern industry requires creation of high-active environmental safe catalytic materials. The molecular technologies enable novel catalysts design and upgrade [1].

Compounds containing molybdenum oxo-clusters or nanosized Mo_xO_y particles with hydrophobic or hydrophilic character can be obtained by varying of sol-gel synthesis conditions. These species are potentially interesting nano-building blocks (NB) in the design of textured materials. The reactivity of hydrophobic NB towards different nucleophiles has been studied in order to understand the processes taking place in the formation of meso-organised hybrids. Subsequently, different synthesis conditions were used to generate textured molybdenia-based hybrid phases, using PEO-based surfactants as templating agents. The tuning of the interactions between the template and the different kinds of nano-building blocks allow worm-like and mesoporous oxomolybdenium-based hybrid phases to be reproducibly obtained.

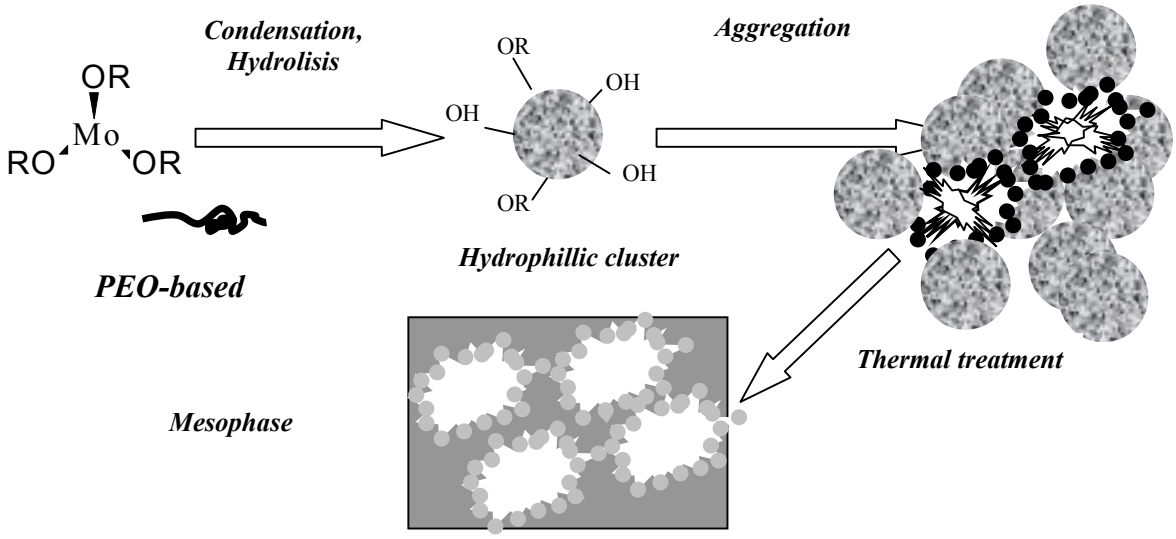

References:

[1] Lisnyak V.V., Yatsimirsky V.K. *et al.*, *Studies in Surf. Sci. & Catalysis,* Ed. A. Corma, Vol. 130, *Elsevier* (2000) 3807.

CONTENT

Russian-American Seminar

"Advances in the Understanding and Application of Catalysts"

ABSTRACTS

Editors: **Professor Valentin N. Parmon**
Professor Valerii I. Bukhtiyarov

The most of abstract are printed as presented in camera-ready texts and all responsibilities we address to the authors. Some abstracts underwent a correction of misprints and rather mild editing procedure.

Compilers: Lyudmila Ya. Startseva
Elena L. Mikhailenko

Computer processing of text: Yulia V. Klimova
Computer processing of eBook: Alexei A. Spiridonov